

## Study of mechanical properties in the simulation of 3D garments

LUIBLE, Christiane

### Abstract

Today, impressive simulation technology is available, allowing the creation of virtual garments that look incredibly realistic. Experimental values for the mechanical fabric properties can be derived from standard fabric characterization experiments. These methods have, however, not been designed for use in simulations. This study examines the accuracy of derived fabric parameters from standard measurement methods. Therefore, fabrics are measured and derived parameters are evaluated for static and dynamic virtual garment simulation. For those measurements which are found to be unsuitable, new methods are developed. A prototyping process is developed to compare both the real and virtual processes. It is demonstrated that typical garment assessments such as comfort and utility performance can be accurately simulated. Moreover, important numerical fitting data attest a better performance in the virtual process. The new measurement specifications are leading to the establishment of new measurement standards, which are designed for virtual simulation processes.

### Reference

LUIBLE, Christiane. *Study of mechanical properties in the simulation of 3D garments*.  
Thèse de doctorat : Univ. Genève, 2008, no. SES 678

URN : <urn:nbn:ch:unige-6880>

DOI : [10.13097/archive-ouverte/unige:688](https://doi.org/10.13097/archive-ouverte/unige:688)

Available at:

<http://archive-ouverte.unige.ch/unige:688>

Disclaimer: layout of this document may differ from the published version.



UNIVERSITÉ  
DE GENÈVE



**UNIVERSITÉ  
DE GENÈVE**

**FACULTÉ DES SCIENCES  
ÉCONOMIQUES ET SOCIALES**

# **Study of mechanical properties in the simulation of 3D garments**

Thèse présentée à la Faculté des sciences économiques et sociales de l'Université de  
Genève

Par Christiane Luible

pour l'obtention du grade de  
Docteur ès sciences économiques et sociales  
mention: Systèmes d'Information

Membres du jury de thèse :

Mme Nadia Magnenat-Thalmann, Professeur, Université de Genève, Directrice de Thèse  
M. Dimitri Konstantas, Professeur, Université de Genève, Président du Jury  
M. Thomas Fischer, Professeur, Université de Stuttgart, WHU Otto Beisheim School of  
Management, DITF – Centre for Management Research,  
M. Pascal Volino, Maître Assistant, Université de Genève

Thèse no. 678  
Genève, 2008

La Faculté des sciences économiques et sociales, sur préavis du jury, a autorisé l'impression de la présente thèse, sans entendre, par là, émettre aucune opinion sur les propositions qui s'y trouvent énoncées et qui n'engagent que la responsabilité de leur auteur.

Genève, le 22. Septembre 2008

Le doyen  
Bernard MORARD

Impression d'après le manuscrit de l'auteur

# Acknowledgements

This thesis owes its existence to the help, support and inspiration of many people. In the first place, I wish to express sincere appreciation and gratitude to my thesis supervisor Prof. Nadia Magnenat-Thalmann for her great support and encouragement during the past years of this thesis work. Without her energy and her enthusiasm, this work would not have been possible.

I would also like to address my thanks to the jury members Prof. Dimitris Konstantas (University of Geneva), Prof. Thomas Fischer (University of Stuttgart, WHU Otto Beisheim School of Management, DITF – Centre for Management Research), Prof. Dimitris Konstantas and Dr. Pascal Volino (University of Geneva).

The discussions and cooperation with all my colleagues at Miralab have contributed substantially to this work. In particular, I want to thank Pascal Volino for the indispensable discussions on cloth simulations and physical fabric parameters. I also thank Philip Gedet (MEM Centre Bern) for his advices on mechanical properties of materials and for many fabric measurements at the MEM centre in Bern. I am grateful to Dr. Harriet Meinander, Minna Varheenmaa and the members of the Haptex project research team for many inputs and discussions. I am also very thankful to Marlene Arevalo and Nedjma Cadi for their collaboration for the validation of this work and in particular Marlene for being the real and the virtual mannequin. I extend my thanks to Cecilia Charbonnier for her help for the scanning of the fabric samples and for the development of a viewer for visualizing the scanned fabrics. Thanks go also out to Alessandro Foni for his advices about camera and video settings for the filming of the real garments. I also wish to thank all Miralab members for their discussions, cooperative spirit and the excellent working atmosphere.

I owe a special gratitude to my friend Sarah Donohue for many fruitful discussions and the English proofreading. I also thank my friends for their motivation and support.

Finally I want to specially thank my family for the continuous and unconditional encouragement during all the time I have spent for my PhD.

This research was funded by the European project HAPTEX (<http://haptex.miralab.unige.ch>) and LEAPFROG IP ([www.leapfrog-eu.org](http://www.leapfrog-eu.org)).



# Abstract

Today, impressive simulation technology is available, which allow the creation of virtual garments that look incredibly realistic. Experimental values for the mechanical fabric properties can be derived from existing standard fabric characterization experiments. However, these measurement methods have not been designed for use in virtual simulations. To which extend these characterization methods are suitable to obtain data for virtual simulations is not known.

This study examines the accuracy of derived fabric parameters from standard measurement methods. A broad selection of 42 very different fabric test samples is chosen according to three defined selection criteria. Fabrics are measured using existing standard fabric characterization methods such as FAST and KES-f. Existing measurement methods are compared and evaluated for static and dynamic virtual garment simulation. For those measurements which are found to be unsuitable, new methods are developed, which better replicate real life garment wear. The accuracy of the derived parameters is studied, taking into account a previously defined accuracy spectrum.

Finally the newly derived parameters and the measurement method derivation processes are empirically tested. A prototyping process is developed and parallel tested to compare both the real and virtual processes. It is demonstrated that typical garment assessments such as comfort and utility performance can be accurately simulated in the virtual world. Moreover, additional important numerical fitting data attest a better performance in the virtual process.

The new measurement specifications are leading, in the long term, to the establishment of new measurement standards, which are designed for virtual simulation processes.



# Table of contents

1. Chapter: Introduction.....	1
1.1. Importance and Background.....	1
1.2. Innovation potential.....	2
1.3. Problem statement.....	3
1.4. Motivating applications.....	5
1.4.1. Garment prototyping and fitting .....	5
1.4.2. Garment design.....	8
1.4.3. Garment manufacturing.....	8
1.4.4. Marketing and the e-commerce.....	9
1.5. Objectives of new research.....	9
1.5.1. Most important parameters.....	10
1.5.2. Right values for each parameters.....	11
1.6. Summary.....	11
1.7. Organization.....	12
2. Chapter: Previous and related work.....	13
2.1. Introduction.....	13
2.2. Existing fabric characterization methods .....	14
2.2.1. Subjective fabric hand assessment.....	15
2.2.2. Objective hand measurements.....	16
2.2.2.1. Fundamental research.....	16
2.2.2.2. Kawabata.....	19
2.2.2.3. FAST.....	24
2.2.2.4. Comparison of the FAST and KES-f measurement data.....	25
2.2.2.5. Interpretation of the measurement data.....	27
2.2.2.6. Other measurement systems.....	28
2.2.3. Relation of fabric properties to clothing appearance and performance.....	29
2.2.4. Fabric drape .....	30
2.3. The exploitation of measured fabric properties in virtual simulation systems.....	32
2.3.1. Fabric materials modeled as continuum .....	32
2.3.2. Finite Element Method (FEM).....	32
2.3.3. Particle Systems.....	33
2.3.4. Numerical Integration.....	34
2.3.5. Use of accurate measurement data as input parameters.....	34
2.3.6. Various simulation applications.....	35



3. Chapter: Design of the test method .....	37
3.1. Introduction.....	37
3.2. Open questions.....	38
3.2.1. Suitability of existing measurement methods.....	38
3.2.2. Importance and influence of fabric properties.....	38
3.2.3. Versatility of parameters for the entire garment manufacturing chain.....	38
3.3. Contribution of this research.....	39
3.4. Applied methodology.....	39
3.4.1. Selection of real fabric samples.....	41
3.4.2. Simulation experiments, data analysis and refinement.....	41
3.4.3. Framework of accuracy .....	42
3.4.4. Validation.....	42
3.5. Justification of the applied methodology.....	43
4. Chapter: Data and parameter acquisition.....	45
4.1. Fabric selection .....	45
4.1.1. First selection criteria: raw material.....	47
4.1.1.1. Natural fibers.....	47
4.1.1.2. Man-made fibers.....	48
4.1.2. Second selection criteria: planar structure.....	49
4.1.2.1. Woven textiles.....	50
4.1.2.2. Knitted textiles.....	51
4.1.2.3. Non-woven textiles.....	51
4.1.3. Third selection criteria: dimension.....	52
4.1.3.1. Yarn properties.....	52
4.1.3.2. Finishing treatment.....	52
4.2. Standard fabric characterization.....	53
4.2.1. KES-f.....	53
4.2.1.1. Tensile.....	53
4.2.1.2. Shear.....	55
4.2.1.3. Bending.....	59
4.2.1.4. Thickness.....	61
4.2.1.5. Weight .....	62
4.2.1.6. Friction.....	62
4.2.1.7. Captured data ranges.....	64
4.2.2. FAST.....	66
4.3. Derivation of fabric input parameters.....	67
4.3.1. Various simulation systems.....	67
4.3.2. Applied simulation system.....	68
4.3.3. Derivation process.....	71
4.3.4. Limitations.....	72
4.4. Conclusion.....	75

5. Chapter: Accuracy of fabric input parameters.....	77
5.1. Introduction.....	77
5.2. Definition of the accuracy.....	77
5.2.1. Aspects of fit and importance of fabric properties.....	77
5.2.1.1. Comfort performance.....	79
5.2.1.2. Utility performance.....	81
5.2.1.3. Summary.....	83
5.2.2. Accuracy spectrum.....	83
5.2.2.1. Schemes and value of accuracy.....	84
5.2.3. Conclusion.....	87
5.3. Accuracy of the elasticity parameters tensile, shear and bending.....	88
5.3.1. Earlier fabric parameters.....	88
5.3.2. Elasticity parameters in static simulations.....	89
5.3.2.1. Tensile and shear.....	89
5.3.2.2. Bending.....	93
5.3.2.3. Pressure.....	97
5.3.2.4. Conclusion.....	97
5.3.3. Elasticity parameters in dynamic simulations.....	98
5.3.4. The tensile property in dynamic simulations.....	99
5.3.4.1. FAST – KES-f tensile parameters.....	99
5.3.4.2. New measurement specification: Step tensile measurements (ITT)...	101
5.3.4.3. Comparison KES-f – ITT.....	104
5.3.4.4. Length Driven Measurement (LDM)...	108
5.3.4.5. Comparison KES-f – ITT – LDM.....	114
5.3.5. The shear property in dynamic simulations.....	118
5.3.5.1. Suitability of standard shear measurements.....	118
5.3.5.2. LDSM (Length Driven Shear Measurement).....	119
5.3.6. The bending property in dynamic simulations.....	123
5.3.6.1. Suitability of standard measurements for dynamic simulations.....	124
5.3.6.2. Linear approach to the nonlinear bending behavior.....	125
5.3.6.3. Simulation experiments.....	125
5.3.6.4. Bending hysteresis.....	127
5.3.6.5. Bending in shear direction.....	127
5.3.7. Conclusion for the tensile, shear and bending parameter.....	128
5.4. Accuracy of the viscosity parameters for tensile, shear and bending.....	129
5.4.1. Viscosity in the applied simulation system.....	130
5.4.2. Existing approaches to acquire fabric damping parameters.....	130
5.4.3. New approaches.....	130
5.4.3.1. Measurements at high frequency and creep tests.....	130
5.4.3.2. Elastic potential.....	133
5.4.3.3. New viscosity parameters.....	135
5.4.4. Air Viscosity (Flowing/Damping).....	136

5.4.5.	Conclusion for the viscosity parameter.....	136
5.5.	Friction.....	137
5.5.1.	Friction measurement .....	137
5.5.2.	Friction in simulation applications .....	139
5.5.3.	Static and dynamic friction .....	138
5.5.4.	Friction in warp and weft fabric direction.....	139
5.5.5.	Friction on the front and on the back fabric sides.....	139
5.5.6.	New friction experiment .....	140
5.6.	New fabric measurement specifications.....	143
5.6.1.	Suitable measurements for static simulations.....	143
5.6.2.	Suitable measurements for dynamic simulations.....	143
<b>6.</b>	<b>Chapter: Validation.....</b>	<b>147</b>
6.1.	Experiment description.....	147
6.2.	Comparison of real and virtual garment prototyping processes.....	148
6.2.1.	Real and virtual mannequin.....	148
6.2.2.	2D pattern.....	148
6.2.3.	Real and virtual dresses.....	149
6.2.4.	Comparison real and virtual comfort performance (static simulation).....	150
6.2.5.	Comparison real and virtual utility performance (dynamic simulation)....	155
6.2.6.	Summary of impreciseness and related error sources .....	160
6.3.	Experiments with the new derived parameters for other applications.....	161
6.3.1.	Accurate simulation for robotic driven sewing processes.....	161
<b>7.</b>	<b>Chapter: Conclusion.....</b>	<b>163</b>
7.1.	Contributions.....	163
7.2.	Limitations and future research.....	165
7.2.1.	Rheology aspects.....	165
7.2.2.	Automation of parameter derivation processes.....	165
7.2.3.	Accuracy of body deformations in dynamic simulations.....	165
7.2.4.	Quantification and exploitation on numerical fitting data.....	165
7.2.5.	Parameters for extreme wearing situations.....	165
7.2.6.	Fabric performance.....	166
7.2.7.	Simulation of additional fabric characteristics.....	166
7.2.8.	Fabric Appearance.....	166
	Bibliography.....	167
	Publications resulting from this research.....	176
	Other publications.....	176

<b>Annex</b> .....	177
Annex A: Technical terms.....	177
Annex B: Fabric selection.....	181
Annex C: 16 KES-f characteristic fabric hand values.....	183
Annex D: Elasticity force-deformation envelopes.....	189
Annex E: Alternative friction tests.....	226
Annex F: Parameter derivation example fabric 11_flannel.....	227
Annex G: Derived fabric parameters.....	231
Annex H: Simulation settings.....	241
Annex I: Remarks.....	243
Annex J: List of Figures.....	244
Annex K: List of Tables.....	249



# Chapter 1

## Introduction

### 1.1. Importance and Background

*“The manufacture of clothing in particular needs to change to more technologically advanced forms of manufacturing in the future. No doubt many of us have our eyes on this area as the candidate for development into the new century.” [Stylios 04]*

In open markets, each sector of industry faces challenges due to competition and is therefore subject to constant change. For some time now, the European textile and clothing industry has been facing one particularly large challenge; that of cheap textile imports. Choices made on how to deal with this will be decisive for the future of the industry. In the last two decades, low-wage countries such as China have begun to flood the European market with cheap products which has severely damaged the European clothing and textile industry. Since 1990, the industry has registered a significant drop in the production index and in some instances, as much as 50% [Guercini 04] [Adler 04] [Jones 04].

In the past, countries used to protect their own markets with the help of trade laws. However, with the globalization movement, governments are agreeing on the removal of trading quotas and it is becoming more and more difficult to protect national industries. As a result of opening trade, and loosening protection laws, a first major loss of market shares for the European textile and clothing industry came after the loosening of the “multi-fiber agreement” in the early 1990’s. In 2005, difficulties increased with the World Trade Organization and the "Agreement on Textiles and Clothing", an accord on the abolition of trading quotas. This caused a further increase in the import of cheap textile goods. In addition to the abolition of trading quotas, and after the entrance of China into the World Trade Organization at the beginning of 2002, the European Union was forced to guarantee the liberalization for China as well [Taplin 04]. Until 2008 the provision of “Temporary Textile Safeguard” is in effect, however after 2008 there will be no renewal and the markets are completely open.

The European textile industry has been seeking methods to enable it to compete with cheap production places and to recapture market share on an organizational level. Various re-engineering methods, for example “just in time” and quick response techniques, paired with the systematic use of teamwork and multi-tasking, improved productivity and quality. The Spanish

company ZARA can be seen as an example of a highly optimized organization with a fast-response global supply production and retail network. ZARA has managed to become a benchmark for speed and flexibility in the garment industry [Dew 03].

Enterprises also have been trying to counter the structural changes in the textile industry with technological innovations, such as new CAD/CAM solutions. Since organizational changes are limited, technological innovations complement the optimization process. The improvement potential of technological innovations is virtually infinite. Lately, companies also invested in new PDM (product development management) and PLM (product lifecycle management) technologies, specialized for the clothing and textile industry, which uses technology to optimize organizational aspects of the production pipeline with better communication and connection of single areas [Runtime], [Matrix].

Despite these efforts, the European apparel industry is still struggling and existing solutions are not sufficient for a reinforcement of the industry. Hence, more sustainable solutions are needed on a high technological level as the potential of technological innovations is infinite. Besides, for technologically high-quality production processes, skilled labor is needed. As long as clothing manufacture continues to be an industry with a low level of technical innovation and minimal capital requirements, the barriers to entry will remain low for cheap manufacturers who, using cheap labor and jobs, will migrate to those countries [Taplin 04]. This trend can only be stopped with the creation of working places on a high technological level.

## 1.2. Innovation potential

The entire clothing and textile industry can be divided in three main fields (Figure 1):

- Fibers and yarns
- Textiles and finishing treatments
- Garment manufacturing

The potential for technological innovation in each of the three areas is different. Fibers and yarns is the most automated and high tech area, producing nanofibers and nanocoating, followed by the field of textiles and finishing treatments with new developments in nano and smart textiles. Innovation examples include 3D simulation technology for the simulation of new fiber assemblies [Roberts 04], shape memory materials (according to temperature), phase change materials (heat storage), chromatic materials (changes the color according to the environment) and wearables. The smart textile market is expected to grow exponentially, particularly in developed countries, from \$370 million in 2006 to over \$1 billion by the year 2010 [Wiwo 08]. The area with the lowest technological level is the field of garment manufacturing. This means on the other side that this area can be seen as the one with the largest innovation potential in the near future.



**Figure 1: Different branches of the clothing and textile industry [Mango], [Fibers], (Miralab – University of Geneva)**

This research contributes to the third area, the field of garment manufacturing, where revolutionary simulation systems will be the key-technologies in the coming years. Thus, this work has to be seen as one small step towards an automated high-tech, product development chain.

### 1.3. Problem statement

Garment manufacturing processes are still executed in a very traditional way. Important tasks such as prototyping and garment fitting are time consuming and costly handwork. For some time now impressive simulation technology have been available, which allow the creation of virtual garments that look incredibly realistic (Figure 2) [Browzwear], [Optitex], [ClothReyes], [ClothFX]. These new developments promise to revolutionize old fashioned manufacturing processes, with high tech solutions. Using these technologies, a completely virtual garment may be developed on a computer, using realistic 3D representations for prototyping and fitting. The implementation of these new technologies would push the garment development process to a higher technological level and save both time and money.





**Figure 2: Four examples of realistic virtual garments (Miralab – University of Geneva)**

But although today new 3D simulation technology for garments and textiles exists, these new applications have not been adopted by the apparel industry. The reason for this fact is often explained by the reserve of the traditional apparel industry towards new technologies.

However, even if this does apply to some companies, recent economic pressure forces all of them to be open to any kind of innovation. After all, fashion companies have recognized the potential of new technologies and most of them incorporated CAD/CAM and PDM/PLM technologies into their production processes (also see Annex 1: technical terms). Hence, this implies that the reason for the non-acceptance of promising simulation technologies has to be found within the new technology itself and not the reserve of the traditional apparel industry. Upon closer inspection it becomes clear that further research is necessary.

Garment prototyping and fitting are complex processes, where the garments comfort with its multiple aspects is proved. Most important aspects are the interaction between body and garment (garment fit), physiological comfortability, or the overall visual appearance of the garment according to aesthetic rules, tendencies and trends. Influencing factors for these aspects can be seen in the dimension of the garments 2D patterns and also in the fabric quality used. Today, 2D patterns can be easily and precisely handled by CAD/CAM and 3D simulation systems. The simulation of specific fabric qualities, determined by their physical properties is, on the other hand, a much more difficult task.

Fabrics are complex mechanical systems. Experimental values for the main mechanical and physical fabric properties, necessary for the virtual recreation of a textile, can be derived from standard fabric characterization experiments. It is widely believed that the integration of mechanical and physical fabric parameters into the virtual simulation systems is an easy task and almost automatic, as we are able to measure some of the fabric properties. But this is far from true. Existing fabric characterization experiments have not been designed for use in virtual simulations, but to distinguish fabrics from one another for their different usages. To which

extend these measurement methods are suitable to obtain data for virtual simulations and if this data is precise enough, we do not know today as any detailed study is lacking.

On the other hand, the clothing industry calls for a virtual simulation tool that not only satisfies the human eye with a realistic representation of the garment, but also mimics precisely the real physical and mechanical behavior of fabrics so as to be able to truly judge a new garment design on the basis of a virtually calculated cloth. Precise material properties play a very important role, since only they can guarantee the technical and aesthetical "feasibility" of a new garment. Only an accurate virtual prototype could replace the real thing and provide sufficient information. Thus, for as long as the mechanical and physical properties can not be accurately reproduced virtually, simulation tools will not meet the expectations for replacing precise manufacturing processes and will therefore not be integrated into manufacturing processes.

## 1.4. Motivating applications

A study of the accuracy of fabric properties would push the virtual simulation of clothing further, so that important manufacturing processes could be replaced by those tools and brought to a higher technological level. This also would accomplish a big step towards the goal of the automation of manufacturing processes, similar to other fields of production. The implementation of this new technology would accelerate, improve and rationalize processes and save high development costs, which are the most crucial factors for the apparel industry. New garment products would also be marketed more successfully, since less rejects would be produced.

Miralab (Prof. Nadia Magnenat-Thalmann) has defined and led the fundamental research project HAPTEX [Haptex 07]. In the framework of which this research has been done (HAPTEX) the goal is to integrate a visual representation of virtual textiles with a haptic/tactile interface, thus allowing the user to have the sensation of feeling the virtual garment. In this thesis, we have worked on the precise measurements and analysis of the physical parameters of fabrics.

We also have been partly working for the project Leapfrog [Leapfrog 08].

### 1.4.1. Garment prototyping and fitting

Accurate virtual simulations would have most impact in the field of garment prototyping and fitting as present day procedures are the most time consuming and costly processes in the manufacturing chain, because each sample model is a product made to specification. Improvements therefore would be multi-fold:

- Precise numerical fitting data

During fitting, designers and modelists are optimizing the fit and cut of the sample model with their expert knowledge. Depending on the complexity of a garment design, up to 5 prototypes are necessary for a final garment product [Hohenstein]. If the virtual tools are proved to be precise, important fitting processes can be replaced by calculated replicas of a new garment design. In doing so, the designers and modelists would have the possibility to not only rely on their experience, but also on exact numerical fitting data, returned by the simulation system (Figure 3). The garment prototype becomes more “transparent”, regarding its interaction with the body. Misfits can be better and more quickly identified and fewer sample models are necessary.



**Figure 3: Virtual prototyping of men suits visualizing numerical fitting data (Miralab-University of Geneva), real men suits [Zegna]**

An increasing development of highly specialized fabric materials also requires an up-to-date fitting method, to guarantee an optimal exploitation of their potential. For example in active sportswear, high tech compression garments have been developed, for an optimized muscle performance. Those characteristics are most accurately measurable with virtual tools. Real fitting processes will always be subjective as it is difficult for a real person to tell how much pressure a garment puts on her body and it is not possible to tell by how much a fabric is elongated.

- Immediate feedback

A time consuming part of real fitting processes is the transfer of the performed modifications from a garment prototype back to the 2D pattern and to sew a new sample model. Therefore, designers and modelists still work with artisan tools such as scissors, pins and crayons. In precise virtual applications, designers and modelists would be able to correct misfits on the flat digital 2D pattern and immediately see the corresponding 3D output with no temporal delay. This resulting acceleration of garment fitting and thus, gain of time, would allow designers and modelists to execute many more correction possibilities for one prototype without the additional cost of a new sample model.

- Fitting of multiple sizes

As their production is expensive, garment prototypes are generally produced in only one size, the base size. However, in the majority of cases the biggest and smallest garment sizes, which are constructed out of the base size by grading rules, cause the most difficulties, as those people's body proportions are much more complicated to grasp. Hence, it would be an important element of quality control to fit those sizes on corresponding mannequins as well. Virtual fitting mannequins can be easily created in any possible body dimension and new simulation technologies allow the switch between different garments sizes, once created. Thus, the virtual application permits the fitting process in all available garment sizes with negligible extra work. The production of clothes in all possible sizes can therefore be highly optimized.

- Fitting in motion

Traditional fittings are generally performed on simple comfortability movements of the mannequin. However, to guarantee a high quality of clothes it becomes increasingly important, to assure a garment's comfort also for special exercises (work clothes, sports clothes, etc.). To assess garments for that purpose, garment prototypes are often given for trials to professionals and their feedback is taken into consideration. However, virtual fitting mannequins can be animated with any kind of expert motion, thanks to motion capture technology. Precise virtual fitting processes are then able to accurately visualize the garment comfort during any kind of movement, returning exact fitting data for each position (Figure 4).



**Figure 4: Numerical fitting data while running in Weft-direction, Warp direction (Miralab-University of Geneva)**

- Sampling of multiple fabric materials

If a fabric material is detected to be unsuitable for a garment, a different fabric material can be selected with one mouse-click, without the necessity to sew a new prototype.

- Protection of resources

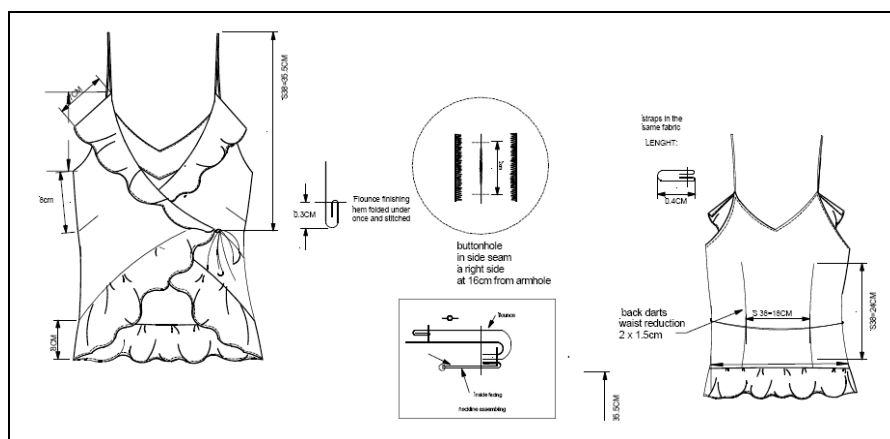
Moreover virtual garment prototypes are “produced” with no raw material waste and resources would be conserved.

### 1.4.2. Garment design

Precise virtual simulation tools, once implemented in the garment production chain, would have not only an impact on prototyping and fitting processes, even if this is the field, where accuracy is inevitable. Also other fields could be improved with this new technology. The design of new garments is mostly done in the form of technical sketches. There are some new design tools on the market, which enable the simulation of new silhouettes and test of color combinations [Browzwear], [Optitex]. However, only accurate simulated fabric characteristics would help the designer to really judge a new design, for the look and its feasibility. Hence, fewer corrections would be necessary later on and the creation of real sample models could be limited.

### 1.4.3. Garment manufacturing

Today, information for the manufacturing of new garment designs is communicated on a low technological level, the specification sheet, accompanied by technical sketches (Figure 5).



**Figure 5: Low technological sketches and garment description (Miralab-University of Geneva)**

Within this part of the production chain, an accurately calculated garment prototype could be used as an accompanying visual language, to communicate data on a higher technological level (Figure 6). The virtual garment sample could be sent to overseas producers, crossing both linguistic and geographic barriers.



**Figure 6: Corresponding virtual 3D garment, used as visual language (Miralab-University of Geneva)**

Today, the garment sewing is still done by people using sewing machines. However, to be able to compete with cheap producers, automatic robotic driven manufacturing processes are a long term goal for the European apparel industry. First attempts are conducted [Leapfrog 08], where robots partly sew together a garment. Therefore, an accurately simulated garment prototype is necessary as a “sewing reference”, for the adjustment of robots. Additionally, mechanical and physical fabric characteristics are important for the calibration of automatic sewing machines, to anticipate the fabric compartment during sewing. If implemented, virtual garment prototypes could be directly sent to production centers to deliver this kind of input data.

#### 1.4.4. Marketing and the e-commerce

To present new garment collections to the retail industry, fashion companies are obliged to produce several expensive sample collections, so that each store can assemble his assortment. If implemented, final virtual garment prototypes could be used for the representation of new garment collections, with the advantage that they could be endlessly cloned and send by e-mail. Garment stores, offering “made to measure” clothing, such as for example men suits, could use virtual prototypes for the representation of all available fabric qualities in all available colors, so that the customer can better visualize the final product (Figure 7).



**Figure 7: Virtual try on of men suits in various colors (Miralab-University of Geneva)**

In addition, virtual garment collections could be used for marketing purposes, with inherent savings on expensive catalogues and brochures. The virtual collections could also be placed on the company’s web-site for information and e-commerce applications.

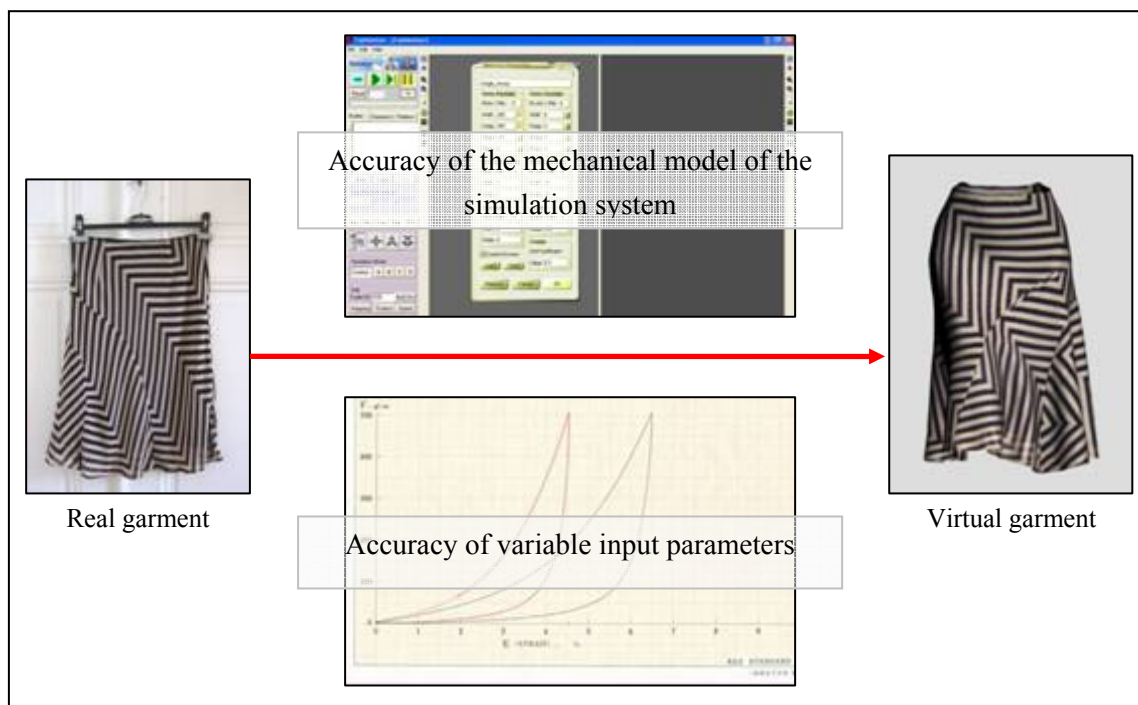
#### 1.5. Objectives of new research

There are two main critical aspects, with regard to the accuracy of fabric properties in virtual cloth simulations (Figure 8):

- (1) The accuracy of the implemented mechanical model of the simulation system.
- (2) The precision of variable input parameters for the simulation system.

The research on mechanical models for cloth simulations is an important field of research since a long time. Former cloth simulation models strongly simplified the complex fabric behavior and accurate fabric parameters were not needed. Until today the algorithms were optimized to such a level, that accurate simulations finally became possible. [Terz 87], [Lafleur 91], [Collier 91], [Yang 91], [Carignan 92], [Baraff 98], [Volino 00], [Metzger 03], [Keckeisen 04], [Volino 05], [Volino 06].

But, as accurate input parameter did not play a very important role in the past, this field constitutes the least investigated today. More precisely, the precision of mechanical and physical fabric properties which describe the behavior of virtual textiles and their correct “copying” to the simulation system constitute the main field of this research.



**Figure 8: Two aspects of accuracy in virtual simulations**

Other input parameters, beside the physical and mechanical parameters, comprise surface parameters and simulation settings.

### 1.5.1. Most important input parameters

First of all the most important parameters, responsible for an accurate simulation, need to be identified. This is an important knowledge, for the fine tuning of existing measurement methods, parameters and simulation settings.

Accuracy and speed are the two crucial and complementary aspects for the competitiveness of virtual systems. Linear derived fabric characteristics generally use less computation power than complex and precise interpreted nonlinear fabric parameters, which are far more challenging calculations. However, if a virtual cloth would not be precise enough, it could not be used as a prototype for fitting. But on the other hand, if the virtual simulation of the sample model would need more time than its real production, the advantages of virtual tools would not be convincing. Thus, the overall goal in virtual simulation is to accurately simulate a garment in a reasonable time. If the influence of one mechanical parameter is found to be less important in terms of its accuracy, a compromise between precision and calculation time needs to be found. Better knowledge about the importance of single fabric parameters therefore also allows a more precise optimization of the implemented mechanical model of the simulation system.

### 1.5.2. Right values for each parameter

In the second step, the right value for each input parameter and in particular for mechanical and physical parameters needs to be found. An in-depth analysis of real dynamic fabric behavior will give better knowledge of how fabrics should be tested, to adapt the fabric characterization methods to demands in virtual simulations and thus, to bring them to a higher level. A deeper examination of measured data, should allow a more accurate mapping of the fabric properties in the virtual simulation system. Based on this knowledge, new measurement evaluations and specifications will be proposed. Other input parameters, such as simulation settings and surface parameters are studied and refined in accordance with the new derived mechanical fabric parameters.

## 1.6. Summary

The implementation of new simulations technologies would accelerate, improve and rationalize processes and save high development costs, which are the most crucial factors for the apparel industry. Furthermore, an increasing development of highly specialized fabric materials requires an up-to-date fitting method, to guarantee an optimal exploitation of their potential such as compression garments or smart textiles. Finally, the accurately virtual simulated garment prototypes can be exploited for new robotic driven sewing processes, an important task for the automation of processes.

But as long as the mechanical and physical properties can not be accurately reproduced virtually, simulation tools will not meet the expectations for replacing precise manufacturing processes and will therefore not be integrated into manufacturing processes.



The main research questions can be summarized as following:

- (1) Existing fabric characterization methods have not been designed for use in virtual simulations, but to distinguish fabrics from one another for their different usages. To which extend existing measurement methods are suitable to obtain data for virtual simulations and if this data is precise enough for the derivation of accurate fabric parameters we do not know.
- (2) An increasing development of highly specialized fabric materials requires an up-to-date fitting method, in order to guarantee an optimal exploitation of their potential. Those characteristics can most accurately be measurable with virtual tools. However, if the number of measured properties from standard characterization methods is sufficient for an optimal exploitation of the potential of virtual simulation systems is not assessed until today.
- (3) To be able to compete with cheap producers, automatic robotic driven manufacturing processes are an important long term goal for the European apparel industry. Therefore, accurately simulated garment prototypes and accurate fabric parameters are needed for the robot adjustment and the calibration of automatic sewing machines. Thus, the suitability of standard fabric measurements should not only to be tested for known processes such as prototyping and fitting, but also meet the requirements of new high-tech manufacturing processes.

## 1.7. Organization

This document proceeds as follows:

In the next chapter, the fundamental research and the state of art of fabric characterization experiments is explained. Standard and other existing measurement methods are outlined. Following their exploitation in virtual simulations systems is described. Chapter three discusses first the open questions regarding fabric characterization methods and input parameter for virtual simulations, followed by the description and discussion of the applied methodology.

In Chapter four, the data acquisition for the subsequent study is explained, from the fabric selection to the derivation of first mechanical properties. Chapter five discusses the applied scheme of accuracy, which is based on real tailoring processes. In addition, fabric properties are classified with regard to their importance for accurate garment simulations. In Chapter six, the precision of the important fabric properties is tested. Existing test methods are examined and for some properties, new measurements are proposed. Chapter seven illustrates the validation of the newly derived fabric parameters on an actual garment fitting example, which directly compares the real and the virtual process. Chapter eight first discusses the limitations of this work, followed by a conclusion and an outlook for future studies.

# Chapter 2

## Previous and related work

### 2.1. Introduction

*“Even very simple systems can not be completely replicated with scientific methods, as it would be impossible to know the coordinates of all particle elements, at each time, their temperature, their movement and transformations. In scientific approaches, people are dependant on conceptual models, to reduce problems and questions to the essential.” [Romberg 04]*

Mechanical models approach reality by considering forces and impulses. Other influencing factors, necessary for a 100% identical imitation, are neglected. Mechanical models for virtual garment simulations represent the environment in which a virtual cloth is reproduced. At this the number of possibilities for different materials is infinite. On the other hand, to be able to simulate one specific fabric material, the precise virtual imitation of its real mechanical and physical characteristics is indispensable.

Regarding mechanics, fabrics are complex viscoelastic materials. Generally, materials can be divided into three main different types: solids, fluids and gases. A solid material, subjected to stress, recovers its original state as soon as the stress is removed. In contrast, if a fluid material is subjected to stress it flows and only gradually comes to rest when the force is removed. Materials such as textiles, which show characteristics of both, liquids and solids, are called viscoelastic materials [Ask 05]. Their simulation is not easy, as their behavior is difficult to describe and predict. Fabrics must have sufficient strength and at the same time they have to be flexible, elastic and easy to pleat and shape. The knowledge of the viscoelastic behavior of a material is based on empirical data from characterization experiments.

For fabrics, the research on mechanical properties has been driven for many decades by the need of a generalized, objectively measurable quality assessment. Therefore, important properties have been identified and their correlation has been studied. Investigations resulted in standardized fabric characterization experiments. Lately this research has been exploited for virtual simulations of textiles, because from the measured data, important input parameters for virtual simulations can be derived.

## 2.2. Existing fabric characterization methods

The oldest known textiles (wool and cotton) date back to around 7,000 years ago and appeared with the invention of proficiencies such as spinning and weaving. In comparison to fabrics based on natural fibers, synthetic fibers are a relatively recent achievement. Only at the beginning of the 20th century were the first full chemical fibers, the so-called “Synthetics”, invented [Loschek 94]. Over the millennia the variety of textile materials increased continuously. Fabrics for different activities, climates or tendencies and trends have been developed to guarantee an optimal comfort of garments. With the development of new fibers (synthetics) and the continuous enhancement of new material structures, the variety of different fabric materials has become immense over the years and is still increasing (smart textiles). However, the development of such a variety of new fabric materials has led to an increasing difficulty in evaluating fabrics according their quality and suitability.

Each textile possesses specific characteristics, which are advantageous for some types of garments, but can be unfavorable for others, regarding comfort. Fabric characteristics are primarily influenced by the textiles raw material, yarn structures (degree of twist), planar structure (weave, knit) and finishing treatment (Figure 9). They can be either of physiological or aesthetical importance [FAST 95]. For example synthetic fibers are easy to care for and keep their shape well, but do not conduct humidity well and lead easily to sweat.

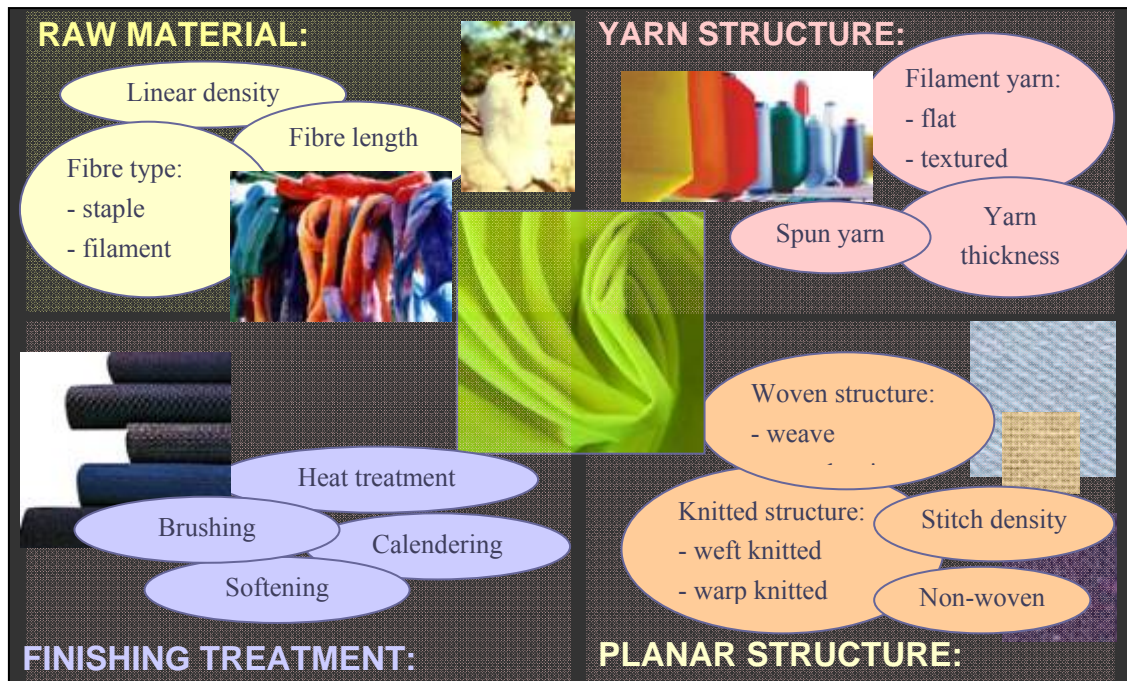


Figure 9: Scheme on influencing factors [Mae 05]

Aesthetical properties are the ones which are more subjective, complex and more difficult to grasp, for example firmness/smoothness, resistance to wrinkling or pilling resistance. The wrinkling of linen fabrics is a typical aesthetic fiber characteristic. The use of unsuitable or inferior fabrics is often the fundamental aspect that determines the success or failure of a textile product [Mae 05]. Also the increasing automation of apparel manufacturing processes demands a more precise control of fabric characteristics [Zhou 98]. Thus, it became more and more important to judge textiles before any production process.

The concept of “fabric hand” was an important method of fabric assessment which was introduced by the apparel and textile industry. The term “fabric handle” or simply “handle” or “hand” is also used. Fabric hand refers to the total sensation, experienced when a fabric is touched or manipulated in the fingers. The attractiveness of a fabric’s handle depends on its end use, as well as on possible cultural and individual preferences of the wearer [FAST 95]. Fabric hand attributes can be obtained through subjective assessment or objective measurement.

### 2.2.1. Subjective fabric hand assessment

Subjective assessment is the traditional method of describing fabric handle. Textiles are touched, squeezed, rubbed or otherwise handled by experts to judge their hand (Figure 10). The subjective assessment may thus be defined as a psychological reaction to the sense of touch [Mae 05]. Disadvantages of the subjective hand assessment are on the one hand the varying sensitivity of people according to age, gender, skin hydration or cultural backgrounds in a tested population and on the other hand the difficulty of finding common standard expressions for specific hand sensations. Therefore, the organization AATCC (American Association of Textile Chemist and Colorists) has published guidelines for the generalization of the conditions during subjective hand evaluation [AATCC 02].

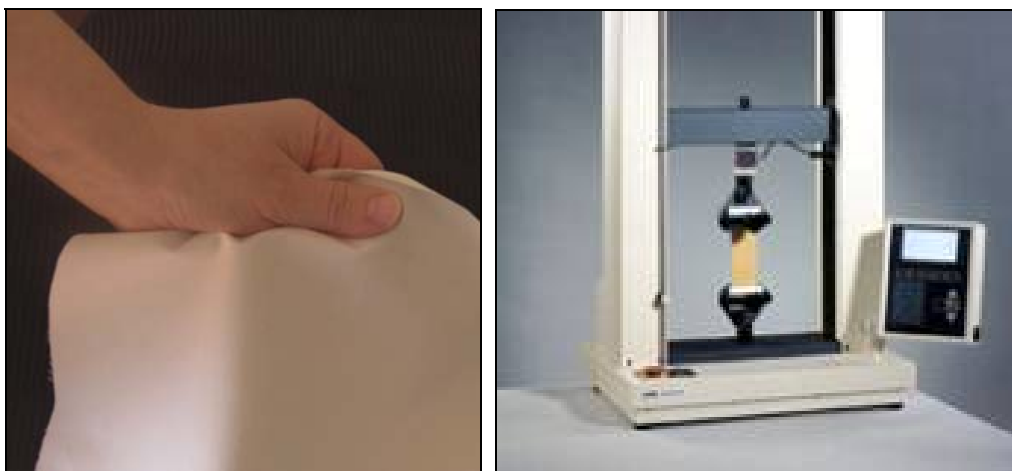


Figure 10: Subjective fabric assessment, Objective measurement device [Instron 06]

## 2.2.2. Objective hand measurements

Researchers have recognized the need to devise physical tests that analyze and reflect the sensation felt during subjective assessment and to describe the sensation of touching by a numerical value [Peirce 30]. Resulting objective assessments improved and standardized the communication on the abstract hand expressions and removed some of the “felt” subjectivity [FAST 95]. During objective assessment, the fabric characteristics are measured with instruments and one “hand” value is calculated by relating the instrumental data. Important physical and mechanical properties are flexibility, compressibility, elasticity, resilience, density, surface contour (roughness, smoothness), surface friction and thermal character. These characteristics are the result of a broad fundamental research on fabric properties. Important standard measurement devices consist in the “Kawabata Evaluation System for Fabrics” (KES-f) and the “Fabric Assurance by Simple Testing” (FAST) method.

### 2.2.2.1. Fundamental research

The first research on fabric mechanical properties dates back to Peirce in 1930, who can be seen as the pioneer in that field. In his first studies, he described a way of linking fabric properties in order to predict their behavior. However, until the 1980’s, when Kawabata conducted his study on the standardization of objective hand assessment, neither a generally accepted definition of hand, nor an accepted definition of its components existed. Until then, the fundamental research on mechanical fabric properties was driven by three main questions:

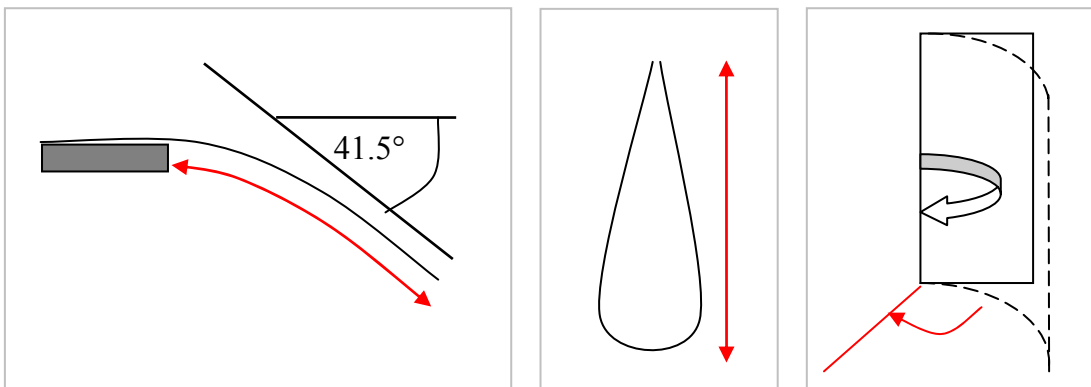
- (1) What are important fabric hand characteristics?
- (2) How to measure them?
- (3) By what are they influenced and how are they related to each other?

#### (1) What are important fabric hand characteristics?

The importance of fabric properties varied over time, depending on needs in manufacturing and the state of the art of fabric materials. On the one hand, until the 1960’s, very little attention was given to the elasticity of fabrics. On the other hand, fabrics containing elastane did only exist from 1962 on, following the invention of synthetic materials [Lycra]. In the beginning of the fundamental research the focus was on the stiffness parameter (or bending, flexibility). In comparison to other characteristics, stiffness was an important tailoring and drape aspect and also probably the property, which was the most difficult to understand. Also Peirce considered stiffness properties, such as bending length and flexural rigidity, as the most important properties regarding hand [Peirce 30]. After 1960, researchers also focused more on fabric buckling and shear properties. Other fabric hand properties such as compressibility, friction or the surface contour were easier to grasp and describe and thus, their investigation seemed to be less important.

(2) How to measure them?

Researcher thought of different experiments for the measurement of each single fabric property. Tensile measurements are designed to return the fabric elongation for a corresponding force. Bending measurements can be classified in two main categories. The first group measures the bending deformation of a fabric under its own weight. Within this category, Peirce developed several stiffness testing methods. The most important one was the Cantilever method, which uses the engineering principles of beam theory. A fabric is moved forward to project as a cantilever from a horizontal platform. As soon as the leading edge of the fabric reaches an angle of  $41.5^\circ$  to the horizontal platform, the bending length is measured. The principle of this method is used in the FAST method (see 2.2.2.3.). Apart from the Cantilever method, folded loop methods have been invented, where the fabric is fold back on itself and the height of the loop measured.



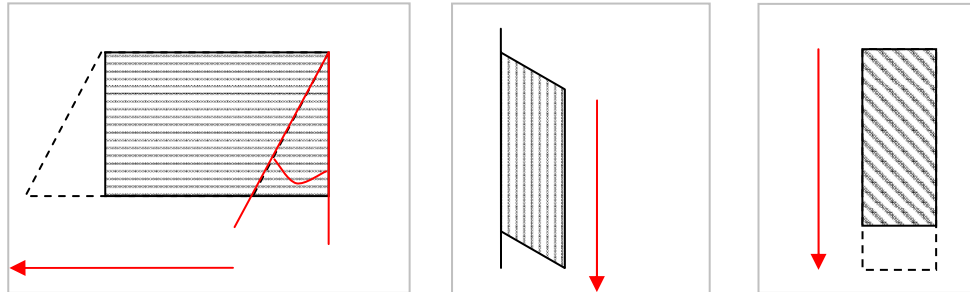
**Figure 11: Group 1: Cantilever principle (left) and loop method (middle), Group 2: moment – curvature method (right)**

The second group of bending measurements is designed to return the moment-curvature relationship by measuring forces or moments. In 1957, [Isshi 57] developed the predecessor of Kawabata's bending testing apparatus (also see 2.2.2.2.), which is based on that principle. A fabric is fixed between two clamps and the specimen is bent in an arc of constant curvature and the curvature changes continuously. The curvature is returned by a pointer, which is fixed on the moving clamp.

In 1951, Abbott compared five different objective stiffness measurement devices with subjective assessment: Cantilever (Peirce), Heart loop (Peirce), Schiefer Flexometer, Planoflex, and Drapometer. Results indicated a significant correlation in four of the five methods. Peirce Cantilever was detected to return the closest results to subjective stiffness tests [Abbott 51].

In 1961, Behre, Lindberg and Dahlberg conducted an important three-fold study on the relationship of fabric shear, buckling properties and garment appearance. This research contributed a lot to today's standard measurement methods, even their analysis was simplified by treating fabrics as thin plates and assuming isotropic behavior. Behre in 1961 proposed two alternative methods for measuring shear properties. He analyzed the stress distribution in a fabric sample, subjected to shear and used the results to construct a shear tester for routine

testing. He described the relation of shear to the extension-compression in the bias direction of a woven fabric, as well as that a sample subjected to shear can be regarded as a cantilever, where the height is much larger than the width. For his shearing experiments, the measurements have been taken at a maximum force and the angle is measured (opposite to KES-f, see 2.2.2.2.).



**Figure 12: Angle force method (left), Shear seen as Cantilever (middle), Shear in 45° (right)**

(3) By what are they influenced and how are they related to each other?

During measurement, each fabric property is treated independently, whereas in reality all fabric characteristics are somehow related. Thus, measurements allow the characterization of single properties, but to really understand the behavior of an entire fabric it is important to know the mutual influences of the single properties to each other.

[Cooper 60] tried to derive the fabric stiffness property from fiber stiffness properties in studying their complex relationship. His studies revealed that regarding fabric stiffness, it is important whether the fiber inside the yarn or the yarn inside the fabric can move freely. The free fiber movement is basically inhibited by the fabric structures or finishing. For fabrics with a tight structure, the stiffness increases towards that of a solid sheet of material, which state is however never reached in practice. Weave differences are also important, especially the floats/satin, as with floats the fabric is looser.

[Livesey 64] later stated that the correlation of inter-fiber friction and fiber movement is the major cause of the nonlinear bending behavior.

In 1966 Grosberg also conducted research on the nonlinear behavior of bending. He found out that due to the frictional restraints, the fabric bending behavior is initially indeed nonlinear, but that with increased loads, the behavior becomes linear. He showed that the Cantilever is suited for a rapid measurement of the parameters of cloth with small frictional restraint, while the buckling method is more suitable for rapid measurement of cloth with large frictional restraints.

[Grosberg 66]

In the third part of their study, Lindberg and Dahlberg demonstrated that there is a linear relationship between bending stiffness and the buckling load and that there is also a relationship between the formability in the bias direction and the shear angle of a fabric (the highest formability of a fabric is generally in the bias direction). However, they found that there was no relationship between bending stiffness and shear angle. They invented the drawing of “fabric maps”, considering bending stiffness and shear angle. The character of a material depends on its position on the map. FAST later uses a similar concept for their fabric “fingerprints”. [Behre 61] [Dahlberg 61] [Lindberg 61]

In 1961, Cusick discovered the relationship between complex bending and the shear property. Cusick was better known for his studies on fabric drape. However, shear is an important influencing property on fabric drape. Cusick stated that because of the low flexural rigidity of fabrics (compared to other materials), a woven fabric may be bent into single curvature without any shear deformation, but if a fabric is bent into double curvature or more complex curvature, then shearing occurs. For his studies, he performed a series of experiments, where the fabric is sheared for two cycles in reversed directions until the fabric is observed to start to buckle. Later Kawabata adopted this method, but standardized it to a maximum shear angle of 8°. [Cusick 61], [Cusick 65], [Cusick 68]

[Peirce 37] also was the pioneer for the prediction of fabric properties with statistical methods, in order to reduce the number of time consuming characterization experiments. Therefore, he described the fabric structures with mathematical forms and tried to discover quantitative relations between fabric properties of general validity, by assuming simple geometrical forms and idealized characteristics of materials.

In 1985, Ly developed a model for predicting shear buckling that combined the anisotropic characteristics of the fabric with bending stiffness properties. [Ly 85]

Recently, researchers worked on the relation and prediction of fabric handle parameters through the help of so-called “neural fuzzy networks” [Hui 04].

#### 2.2.2.2. Kawabata (KES-f)

In the 1970's, Kawabata conducted research on mechanical fabric properties; however, his main achievement was the concentration of the so far obtained fundamental knowledge on fabric mechanics in one standardized fabric characterization methods. Since, his achievements represent the most wide spread and well-known method for the objective assessment of fabric hand. Until then, fabric hand experts in factories, sales engineers or consumers executed fabric hand assessments subjectively without any common concept or definition of hand, in spite of the importance. [Kaw 80]

Kawabata's standardization study was two-fold. On the one side he organized an expert committee with different people from the apparel industry, who assessed traditionally in total around 1500 different fabric materials. According to the expert team, a “good” hand meant for example that to the touch the fabric is extremely smooth and both, stiffness and fullness/softness are moderate. The main goal of the expert team was to identify the most important hand expressions and to relate these touch sensations to measurable fabric properties. Kawabata then developed a method for relating the measured data in a way, so that 16 characteristic values are calculated, where from a “good” or a “poor” hand feeling is derived (Table 2). This part of Kawabata's studies can be seen as the standardization procedure. [Kaw 80]



KES-f automatic calculated characteristic hand values:

Device	Tested property	Characteristic value	Definition
KES-FB 1	Tensile	LT	Linearity
		WT	Tensile energy
		RT	Resilience
KES-FB 1	Shear	G	Shear rigidity
		2HG	Shear hysteresis at 0.5°
		2HG 5	Shear hysteresis at 5°
KES-FB 2	Bending	B	Bending rigidity
		2HB	Bending hysteresis
KES-FB 3	Compression	LC	Linearity
		WC	Compression energy
		RC	Resilience
		T	Thickness
KES-FB 4	Surface properties	MIU	Mean friction coefficient
		MMD	Mean deviation friction coefficient
		SMD	Mean deviation of surface roughness
Balance	Fabric weight	W	Fabric weight

**Table 1: KES-f calculated characteristic fabric hand values**

Besides his studies on the standardization of objective fabric hand assessment, Kawabata went on with research on measuring mechanical and physical fabric properties. This part of research was driven by the question of how a broad variety of fabrics should be tested in the same way so that the obtained data represents a significant statement about that textile. When a fabric is touched and squeezed during subjective hand assessment, only small forces occur. For example, no fabric would brake during this manipulation. For this reason, Kawabata designed his measurement standard for small deformation regions. In conclusion, Kawabata considered 6 measurement blocks, which were improved in 1980, named KES-FB and reduced to only 4 machine blocks, KES\_FB 1, 2, 3 and 4 [Kaw 80]:

KES-FB 1 = Tensile and shearing test (Figure 13, 14):

Tensile deformation is applied along the length. The specimen size is 5cm length to 20cm width. The strain in the width direction becomes approximately zero because the force is applied to the long sides of a rectangular specimen. This type of deformation is also called “strip biaxial deformation”. After the tensile force attains at  $F_m = 500 \text{ g f/cm}$ , the recovery process is recorded. The tensile and shear tests can be conducted with velocities of either 0.1 or 0.2 mm/sec.

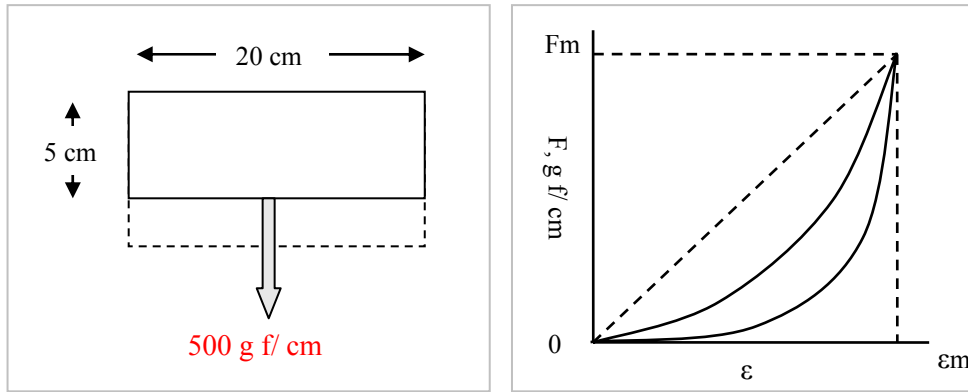


Figure 13: Scheme of measuring tensile, tensile hysteresis envelope [Kaw 80]

Derived characteristic values:

**LT:** Linearity

**WT:** Tensile energy per unit area ( $\text{gf} \cdot \text{cm} / \text{cm}^2$ )

**RT:** Resilience (%), (To which degree the fabric recovers, after the release of the force)

These characteristic values are defined by:

$$LT = WT / WOT$$

$$WT = \int_0^{\varepsilon_m} F(\varepsilon) d\varepsilon \quad (\text{gf} \cdot \text{cm} / \text{cm}^2)$$

$$RT = (WT' / WT) \cdot 100$$

Where:

$WOT = F_m \varepsilon_m / 2$  (area surrounded by dotted line in Figure 13)

$F$ ; Tensile force per unit width. ( $\text{gf} / \text{cm}$ )

$\varepsilon$ ; Tensile strain ( $\varepsilon$  has not % unit but is a dimensionless quantity).

$F_m$  and  $\varepsilon_m$ ; Maximum values of  $F$  and  $\varepsilon$ .

$$W' = \int_0^{\varepsilon_m} F'(\varepsilon) d\varepsilon \quad (\text{recovering energy per energy unit area})$$

$F'$ ; Tensile force in recovering process

In a more recent study of the relaxation phenomena of fabrics containing elastane yarns, a modification of the KES-FB standard from 500  $\text{gf} / \text{cm}$  to 490.5  $\text{N} / \text{m}$  is recommended for fabrics containing elastane, as their relaxation is different from those, without any elastane [Gersak 05].

Shear properties are obtained by shearing the same specimen  $8^\circ$  in one direction, moving it back to the origin and shearing it in the opposite direction until an angle of  $-8^\circ$  is reached. Applied forces are recorded. A constant tension of  $W = 10 \text{ gf} / \text{cm}$  along the orthogonal shearing direction is applied, to overlap initial biaxial tensile and shear forces.

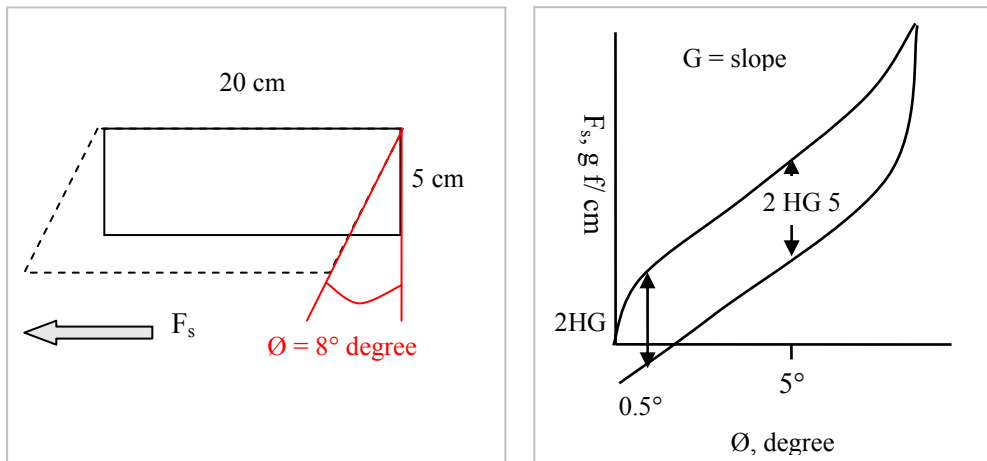


Figure 14: Scheme of measuring shear, shear hysteresis envelope [Kaw 80]

Derived characteristic values:

**G:** Shear rigidity (gf/cm \* degree)

**2 HG:** Hysteresis at shear angle  $\emptyset = 0.5$  degree (gf/cm).

**2 HG5:** Hysteresis at shear angle  $\emptyset = 5$  degree (gf/cm).

G is defined as the (shear force per unit length) \* (shear angle). G can also be defined as the slope of  $F_s - \emptyset$  between  $\emptyset = 0.5^\circ$  and  $5^\circ$ . If the curve is not linear in this region, the mean slope over this region is taken. For fabrics with a non-symmetric weave structure, the curves are different between positive and negative regions. In this case, the measurement of both regions is necessary.

KES-FB 2 = Pure bending test (Figure 15):

Kawabata measures bending with an apparatus that bends the whole sample in an arc of constant curvature, where the curvature is changed continuously. This allows the detection of the relationship between bending momentum and curvature. The bending tester measures the forces to bend the specimen up to  $150^\circ$  followed by the opposite direction. ( $K = -2.5 \text{ cm}^{-1}$  and  $2.5 \text{ cm}^{-1}$ ). Specimen size is 20 cm by 1cm width. The rate of curvature change is  $0.50 \text{ cm}^{-1} / \text{sec}$ .

Derived characteristic values:

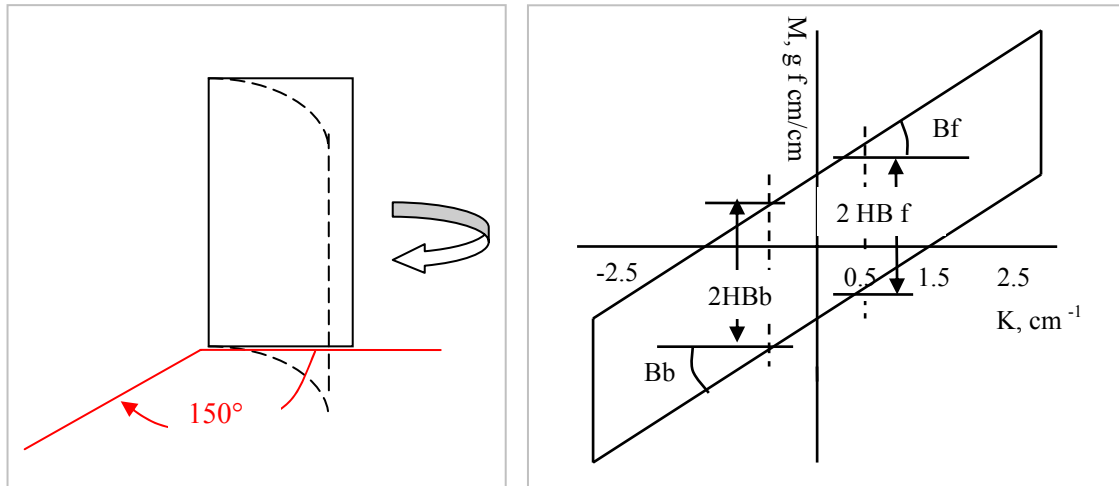
**B:** Bending rigidity per unit length (gfc $\text{m}^2/\text{cm}$ )

**2 HB:** Momentum of hysteresis per unit length (gfc $\text{m}/\text{cm}$ )

Where:

$$B = (B_f + B_b)/2$$

$$2HB = 2 (HB_f + HB_b) / 2$$



**Figure 15: Scheme of bending, bending hysteresis envelope [Kaw 80]**

B is defined by the slope between  $K=0.5$  and  $2.5$  for  $B_f$  and between  $K=-0.5$  and  $-1.5$  for  $B_b$ . Four types of bending are important: Face ( $B_f$ ), Back ( $B_b$ ) in weft and warp.  $2HB$  is taken between  $K=0.5$  and  $1.5$  for  $HB_f$  and between  $K=-0.5$  and  $-1.5$  for  $HB_b$ . For the calculation of the hand value, the mean value of all four is taken.

**KES-FB 3 = Compressional test:**

Compression tests measure the compressibility of a textile as well as physical characteristics such as thickness and weight. Thickness  $T$  in mm is measured with a fixed pressure of  $P = 0.5$   $gf/cm^2$ . Weight  $W$  is expressed as mass density ( $mg/cm^2$ ).

**KES-FB 4 = Surface test:**

Within the surface tests, friction is measured with piano-wire. The piano-wire is used under a constant force of  $10g$  and frequency is  $30$  Hz. The sample size is  $20cm \times 3.5$  cm.

Derived characteristic values:

**MIU** (mean value of the coefficient of friction)  $= \frac{1}{x} \int_0^x \mu dx$

**MMD** (mean deviation of the coefficient of friction)  $= \frac{1}{x} \int_0^x |\mu - \mu'| dx$

**SMD** (mean deviation of surface roughness)  $= \frac{1}{x} \int_0^x |T - T'| dx$

Where:

$\mu$ ; frictional force

$x$ ; displacement of the contactor on the surface of the specimen

$X$ ;  $2$  cm is taken in this standard measurement

$T$ ; Thickness of the specimen at position  $x$ , the thickness is measured by the contactor

$T'$ ; Mean value of  $T$

### 2.2.2.3. FAST

Although Kawabata's objective assessment method is precise from a mechanical point of view, it was not widely adopted by the textile and clothing industry. Many companies still used the subjective evaluation to assess fabric hand. The main reason for this situation was the repetitive and lengthy process of measurements and expensive equipment. In the late 80's CSIRO Division of Wool Technology in Australia realized the importance of a simpler and cheaper alternative to KES-f and developed the FAST -method. The SiroFAST characterization standard resulted in three instruments and one test method, returning 16 measured and calculated characteristic values (Table 3). [FAST 95], [FAST 94]



**Figure 16: SiroFAST bending measurement machine [CSIRO 07]**

#### SiroFAST – 1: Compression meter:

Compression is taken at two loads: 2 g/cm<sup>2</sup> and 100 g/cm<sup>2</sup>. The measurements are taken once and are then repeated after the fabric has been relaxed with steam. Original surface thickness and the released surface thickness are measured and can be used to assess the stability of the finish of the fabric under garment manufacturing conditions such as pressing and steaming.

#### SiroFAST – 2: Bending meter (Figure 16):

This instrument measures the bending length using the cantilever bending principle. From the bending length, the bending rigidity is measured. Bending is measured in three directions, machine, cross and bias (45°) direction.

#### SiroFAST – 3: Extensibility meter:

The Extensibility meter measures the extensibility of a fabric under three different loads (5, 20 and 100 g/cm width). These loads are chosen to simulate the level of deformation that a fabric is likely to undergo during garment manufacture. This device is also used to measure the bias extensibility of the fabric (= shear) under a low load 5 gf/cm. Bias extensibility is not used directly but rather it is used to calculate shear rigidity. In addition, formability parameters can be derived from SiroFAST-3 measurements in conjunction with data from SiroFAST-2.

#### SiroFAST – 4: dimensional stability test:

The dimensional stability test is a procedure for measuring dimensional properties of fabrics such as hygral expansions and relaxations of fabrics (important for wool).

Characteristic values resulting from the FAST measurement:

Device	Tested property	Characteristic value
FAST 1	Measured:	P1 = thickness at 2 gf/cm <sup>2</sup> (T <sub>2</sub> ) in mm P2 = thickness at 100 gf/cm <sup>2</sup> (T <sub>100</sub> ) in mm
	Calculated:	P3 = Surface thickness (ST) ST = T <sub>2</sub> – T <sub>100</sub>
FAST 2	Measured:	P4 = bending length (C) in mm P5 = bending rigidity (B) in μN.m
	Calculated:	B = 9.8 WT C <sup>3</sup> 10 <sup>-6</sup>
FAST 3	Measured:	P6 = elasticity at 5 gf/cm in % (E <sub>5</sub> ) P7 = elasticity at 20 gf/cm in % (E <sub>20</sub> ) P8 = elasticity at 100 gf/cm in % (E <sub>100</sub> ) P9 = elasticity in shear direction in % (EB <sub>5</sub> )
	Calculated:	P10 = shear rigidity (N/m) G = 123/ EB <sub>5</sub>
FAST 4	Measured:	Dimension stability test L <sub>1</sub> : dry dimension L <sub>2</sub> : wet dimension L <sub>3</sub> : final dry dimension
	Calculated:	Relaxation shrinkage Hygral expansion
Balance		Weight in g/m <sup>2</sup> (WT)

**Table 2: FAST calculated characteristic fabric hand values [FAST 95]**

Parameters which describe the resistance to deformation, such as tensile, bending and shear are considered as the most important. Similar to Kawabata, all measurement devices are designed for small deformation regions. FAST -1, 2, 3 test samples must be 10 cm x 5 cm. The force is applied on the smaller side of the specimen. The same samples are used for all of the tests. For Kawabata, new samples are used for each test. About 6-10 different fabrics can be measured in one day. The measuring conditions are the same as for KES-f. The test results are summarized in the FAST control chart, also called fingerprint. [FAST 95], [FAST 94]

#### 2.2.2.4. Comparison of the FAST and KES-f measurement data

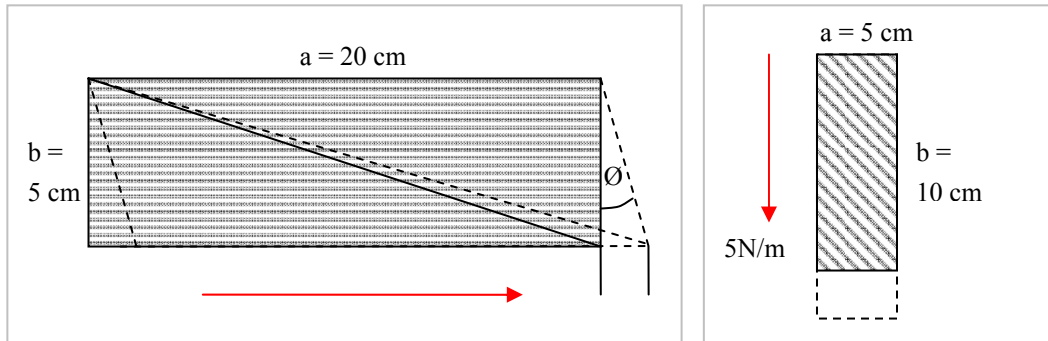
For some properties both methods use different measurement principles. Also the size of the measured sample is different: 5 cm x 10 cm for FAST and 20 cm x 5 cm for KES-f.

- Tensile

A direct comparison of the measured data for the tensile parameter is only possible at 100 gf/cm (max. measured load of FAST).

- Shear

A direct comparison of the shear data from KES-f and FAST is difficult as both standards apply different measurement principles (Figure 57). FAST measures the bias extensibility at 45° with one small load of 5 N/m, whereas KES-f shears the fabric horizontally until an angle of +/-8° degree is reached.



**Figure 17: KES-f shear elongation scheme (left), FAST shear deformation scheme (right)**

Also the characteristic shear rigidity value is calculated differently by both methods:

FAST shear rigidity G:  $P_{10} = \text{shear rigidity (N/m)} \quad G = 123 / EB_5$   
 (Where  $EB_5$  is the elasticity in shear direction in % at 5N/m)

KES-f shear rigidity G: (gf/cm \* degree)

KES-f returns the shear rigidity G as characteristic value. However, the standard value G is different from the definition of shear modulus. If the shear strain is taken instead of the shear angle for defining G, the value is equal to shear modulus [Kaw 80].

$$\text{Shear modulus} = (\text{shear force } F_s \text{ (gf/cm)}) / (\text{shear strain} = \tan \emptyset)$$

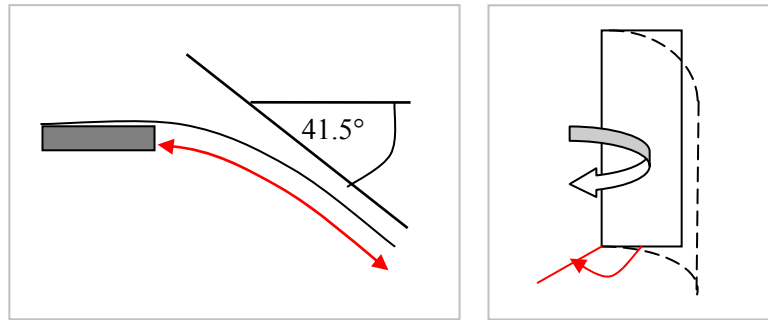
The relation between the two values of G defined by  $\tan \emptyset$  and by  $\emptyset$  degree is:

$$G(\tan \emptyset) = 57.3 G(\emptyset \text{ degree})$$

FAST and KES-f shear measurements relate, similar to the tensile property, forces to elongations. At FAST the force is fixed, whereas during KES-f the elongation is fixed by the maximum shear angle.

- Bending

Different measurement principles are also applied to bending. FAST applies the Cantilever method, which involves pushing a fabric over a vertical edge until it bends to a specified angle 41.5°. KES-f applies the moment-curvature principle.



**Figure 18: FAST cantilever method, KES-f moment curvature method**

Both methods return the bending rigidity as characteristic value:

FAST Bending rigidity B: bending rigidity (B) in  $\mu\text{N.m} = 9.8 \text{ WT C}^3 10^{-6}$   
(Where WT = weight, and C = bending length in mm)

KES-f bending rigidity B (gf.cm): bending rigidity (B) =  $(a + b)/2 * 0.05 \text{ gf cm/cm}$   
(Where “a” is the slope of the front bending and “b” the slope of the back bending)

FAST also measures the bending property in shear direction. This measure is not obtained from the KES-f method.

- Other properties

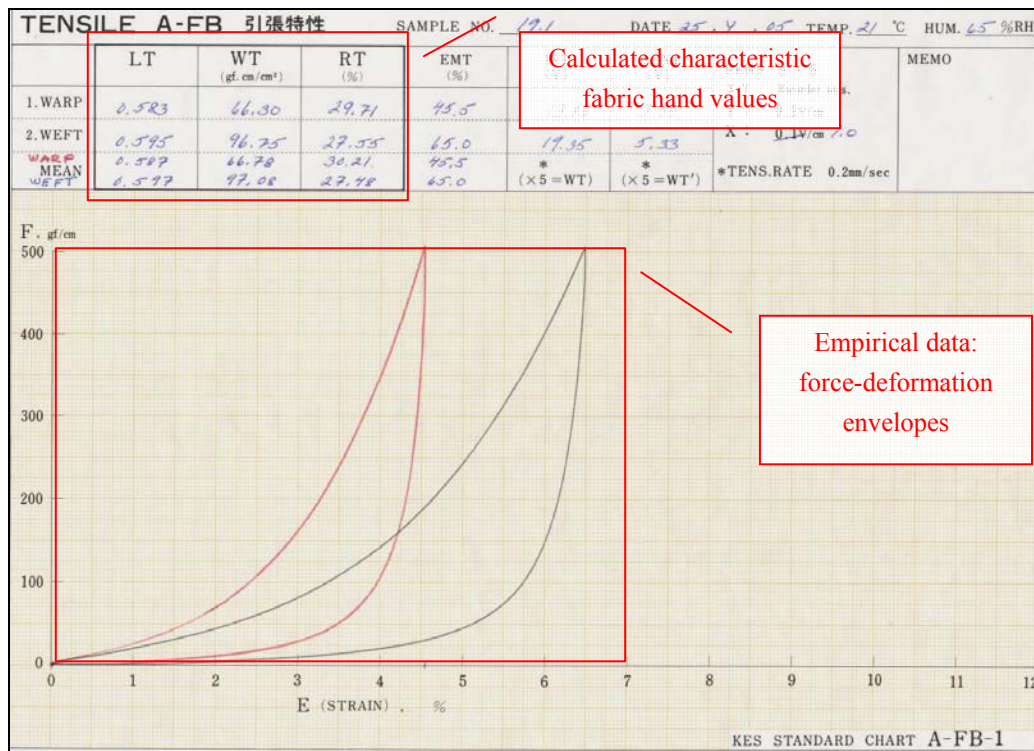
The thickness property is a characteristic fabric hand value. However it is measured applying different loads in both standard methods. KES-f measures the thickness with a fixed pressure of  $P = 0.5 \text{ gf/cm}^2$ , whereas FAST takes the values at  $P = 2 \text{ g/cm}^2$ . Hence, thickness parameters from the KES-f system are slightly higher values.

KES-f also measures the friction characteristic, which is not assessed by the FAST system.

#### 2.2.2.5. Interpretation of the measurement data

From the standard fabric measurements linear (FAST, KES-f) and nonlinear (KES-f) parameters can be derived by mathematically interpreting the empirical data (Figure 19). Correlations between the fabric components (raw material, yarn and planar structure, etc.) and the acquired measurement data can be established to detect the influencing factors for each single property. Various simple and complex input parameters can be obtained for each fabric property.





**Figure 19: KES-f tensile measurement report page for fabric single-jersey**

#### 2.2.2.6. Other measurement systems

Today, in the community of garment physiology and engineering, there are discussions about the suitability of existing measurement and garment evaluation methods. Most knowledge and methods date back to the 1970's and 1980's, where the textiles have been quite different from today. The assessment methods have to be adapted to new fabric materials, which possess different characteristics. One new generation measurement method is the FAMOUS system.

- FAMOUS - Fabric Automatic Measurement and Optimization Universal System

The general understanding of the current provision of equipment, following the extensive scientific and industrial use of the last 20 years is that the KES-f is regarded as a scientific device for research and FAST as a simplified alternative device for industrial use [Stylios 05]. Results of KES-f are precise but the measurement equipment is expensive and the testing procedures are time consuming. FAST is a cheaper alternative to KES-f, but the tests are limited to single measured loads and do not provide a complete stress/strain profile. FAMOUS tries to offer a new measurement method, consisting of only one apparatus to reduce equipment costs. The second aim is to reduce the time and complexity of the measurement procedure and to increase the accuracy. During measurement of a textile, only one sample of 20 cm x 20 cm is needed and complete suite of measurements is taken in only five minutes. [Stylios 05]

- Tensile Tester

Tensile and shear properties can also be measured with alternative measurement devices such as the Instron Tensile Tester [Instron]. These alternative devices are often used to test breaking loads of materials and fabrics. Small and large deformation regions can be measured.

Commercial applications from [Browzwear], [Lectra] and [Optitex] offer fabric measurement methods which are based on the existing standard measurement method. Lectra’s system is based on the KES-f system, whereas the solution from Browzwear and Optitex is based on the simpler FAST method. Browzwear uses a different sample size and Optitex calculates the characteristic values differently.

### 2.2.3. Relation of fabric properties to clothing appearance and performance

Because of the way, how fabrics have been assessed, i.e. by tactile/touch/feel, and the terminology used, i.e. fabric handle or hand, it is sometimes incorrectly assumed that the assessment was purely aimed at arriving at a measure of the fabric tactile related properties. In fact, in reality, the fabric handle, provided a composite measure of the overall garment related quality of the fabric, including garment making-up, comfort, aesthetics, appearance and other functional characteristics (Table 4) [Fan 05]. Researchers therefore use the objective measurements of fabric properties not only for the derivation of the “total hand value” (THV), but also for a “total appearance value” (TAV) [Fan 05]:

1.	Objective measurements are used for the assessment of fabric quality and handle and their primary components for various textile products.
2.	Design and production of a diverse range of high quality yarns and fabrics using objective mechanical and surface property data.
3.	Objective evaluation and control of textile processing and finishing sequences for the production of high quality yarns and fabrics.
4.	Objective evaluation of fabric tailorability and finished garment quality and appearance.
5.	Objective specification by tailoring companies for fabric selection, production planning, process control and quality assurance, using fabric mechanical and dimensional property data.
6.	Measurement and control of the comfort, performance and stability of fabrics and clothing during use.
7.	Evaluation of the effect of changes in fabric finishing routines, including decatizing, on fabric tailorability.

**Table 3: Different applications of fabric objective measurement technology**

In 1983, [Postle 83] already investigated the relation of fabric properties to garment performance and appearance. Therefore, he related each mechanical property to typical fabric and garment comportment (Table 5).

<b>Fabric mechanical property</b>	<b>Quality and mechanical performance</b>
Uniaxial and biaxial tension	Fabric handle and drape Fabric formability and tailoring properties
Shear under tension	Garment appearance and seam pucker
Pure bending	Mechanical stability and shape retention
Lateral compression	Relaxation shrinkage, dimensional stability and hygral expansion
Longitudinal compression and buckling	Wrinkle recovery and crease retention Abrasion and pilling resistance
Surface roughness and friction	Mechanical and physiological comfort

**Table 4: Fabric properties and their relation to performance and appearance in wear and handle**

The CSIRO Wool Association, who developed the FAST method, also dedicated a large share of their studies to explore the connection of fabric properties and garment appearance and performance during manufacturing. To facilitate the interpretation of the measured data, the so called „finger print“ has been developed. The finger print of a fabric material predicts, based on the combination of the measured characteristics, the comportment of the material and possible manufacturing problems [FAST 95].

Lately, researchers focus on a distinct importance of single fabric properties regarding clothing appearance and performance. Kawabata and Niwa specified three performance categories: utility performance (strength, etc.), comfort performance (fitting to the human body) and fabric performance for the clothing manufacturing [Kaw 89]. After Kawabata and Niwa, the important related fabric properties are bending, shear, compression and extension, as well as dimensional stability. [Kaw Niwa 98]

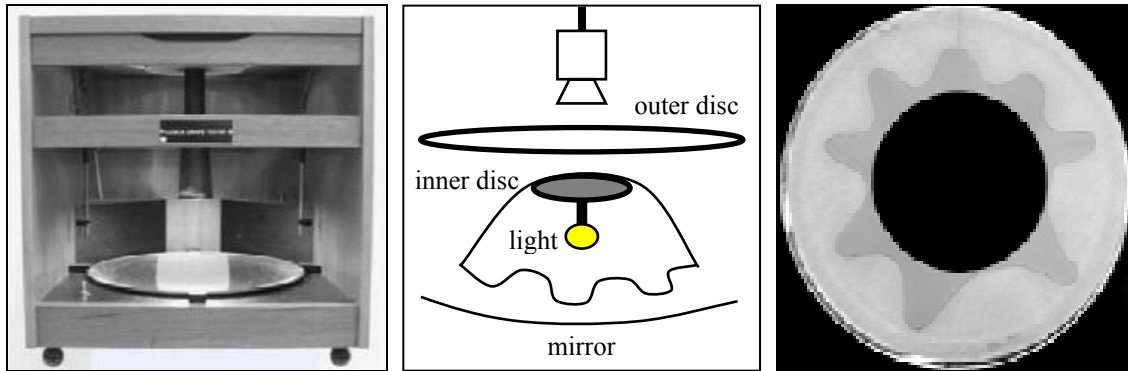
Gersak considered tailoring components such as formability, elastic properties and drape as most important. Formability is related to the bending rigidity and the extensibility of a fabric, thus elasticity, bending and shear properties. [Gersak 02]

The wear of garments involves another comfort and fit aspect, which is related to fabric mechanics: Depending on its type and function, each garment produces more or less some kind of pressure on some body parts (belt, cuffs, fabric weight, bodices, compression garments, etc.). Each individual subjectively perceives this pressure as positive or negatively. Researchers investigated this subjective, pressure and elasticity related comfort aspect. [Li 40], [Hui 03]

#### 2.2.4. Fabric drape

Fabric drape is not a mechanical or physical hand property but an important aesthetical parameter of fabrics. Drape determines the adjustment of clothing to the human silhouette and is defined as the extent to which a fabric will deform whilst hanging under its own weight. The ability of a fabric to drape can be seen as the main distinction between textiles and other sheet materials. An important measurement device is the drapemeter, where a circular piece of fabric is placed over an inner circular disc and an outer annular disc. During the drape test, the sample

is placed over the two discs and the outer annular disc is lowered gradually, allowing the fabric to drape inside (Figure 18).



**Figure 20: Photo drapemeter [Kenkare 05], Scheme drapemeter, Output picture [Kenkare 05]**

Cusick developed a drapemeter, where one characteristic value, the drape coefficient, is calculated for a tested fabric. The drape coefficient can be defined as the percentage of the area of the annular ring covered by a vertical projection of the draped fabric [Cusick 68]. A high drape coefficient means that there is little deformation and vice versa.

$$\text{Drape coefficient} = \frac{\text{Shaded area} - \pi (r^2) * 100}{\pi (R^2 - r^2)}$$

**R is the radius of the outer and r the radius of the inner circle**

Other research has been conducted to study the relationship of drape to corresponding fabric mechanical properties. Cusick found that drape is strongly related to bending rigidity and shear stiffness [Cusick 65]. Later on it was thought that the fabric weight and bending modulus are the most influencing factors on fabric drape [Kawabata 89]. Collier claimed that shear and shear hysteresis are the most important influences on the fabrics drape characteristics [Collier 91]. [Leapfrog 08] is a large European project, which aim is to automate the entire clothing production chain with the help of new technologies. One goal of the project is the prediction of mechanical fabric properties out of drape characteristics, as fabric drape is faster, easier and cheaper to measure than precise mechanical properties. Thus, in the future, only the drape of new textiles should be recorded and mechanical parameters allocated. The FAST method and the Drapemeter have been used for this research. Correlations between the drape and mechanical parameters have been studied. However, no significant correlations between the fabric drape and the mechanical parameters have been found, except for the bending property and weight.

## 2.3. The exploitation of measured fabric properties in virtual simulation systems

Since the late 1980's, researchers focus on cloth simulation methods, where measured physical and mechanical parameters of fabrics constitute important input parameters for realistic virtual imitations of real textiles. During the simulation of fabrics, its behavior, derived from measurement experiments, is combined with mechanical laws, resulting in complex mathematical equations. These complex differential equations can be solved by various methods. Different methods are applied for temporal and spatial discretizations. Spatial discretization can either be accomplished through numerical solutions or be part of the mechanical model itself, as in the particle system models [Volino 00]. Resulting equations from spatial discretizations are integrated over time using explicit and implicit algorithms. The discretization methods mainly influence the accuracy and the speed of the simulation system, since the fabric behavior is computed differently for each method.

### 2.3.1. Fabric materials modeled as continuum

Fabric materials modeled as continuum represent the state of the surface material (mechanical and physical parameters) by a scalar or vector value that continuously varies with position and time. Mechanical laws are represented by a set of partial differential equations, which relate the surface deformation energy to the local surface deformation (tensile, shear and bending). A well known continuous model is proposed by [Terz 87] [Terz 88]. Subsequent work such as done by [Lafleur 91], [Carignan 92] and [Yang 91] extended existing methods for cloth and garment simulations on virtual humans.

### 2.3.2. Finite Element Method (FEM)

FEM computes mechanical energies within a predefined discretization. The FEM is a method where functions are replaced by a piecewise approximation. At each node of the mesh, a proper number of degrees of freedom are considered (displacement, rotation). Also the number of nodes per element and the polynomial degree of the shape functions varies (bilinear, trilinear, quadrilinear, etc.). After the computation of each single element, the contributions of all elements of the surface are successively assembled and solved [Volino 00]. The FEM is the preferred solution technique in numerical analysis and engineering applications because of its versatility, sound derivation and superior convergence with respect to integral norms. Regarding garment simulations, it is possible to accurately simulate all kinds of aspects. However, compared to the field of engineering, the time factor is crucial for the fast processes in the garment industry as well and the computational effort of FEM's is too large. Therefore, some approaches assume a simplified mechanical behavior (linear, isotropic materials) and restrict the

applications to simple garments, what makes these systems on the other hand less accurate. Two important approaches for this kind of cloth simulation are described in [Eischen 96] [Hauth 03].

### 2.3.3. Particle Systems

Particle systems are simpler methods of space discretizations. The fabric surface is represented by a set of vertices. The position of the vertices is computed by imitating the mechanical force-deformation behavior of materials. Variations of particle systems exist and among them the spring-mass method is the simplest and most applied. The Spring-mass method considers as only deformation the distance between two adjacent particles (Figure 19). With this simplification of the mechanical behavior it is however difficult to represent the anisotropic tensile and bending strain-stress relationships.

Some more accurate models are based on a regular quad grid where the tensile stiffness is modeled along the edge in warp and weft yarn fabric direction and the shear stiffness along the diagonal. This model is however still inaccurate because of the inevitable cross dependencies between the deformation modes, relative to the respective spring. It is also not suited for nonlinear elastic behavior simulations and large deformations.

In comparison to the tensile stiffness, the bending stiffness is more complicated to simulate, as several neighboring mesh elements have to be considered simultaneously. Bending stiffness in spring-mass methods is represented as additional springs (cross-over springs) as shown in Figure 19 [Provot 95] [Ebe 96]. More accurate bending models represent forces as out-of-plane forces along surface normals (Figure 20) [Thom 06]. This approach however requires significant more computational power.

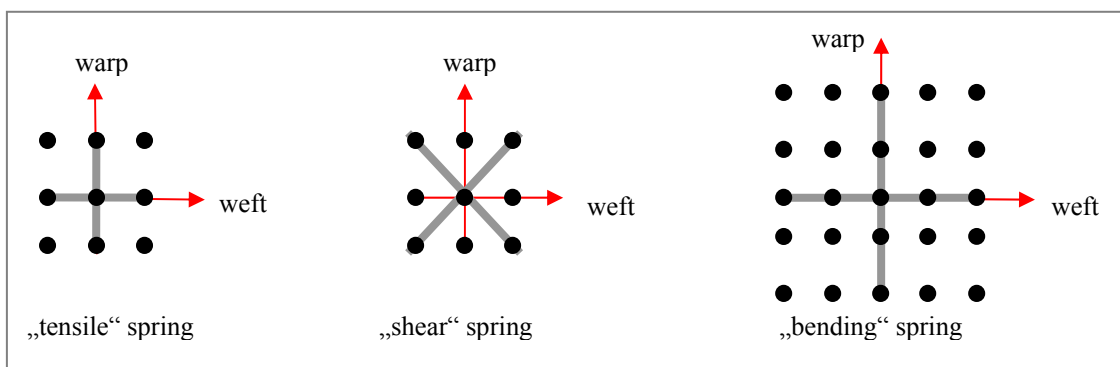
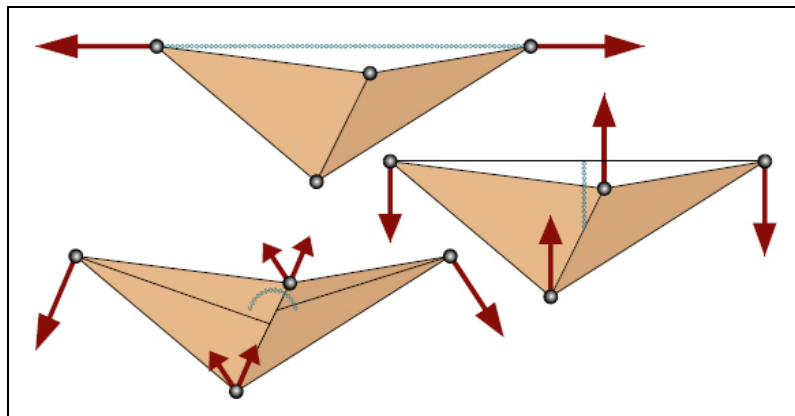


Figure 21: Spring-mass model by [Provot 95]

[Volino 05] proposed a more accurate particle system model, where the three particles of a triangle interact simultaneously. This model allows the accurate simulation of the nonlinear fabric tensile and shear behavior, even for large deformations. He also proposed a simpler, linear and accurate bending model, which evaluates the forces from a weighted sum of vertex positions (Figure 20) [Volino 06]. As this is the applied simulation system for this research

work, a more detailed description is given in Chapter 4.3. [Goldenthal 07] proposed a novel Constrained Lagrangian Mechanical formulation focusing on fast and realistic simulations.



**Figure 22: Three ways of creating bending stiffness in a triangle mesh: Crossover springs (top), forces along normals (bottom), and forces as weighted sums of vertex positions (right) [Volino 06]**

#### 2.3.4. Numerical Integration

Explicit and implicit methods are numerical approaches for solving time dependant ordinary and partial differential equations (time discretizations). Explicit methods calculate the state of a system at a later time from the state of the system at the current time. Implicit methods solve equations relating the current and the later state of the system. The choice between explicit or implicit method depends on the problem to be solved. [Terz 87] first used an implicit integration method for his work. Subsequently, mostly explicit methods have been used [Breen 94] [Ebe 96]. [Baraff 98] used again an implicit numerical method and his work constitutes an important contribution for the reduction of computation time. Implicit methods can be much harder to implement, but are suited for many calculations such as the computation of stiff materials, where explicit methods would require impractically small time steps [Volino 00\_2]. [Choi 02] used a semi-implicit method, allowing the use of large time steps to handle instabilities. Suitable time step parameters need to be specified for systems using implicit integration methods. (Also see Annex H).

#### 2.3.5. Use of accurate measurement data as input parameters

The algorithms of the first developed methods such as [Terz 87] [Lafleur 91] [Carignan 92] or [Yang 91] were not yet able to accurately handle the complex behavior of fabrics. Fabric properties were simplified through linear and isotropic behavior assumptions and set arbitrarily. Later, more accurate models started to use KES-f measurement data as input parameter [Breen 94]. [Ebe 96] tested the efficiency of various integration methods with KES-f parameters. Later, other simulation systems [Rizzi 04], [Bottino 01], [Eischen 00], [Collier 91], [Volino 05], tested

the versatility of their applications with KES-f data. [Ebe 96], [Ebe 97], [Ebe 99] used energy potentials and included both the loading and unloading KES data. [Collier 89] also used the Drapemeter for the derivation of input parameters. KES-f data was used for tensile data and shear. [Eischen 2003] used the fabric drape as validation tool, to prove the accuracy of his virtual simulations, by comparing real draped fabric samples to their virtually simulated counterparts. Real fabric specimens were scanned and overlaid with the virtual simulated copy, using KES-f data for the derivation of input parameters. The commercial application Optitex has been used as simulation tool.

In the German Research project “Virtual Try On”, the properties of fabric combinations and processed materials, such as fused or interlined textiles, are measured for the first time. Therefore the KES-f method has been used [VTO 04]. The aim of European project Haptex is the virtual simulation of the touch of fabrics in real time. The KES-f method is used for the determination of fabric input parameters [Haptex 07]. In this project we have made our research on physical parameters.

### 2.3.6. Various simulation applications

Research on the modeling of the fabric behavior is conducted in two main fields: computer graphics and textile engineering. While the computer graphics community focuses on the visual approximation of the fabric materials, the textile engineering society is searching for models which are physically justified.

The computer graphics community uses simple mechanical models such as spring-mass particle systems with the basic parameters such as elasticity, viscosity and gravity. These tools are usually integrated as plug-ins to 3D applications. The most important examples are Syflex [Syflex], MayaCloth [Autodesk], ClothFX [Autodesk] and Reactor [Havok].

- *Syflex* seems to be the most used plug-in for commercial productions. The simulation of the materials is based on 2D patterns. Basic seaming functions are available. [Syflex]
- *MayaCloth* simulates the materials with a spring-mass model. To obtain 2D patterns, the Maya splines are converted into garment patterns. Basic seaming functions are available, which attach the 2D patterns. (Fabric parameters see table below) [Maya]
- *ClothFX* (former Stitch plug-in) is a basic spring-mass simulation model. To obtain 2D patterns, the 3DSmax splines are converted into garment patterns. Basic seaming functions are available, which attach the 2D patterns. [ClothFX]
- *HavokCloth* (former Reactor) is a basic physical-based simulation of surface materials. The model is a spring-mass system with parameters such as stretching, damping, and bending. No 2D pattern editing tools are available, hence no seaming is possible. [Havok]



The garment engineering society focuses on garment draping on virtual mannequins, an accurate mechanical reproduction for visualization (virtual try on) and prototyping purposes (virtual prototyping). Applications are specialized on the simulation of pattern assembly and garment draping using more accurate mechanical models of fabrics. The visualization applications take advantage of geometric techniques for generating quickly realistic dressed mannequins out of design choices. Applications are either standalone environments which are directly linked to professional 2D CAD software (Browzwear/V-Stitcher with Gerber) or are integrated within the 2D CAD software (Lectra, Optitex Runway or Assyst Bulmer/Vidya).

- The software *Runway* from Optitex is a 3D simulation software (seaming, texture mapping, etc. Optitex provides software that governs the processes from 2D pattern making to 3D animation of the cloth). A tool for the customization of bodies is integrated. [Optitex]
- *Vidya* from Assyst Bulmer governs the processes from 2D pattern to 3D animation of the cloth (seaming, texture mapping, etc.). No customization of bodies is available. [Assyst/Bullmer]
- *V-Stitcher* from Browzwear is integrated within the Gerber 2D CAD platform. The software governs the processes from 2D pattern to 3D static simulation of garments including seaming and texture mapping functions. A tool for the customization of bodies is integrated. [Browzwear]

# Chapter 3

## Design of the test method

### 3.1. Introduction

The accurate virtual imitation of the fabric behavior is an indispensable aspect regarding the use of simulation tools for precise manufacturing processes. Recently, the use of measured data from fabric characterization experiments seems to promise precise calculations of distinct fabric materials. Consequently, the fact that virtually simulated garments look realistic (Figure 22) easily leads to the assumption that the simulations are also accurate from a mechanical point of view and that those available standard fabric characterization methods are satisfactory for exploitation in virtual applications. But upon closer inspection, it becomes clear that this is not the case.



**Figure 23: Virtual garment examples**

Until today simulation systems have evolved to such an extent that we are not only able to simulate simplified, static clothes, but also precise, complex and dynamically moving garments, in the timeframe expected by the clothing industry. This evolution of the simulation systems brought new challenges for fabric characterization methods as well. The improved algorithms can handle complex fabric parameters and now the fabric measurement methods and the evaluation and derivation of fabric parameters have to be pushed forward as well.

## 3.2. Open questions

### 3.2.1. Suitability of existing measurement methods

Existing fabric characterization methods have not been developed for a use in virtual simulations but to distinguish fabrics from one another for their different usages. During the measurement experiment each fabric is exposed to the same mechanical stress in order to be able to compare the measurement results and to make a statement about each material.

In virtual simulations the input parameter defines the relationship between occurring strains and stresses for all mechanical properties. Thus, taking the measured data from standard characterization experiments as input parameters, we have to consider that our computation system is only accurately calibrated for the mechanical occurrence of the measurement. The simulation system might not be accurate any more, if the emerging mechanical stress deviates from the applied stress of the measurement, as there the system is not calibrated any more. With regard to the small force range of standard fabric measurements it is however very likely that appearing strains and stresses are not correlating. For that reason it is important to study the suitability of existing measurement methods for a use in virtual simulations and if necessary to define new measurement methods.

### 3.2.2. Importance and influence of fabric properties

Standard fabric measurements are objectively imitating the traditional subjective fabric assessment. At this, eight fabric properties are measured, which have been defined as being important for the subjective perception of a textile.

In virtual garment simulations, the objective is however a different one. The measurements are utilized for an accurate replication of the mechanical fabric behavior. Therefore, the influencing fabric properties might be different from the eight measured characteristic. For that reason, another determining point of research is the identification of important and influencing fabric properties for the recreation of the mechanical fabric behavior. Only if all relevant properties are considered and measured, the potential of virtual simulations can be optimal exploited.

### 3.2.3. Versatility of parameters for the entire garment manufacturing chain

The automation of manufacturing processes becomes a more and more important factor today. First attempts for automatic robotic driven sewing processes are in their test phase [Leapfrog 08]. For this new way of manufacturing, accurate simulations constitute important precise input parameters (robot adjustment). These new developments underline again the importance of accurate fabric parameters, not only for prototyping processes, but for the entire garment development chain. It is therefore also important to already consider and define at this stage the requirements of long-term developments regarding fabric parameters. Thus, generally versatile fabric parameters can be developed, which guide the entire virtual garment development process.

### 3.3. Contribution of this research

The main goal of this research is the creation of new precise and versatile fabric parameters for accurate mechanical simulations, which can be used in virtual garment manufacturing processes. Therefore, existing standard measurement methods are studied and further developed.

Existing research for the improvement of fabric characterization experiments pursue different goals: The measurement systems were on the one hand simplified in their usage [FAST 95], [Stylios 05] and on the other hand optimized for a variety of different fabric materials [Maklewska 07], [Hui 07] [Gersak 05].

Research on the side of the computation systems mainly followed the goal of an optimization of algorithms and numerical integrations (Chapter 2.2.9.). No research was conducted to the way of measuring fabrics and to derive fabric parameters. Only standard measurement experiments have been employed.

The aim of this research is however not the improvement or further development of state of the art measurement methods for the same field of application, the fabric assessment. Nor is the goal the optimization of the computation systems. Within this work, the existing measurement routines are studied and developed further for a completely new field of application, the virtual garment simulation. Thus, conditions and requirements of the virtual computations are brought into correlation with the state of the art knowledge of characterizing fabrics in order to refine existing measurement methods and if necessary to define new test methods. In a longer term, this research should lead towards the definition of a new standard fabric characterization for virtual garment manufacturing.

This interdisciplinary work is hence a first experimental approach to analyze the possible accuracy of virtual garment simulations by merging the requirements and methods of two completely different disciplines: the apparel industry and the field of computation systems, two domains, which only co-existed until today.

The leading aspect for the experiments is that the accuracy of the virtual garment simulation has to meet the precisions of real fitting and prototyping processes and not only be graphically realistic.

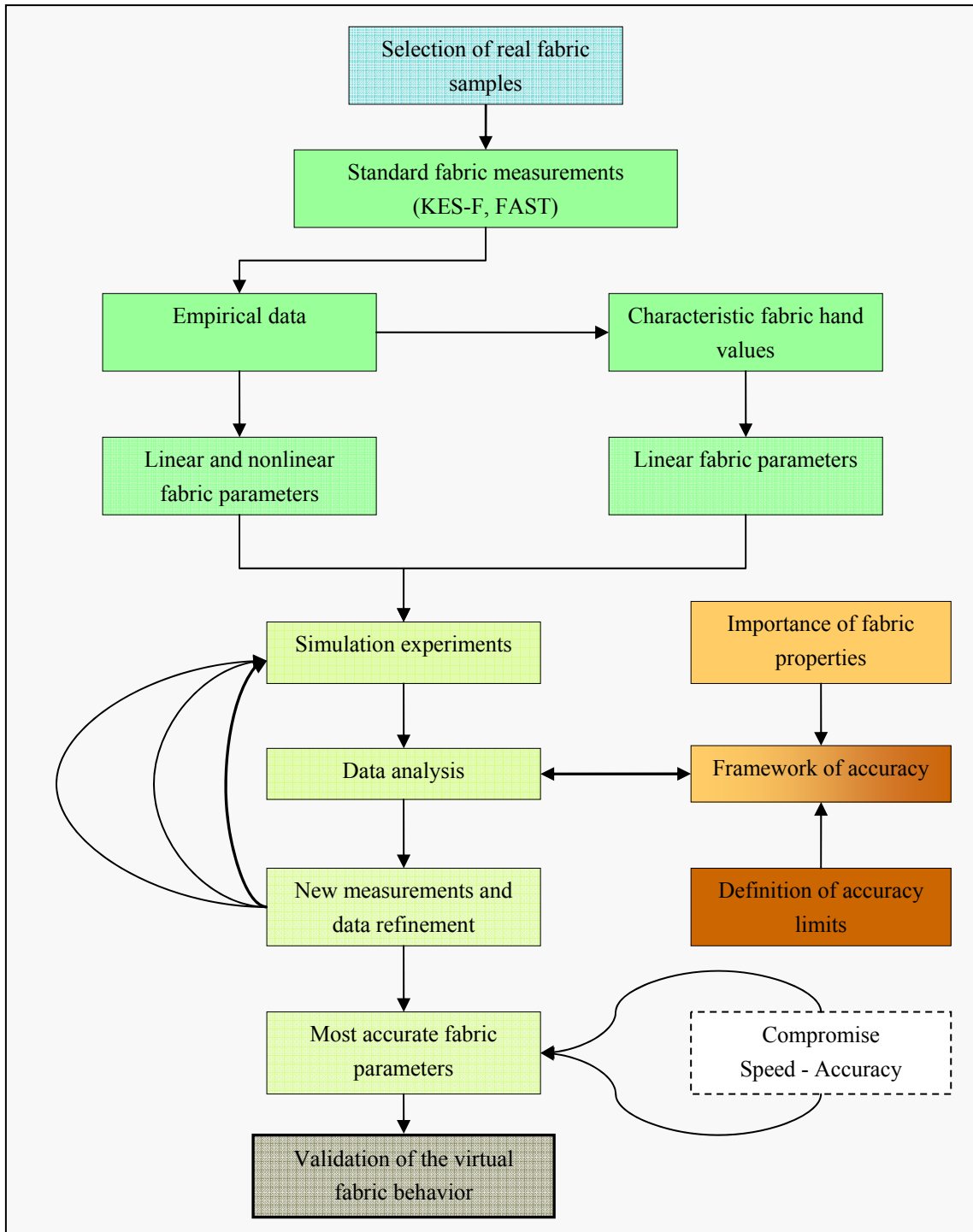
### 3.4. Applied methodology

In order to approach reality with as much accurate parameters as possible, the proposed test method is primarily characterized by a constant alignment of the virtual and the respective real process. Therefore, the fabric properties are systematically analyzed, measured and evaluated in order to derive accurate fabric input parameters for the virtual simulation systems.

The applied method is divided in five main modules, which are illustrated with different colors in the workflow scheme (Figure 23):

- Module 1: Selection of real fabric samples
- Module 2: Standard fabric measurements
- Module 3: Framework of accuracy
- Module 4: Simulation experiments, data analysis and measurement refinement
- Module 5: Validation

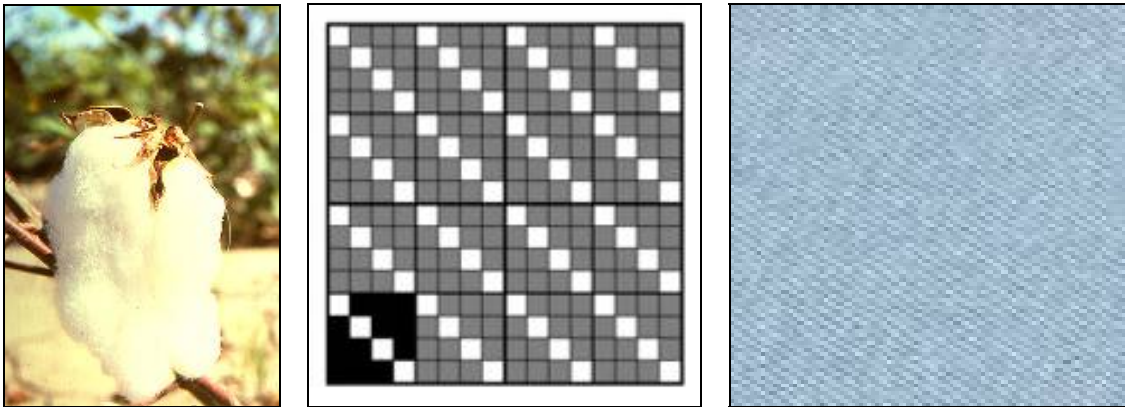
Workflow of the proposed method:



**Figure 24: Workflow**

### 3.4.1. Selection of real fabric samples

The first module of the test method consists in the selection of real test fabric samples. Textile surfaces are highly diverse materials, which correspond to a broad variety of demands of the apparel industry such as protection, comfort or aesthetic rules. This extreme inhomogeneity of textiles is possible because of a large choice of raw materials and complex manufacturing methods (Figure 24).



**Figure 25: Cotton plant [Fibers] (left), scheme twill [Loschek 94] (middle), denim fabric (left)**

For that reason, the first important step for studying fabric characteristics is a good choice of test fabric samples, as this selection is considerably influencing the final result. In order to represent a broad diversity of dissimilar fabric materials, textiles of different raw materials (fibers origin), yarn structures (degree of twist), planar structures (weave, knit) and finishing treatments are chosen for the experiments.

### 3.4.2. Simulation experiments, data analysis and refinement

The simulation module is designed as a try and error system, which compares each simulation result with a previously defined framework of accuracy (module 4). Based on the outcome of this alignment, the parameter and the corresponding measurement method are evaluated. If necessary, a new measurement specification is proposed and the same test cycle carried out again. Only if the simulation result meets the requirements of the previously defined accuracy framework, a parameter is judged as accurate.

A state of the art simulation system, suited for the computation of dynamic simulations with high accuracy is used for all experiments. For each fabric property a suitable simulation test experiment is designed.

### 3.4.3. Framework of accuracy

Within the fourth module, a framework of accuracy for virtual simulations is defined, which is based on the possible precision of the corresponding real processes. Garment fitting is a subjective and complex procedure, where multiple aspects of comfort are assessed. For the virtual simulation it is first of all important to reproduce the garment virtually in such an accurate way so that the same errors and problems as during the real fitting process can be detected (Figure 25). This means on the other hand that the virtual system can be judged as accurate if it corresponds to the possible precision of real processes.



**Figure 26: Real fitting processes [San], [Reflexstock]**

The framework of accuracy defines on the one hand the accuracy limits for each property, which should be reasonable and correspond approximately to the smallest, by humans' perceivable values. On the other hand, the accuracy framework classifies the properties with regard to their importance.

Before the final validation, each fabric parameter is evaluated again regarding precision and speed, where the requirements of the reality (accuracy) and the possibilities of the virtual world (speed – fast simulation) are weighed against each other.

### 3.4.4. Validation

In the preceding simulation experiments, single parameters for each fabric property are tested. In the final validation, one overall fabric parameter, which is composed of several single parameters, is examined. (The total of relevant single parameters is defined in module three and four). Two main aspects are tested within the validation procedure:

- (1) Accuracy of mechanical virtual fabric behavior.
- (2) Aesthetical accuracy of the simulated textile.

Similar to [Eischen 03], the scanning method is applied which compares the scanned drape of a fabric and the simulated virtual counterpart by superposing both surfaces. Both, the physical/mechanical and the aesthetical accuracy are verified within this test.

The traditional method for the comparison of the real and the virtual world is by filming. Therefore, the real model will be filmed, performing various actions. Subsequently, the model is virtually recreated and captured with identical camera setting. With this method, the mechanical and the aesthetical accuracy of the input parameters will be tested.

### 3.5. Justification of the applied methodology

Until today, no research has been conducted to adapt and to development further fabric input parameters for new state of the art simulation systems, which finally allow the computation of the complex fabric behavior.

The applied methodology exemplifies the very experimental nature of the present work. Beside the fabric selection, each module is designed in an open way in order allow its application for any kind of test result from a previous module.

The test fabric selection is conducted in a way so that the largest possible bandwidth of various fabric materials is represented and not only those textiles, for which a good simulation is expected. In the next module, not only simple linear fabric descriptions but complex nonlinear parameters are derived from the empirical data. The suitability of the derived parameters is not judged intuitively, but on an original scheme of accuracy, which is based on real prototyping processes. And the try and error simulation module guarantees the flexibility in order to find the best suitable measurement method for virtual simulations. Finally, based on this knowledge, exact parameters are obtained and validated.

This method thus delivers important data for an accurate clothing simulation and can hence be seen as one step towards and entire automation of the garment development process.





# Chapter 4

## Data and parameter acquisition

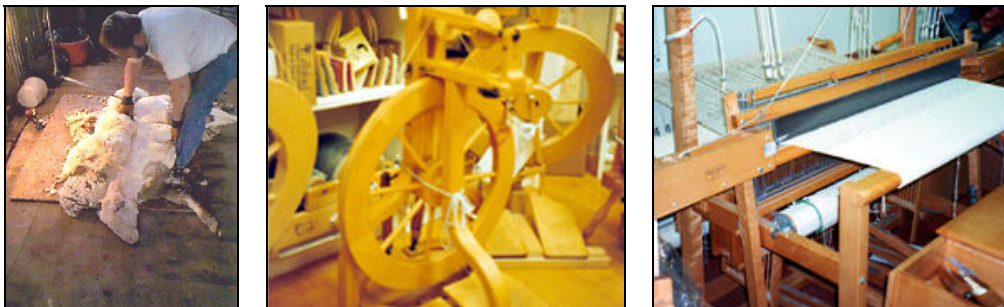
### 4.1. Fabric selection

For the study of fabric characteristics, the choice of test fabric samples is essential, as this selection is considerably influencing the final result. In general, fabrics are very diverse materials, which study constitutes several fields of research. For example, knitted and woven fabrics are rarely subjects of the same investigation, because of their very dissimilar mechanical properties. The goal of this research, however, is to test the accuracy of simulation systems for a broad field of application, primarily for garment prototyping, where all kinds of fabrics can be found. Therefore, an explicit broad bandwidth of very different textiles is searched with this selection.

To enable a detailed comparison of the properties of similar fabrics, the fabric selection process is carried out in two cycles. The first fabric selection consists of a broad variety of 32 very different textiles. The second fabric selection contains 10 specimens of like textiles, which are various knits and men's suit fabrics. Their expected similar mechanical behavior should allow a deeper study of the precision of each property.

As textiles are a manufactured assembly of fibers and yarns, the diversity of their mechanical and physical properties results from three major factors (Figure 26). These three factors have been chosen as the basis for the fabric selection criteria (Figure 27):

- Raw material (fiber origin)
- Planar structure (the method by which the fibers and yarns are assembled)
- Dimension (yarn and finishing treatments)



**Figure 26: Traditional fabric manufacturing processes a) wool shearing, b) fiber spinning-wheel, c) weaving. Today the manufacturing is more automated**

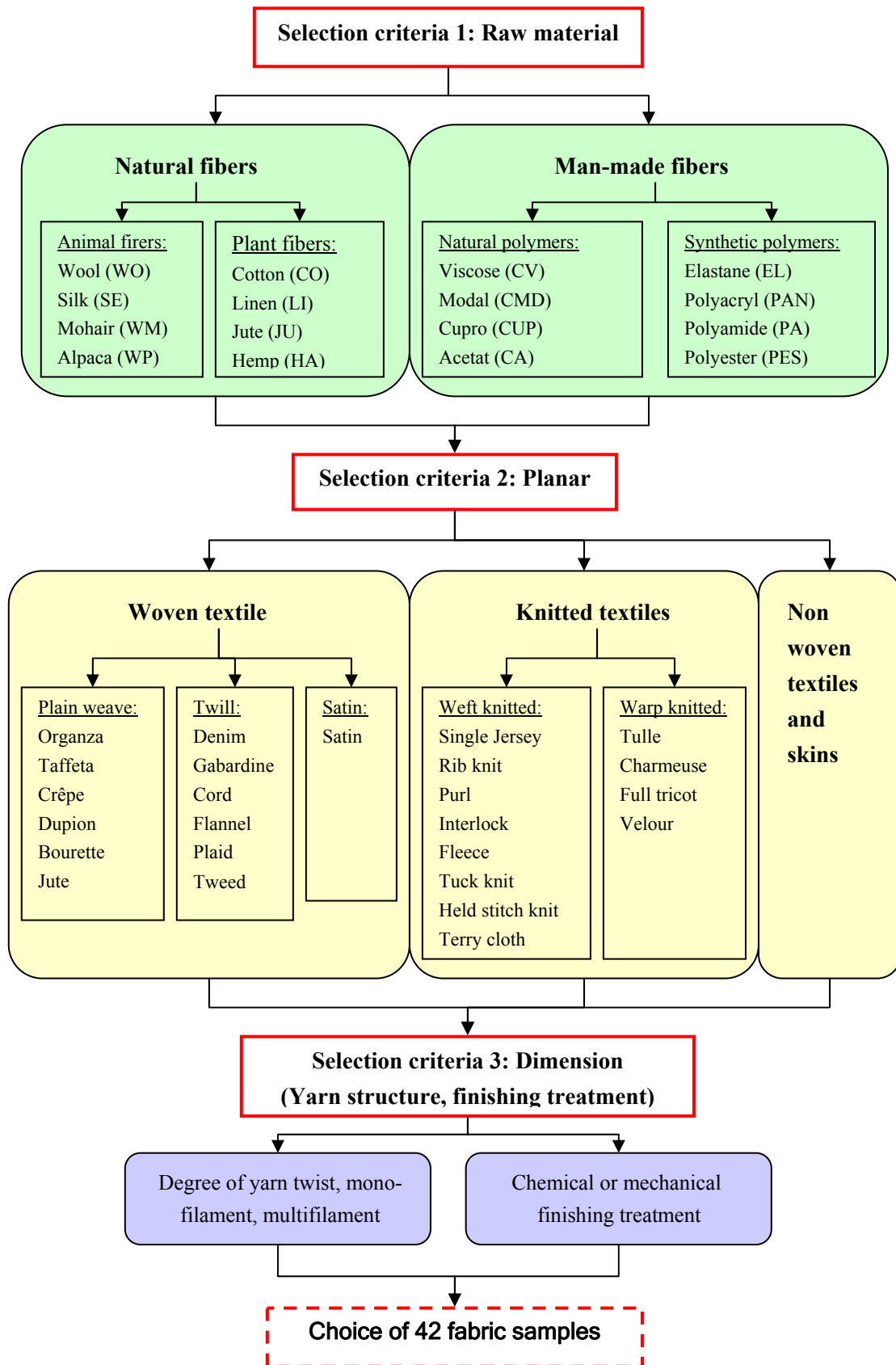


Figure 28: Fabric selection criteria (detailed fabrics selection list can be found in Annex B)

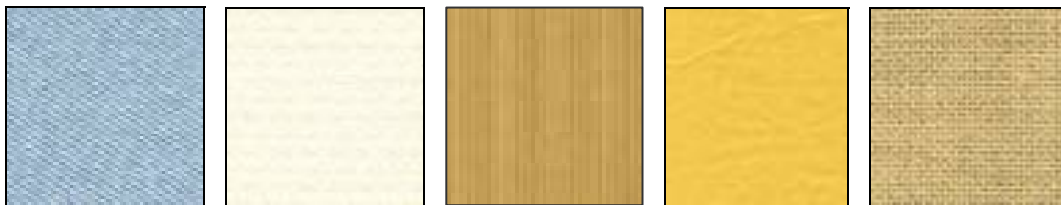
#### 4.1.1. First selection criteria: raw material

The term raw material could be misleading, as there is only one raw material for textiles, the fibers. However, fibers can be obtained from several resources such as plants, animals or can be custom-made. Fibers are relatively thin and flexible structures. Their main characteristics, beside their origin, are their length (staple or filament) and their linear density (diameter/size). The finer the fibers, the smoother and more flexible is the yarn, resulting in a fabric, which will drape beautifully. Also the fiber length and cross-sectional shape influences the smoothness of the yarn. The longer and thinner the fiber, the smoother is the spun yarn.

##### 4.1.1.1. Natural fibers

Natural fibers are divided into vegetable and animal fibers, where vegetable fibers are less elastic than animal fibers. All natural fibers except silk are staple length fibers.

Cotton (CO) is produced from the seed fibers of the cotton plant, whose length lies between 2cm to 4cm. Pure cotton samples, chosen for this research, are 01\_denim, 02\_shirt-cotton and 03\_cord. Blended samples containing cotton are 12\_denim, 15\_velvet, 19\_easy-care, 36\_overcoat and 38\_weft-knit. Linen (LI) fibers are obtained bundled from the stem of the flax plant and are much longer than cotton fibers with a length of 50cm to 90cm. Therefore, linen textiles are inelastic and tend to wrinkle easily. However, linen wrinkles are a typical aesthetic feature of this type of fabric. Linen also possesses a typical shine, resulting from a smooth fiber surface. One pure linen sample is 04\_linen. Jute (JU), like to linen, is a bast fiber with similar fiber lengths. However, it is a much stiffer material. One jute sample is 10\_jute.



**Sample 01\_Denim, Sample 02\_Shirt cotton, Sample 03\_Cord, Sample 04\_Linen, Sample 10\_Jute**

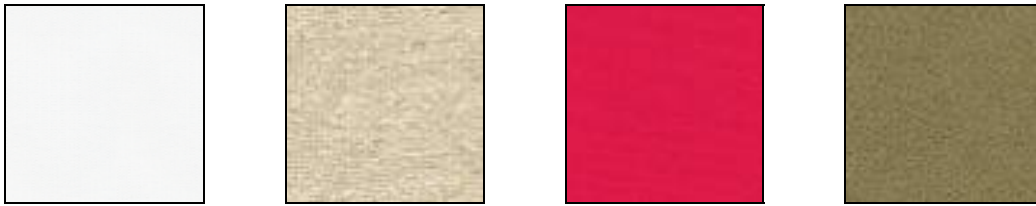
Wool (WO) fibers are thick, heavy and usually obtained from the fleece of lambs and sheep. High quality merino wool fibers are thin, soft, very curly and short with a length of around 2cm. Low quality Shetland wool fibers are rougher, less curly and longer measuring approximately 4cm. Wool fibers are rather elastic and do not wrinkle easily. The shear resistance of textiles out of those fibers can be higher for the curly rough fibers.



**Sample 05\_Gabardine, Sample 06\_Crepe, Sample 11: Flannel, Sample 13\_Plaid, Sample 14\_Tweed**

Silk (SE) is produced using silk fibers from the silkworm. The mulberry silk is obtained from cultivated living silkworms, which are killed in boiling water so that the silk thread can be unrolled undamaged. This purely natural filament is responsible for the mulberry silks inelasticity and its typically smooth surface. Tussah silk fibers are taken from damaged cocoons of slipped savage silk worms. Tussah silk fibers have staple length and are less smooth. Waste fibers from silk production are re-manufactured into lower quality bourette silk. Silk fabrics tend to have a high tensile resistance with a low bending resistance. Also the shear resistance generally is low because of the very smooth threads. Three silk fabrics out of each category have been chosen, 07\_mulberry silk, 08\_bourette silk and 09\_tussah silk.

Leather is a skin and not a fiber product. However, it has been chosen due to its importance to the garment industry.

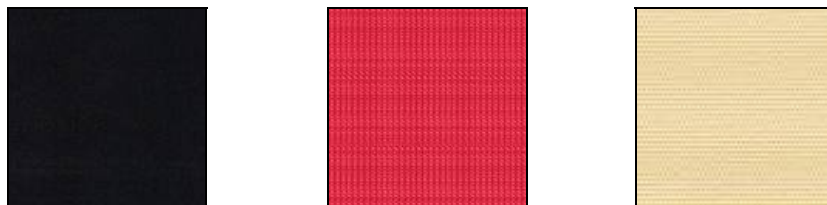


**Sample 07\_Mulberry silk, Sample 08\_Bourette silk, Sample 09\_Tussah silk, Sample 32\_Leather**

#### 4.1.1.2. Man-made fibers

Man-made fibers are divided into two categories, natural and synthetic. Man-made fibers were invented as cheaper and more durable imitations of their natural counterparts. Completely new fabric characteristics appeared with the invention of synthetics, such as nylon and elastane, which have been developed to “imitate” the skin. The second generation of synthetics now tries to “improve” the skin, with the development of smart textiles. It is impossible to classify man-made fibers according to their mechanical properties, because all kinds of mechanical properties can be synthetically imitated.

Man-made fibers based on natural polymers are manufactured from the celluloses of different kinds of wood. Through different treatments, various types of custom-made fibers can be obtained. Samples such as 15\_velvet (8% modal, CMD), 22\_taffeta (100% acetate, CA) or 21\_single-jersey (98% lyocell, CLY) represent this category.



**Sample 15\_Velvet, Sample 21\_Single-jersey, Sample 22\_Taffeta**

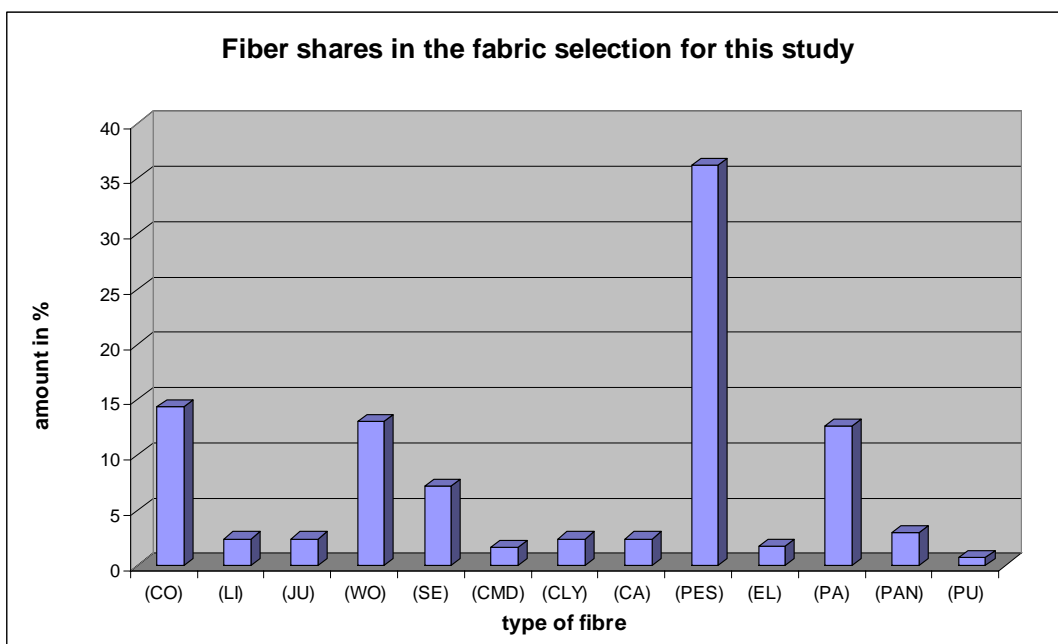
Man-made fibers based on synthetic polymers are called synthetics. Preliminary products are produced from coal, tar, natural gas and oil, which can be divided into several subgroups: Polyamide (PA) (Nylon, Perlon), Polyester (PES) (Trevira, Diolen and Dacron), Polyacryl

(PAN) (Orlon, Dralon), Polyurethane (PU) and Elastane (EL). This category is represented by the samples 23\_crepe, 24\_stain, 25\_felt, 26\_orgaza or 27\_felt.



**Sample 23\_Crepe, Sample 24\_Satin, Sample 25\_Felt, Sample 26\_Organza, Sample 27\_Fleece**

The quantity of test specimen per type of fiber is determined by the fibers importance on the textile market (Figure 28). Until 2003, the most used fiber on the market was cotton. Since 2003 cotton has lost market share to polyester, which is today the most popular fiber in textile production. Linen production is expensive and therefore linen represents only 2% of the world’s fiber consumption. Wool is the most used animal fiber. In general there is a continuing increase in the consumption of man-made fibers. They are also often used in blended textile materials.



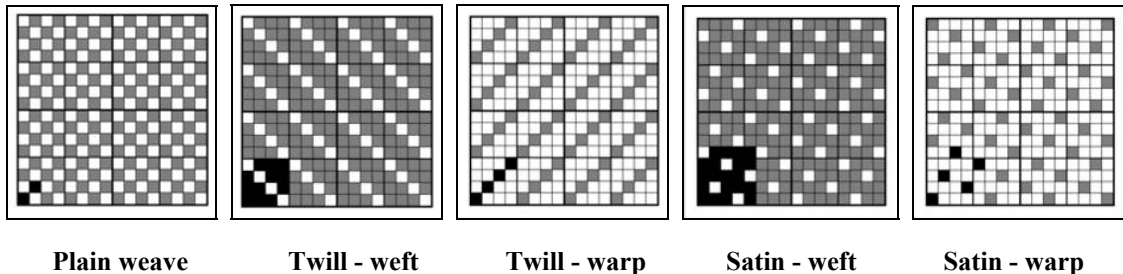
**Figure 29: Fiber shares in the two fabric selection cycles**

#### 4.1.2. Second selection criteria: planar structure

The way of crossing threads into a planar surface influences the mechanical behavior and the look (aesthetic) of a fabric. The planar surface structure can be knitted, woven or nonwoven. In general we can say that woven or knitted structures are usually more firm than the same material made out of the non-processed source material (yarn or fiber).

#### 4.1.2.1. Woven textiles

The type of weave and the yarn density affect the mechanical properties. Variations in warp and weft densities are possible. Many fabrics are produced out of different weft and warp yarns, since different characteristics are desired for each fabric direction. The three main types of weaves are plain weave, twill and sateen, wherefrom all other variations can be traced back.



Plain weave (e.g. sample 10\_Jute) is the simplest form, where each weft thread comes alternately over and under one warp thread. It is also the only weave, which creates a “homogeneous” textile, which is the same from all sides. It is also the weave with the most thread crossing points that creates the firmest textiles with often high shear resistances.

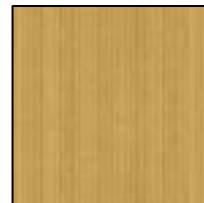
Velvet is a frequently used derivation of plain weave, but with an additional pile on one side of the fabric. A second set of warp yarns is added and cut for the pile, giving the typically smooth feeling on the pile side. Velveteen on the other hand is a typical derivation of the velvet weave and is characterized by a ribbed velvet pile. The mechanical characteristics of velvet and velveteen are strongly direction and side dependant.



**Sample10\_Jute,**



**Sample15\_Velvet,**



**Sample 03\_Cord (velveteen)**

The twill binding is characterized by its diagonal structure. Each weft thread comes alternately over and under two or more warp thread. Hence, twill woven fabrics have less crossing points. Depending on the form of variation, the twill binding can be loose and soft or dense and hard-wearing. Variations include combined twill and herringbone.

The sateen weave is characterized by equal spread thread crossing points. In comparison with previous weaves, it has the least crossing points, which are not in contact, resulting in a smooth fabric with low shear resistance, which is suitable for draping.

The jacquard is a special weave technique, where the weft and warp thread alteration is machine controlled in order to produce a customized weave pattern on the fabric. The number of thread crossing points is pattern dependant.

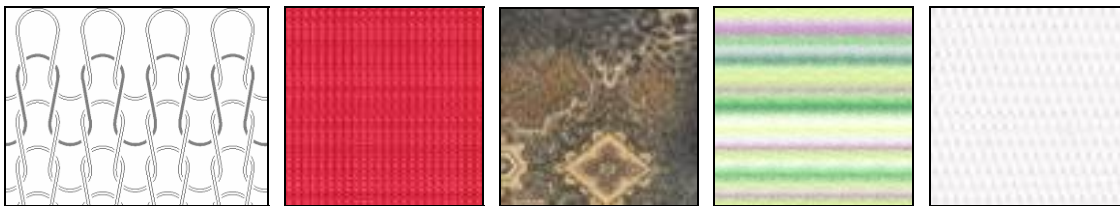


**Sample 01\_Denim, Sample 34\_Men suit fabric, Sample 24\_Satin, Sample 28\_Woven jacquard**

#### 4.1.2.2. Knitted textiles

Knitted textiles are thread systems, composed of successive loops of one continuous thread. Their density depends on the gauge (needle density) of the knitting machine. In comparison to weave, the mechanical behavior of knitted textiles is quite different and fabrics are generally much more elastic in all directions.

Differentiations are made between weft knitted and warp knitted textiles. A weft knitted fabric consists of horizontal, parallel yarn courses, which are mainly produced on knitting machines, whereas the warp knitted fabrics are composed of vertical yarn courses, which can be manufactured by hand or machines [EN ISO 03].



**Knitting scheme, Fabric sample 21\_Single-jersey, Sample 17\_Rib-knit, Sample 27\_weft knit, Sample 30\_Tulle,**

Plain jersey stretches equally in the two axial directions, but floats reduce stretch significantly at cross direction. Another common group of weft knits are rib knits, which have greater stretch crosswise than lengthwise. Warp knits are less elastic than weft knits, if no elastane yarn is used. 11 knit weft and warp fabrics have been chosen.

#### 4.1.2.3. Non-woven textiles

Non-woven fabrics (Sample 25\_Felt) are not based on yarns, but on single fibers, which are directly connected to a surface by different means. The fiber composition of non-woven fabrics influences their performance, much more than for woven fabrics.

Regarding planar fabric structures, knitted textiles have the largest share of 70% of the textile and clothing market. Nevertheless, 24 knitted fabrics have been chosen and 28 woven (14 plain weave, 12 twill including variations, 1 satin and 1 herringbone) because of the broader variety of woven structures. Additionally one skin and one non-woven fabric have been chosen.



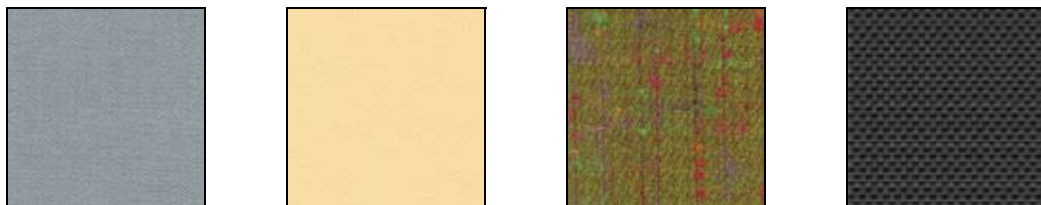
### 4.1.3. Third selection criteria: dimension

The dimensional fabric aspects, which are mainly influenced by the yarn structure, yarn density and loops as well as by finishing treatments, have been chosen as the third selection criteria.

#### 4.1.3.1. Yarn properties

The degree of twist in the yarn is the main influence over its characteristics, as the fibers or filaments come closer to each other. A high twist is responsible for a greater bending stiffness. The stiffness of plied yarns, i.e. two or more single yarns twisted together is greater than that of single yarns.

Filament yarns made from one filament are called monofilament yarns. Those with many filaments are called multifilament yarns. In apparel fabrics multifilament yarns are usually used. Multifilament yarns are finer and smoother, contain more filaments, are straighter and better aligned around the yarn axis than their monofilament counterparts. Filament yarns with greater apparent volume due to physical, chemical or heat treatments are named textured yarn. Textured yarns are softer and feel less synthetic [Hatch 93]. Crepe is a fabric made out of hard twisted yarns such as samples 06\_Wool-crepe and 23\_Poly-crepe. Sample 14\_Tweed is made out of textured yarns.



**Sample 06\_Wool crepe, Sample 23\_Polyester crepe, Sample 14\_Tweed      Sample 18\_Coated**

#### 4.1.3.2. Finishing treatment

Finishing is an extremely complex subject due to the large number of changes that can occur to a fabric. By using various finishing treatments different kind of end products can be produced from the same unfinished woven or knitted fabric and original typical mechanical characteristics can be vanished completely. Finishing treatments are applied on fibers, yarns or textiles. It follows the actual manufacturing processes and preserves and optimizes important fabric characteristics for an intended usage. Finishing treatments can be chemical (bleaching, iron-less, anti-dust, anti-bacteria, etc.) or mechanical (brushings, heat treatments, calendaring, softening). Sample 18\_motorcye wear fabric is a heat treated fabric.

## 4.2. Standard fabric characterization

After the test fabrics have been selected according to influencing factors on mechanical properties, the textiles are characterized with the existing standard measurement methods. All fabrics of the two selection cycles are measured with the KES-f method, which allows the assessment of the fabrics nonlinear hysteresis behavior. Six different fabrics from the first selection cycle are additionally measured with the simpler FAST measurement procedure, in order to be able to compare both standards.

A lot of information can be gathered from the measured data. For this study however the necessary characteristics for the derivation of parameters for virtual simulations are of interest. These are on the one hand the calculated characteristic fabric hand values and on the other hand the force-deformation curves, illustrating the hysteresis behavior of the single properties.

### 4.2.1. KES-f

The KES-f measurement method is described in Chapter 2.2.2.2. Each characteristic is measured twice and the mean value of both measurements is taken for the calculation of the 16 characteristic values (Annex B). Examples of related force-deformation profiles for all properties are shown in the course of this work.

#### 4.2.1.1. Tensile

The tensile measurement can be seen as fiber and yarn stretching processes, in contrast to the shear measurement, which is a stretch of the fabric structure. Deformations are characterized by three different phases: (1) Inter-fiber friction, (2) Decrimping and (3) Yarn-extension.

The greatest measured elongation at the maximum force of 500gf/cm is returned within the characteristic value EMT for warp and weft (Annex C) and gives the following results for our fabric selections:

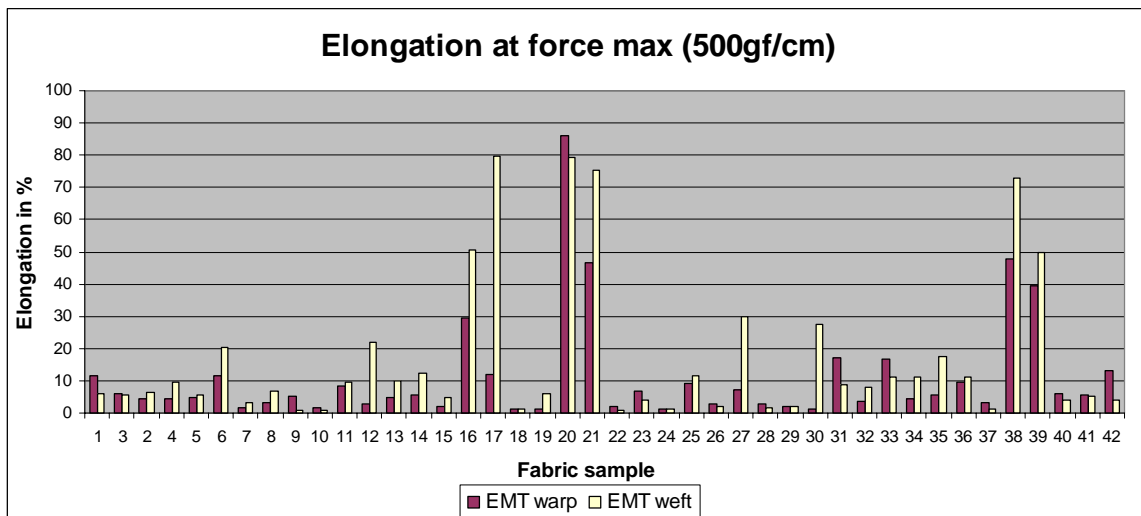
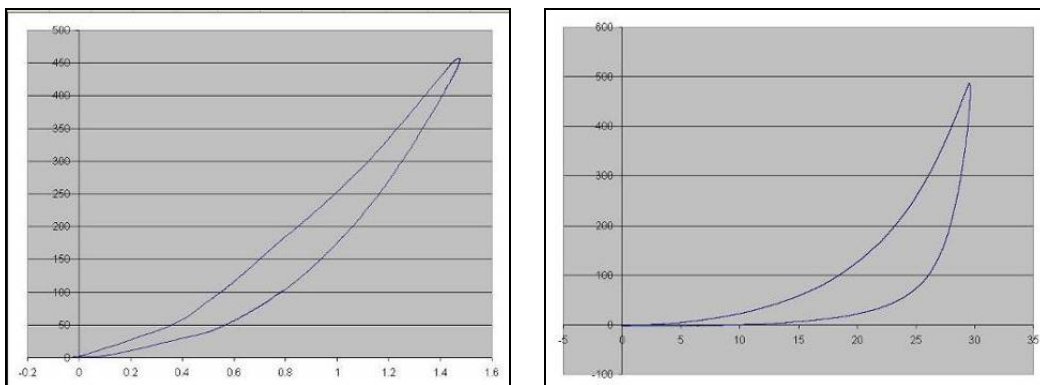


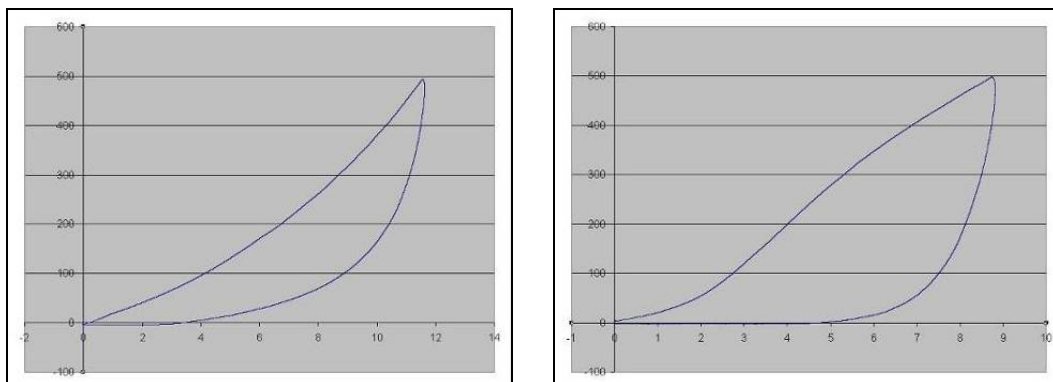
Figure 30: EMT warp and weft for the first fabric selection cycle

As illustrated in Figure 29, a broad variety of typical anisotropic fabric materials with quite different elastic properties is tested. The measured data varies from the lowest elongation of 0.7% (sample 09\_tussah-silk, weft) to the highest of 85.9 % (sample 20\_knit velour, warp). Knitted fabrics such as sample 16\_lurex-knit, 20\_warp-knit-velour and 21\_single-jersey are the most elastic. The three most rigid fabrics are sample 24\_satin, 10\_jute and 18\_woven motorcyclist wear, followed by 22\_taffeta and 07\_silk. Five of the six most rigid fabrics are in plain weave.

Each material deformation involves internal reversible and deformational energy, where the deformational energy is related to a thermodynamic change. After the release of the load, potential energy is transformed into kinetic energy and the material tends to recover its original shape and size, the equilibrium state. The part of energy that is dissipated in the form of heat is the cause of plastic deformation. Regarding fabric materials, the resulting deformation can be more or less reversible, depending on the load intensity and duration of loading, as well as on relaxation time [Gersak 04]. This typical hysteresis behavior of fabrics, to not immediately recover after the release of the force, is visible on each affiliated force-deformation or hysteresis envelope (Figure 30 – 33).



**Figure 31: Tensile force-deformation curve 07\_silk, Figure 31: Force-deform. curve 16\_Lurex-knit**



**Figure 33: Tensile force-deformation curve 01\_denim, Figure 34: Force-deformation curve 25\_felt**

Hysteresis envelopes of elastic fabrics are generally larger and characterized by a higher increasing slope (Figure 31). The recorded elongation and relaxation curves are generally more similar for rigid fabrics such as Sample 07\_silk (Figure 30).

The size of the enclosed area of the hysteresis envelope is expressed by the characteristic fabric hand value tensile resilience or RT (Figure 34). This value is highest (smallest envelope) for tightly woven fabrics such as samples 05, 07, 18, 22, 26, 29 and lowest (largest envelopes) for knitted fabrics such as samples 16, 21, 25 and non-woven sample 25.

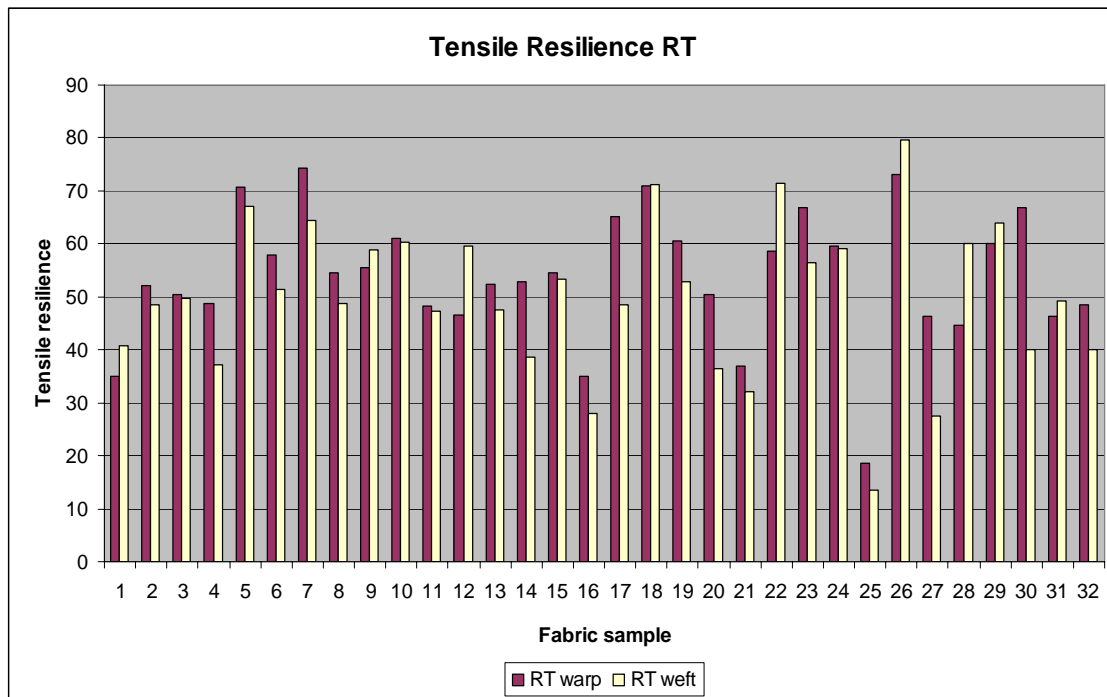


Figure 35: Tensile resilience

#### 4.2.1.2. Shear

For woven textiles, the shear property can be quite different from the tensile behavior. The elongation of the fabric structure can be attained with relatively smaller forces than the stretch of the fiber and yarn. Hence, the fabric is more elastic in the shear direction. The more thread crossing points the fabric structure possesses (plain weave), the greater the frictional restraint during structure change.

The crossing threads of knitted fabrics are not strictly orthogonal, however, because of the knitted loops, they are quite elastic in all directions. Generally they are most elastic in the knit direction. The calculated characteristic value 'shear rigidity'  $G$  (gf/cm \* degree) describes the fabrics resistance to shearing forces and is illustrated in Figure 35. A broad variety of different shear properties is measured by our fabric selection.

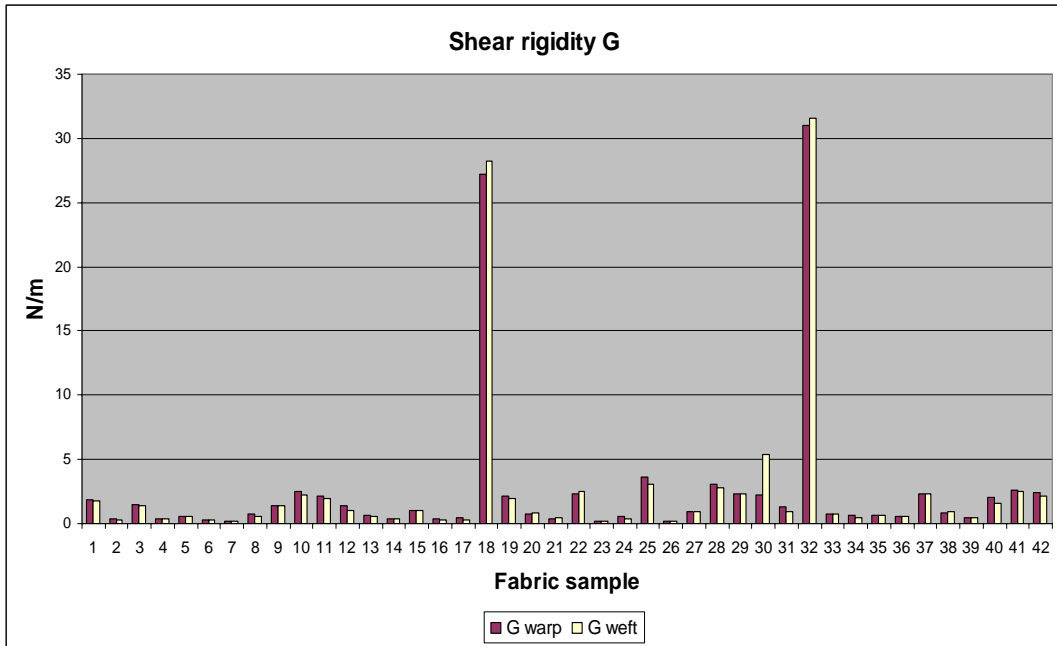


Figure 36: Shear rigidity values G

Forces necessary to shear the fabric samples vary from 1.15 gf/cm (sample 23\_crepe) to 33.28 gf/cm (30\_tulle). For two textiles (sample 18\_jute, 32\_leather) the shear rigidity is particularly high and forces of up to 174.38 gf/cm are needed to shear the fabric. Crepe fabrics such as sample 23, whose threads are hard twisted, drape very easily and thus possess the lowest resistance to shear. Knitted fabrics (e.g. 16\_lurex knit, 17\_crepe-jersey, 20\_warp-knit velour and 21\_single-jersey) and some woven fabrics (e.g. combined twill, crepe structures and loose woven fabrics such as samples 02\_shirt-cotton, 06\_wool-crepe and 14\_tweed) possess low shear rigidity.

The shear property is measured in weft and warp direction. The weft and warp shear behavior varies slightly for knitted, woven and non woven fabrics (Figure 35). Sample 30\_tulle varies by far the most. Sample 30 also differs most for weft and warp tensile measurement. However, no relation between the ratio of weft and warp tensile and the ratio of the weft and warp shear measurements could be detected (Figure 36).

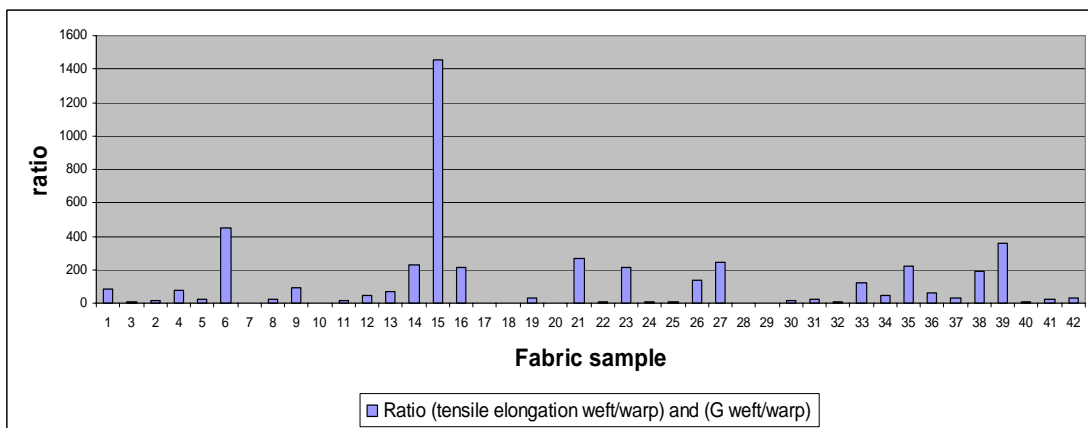
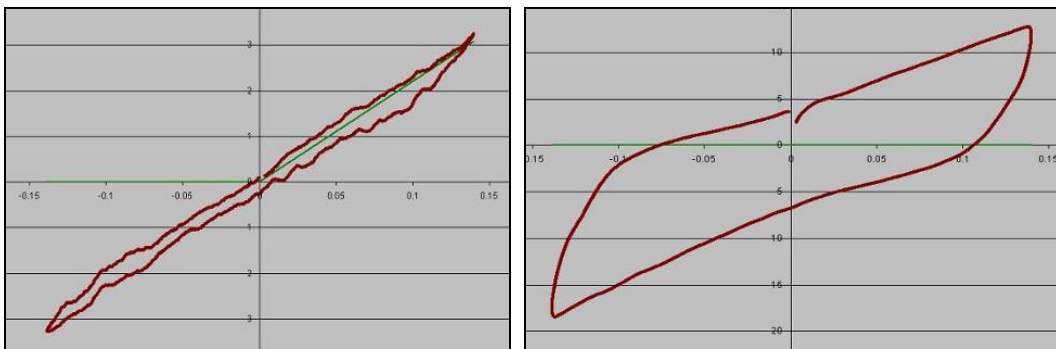
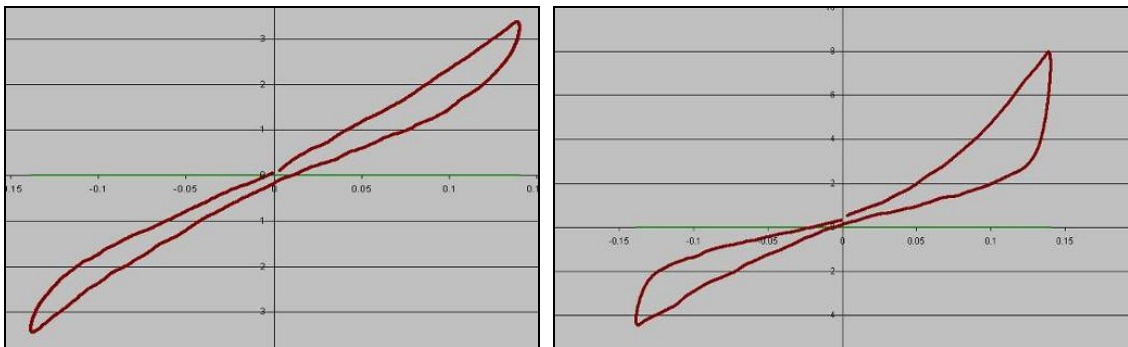


Figure 37: Ratio (tensile elongation weft/warp) and (G weft/warp)

Shear hysteresis envelopes are different from the tensile force-deformation profiles as the influencing factors are different. The influencing factors of the shear resistance are the structure (weave/knit), the yarn density or finishing treatments. For woven fabrics the shear hysteresis can be defined as friction force at the interlacing points of the warp and weft yarns. For closely woven fabrics, there is not much place for slippage, resulting in a higher friction between the yarns. For more loosely woven fabrics, there is less friction between warp and weft yarns. This means that slippage between warp and weft yarns causes increasing shearing strain as the straining action commences, it then remains stable before finally increasing again towards the end. [Lindberg 61]. Homogeneous materials exhibit linear shear hysteresis.



**Figure 38: Shear force-deformation curve 21\_single-jersey (knit), Figure 39: 09\_wild-silk (plain),**



**Figure 40: Shear force-deformation curve 02 shirt cotton (plain) Figure 41: Sample 24\_satin (satin)**

From the first broad selection 50% of the fabrics have a linear shear behavior (such as Figure 37). Another 8% show a quite linear behavior but on a larger envelope (Figure 38). Around 30% of the fabrics have a linear deformation curve and a more nonlinear relaxation curve (Figure 39). Only 12% exhibit a curved deformation and relaxation curve (Figure 40). This means that 88% of the fabrics demonstrate linear behavior during the deformation process.

As characteristic fabric hand value the shear hysteresis is measured at  $0.5^\circ$  and  $5^\circ$  degree (Figure 41). The shear hysteresis is lowest for samples 04\_linen, 06\_wool-crepe, 07\_mulberry-silk and 23\_poly-crepe and highest for samples 18\_motorcycle wear, 22\_taffete, and 32\_leather.

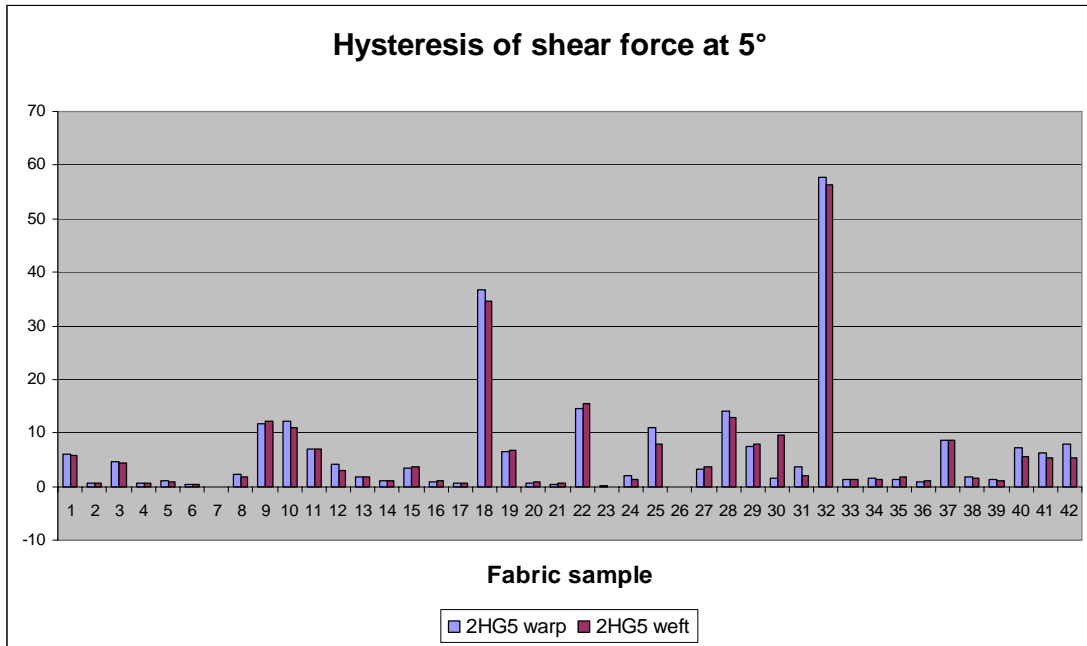


Figure 42: Hysteresis of shear force at 5°

In contrast to the tensile property, shear weft and warp force-deformation envelopes additionally return two curves for the opposite shearing direction (right side +8°, left side -8°). Therefore, fabrics with non-linear shear properties will have four non-identical force-deformation curves (Figure 42, 43, 44).

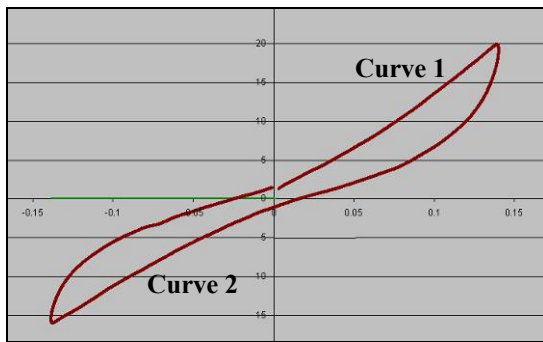


Figure 43: Sample 01\_denim (warp)

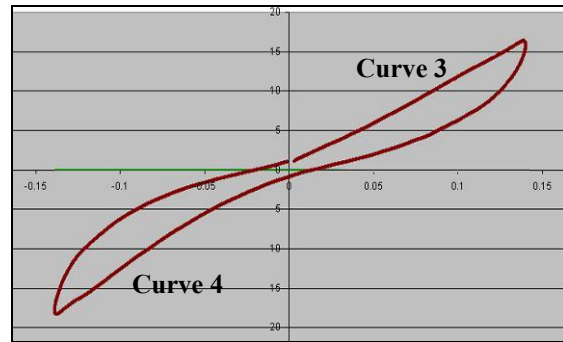


Figure 44: Sample 01\_denim (weft)

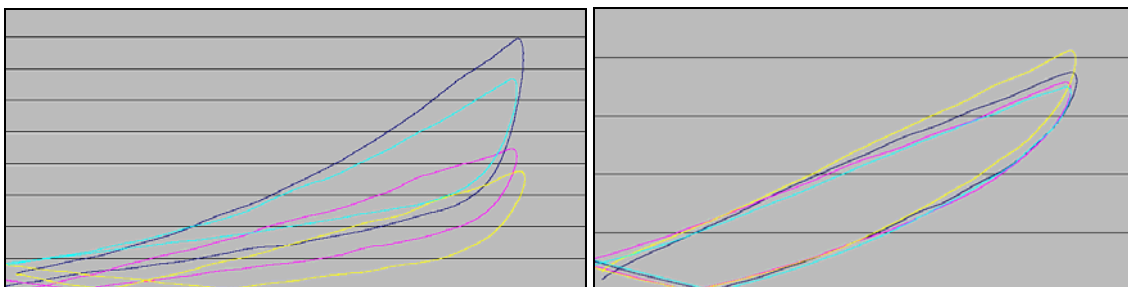


Figure 45: Four shear force-deformation curves sample 24\_satin (left) and 11\_flannel (right)

#### 4.2.1.3. Bending

In comparison to the two-dimensional tensile and shear elongation, bending is a three-dimensional deformation. The fabric thickness, together with the bending length and fabric density, mainly influences the bending rigidity (Figure 45) [Peirce 30]. Doubled thickness of a fabric can result in an eight times higher bending rigidity.

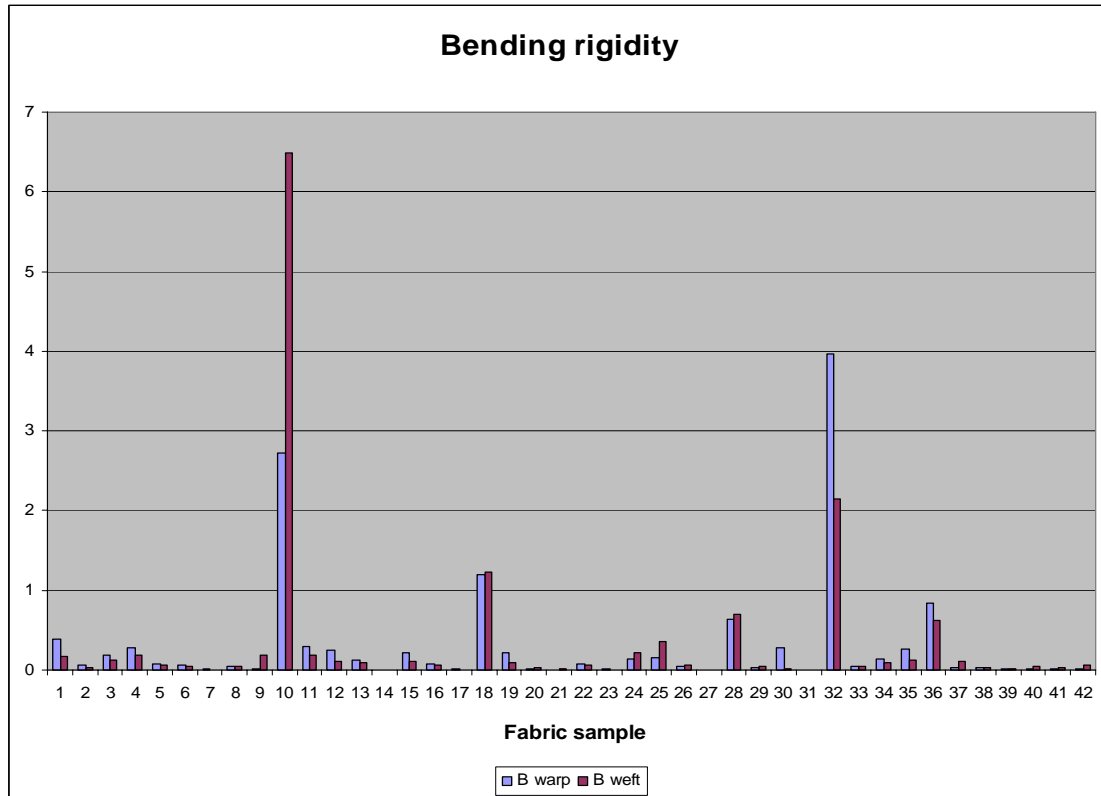


Figure 46: Bending rigidity of the measured samples in KES-f system

Most applied bending forces are between  $0.22 \mu \text{ N.m}$  (31\_warp knit tricot satin) and  $100 \mu \text{ N.m}$  (18\_woven motorcycle wear). Samples 31\_warp-knit tricot satin, 17\_crepe-jersey and 21\_single jersey possess the lowest bending rigidity. Two fabrics have a particular high bending rigidity (sample 10\_jute, 32\_leather), wherefore forces of up to  $560 \mu \text{ N.m}$  are needed to bend the fabric. However, the two extreme fabrics regarding bending are not the same as the two extremes for the shear property. Compared with the forces to stretch or shear a fabric, much smaller forces are needed to bend a fabric. Two fabric samples (14\_tweed and 27\_fleece) have a thickness of 3.9 mm which is too thick to be measured by the KES-f bending apparatus. Sample 16\_lurex-knit with 2.94 mm is the thickest fabric sample which can be measured.

The bending behavior of textiles is slightly nonlinear mainly because of the inner friction between the fibers. Because of different fiber and yarn compositions, each fabric has its typical bending hysteresis envelope. Initial bending strain causes linear growth of the moment-bending curvature, while at higher loads a change of the linear part into a curve can be observed [Pavlinic 03].



The characteristic fabric hand value 2HB (Hysteresis of bending moment), returns again information about the enclosed area of the force-deformation envelope and is once again a measure for the fabric's ability to recover after the force is released. Fabric 10\_jute and 32\_leather possess the largest bending hysteresis envelopes (Figure 46).

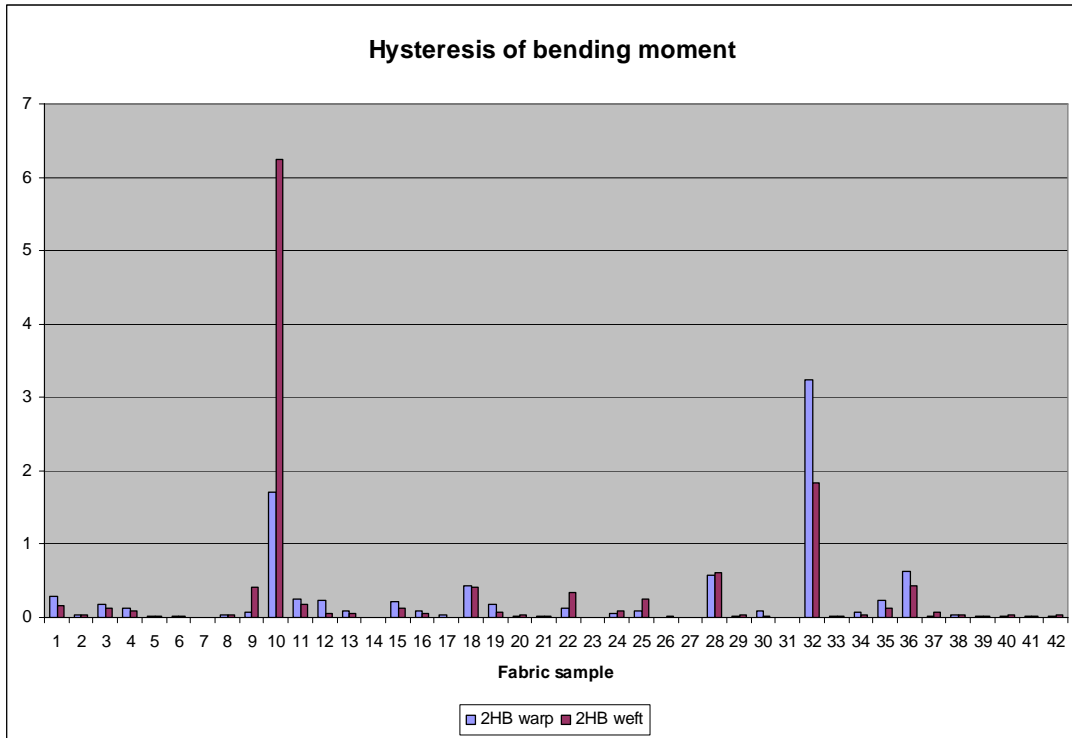


Figure 47: Hysteresis of bending moment

Typical hysteresis envelopes vary from thin to medium and large envelopes (Figure 47, 49, 50) and from symmetric to unsymmetrical ones (Figure 47 and 48).

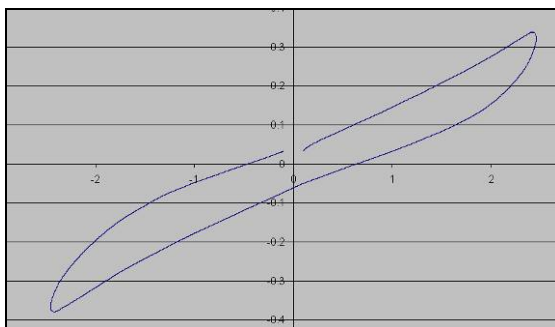


Figure 48: Sample 03\_cord,

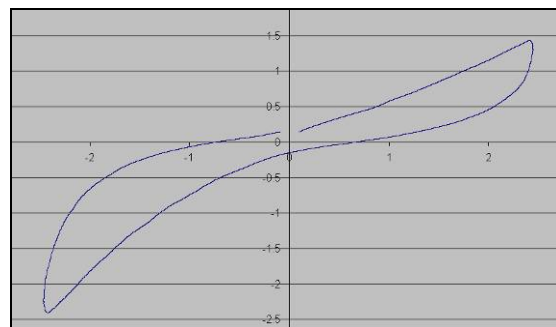
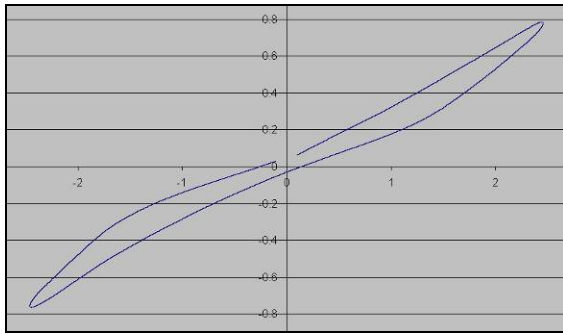
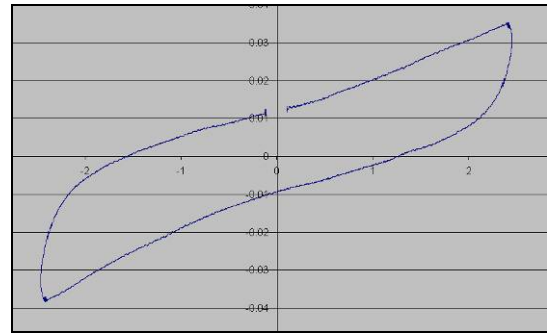


Figure 49: Sample 28\_woven upholstery fabric



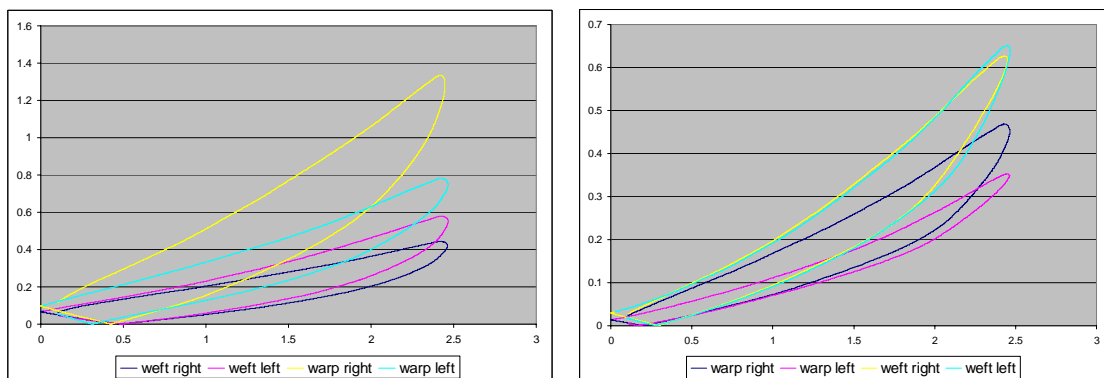
**Figure 50: Sample 18\_woven motorcycle fabric,**



**Figure 51: Sample 17\_crepe-jersey**

Around 80% of the obtained bending force-deformation envelopes show fairly linear behavior, of which approximately 35% have thin, 35% have medium and 10% have large envelopes. The remaining 20% of the measured force-deformation envelopes exhibit more nonlinear behavior and have medium to large envelopes. However, none of the curves demonstrate significantly nonlinear bending behavior.

The bending property is, similar to the shear property, not only measured in weft and warp direction, but additionally to the front and back, returning a total of four hysteresis envelopes, two for warp and two for weft. Fabrics rarely bend in the same way to the front and the back side, visible in the dissimilar left and right curves of force-deformation envelopes. For 30% of the envelopes the left and right curves are visibly dissimilar to various extensions (Figure 51).

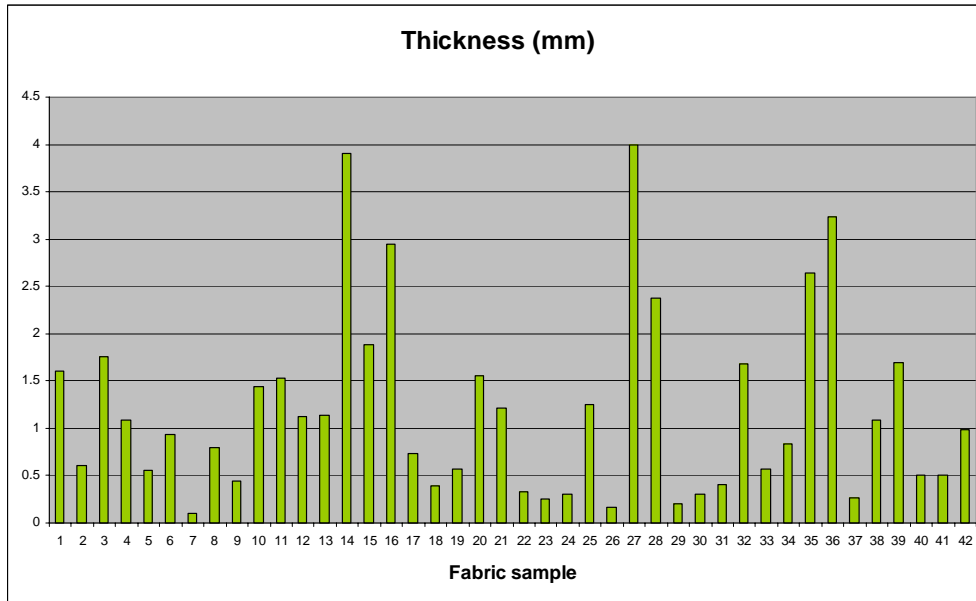


**Figure 52: Four bending force-deformation curves for fabric 01\_denim (left) and 24\_satin (right)**

In summary, a broad variety of very different bending rigidity and bending hysteresis characteristics are captured.

#### 4.2.1.4. Thickness

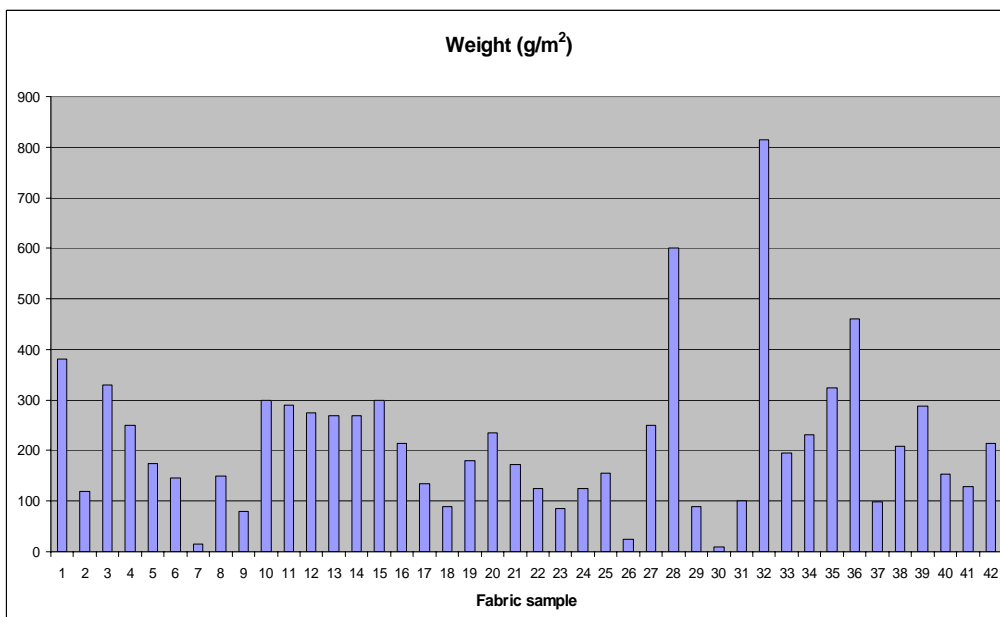
The fabric's thickness is a fabric hand characteristic, which is derived from the compression measurement. The thickness varies from 0.1 mm for sample 07\_Silk to 3.9 mm for sample 14\_Tweed (Figure 52).



**Figure 53: Thickness first fabric selection cycle**

#### 4.2.1.5. Weight

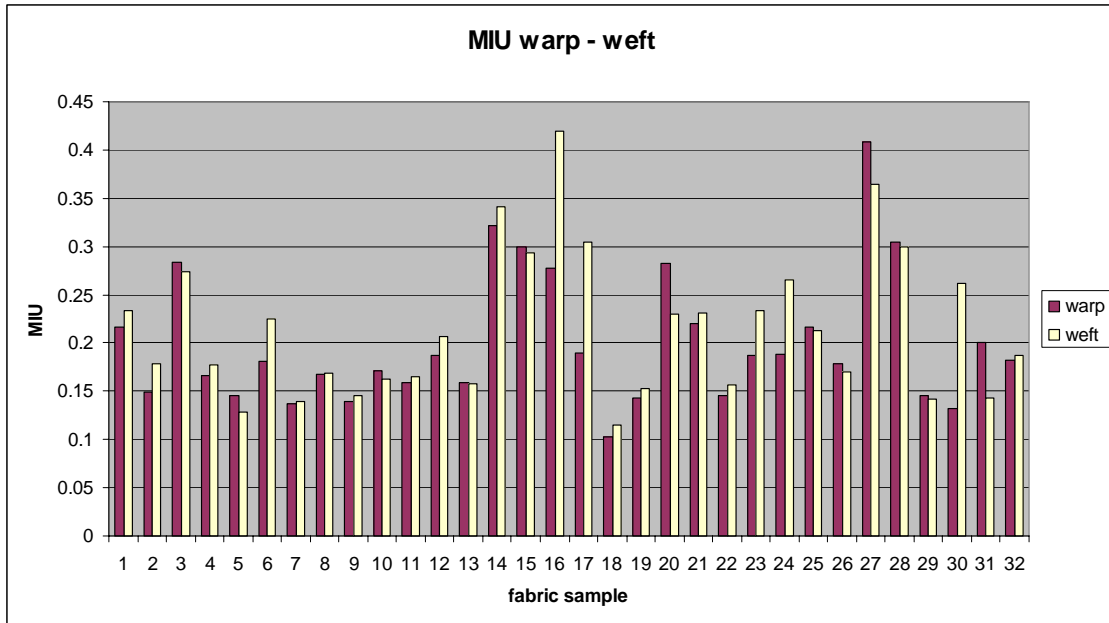
The fabric weight varies from 15 g/m<sup>2</sup> for sample 07\_Silk to 815 g/m<sup>2</sup> for sample 32\_leather, with the rest of the samples being evenly dispersed between these two values (Figure 53).



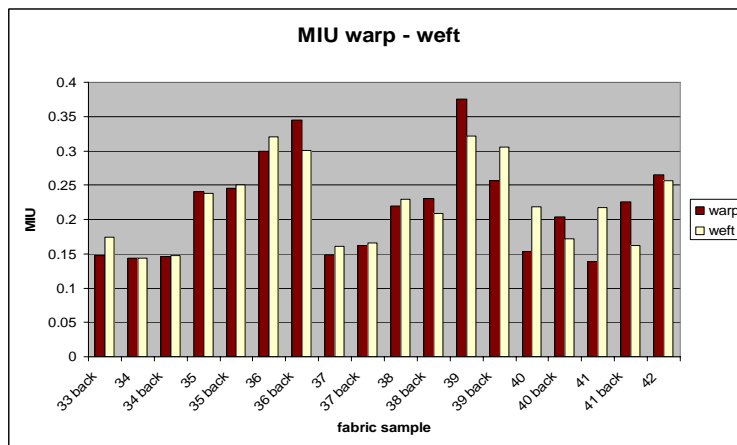
**Figure 54: Fabric weight**

#### 4.2.1.6. Friction

The coefficient of friction (MIU) is a fabric hand characteristic, which is calculated by taking the average friction over a predetermined area (Figure 54, 55).



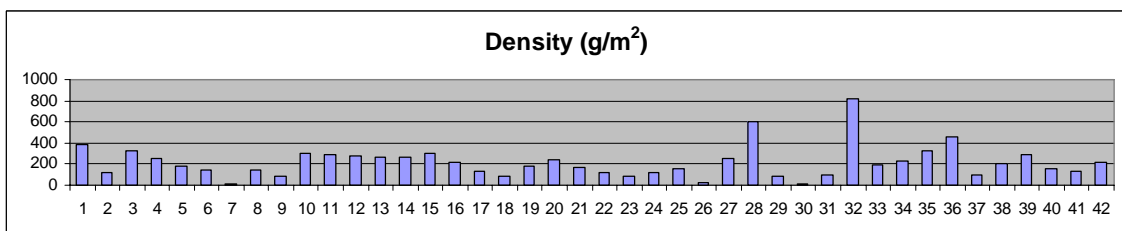
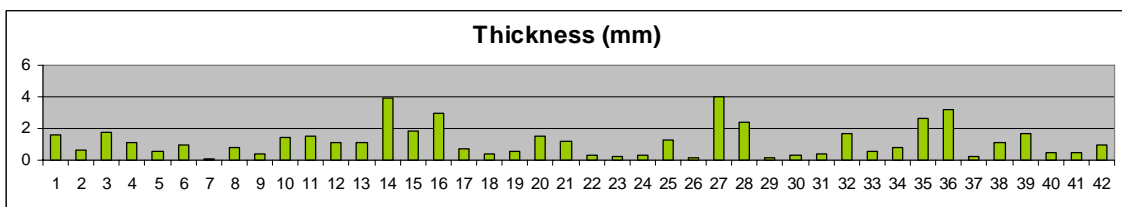
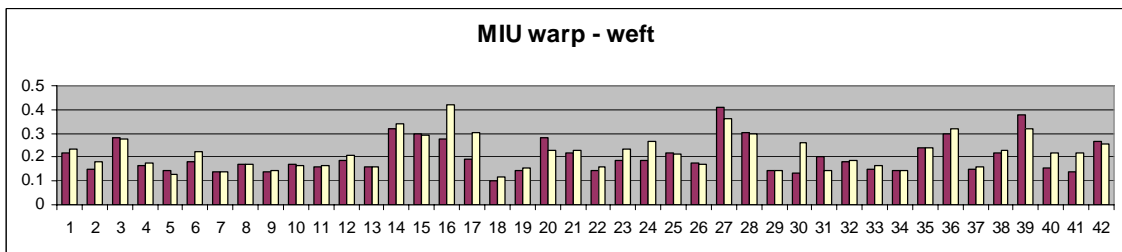
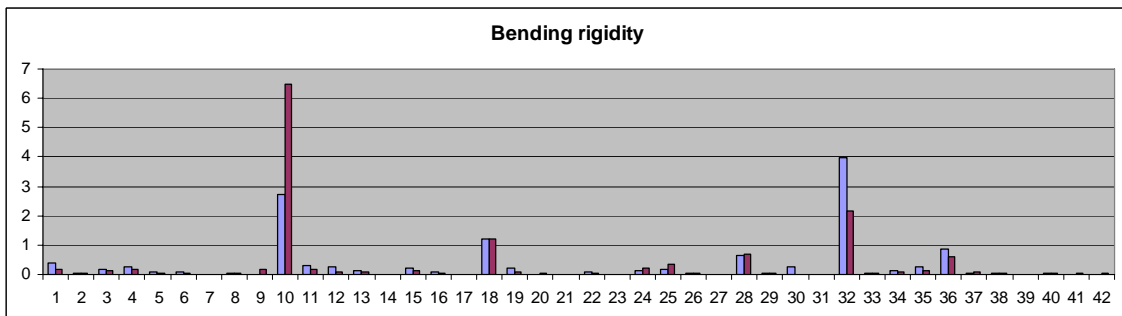
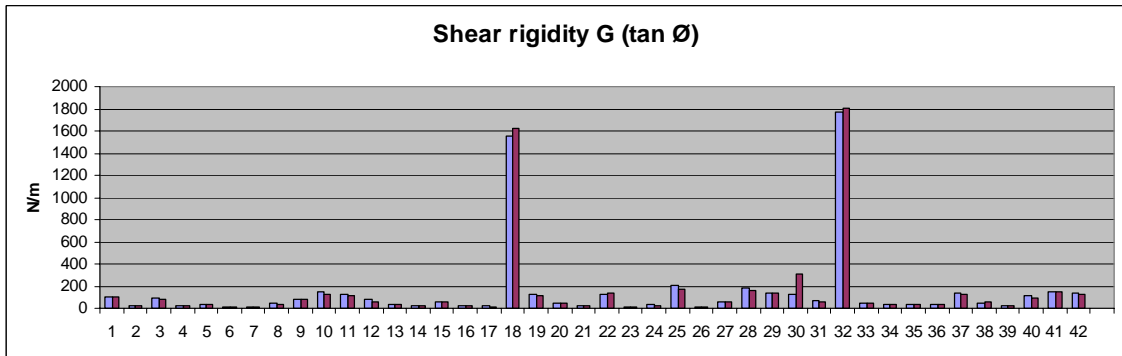
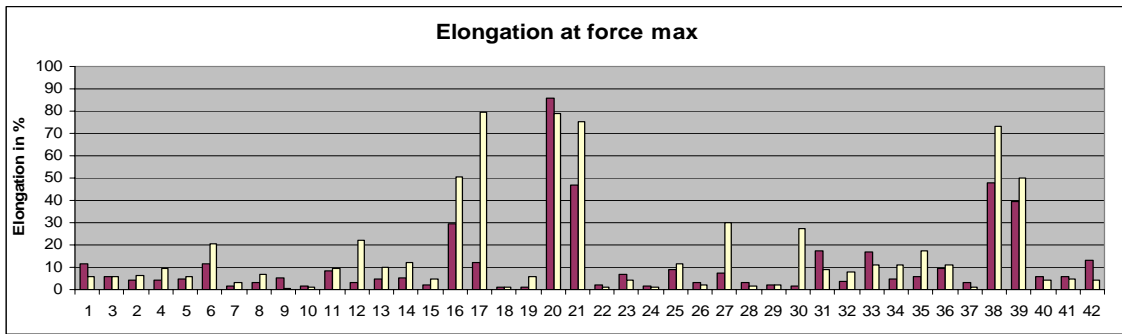
**Figure 55: MIU in weft and warp direction for the first fabric selection**



**Figure 56: MIU in weft and warp direction for the second fabric selection**

The highest measured friction is 0.408 for sample 27\_fleece. The lowest measured friction is 0.103 for sample 18\_motorcyclist wear. Higher friction forces were generally observed for knitted fabrics (16\_lurex-knit, 17\_crepe-jersey, 20\_warp-knit velour), the velour and cord fabrics (03\_cord, 15\_velvet) and for the jacquard weave (28\_woven upholstery fabric). Lower friction forces were observed for plain weave and twill fabrics samples 05\_gabardine, 07\_silk, 09\_tussah-silk and 29\_woven outdoor leisure wear. The friction coefficient differs for weft and warp direction. Most differences in weft and warp direction are visible for the more rough knitted fabrics and the samples 16\_lurex-knit, 17\_crepe-jersey and 30\_tulle. Hence, also a broad variety of friction properties has been observed.

#### 4.2.1.7. Captured data ranges



In summary, the measured data ranges regarding each fabric property are:

	<b>Lowest and highest measured values</b>	<b>Lowest</b>	<b>Highest</b>	<b>Ratios low - high</b>
<b>Tensile</b>	<b>1.02 - 148 %</b>	20_Velour 21_Single-jersey	10_Jute 18_Motorcycle	<b>1 : 145</b>
<b>Shear</b>	<b>10 - 1588 N/m</b>	10_Silk 17_Crepe-jersey	18_Motorcycle 32_Leather	<b>1 : 158</b>
<b>Bending</b>	<b>0.22 - 647 <math>\mu</math> N.m</b>	17_Crepe-jersey 21_Single-jersey	10_Jute 32_Leather	<b>1 : 2940</b>
<b>Thickness</b>	<b>0.1 - 3.99 mm</b>	7_Silk 26_Organza	14_Tweed 27_Fleece	<b>1 : 39</b>
<b>Weight</b>	<b>10 - 815 g</b>	7_silk 30_tulle	28_Upholstery 32_Leather	<b>1 : 54</b>
<b>Friction coeff.</b>	<b>0.103 - 0.408</b>	7_Silk 18_Motorcycle	16_Lurex-knit 27_Fleece	<b>1 : 4</b>

**Table 5: Data ranges**

Clearly the ratios of highest to lowest measurements show that the bending property varies most, followed by the tensile and shear property, considering the entire fabric selection. The friction coefficient is the most uniform data range.

On the other the typical characteristics of certain fabrics (regarding their structure or origin) described in the fabric selection process, could be proved with our standard measurements. The fabric structure is highly influencing the fabrics elasticity characteristic. Knit fabrics possess the highest extensibility. Knit fabrics also bend more easily than woven's.

Regarding the fiber origin, silk fabrics are the most rigid natural textiles (monofilament). Wool fabrics are generally more elastic. All kind of characteristics can be found among Polyester fabrics (synthetics). As they are made out of man-made fibers, all kind of properties can be manufactured.

<b>Type of fabric</b>	<b>Elasticity (N/m)</b>			<b>Bending in N.m (<math>10^{-6}</math>)</b>		<b>Density (g/m<sup>2</sup>)</b>	<b>Thick-ness (mm)</b>	<b>Friction</b>
	<i>Weft</i>	<i>Warp</i>	<i>Shear</i>	<i>Weft</i>	<i>Warp</i>			
<b>Knits</b>	40 to 2000	80 to 3000	19 to 219	0.4 to 6.1	0.22 to 8.1	10 to 288	0.3 to 3.99	0.12 to 0.41
<b>Woven</b>	400 to 12000	1000 to 13000	10 to 1588	0.7 to 647	1.4 to 396	15 to 600	0.1 to 3.9	0.1 to 0.32
<b>Cotton</b>	1000 to 3000	1800 to 3000	20 to 102	3.3 to 17	5.7 to 39	120 to 380	0.6 to 1.88	0.12 to 0.31
<b>Silk</b>	1500 to 10000	1500 to 6000	10 to 80	0.7 to 4	1.4 to 4	15 to 150	0.1 to 0.8	0.12 to 0.18
<b>Wool</b>	600 to 1200	1300 to 3000	14 to 118	6.3 to 19	6.5 to 29	145 to 219	0.55 to 1.53	0.11 to 0.22
<b>Polyester</b>	40 to 10000	80 to 4000	11 to 1588	0.4 to 122	1.6 to 119	25 to 600	0.16 to 399	0.1 to 0.41

**Table 6: Data ranges regarding various types of materials and structures**

#### 4.2.2. FAST

For the specification of the measurement standard see Chapter 2.2.2.3. Fabric samples 04\_linen, 05\_gabardine, 07\_silk, 11\_flannel, 21\_single-jersey and 24\_satin are measured with the FAST method. The output data consists in single measured values for each property:

Sample Nr	Extensibility at 100g/cm warp in %	Extensibility at 100g/cm weft in %	Shear Rigidity (N/m)
11_flannel	3.8	5.3	90
05_gabardine	2.3	3.5	31
04_linen	2.8	6.5	29
21_single-jersey	20.9*	20.9*	21
07_silk	2.2	2.7	15
24_satin	0.8	0.4	30

**Table 7: FAST data extensibility warp, weft and shear, \* exceeded the test machine limit - 21%**

Sample Nr	Bending rigidity warp $\mu$ N.m	Bending rigidity weft $\mu$ N.m	Bending rigidity shear $\mu$ N.m
11_flannel	34.0	25.9	29.7
05_gabardine	9.7	8.7	9.2
04_linen	45.2	21.7	31.2
21_single-jersey	5.9	6.1	6.0
07_silk	1.2	2.7	1.8
24_satin	14.6	20.1	17.1

**Table 8: FAST data bending**

Sample Nr	Weight g/m <sup>2</sup>	Thickness at 2g (mm)	Thickness at 100g (mm)	Surface thickness (mm)
11_flannel	282	1.244	0.926	0.317
05_gabardine	169	0.484	0.376	0.108
04_linen	239	0.766	0.477	0.290
21_single-jersey	216	0.778	0.709	0.069
07_silk	22	0.058	0.043	0.016
24_satin	132	0.232	0.204	0.028

**Table 9: FAST data weight, thickness and friction**

The FAST standard measurement also provides information on fiber, thermal and formability properties. However, as these properties are not part of this study, they are not listed in the table.

### 4.3. Derivation of fabric input parameters

The parameter derivation depends on the one hand on the available empirical data and on the other hand on the complexity of the computation system used. For that reason several simulation systems and the parameter integration are first studied in more detail. Subsequently the applied simulation system is described.

#### 4.3.1. Various simulation systems

For the comparison of various existing simulation systems a cotton fabric is draped over a sphere on a stand. The simulation of a cloth using three different simulation systems (MIRALab, 3DS max, MayaCloth) returns similar results for the cotton parameter (Figure 20). All the three fabrics give however the impression of a quite elastic textile. Having a look at the corresponding input parameter (Table 6) we can see that a comparison of the values is difficult:



**Figure 57: Simulated cotton fabric with MIRALab's in-house simulation application, Figure 58: 3ds max 9 (ClothFX) simulation application, Figure 59: Maya 8.5 (MayaCloth)**

Applications such as 3Dmax, Maya [Autodesk] allow the modification of parameters, but their units are not displayed (Table 6). Hence, it is not possible to enter precise input parameters and the users have to rely on the proposed settings. The comparison of the parameters shows that quite different values are used within each system for the description of a cotton fabric. This can be on the one hand related to the fact that very different textiles have been measured or on the other hand that different units are used.



<b>Cotton</b>	<b>MIRALab</b>	<b>3DSmax 9 (ClothFX)</b>	<b>Maya 8.5 (MayaCloth)</b>
<b>Elasticity parameters</b>	<b>Tensile:</b> Weft: 16 N/m Warp: 16 N/m Shear: 8 N/m	<b>Tensile:</b> no units U Stretch: 75 V Stretch: 75 Shear: 225	<b>Tensile:</b> no units U Stretch Resistance: 200 V Stretch Resistance: 200 Shear Resistance: 50
	<b>Bending:</b> Weft: $0.8 \times 10^{-6}$ N.m Warp: $0.8 \times 10^{-6}$ N.m Shear: 0 N.m	<b>Bending:</b> no units U Bend: 25 V Bend: 25	<b>Bending :</b> no units U Bend Resistance: 100 V Bend Resistance: 100  <b>Bend Rate:</b> (for nonlinearity) U Bend Rate: 0.3 V Bend Rate: 0.3
<b>Viscosity and damping parameters</b>	<b>Tensile Viscosity:</b> Weft: 0.16 N.s/m Warp: 0.16 N.s/m Shear: 0.08 N.s/m	Damping: 0.1 Plasticity: 0	Cloth Damping: 0.2
	<b>Bending Viscosity:</b> Weft: $0.8 \times 10^{-9}$ N.m.s Warp: $0.8 \times 10^{-9}$ N.m.s Shear: 0 N.m.s		
<b>Density</b>	Density: $0.16 \text{ kg/m}^2$	Density: 0.01	Density: 0.01
<b>Thickness</b>	Thickness: 2 mm	Thickness: 0.2	Thickness: 0.2 Thickness force: 1
<b>Friction coefficient</b>	Body: 0 Fabric: 0.2	Static: 0.5 Dynamic: 0.1 Self: 0.5	Static friction: 0.7 Dynamic friction: 0.7 Cloth friction: 0.6
<b>Environment parameters</b>	<b>Air Viscosity:</b> Omni: $20 \times 10^{-3}$ N.s/m <sup>3</sup> Norm: $200 \times 10^{-3}$ N.s/m <sup>3</sup>	Air Resistance: 0.02 Repulsion: 2	Air Damping: 0.05

**Table 10: Overview of input parameters of different simulation applications**

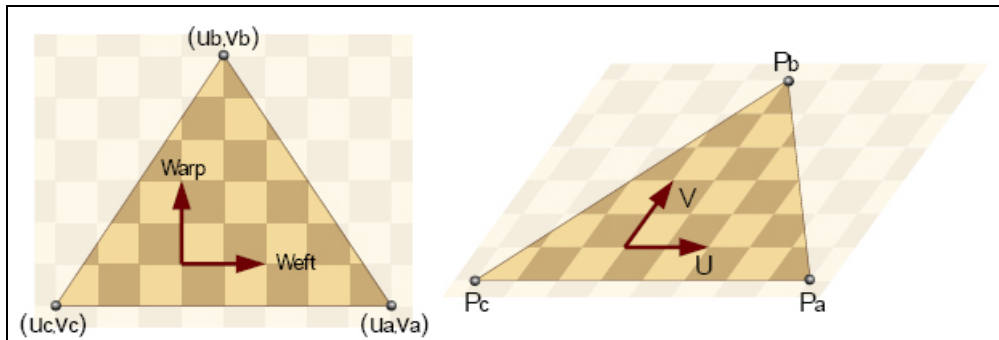
#### 4.3.2. Applied simulation system

The applied simulation method is an accurate state of the art particle system, where the energy minimization scheme corresponds to that of first-order finite elements. [Volino 05] [Volino 06]

- In-plane deformations

The mechanical behavior of a textile, which approximates that of a thin surface, is composed of two-dimensional (tensile, shear) and three-dimensional (bending) deformations. The two-dimensional in-plane behavior is described by relationships that link the stress  $\sigma$  to the strain  $\epsilon$  and its speed  $\epsilon'$  according the laws of viscoelasticity. In the applied model the stresses of triangular elements in weft, warp (uu, vv) and shear (uv) modes are computed precisely

according to the current 3D position of the triangle vertices (Figure 61). Subsequently, the actual strain-stress curves (modeled as piece-wise polynomial splines and derived from the fabric measurements) are used to compute the resulting strain on the element, and equivalent forces are applied on its vertices. The fabrics shear behavior is integrated in the same way as a change of length in the diagonal direction (and not as a change in the angle of orthogonal threads, as measured by KES-f). [Volino 05]

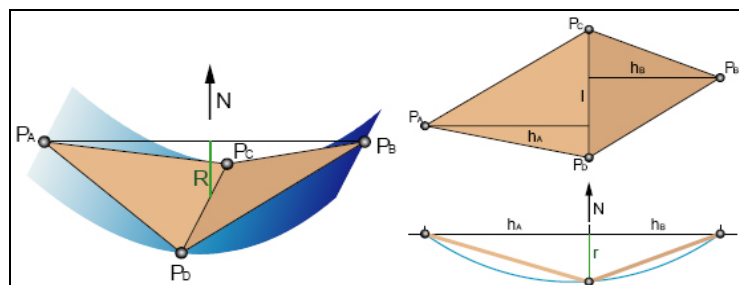


**Figure 60: A triangle element deformed in 3D [Volino 05]**

Generally, there is a dependency between the different elongation modes ( $uu$ ,  $vv$ ) and shear ( $uv$ ). For example, elongating a fabric in the warp direction will tend to shrink it in the weft direction. This behavior is described by the poisson coefficient. In the applied simulation system, the poisson coefficient is not considered and assumed to be null. Hence, the three deformation modes are independent.

- Out of plane deformations

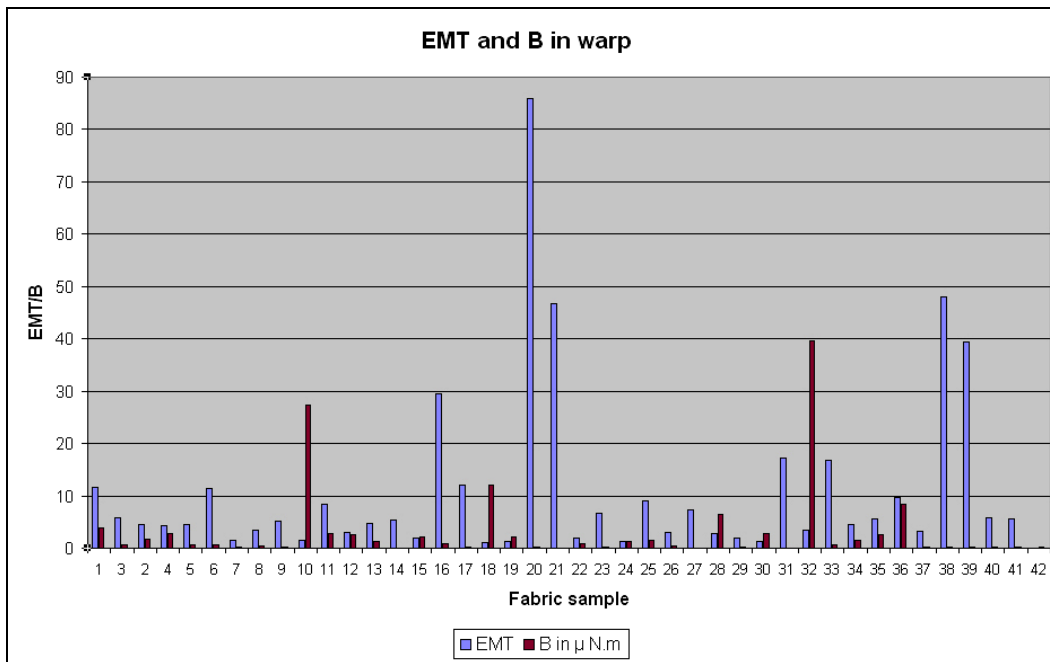
A simple and accurate linear bending model is integrated that relates the bending momentum to the surface curvature in weft, warp and shear direction. For this approach, a “bending vector” is computed that represents the bending of the surface through a simple linear combination of particle positions. This vector is then redistributed as particle forces according to the bending stiffness of the surface. [Volino 06]



**Figure 61: Scheme of the applied bending model [Volino 06]**

The bending stiffness in the applied simulation system is, however, still coupled to the tensile stiffness to some extent, as only the normal-based method allows a perfect separation of tensile

and bending stiffness. This coupling results in some additional tensile stiffness for small edge bending, which has no noticeable effects on the global fabric drape. For large edge bending, some tensile compression effects are obtained that could squeeze the mesh elements which have a low tensile stiffness compared to the bending stiffness [Volino 06]. However, the graph below (Figure 63) illustrates that this characteristic rarely applies for fabrics used for garment productions. Fabrics with a low tensile stiffness (high EMT) generally possess a low bending stiffness.



**Figure 62: Ratio of EMT (max elongation) and B (Bending stiffness)**

- Energy damping

In the applied simulation system, the fabric behavior functions are potential energy functions related to the position of the vertices. In addition damping forces are integrated that specify the position and the velocity of the vertices. Therefore a suitable damping value has to be specified for each elasticity parameter to prevent anomalous in-plane oscillations. These parameters cannot, however, be derived from standard fabric measurements and have to be evaluated by experiments.

- External forces

The integrated external forces in the applied simulation system include gravity, anisotropic viscous aerodynamic drag (wind) and collision effects (friction).

Input parameters	Measured	Approached	Set
<b>In-plane deformations (2D)</b>	Tensile Elasticity: weft, warp, shear	Tensile viscosity: weft, warp, shear	
<b>Out of plane deformations (3D)</b>	Bending Elasticity: weft, warp, shear	Bending viscosity: weft, warp, shear	
<b>External forces/ contact reactions:</b>	Gravity Friction	Air Viscosity	
<b>Physical properties:</b>	Density, Thickness		
<b>Related simulation settings:</b>			Tim step, Surface resolution,
<b>Derivation method:</b>	KES-f, FAST, etc.	Simulation tests	Simulation tests

Table11: Overview of input parameters in the applied simulation system

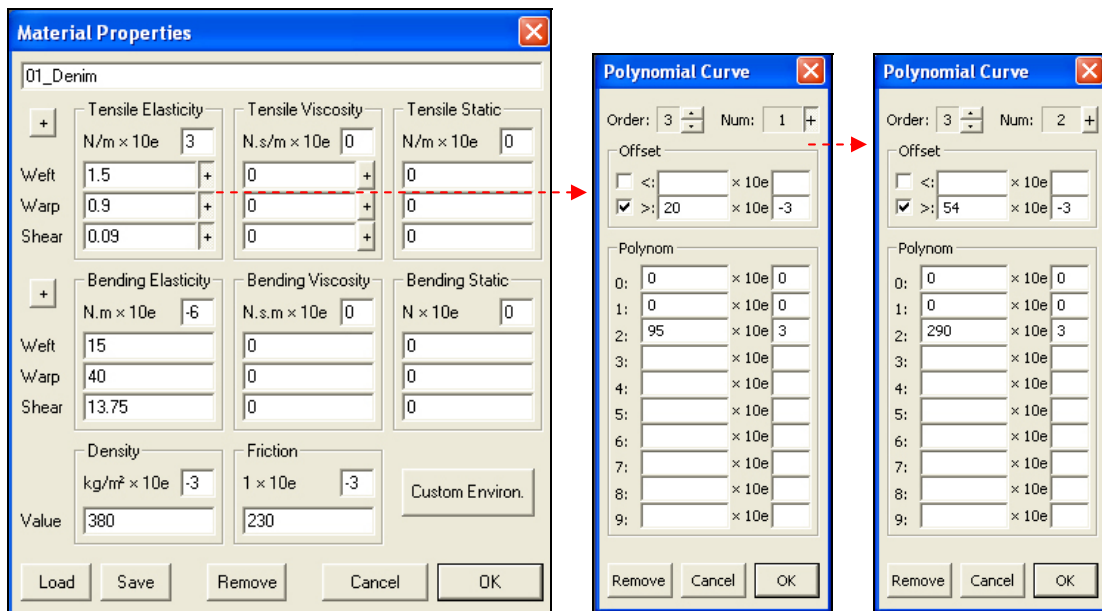


Figure 63: Input parameter box of the used simulation system

#### 4.3.3. Derivation process

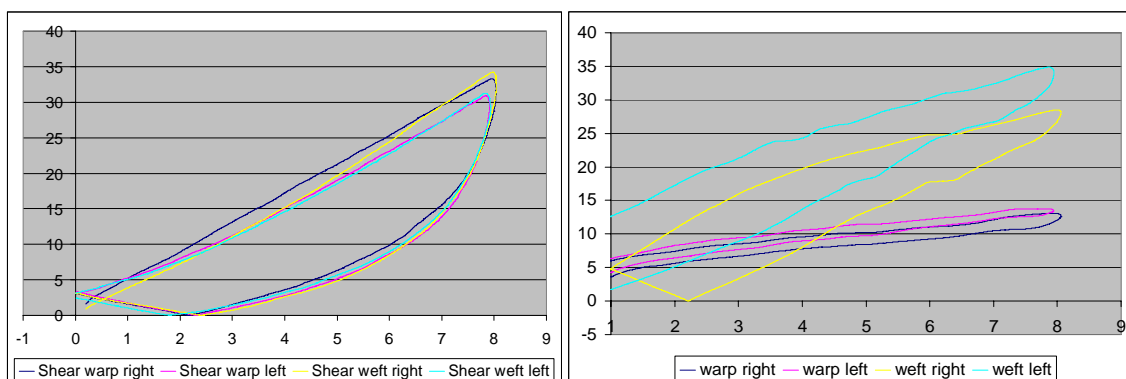
During the actual input parameter derivation process, a suitable mathematical description of the measured data is sought. The applied computation system allows the accurate simulation of the nonlinear tensile and shear behavior. From the FAST data set, linear parameters can be obtained for the six tested fabrics. From the KES-f measurements linear and nonlinear parameters can be obtained for all 42 fabrics. The automatically calculated characteristic fabric hand values can be taken as linear parameters. Nonlinear descriptions are obtained by fitting the force-deformation profile with polynomial splines. The bending property is linear modeled. Thus, a simple linear mathematical interpretation for the bending behavior is sufficient. The bending rigidity value  $B$  is the gradient of the measured data and is hence suitable as linear bending characteristic. The

characteristic fabric hand value MIU (mean friction coefficient) from the KES-f measurements are taken as friction parameter. Viscosity damping parameters can not be derived from the standard measurements. The derived parameters constitute the starting point for further experiments.

#### 4.3.4. Limitations

- Simplification of the shear parameter

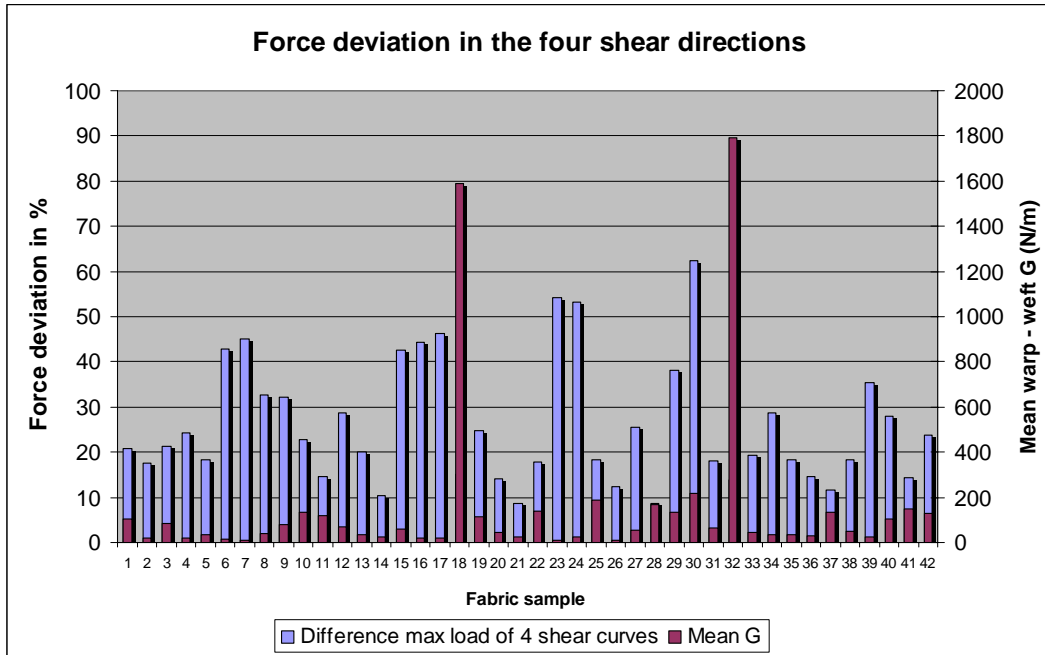
KES-f shear measurements are carried out both, in weft and warp directions, returning four shear behavior curves (Figure 44). The difference of the four maximum measured shear forces for one textile vary from 8.6% (28\_upholstery, Figure 65 left) to 63.1% (30\_tulle, Figure 65 right). As shear input parameter, an average value is taken and hence, the actual shear deviation error can be up to 31.5%. As we can see from the force-deformation shear curves in Annex D, differences occur, on the one hand, by shearing the fabric to the right and to the left side (same fabric direction) and on the other hand, by shearing the fabric in warp and weft direction.



**Figure 64: Four measured KES-f shear force-deformation envelopes for fabric 28\_upholstery fabric (left), Figure 65: 30\_tulle (right)**

The greatest deviations occur for fabrics with a rather different warp and weft tensile behavior and for fabrics where the shear resistance is much lower than the tensile resistance (07\_silk, 23\_crepe, 24\_satin, 30\_tulle, Figure 65). In Figure 66 we can see that by bringing this deviation into correlation with the mean shear resistance  $G$ , the resulting error is considerable.

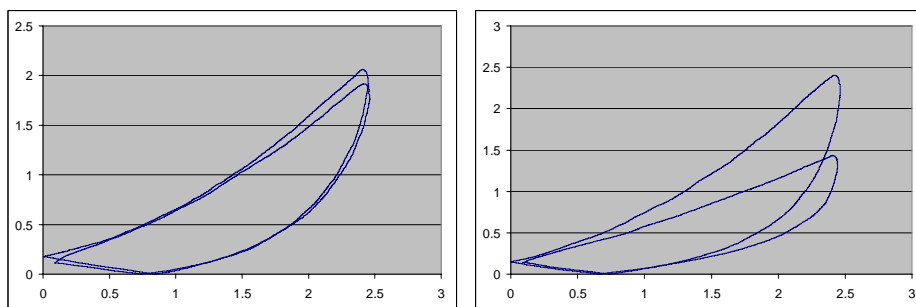
Therefore, we can say that the fabrics shear behavior is direction dependant and for an accurate simulation, the different shear directions should be integrated. However, in the simulation system only one shear mode is considered, supposing a dependency between various shear modes. For that reason, the simplified shear testing method of measuring the bias extensibility of fabrics (FAST) seems to be sufficiently precise for existing fabric simulation applications (what is assessed in Chapter 6).



**Figure 66: Force deviation in % for the four measured shear directions**

- Simplification of the bending parameter

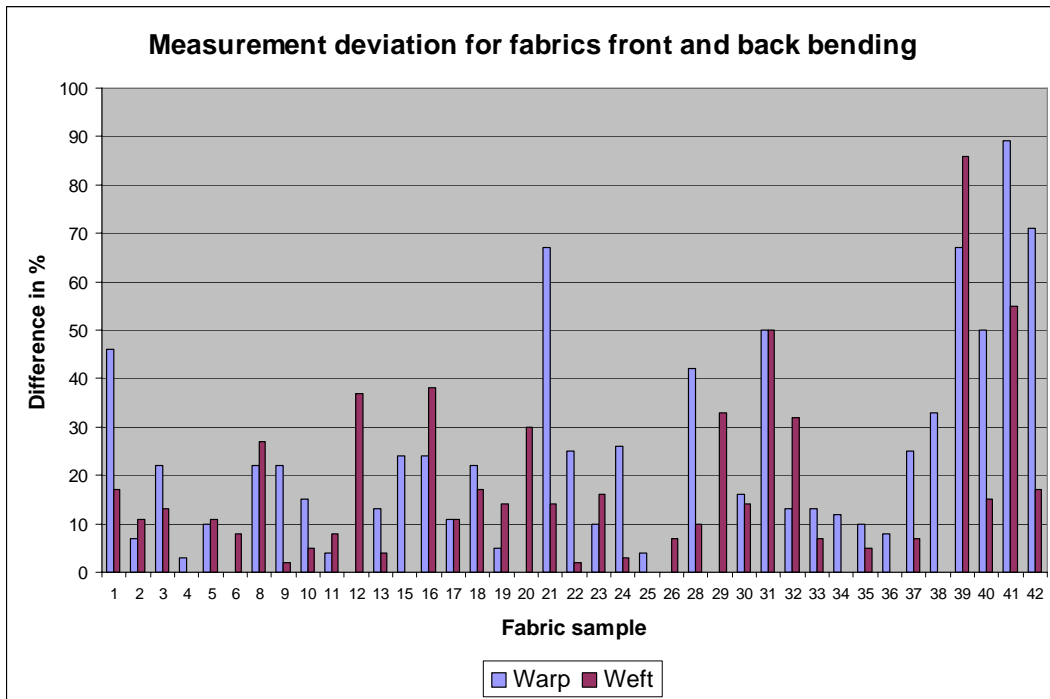
In comparison to shear, the four bending hysteresis envelopes are not reduced to one but to two linear parameters, one for warp and one for weft. The bending behavior is thus less, but still simplified by combining the dissimilar front and back bending within one descriptive parameter. In Figure 67 (left) we can see that for some textiles, the front and back bending moment-curvature relationship is similar. For others (Figure 67 right), a considerable divergence is observed.



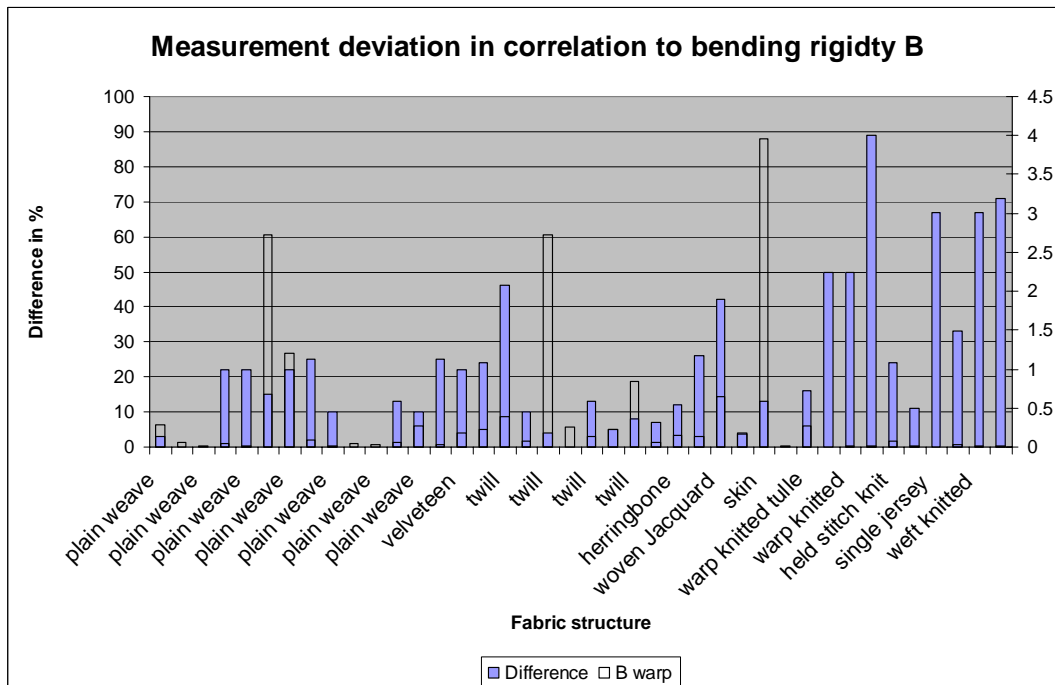
**Figure 67: Good and bad correlating front and back bending force-deformation envelopes sample 28\_upholstery fabric (warp left, weft right)**

The comparison of the front and the back bending measurement returns a good correlation for 30% of the fabric samples. 32.5% of the data shows a medium good correlation and 37.5% of the fabrics show a suboptimal correlation for the front and the back bending (Figure 68). The deviations are smaller for the measurements in weft direction (Also see Annex D, bending

moment-curvature envelopes) and vary from 0% for several textiles to 89% for fabric 41\_warp knitted mesh fabric.



**Figure 68: Measurement deviation for fabrics front and back bending for warp and weft measurements**



**Figure 69: Deviation according to fabric structures in comparison with the bending rigidity B (warp direction)**

The second graph (Figure 69) sorts the bending measurement according to the fabric structure and brings the difference of the front and the back bending into correlation with the bending rigidity value B. We can see that the front and back bending measurements generally differ more for knit than for woven fabrics. However, the deviation of most woven materials is still between 10% and 50% and should thus be considered in the simulation system.

- Fabric thickness and compression

In the applied simulation system, the fabric is modeled as a 2D surface, where the thickness parameter describes the distance between the body and the virtual fabric. However, for an accurate simulation of thickness and compression parameters, a three-dimensional modeled surface is required. Hence, no further experiments are conducted for thickness and compression. The mechanical simulation of compression would, however, add some kind of realism for the simulation of thick fabrics.

#### 4.4. Conclusion

42 fabrics have been chosen in two selection cycles, according to three defined selection criteria, which are the raw material, the planar structure and the fabric's dimension. The first fabric selection consists of a broad selection of very different fabrics, whereas the second selection cycle contains similar fabric samples.

All fabrics are characterized using the standard fabric characterization method KES-f. Six very different textiles from the first selection are measured with the FAST method and the data of both methods are compared. An evaluation of the measurement results shows that our fabric selection represents a broad variety of characteristics for each property as well as a wide variety of the different mechanical properties of textiles. Input parameters for the virtual simulation are derived from the KES-f for all fabrics and from the FAST data for the six fabrics.

At this stage, the input parameters are derived in the best possible way. In Chapter 6, the accuracy of the derived parameters is studied.





## Chapter 5

# Accuracy of fabric input parameters

### 5.1. Introduction

The accuracy of the previously derived parameters is studied consecutively, taking into account a defined accuracy spectrum (Chapter 5.2). Special consideration is given to those properties, which are identified to be important with regards to fitting. Each parameter is tested by static and dynamic simulations, as both computations encompass different requirements.

### 5.2. Definition of the accuracy

#### 5.2.1. Aspects of fit and importance of fabric properties

Garment fitting is a subjective and complex process, where multiple aspects of comfort are assessed. Aspects of fit include the 3D body shape, the fabric properties, clothing physical dimensions, social messages, fashion and body cathexis [Gersak 07]. For virtual simulation it is important to reproduce the garment accurately enough so that the same errors and problems encountered during the real fitting process can be detected. According to Kawabata and Niwa (page 29) [Kaw 89] various fitting and garment quality aspects are tested within three different performances:

- Fabric performance, where problems resulting from clothing manufacturing are assessed.
- Comfort performance, where the fitting of the garment to the static human body is tested.
- Utility performance, where the ease of movement and strength is tested.



Figure 70: Fabric performance [Reflexstock], [Fan 04]



**Figure 71: comfort performance [San], [Reflexstock]**



**Figure 72: utility performance [Reflexstock]**

This distinction is particularly interesting for virtual garment simulations, as each of the three performances, constitute different challenges to the virtual computation: Comfort performance can be related to static virtual garment simulations where correlation of the immobile body and the 3D garment are tested. Utility performance can be tested within dynamic garment simulations, where the garment is evaluated on the moving body. The virtual imitation and simulation of the fabric performance is, however, a more difficult field. On the one hand, a detailed replica of the garment would be needed in order to visualize such small details as seam pucker for example. On the other hand, the real garment manufacturing process (for example sewing), which is when most mistakes occur, is not performed virtually. Hence, subsequent problems and errors do not occur in the virtual prototype and the fabric performance can today not be virtually assessed.

The two main components which influence comfort and utility performance are the 2D pattern and the fabric's mechanical and physical properties. The role of the 2D pattern and aesthetic fabric properties are more important during comfort performance, whereas the functional properties such as tensile are more significant for utility performance. If a garment has the right size, but the shape of the 2D pattern does not fit the physiology of a certain body type, the non-fitting parts cause wrinkles, folds or unwanted deformations in the garment (Figure 74). The improvements in the 2D pattern are then made according to the detected unwanted shapes. Therefore, for an accurate improvement of the 2D pattern, it is important that the non-fitting parts of the garments are accurately simulated so that the necessary changes can be made.



**Figure 73: 2D Pattern misfit and related folds [Reflexstock]**

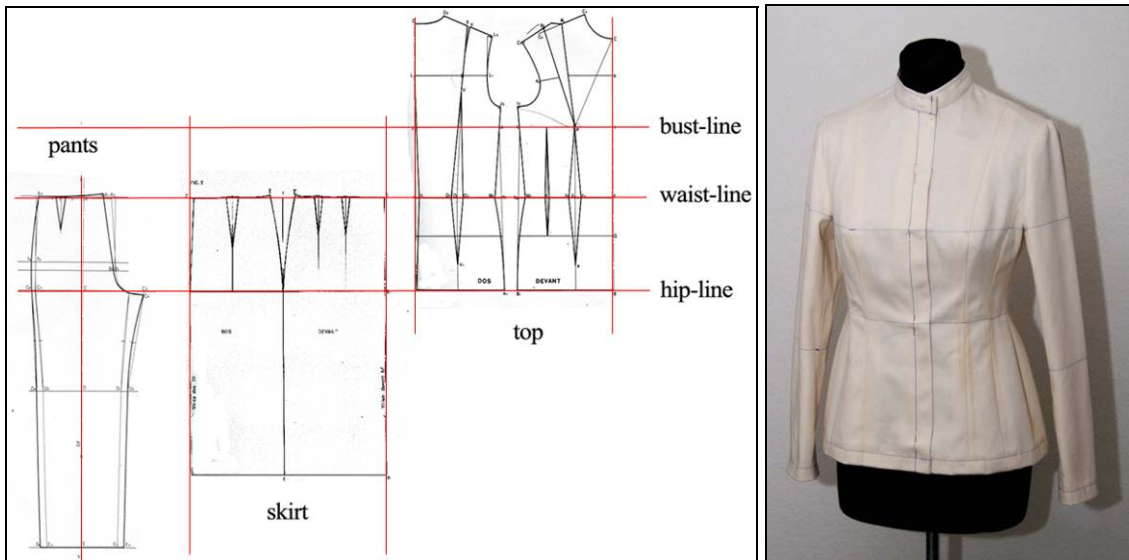
Despite the fact that all mechanical and physical fabric properties affect the fit or the visualization of misfit, their influence can not be generalized, as each characteristic is related to different fabric components. This means that the fabric properties must be classified with regard to their influence on the garment's fit.

We will now examine the importance of each of the eight measured fabric properties on comfort and utility performance. For this, knowledge from the literature as well as own professional tailoring skills (previous profession) are applied.

#### 5.2.1.1. Comfort performance

A piece of clothing is a hull for the human body and therefore the proportions of the human body and the garment have to match. During the design of a new 2D pattern, the contours are constructed over significant horizontal and vertical body lines such as the hips, waist, bust, middle front and middle back. The major horizontal and vertical body lines are then combined with style lines, darts and folds to obtain a characteristic new garment design (Figure 75).

During comfort performance, the correlation of the garment and the static body is tested. At this point, the vertical and horizontal 2D pattern construction lines serve as guides for the evaluation of the fit (Figure 75). Mechanical and physical fabric characteristics are responsible for a smooth drape of the garment on the body. The stiffer the material, the more visible misfits become; the softer and more elastic the material, the smoother the drape of the garment over the body. In the second case, fitting inaccuracies might be blurred by the soft drape. During comfort performance, four important fit elements are tested: Grain, set, line and balance [Fan 04]



**Figure 74: 2D pattern construction with base lines, Figure 75: Garment showing base lines**

- Grain is the horizontal and vertical direction of a fabric. To give a garment an equal and symmetric appearance, the 2D patterns are constructed in such a way that the lengthwise grain runs parallel to the centre front and centre back of the clothing. The crosswise grain should run horizontally to the bust/chest and hip level.
- A good set refers to a smooth fit with no undesirable wrinkles. Undesired wrinkles occur when the form of the garment does not correspond to the form of the body. Hence, a poor set arises for example if a rather straight body shape is dressed with a feminine cut garment. In this case the garment is either too loose or too tight in some areas.
- The line is related to the design and follows the silhouette and circumference lines of the body. During this assessment the correlation of the new real garment to its design idea is tested.
- Clothing that is balanced appears symmetrical from side to side and front to back. For made to measure garments this part can be particularly challenging as the human body and its posture is not symmetric and the garment has to compensate for this.

After the definition of comfort performance, now the question is which of the mechanical and physical fabric properties are the most influential during the comfort performance assessment? The bending property is of aesthetical importance as it is the main influence on the drape of the garment over the body. The tensile property is an important functional property, which is related to the dimensional comfort. The shear property influences the fabric drape and dimension in the bias direction and is, therefore, both an important aesthetical and functional property. Detected unwanted wrinkles occurring from a less good garment set can be compensated to some extent

by the elasticity properties. For example a low tensile, shear and bending stiffness can reduce wrinkles, clouding the judgment.

The friction property plays an important role during the evaluation of the body/garment correlation, as this property can prevent the garment from draping in the right position on the body, thus increasing unwanted wrinkles.

The roughness property of a textile may influence the physiological comfort (i.e. the textile is not comfortable on the skin) but has less influence on the comfort performance.

Thickness, compression and weight properties do not necessarily influence the fit of a garment. However, the influence of these properties increases for extreme values. For example a heavy fabric, used for an asymmetric garment, can elongate the piece of clothing in some places and influence the grain and balance. A very thick textile can adversely influence the set, line and balance. The compression parameter becomes important for thick textiles as well.

Subsequently, elasticity properties and the friction are judged as important for comfort performance. Weight, thickness and compression properties only influence the comfort performance for extremely high and low values. The roughness property has no influence.

	tensile	shear	bending	friction	roughness	weight	thickness	compression
Comfort performance	+	+	+	+	-	o	o	o

**Table 12: + = important, o = medium, - not important**

#### 5.2.1.2. Utility performance

A garment also requires adequate fitting ease to provide comfort and allow room for movement. Additional ease for style reasons is called “design ease” [Fan 04]. The necessary amount of ease of movement depends on the use of the garment. Sports and leisure wear garments need a greater movement ease than, for example, formal evening wear. The ease of movement of a garment emerges either from a loose cut 2D pattern or from an elastic fabric material. For tight garments, generally elastic fabrics are used.

- Influence and importance of standard fabric properties

The most influential fabric properties for the utility performance are the tensile and shear characteristic. Bending is an aesthetic property, which has already been assessed by comfort performance. It does not directly influence the ease of movement of a piece of clothing. However, some fabrics might not drape well during movement, which may result in a garment being rejected. Therefore, bending is still judged to have an importance during utility performance.

The friction property also plays an important role for the body/garment interaction. It influences whether or not a garment falls in the right position during movement and is therefore considered as an important property of utility performance.

Once again the roughness property of a textile has little influence on the utility performance, whilst thickness, compression and weight properties will influence the ease of movement only for extreme values. A very thick or heavy textile, as well as a textile with a high resistance to compression could reduce the ease of movement.

We may conclude that tensile, shear, bending and friction properties are all important for utility performance. Weight, thickness and compression properties only influence the utility performance for extreme values. The roughness property has no influence.

<b>Standard</b>	tensile	shear	bending	friction	roughness	weight	thickness	compression
Utility performance	+	+	+	+	-	o	o	o

**Table 13: + = important, o = medium, - not important**

- Influence and importance of other fabric characteristics (viscosity and plasticity effects)

In contrast to comfort performance, during utility performance, not only the standard eight fabric properties are influencing the behavior of the cloth. The movement of the fabric implies some other, more complex issues, which subsequently also have to be considered during dynamic virtual garment simulations.

As described in Chapter 2.1., fabrics are complex viscoelastic materials. This means, that the fabric material does not immediately or fully recover, after the removal of an applied stress. This effect is most visible for elastic fabrics, containing a low amount of elastane. For example after sitting, the garment would keep for a while the deformation on the back. Some of the deformation might not recover. These effects are related to the fabrics viscosity and plasticity properties. Various fabrics possess very different viscosity and plasticity effects. The viscosity and plasticity characteristic is important for all elastic properties. The bending viscosity property for example is influencing the “movement” of the folds during motion.

As this is also an important aesthetic measure during utility performance (a pants may be rejected during prototyping, if deformations do not recover well), these characteristics have to be considered during the garment evaluation and also be accurately recreated during virtual simulations.

<b>Additional</b>	viscosity	plasticity
Utility performance	+	+

**Table 13a: + = important, o = medium, - not important**

### 5.2.1.3. Summary

In summary, we can state that tensile, shear and friction are the most important mechanical fabric properties for garment evaluation. The bending property is mainly assessed during comfort performance and has a medium importance for utility performance. Weight, thickness and compression may be critical properties for extreme values. Roughness is judged to be of least importance during comfort and utility performance.

	Ten- sile	Shear	Ben- ding	Fric- tion	Rough- ness	Weight	Thick- ness	Compres- sion	Visco- sity	Plasti- city
Comfort performance/ static simulation	+	+	+	+	-	o	o	o		
Utility performance/ dynamic simulation	+	+	+	+	-	o	o	o	+	+
<b>Total:</b>	+	+	+	+	-	o	o	o	+	+

**Table 14: + = important, o = medium, - not important**

Again for comparison, after [Kaw Niwa 98], the important fabric properties for fabric hand are extension (tensile), shear, bending and compression. However, the compression property was considered as important for the touching of fabrics. Hence for the virtual simulation of touch [Haptex 07], the compression is a more important input characteristic. [Gersak 02] considers tailoring components such as elastic properties, formability (possible compression of a fabric until no buckling occurs = bending rigidity \* extensibility) and drape as most important for garment evaluations.

[FAST 94] considers the fabric properties which describe the resistance to deformation, such as tensile, bending and shear as the most important.

### 5.2.2. Accuracy spectrum

In general, virtual simulations give much more detailed information about the fit and comfort of a garment in the form of precise numerical data than the real and merely visual assessments provide. On the other hand, the aim of the virtual simulation is the imitation and replacement of the corresponding real action. Hence, the demand for accuracy of the virtual simulation should be oriented to the real garment fitting and evaluation. Despite the fact that the virtual computation delivers more detailed data, a tested parameter is judged as accurate if it is as precise as the smallest identifiable value of the corresponding real process. It is, therefore, necessary to establish a spectrum of precision for each parameter, based on the real garment assessment.

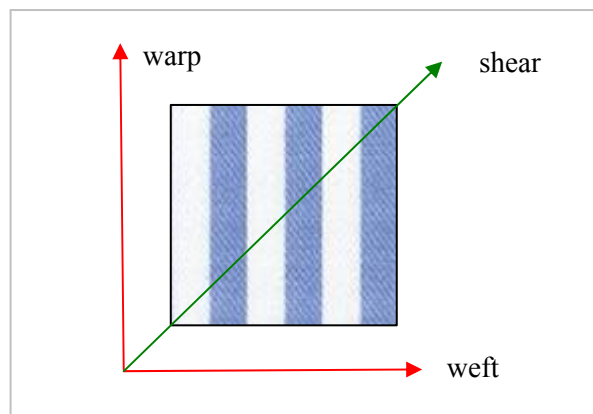


First a scheme of precision is defined for each property, upon which the characteristics are evaluated and real and virtual processes are compared. Precision values are defined for each property, to which the simulation results are compared. The accuracy spectrum is defined for the aesthetic and the dimensional/functional aspects. In general, the limit for aesthetic aspects is determined by the smallest distance which may be detected by the human eye. The limit of dimensional aspects is characterized by the smallest noticeable difference in garment tensions.

#### 5.2.2.1. Schemes and values of accuracy

- Tensile and shear

For the tensile and shear characteristic the dimensional aspects of the fabric in the three directions on the textile are considered for the evaluation of the simulation tests (Figure 76). For tensile and shear the simulated parameter has to be precise for two different aspects of precision: On the one hand the parameter has to be functionally accurate and on the other, aesthetically and visually precise.



**Figure 76: Scheme for the tensile parameter evaluation**

Although it was mentioned before that the meaning of the tensile characteristic (of real textiles) is more a functional one, its virtual replica has to be tested for aesthetic/visual aspects too. The tensile parameter need only be mechanically accurate enough that there is no perceptible difference to the human eye. For example for an accurate judgment, a virtually simulated skirt must not be identifiably longer than the real one. This also applies to smaller fabric pieces on a garment, for example collar reverts and pockets. The smaller the fabric pieces, the easier it is for errors to be detected by the human eye. For a better comparison, several significant distances on a garment are measured, the smallest identifiable differences are specified and the maximum authorized difference returned in % (Table 15, 16):

Garment part	Length	Smallest visual identifiable difference	Maximum allowed difference
Revert	~ 70 mm	0.5 mm	0.7%
Belt width	~ 40 mm	0.5 mm	1.25%
Pocket	~ 160 mm	1 mm	0.62 %
Skirt length	~ 500 mm	1 mm	0.2 %
Pants length	~ 1100 mm	3 mm	0.27 %

**Table 15: Required aesthetical (visual) accuracy for different parts of a garment**

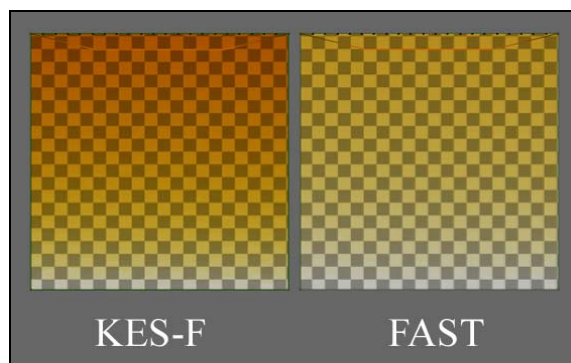
Garment feature	Length	Smallest felt difference	Maximum allowed difference
Bust circumference	~ 900 mm	10 mm	1.1%
Waist circumference	~ 700 mm	5 mm	0.7%
Hip circumference	~ 1000 mm	10 mm	1%

**Table 16: Required functional (felt) accuracy for different parts of a garment**

The smallest visibly identifiable difference values are defined with a safety margin. It would be difficult to recognize a divergence of 3 mm in pants with a length of 1.1 m. However, taking 0.2% as a limiting value for the tensile and shear accuracy is a reasonable value for the comfort performance with a good safety margin. For the utility performance, the tight visual accuracy scale is loosened to the smallest “felt” difference of 0.7%.

Three different simulation tests are applied for the tensile and shear simulation tests:

- (1) A hanging cloth is used for static simulation tests, where the fabric is elongated under its self weight (Figure 77). For tensile tests the fabric is a square and fixed on the upper edge. For the shear tests the fabric is a rectangle and fixed on the side.
- (2) A typical stretch fitting movement, where lower and higher forces are believed to act on the garment, is used for the dynamic simulation tests: the mannequin moves its arms forward and stretches the back of the jacket (Figure 78).



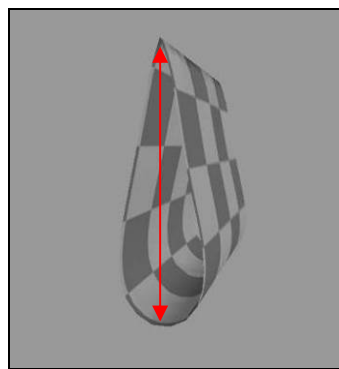
**Figure 77: Hanging cloth (left),**



**Figure 78: Stretch fitting posture movement**

- Bending

For the bending property, aesthetic characteristics are visually evaluated with simulation experiments. At first sight the draping method seems to be suited for these tests. However, at this stage only the pure bending characteristic should be assessed and the influence of other aspects such as shear be minimized. Therefore, the cantilever or the loop test methods (as described on page 17) are suitable where only the bending property is to be assessed. However the virtual hanging cloth of the Cantilever method might be distorted by Air Damping parameters. Therefore the loop method (Figure 79) is chosen. The draping test is used for the final validation tests.



**Figure 79: Bending loop test method**

- Viscosity and Plasticity

As the viscosity and plasticity properties are no measurable characteristics today, it is difficult to define their limit of accuracy. Moreover, we will see later on this work that the modeling of both parameters is still challenging today (see 5.3.3 and 5.4.)

### 5.2.3. Conclusion

Of the three garment evaluation components - fabric, comfort and utility performance - only utility and comfort performance processes can be virtually simulated. Fabric performance can not be assessed today with virtual methods as the correlating processes are not simulateable. We can also say that the comfort performance is a more complex procedure than the utility performance, since more aspects are evaluated in detailed.

Important fabric properties for the garment fitting process are identified as tensile, shear, bending and friction. Thickness, weight and compression are found to be of medium importance, whereas the roughness property has no importance for garment comfort and utility performance.

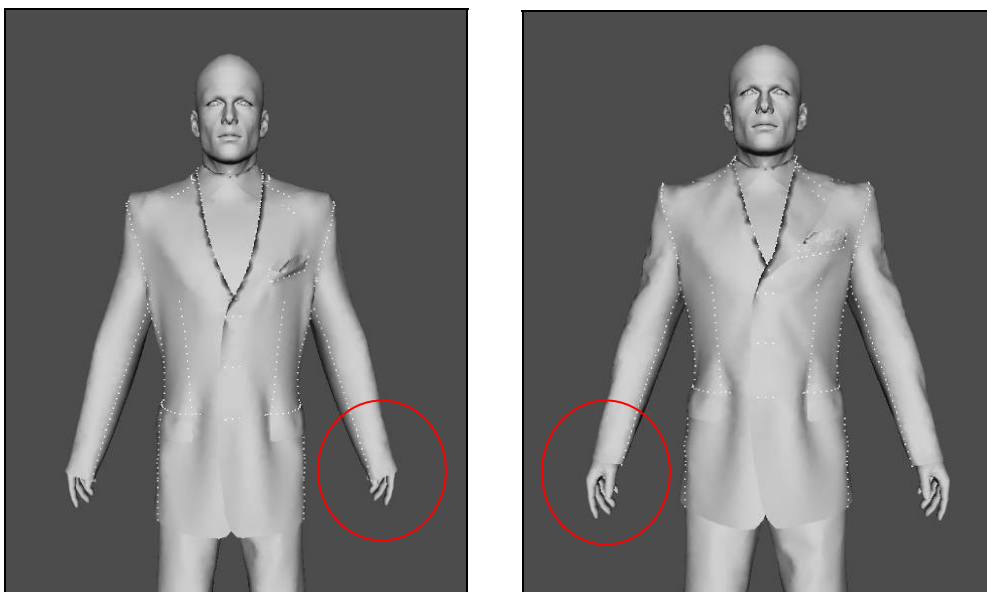
### 5.3. Accuracy of the elasticity parameters tensile, shear and bending

The different elasticity parameters describe the strain-stress relationship for a textile material in various fabric directions: the tensile and shear property constitute the two-dimensional in-plane deformations and the bending property the three-dimensional out of plane deformation. (In comparison to the viscosity parameter, which relates each elasticity parameter to the deformation time/speed). The measurement results from Chapter 4 show that the greatest stresses occur, when a fabric is stretched (as it is when a garment is worn). Lowest forces are needed for the fabric bending.

#### 5.3.1. Earlier fabric parameters

The tensile property is the one which differs the most from earlier imprecise fabric parameters. For example new tensile parameters vary in their linear part for small forces from 50 to 10.000 N/m. In comparison, older fabric parameters varied from 6 to maximum 50 N/m. An earlier cotton parameter describes a fabric, which elongates by up to 60% of its own length at an applied force 100 N/m. A typical new cotton parameter, for example, only elongates 3% under the same applied force. Thus, former tensile parameters describe much too elastic materials and are far from realistic (Figure 80). Former fabric parameters consist of mostly isotropic material descriptions, where the shear behavior is derived from the warp/weft elasticity. As with the tensile property, former shear parameters also describe materials, which have too elastic behavior.

New parameters for bending vary from between  $0.2 \times 10^{-6}$  and  $647.9 \times 10^{-6}$  N.m. Former bending parameters thereafter vary from  $0.8 \times 10^{-6}$  to  $18 \times 10^{-6}$  N.m and are therefore in the very low range of real measurements and describe materials, which bends too easily.



**Figure 80: Former cotton parameter (left) and new linear derived FAST cotton parameter (right)**

### 5.3.2. Elasticity parameters in static simulations (comfort performance)

During static simulations, the fabric's self-weight (SW) acts as a force on the garment. The weight properties of the fabrics in the first and second fabric selection lie between 15 g/m<sup>2</sup> to 815 g/m<sup>2</sup> (see Figure 53). Hence, a garment made out of the lightest silk fabric corresponds to a force of 0.15 N/m for 1 meter of fabric. A garment made out of the heaviest leather fabric corresponds to a force of 8.15 N/m for 1 meter of fabric. (A ready tailored garment, however, can contain approximately between 0.5m and 3m of fabric, which corresponds to forces of 0.075 N/m, 4.07 N/m and 0.45 N/m, 24.45 N/m). The accuracy of the elasticity parameters in static simulations is tested for the six very different fabrics, measured by the FAST and the KES-f method.

The KES-f force-deformation envelopes of the elasticity parameters show that fabrics generally behave in a linear fashion in the low force area, which occurs under the fabric's SW. The fabrics hysteresis behavior can be neglected for static simulations, as only one deformation process takes place. Consequently, it could be thought at a first glance that the simpler linear FAST data set is precise enough for an accurate parameter derivation for static fabric simulations. However, this hypothesis will be investigated by the following two simulation experiments, which apply KES-f and FAST parameters.

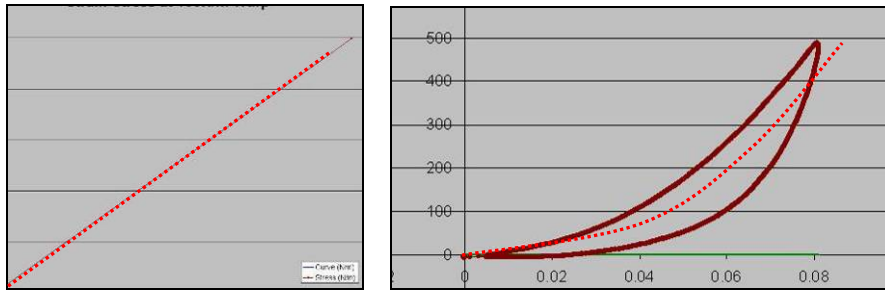
#### 5.3.2.1. Tensile and shear

The elongations shown in Table 17 for the warp and shear direction under the self-weight (SW) are taken from the standard KES-f measurements.

1 m <sup>2</sup> fabric	Weight	Force N/m	Elongation in warp under fabrics SW	Elongation in shear under fabrics SW (mean weft - warp)
04_linen	250 g	2.5 N/m	~ 0.2%	5.45° ~ 0.48 cm = 2.4%
05_gabardine	175 g	1.75 N/m	~ 0.1%	3.56° ~ 0.31 cm = 1.55%
07_silk	15 g	0.15 N/m	~ 0.02%	2.39° ~ 0.21 cm = 1.05%
11_flannel	290 g	2.9 N/m	~ 0.5%	0.71° ~ 0.062 cm = 0.31%
21_jersey	172 g	1.72 N/m	~ 1%	4.19° ~ 0.37 cm = 1.85%
24_satin	125 g	1.25 N/m	~ 0.01%	2.95° ~ 0.26 cm = 1.3%

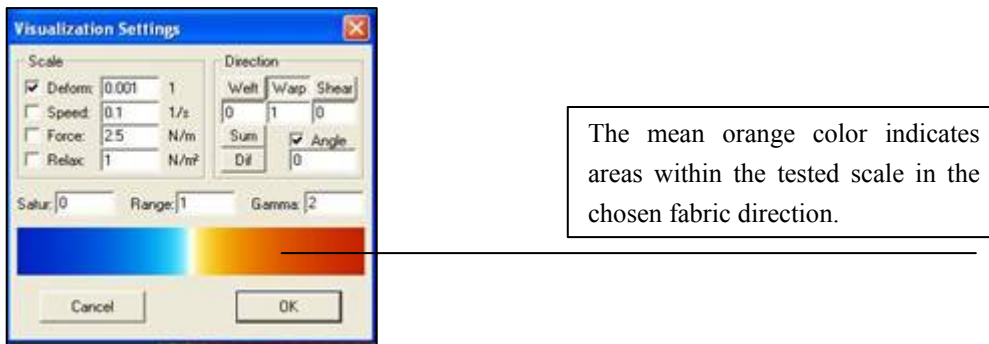
**Table 17: Fabric deformations at their SW**

We can see that all six fabrics are already more elastic in shear direction under their SW. In Chapter 5.2.1., we defined the maximum allowed deformation deviation for the tensile and shear accuracy as 0.2%. Thus, all shear deformations as well as some warp and weft deformations (e.g. fabric 04\_linen, 11\_flannel, 21\_single-jersey) need to be accurately simulated in static simulations.

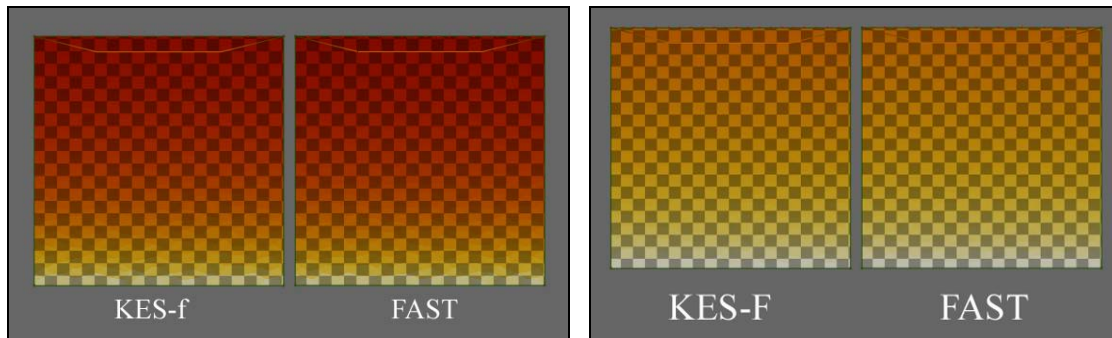


**Figure 81: Linear derived data from FAST, Non-linear interpreted data from KES-f**

Within the first simulation experiment the tensile parameter is tested. Therefore, a piece of cloth with the dimension 1m x 1m, fixed on the upper side is computed. Parameters derived from KES-f and FAST (Figure 81) are applied and the resulting fabric elongations compared with the help of a colorscale (Figure 82).



**Figure 82: Colorscale**

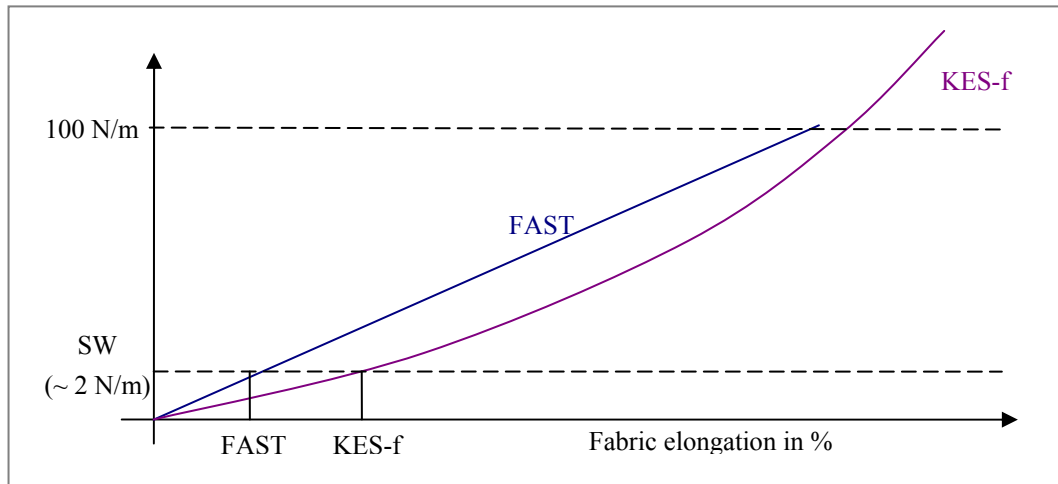


**Figure 83: Tensile deformations under the fabric SW for sample 21\_single-jersey (left) and 11\_flannel (right), deformation scale 0.2% in warp direction**

The first simulation experiment shows that there is no difference in the fabric's tensile deformation. The respective KES-f and FAST parameters give the same simulation result for the six tested fabrics in static simulations (Figure 83). This means that although the linear FAST parameter is slightly inaccurate in the low force area (Figure 84), the difference appears to be too small to noticeably influence the simulation result. The orange colorscale visualizes all fabric elongations around 0.2%. The color shades for all simulations correspond to the fabric

deformations at their self-weight. For example fabric 11\_flannel elongates 0.5% at its SW and shows therefore lighter colors than the mean colorscale (Figure 83).

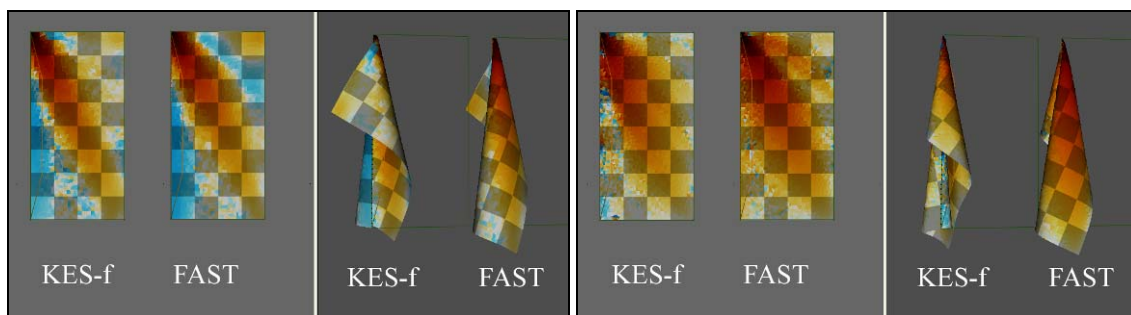
Hence, both, KES-f and FAST tensile parameters are accurate enough for static fabric simulations, where the self-weight acts as force on the textile.



**Figure 84: Scheme – inaccuracies of FAST tensile parameters**

The second simulation experiment investigates the shear parameter for static simulations. This time, a rectangular piece cloth is fixed on the longer side and simulated. Fabric elongations of 0.2% in the shear direction are observed.

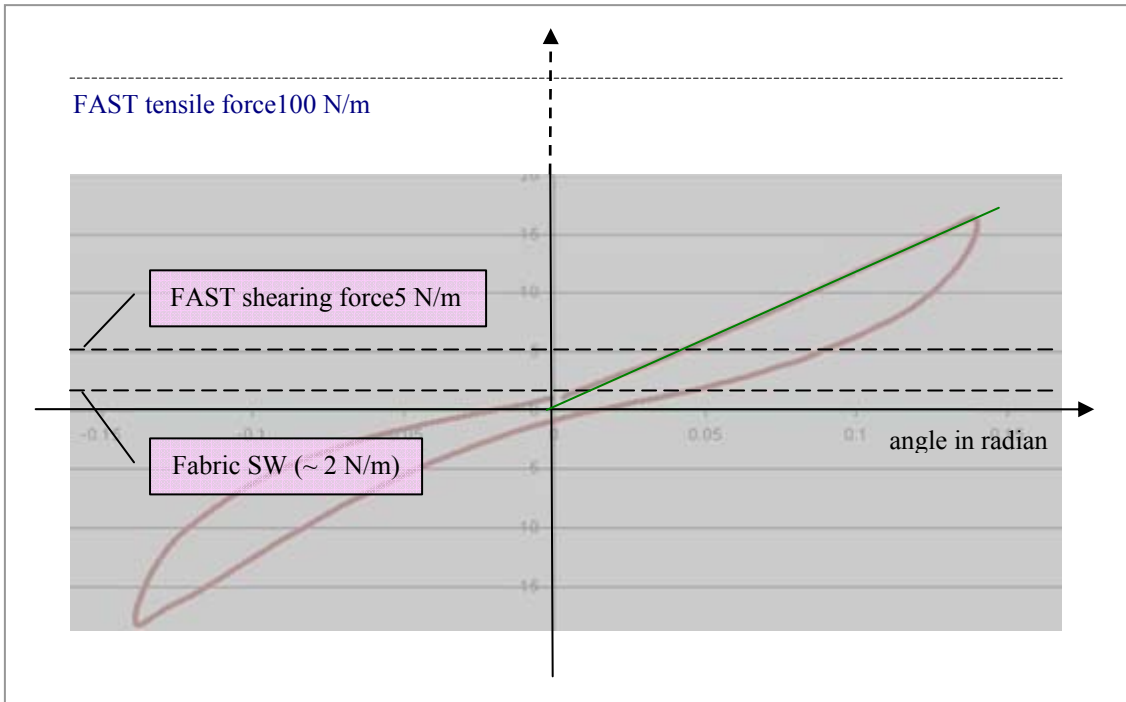
First, the medium to good correlating linear shear parameters, resulting from the different KES-f and FAST shear measurements and calculations of the shear rigidity are applied. The simulation experiments returned almost identical results for all fabrics (Figure 85).



**Figure 85: 2D and 3D view of simulated hanging rectangle, visualizing fabric elongations of 0.1% (accuracy limit) in shear direction. 24\_satin (left) and 21\_single-jersey (right)**

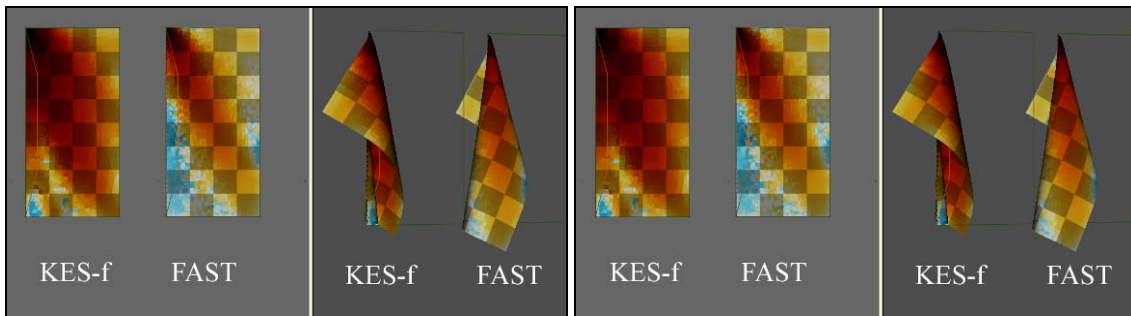
In Figure 86 we can see that for the shear parameter, in contrast to the tensile parameter, the measured forces and elongations correspond much better to the forces of the fabrics SW. This fact seems to indicate that the potential for errors, resulting from a linear data interpretation, should be small. However, fabrics are much more elastic in the shear direction and hence possible inaccuracies are more visible than for the tensile parameter.





**Figure 86: Shear forces, fabrics SW and FAST tensile forces - scheme**

Three of the six tested fabrics show a nonlinear shear behavior (sample 04\_linen, 05\_gabardine and 24\_satin). Simulations comparing the nonlinear KES-f and the linear FAST parameter show different fabric elongations in shear direction for two different fabrics (Figure 87).



**Figure 87: Elongations of 0.2% in shear direction using nonlinear KES-f parameter and linear FAST parameter, 04\_linen (left) and 05\_gabardine (right).**

Looking at table 16, we can see that fabric 04\_linen is the fabric with the highest weight among the three samples. Fabric 04\_linen also shows the greatest deformation difference using the nonlinear KES-f and the linear FAST parameter. Fabric 24\_satin, which is a lighter fabric, does not show any difference for the simulations with the linear and nonlinear parameter.

Hence we can conclude that the KES-f and FAST shear parameters are equally accurate for static simulations of fabrics exhibiting linear shear behavior. For fabrics with a nonlinear shear behavior, inaccuracies can occur for textiles with greater densities. For fabric densities greater than 150 g/m<sup>2</sup> the nonlinear KES-f shear parameter should be used.

Nevertheless, regarding the nonlinear shear parameter, we should not forget that inaccuracies might already be within the parameter, resulting from the simplification of considering only one average shear force-deformation curve out of four. In contrast to dynamic simulation (6.2.5.1.), this simplification however has little influence on the precision of static simulations, as the forces take place in a bandwidth where the four force-deformation curves overlap (Figure 65 and 86).

### 5.3.2.2. Bending

In comparison to tensile and shear, the bending property is an aesthetic characteristic, which is visually assessed. In Chapter 4.3.3. we already learned that the front and the back bending measurement data does not correlate well for 37.5% of the fabrics of our fabric selection and deviations vary up to 89% (fabric 41\_warp knitted mesh, Figure 68). As in the simulation system only one bending parameter per fabric direction is considered, the derived parameter is an average value of the front and the back bending measurement.

For the assessment of the accuracy of the bending parameter in static simulations, the loop length test method is applied. First the real fabric's loop length is tested to the front and to the back and is compared. Subsequently, the average real loop length is evaluated against the virtual simulated one and deviation identified. (For the test specification see Figure 79 and page 17). Afterwards, the test results are again compared to simulations using the simplified FAST parameter. In total, 30 fabrics of both fabric selections are tested (Figure 88 and 91).

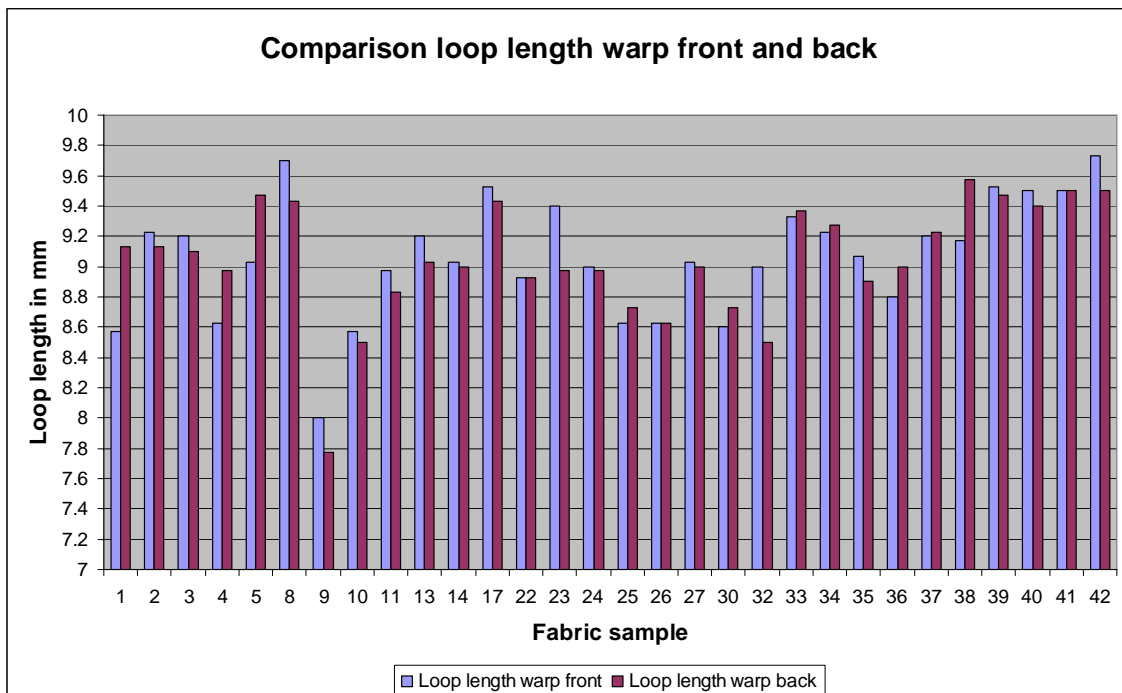


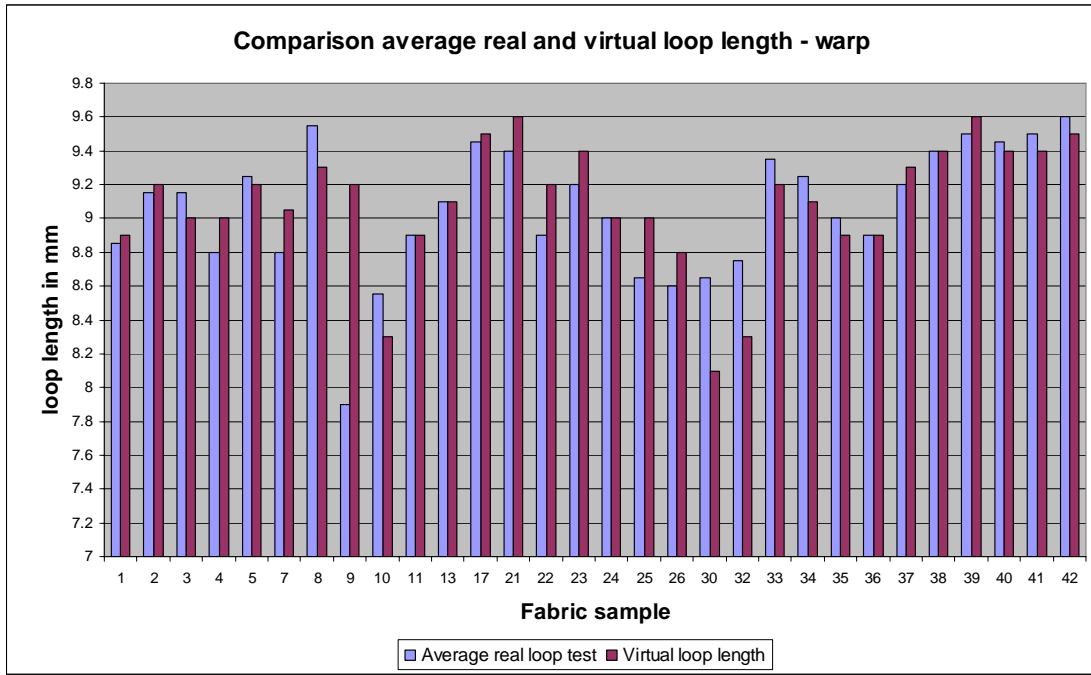
Figure 88: Comparison of real warp front and back bending



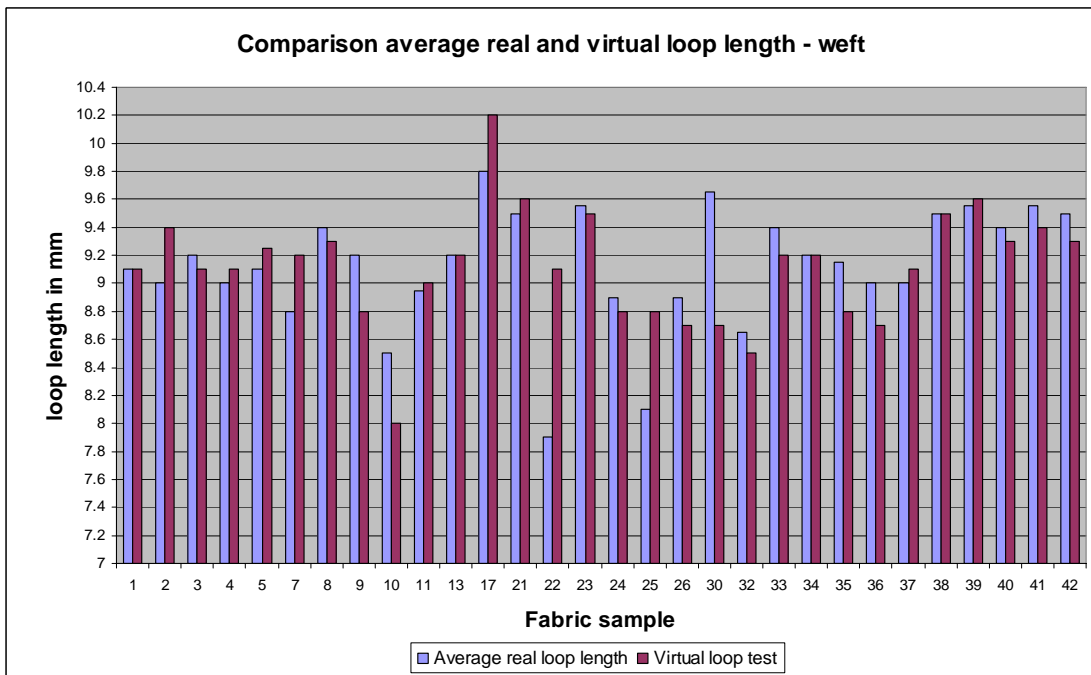
**Figure 89: Comparison of real weft front and back bending**

Observed deviations for the loop length to the front and to the back lie within a smaller scale (0% to 6.1%) than deviations of the KES-f bending measurement (0% -89%, Figure 68). This can be explained with the fact that the KES-f method measures the moment-curvature relationship in a greater bandwidth than occurring during the loop length test, where only the fabric's SW acts as bending force. Hence, deviations are much smaller. The maximum bending parameter deviation, resulting from the simplification of the bending parameter, is thus 3.05% (01\_denim warp) for static simulations (mean value of max deviation of 6.1%). As shown in Figure 88 and 89, most deviations lie however in the range of around 2% (~1-3mm).

Next, the correlation of the average real front and back loop length and the virtual simulated loop length is tested. This comparison returns a good correlation for 26 fabrics in warp direction and for 23 fabrics in weft direction (Figure 90, 91). The sub-optimal correlation occurs for fabrics which are easy drape able and possesses a high bending rigidity (09\_wild-silk, 22\_taffetta). Thus, deviations might be related to drape effects, which prevent the fabric from hanging freely.

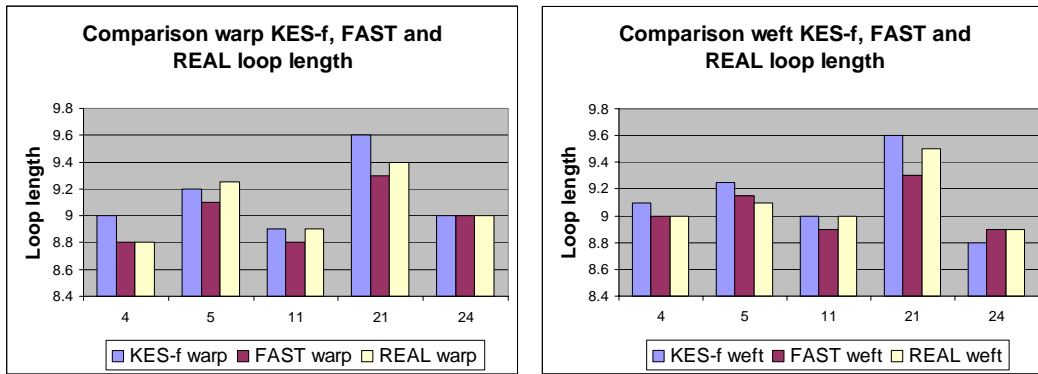


**Figure 90: Comparison average real and virtual loop length in warp direction**



**Figure 91: Comparison average real and virtual loop length in weft direction**

The front and back fabric bending is not individually assessed by the FAST measurement. The returned bending parameter is thus already simplified. The comparison of the virtual loop length simulation using KES-f and FAST bending parameters only correlates for fabric 24\_satin warp. Simulations with the FAST parameter correlate however well to the average real bending for four fabrics (warp: 04, 24; weft: 04, 24).

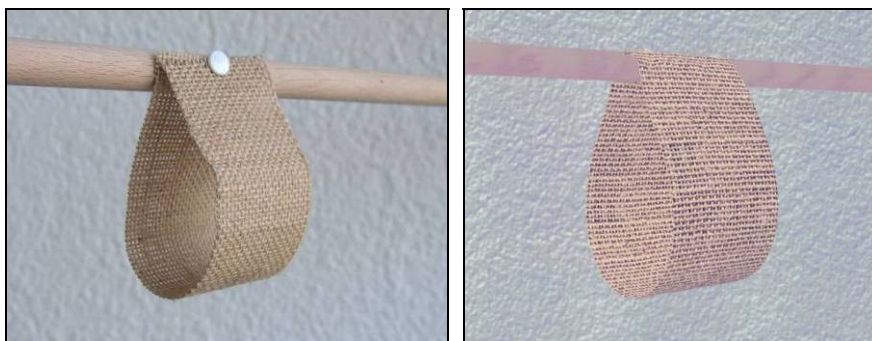


**Figure 92: Comparison KES-f, FAST and average real front and back bending**

The visual comparison of the three simulations is however satisfactory as shown in Figure 93 and 94, vanishing assessed inaccuracies.



**Figure 93: Real bending loop front, KES-f bending loop, FAST bending loop**



**Figure 94: Loop length test 10\_jute real (right) and virtual (left)**

The simulation experiments show that parameters derived from KES-f are slightly inaccurate for static simulations, because of the simplification of the bending characteristic by not considering the front and the back bending. The FAST measurement (based on the Cantilever principle) corresponds better to the simplified bending parameter and to static simulations, but constitutes an inaccurate measurement. The visual comparison of the three different loop length (real, KES-f, FAST) returns however satisfactory results.

During the bending simulation experiment, the resolution of the virtual fabric (amount of triangles) becomes a critical aspect. For the definition of the fabric resolution see Annex H.

#### 5.3.2.3. Pressure

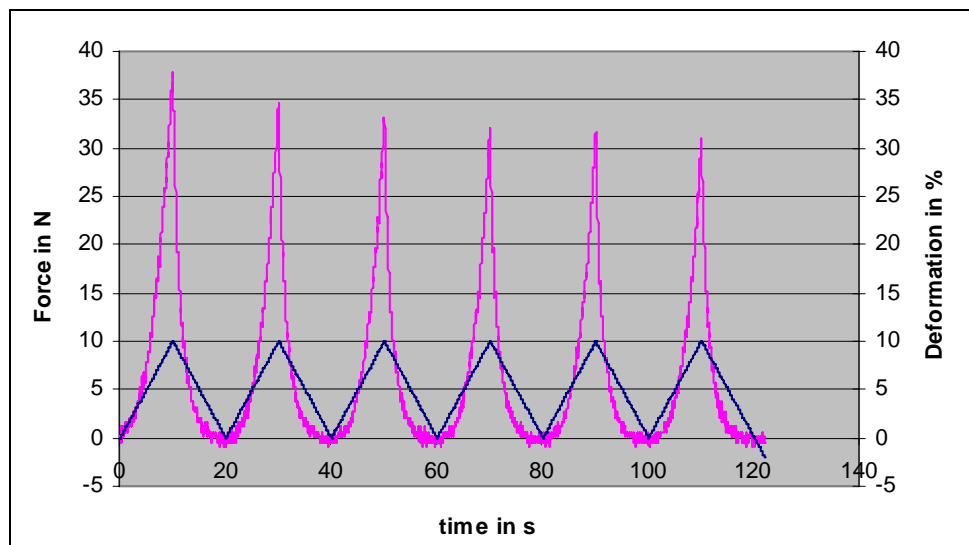
Higher tensile and shear forces than those caused by the fabric self-weight can, however, occur in static simulations in the case of stretch or compression garments, where tight garments exert some kind of pressure on the body. The degree of pressure, generated by a tight garment, is dependant on the fabric elasticity and can be visualized with the colorscale. To determine the accuracy of the pressure property, the elastic parameters have to be studied under greater forces than the fabric's self-weight. These higher forces are treated in the next chapter on dynamic garment simulation.

#### 5.3.2.4. Conclusion

Static garment simulations can be performed reasonably accurate using the KES-f measurement data. This fact is advantageous, since the comfort performance is the more complex evaluation process during garment prototyping and fitting. Only regarding the bending property, small inaccuracy can occur because of the simplification of not considering the front and back fabric bending.

### 5.3.3. Elasticity parameters in dynamic simulations (utility performances)

Compared to static simulations, the virtual imitation of dynamic fabric behavior is a much more complex subject. Depending on the body movement, not only the fabrics self-weight, but very different low and high loads can act on the garment at different frequencies. Thus, it is not sufficient any more to know only the force-deformation relationship. For an accurate parameter derivation for dynamic garment simulations, we also have to know to what extent and at what speed the viscoelastic fabric material recovers after the release of each load, as the preceding deformation cycle influences the subsequent cycle (Figure 95).



**Figure 95: Six deformation cycles of 10% elongation. Less and less force is needed for the same deformation, as the fabric does not fully recover from previous load.**

- Measurement problem

For a truly accurate imitation of the viscoelastic fabric behavior in dynamic garment simulations it would be necessary to measure all possible occurring force sequences at all potential force rates. This however is not possible, as the work load would be far too large. As a result it becomes clear that a fabric parameter for dynamic simulations can never be 100% accurate, (even if the simulation system would be 100% accurate) as it is impossible to measure all potential force sequences and rates that may occur.

- Limitations of the simulation system

In state of the art simulation systems, energy functions compute the 3D position of the vertices. The fabrics hysteresis behavior is not modeled; the spatial displacement process does not consider whether a deformation or a recovery process is concerned, where the energy and hence, the derived vertices position would be different. The decelerated recovery process is imitated by the position and velocity dependant viscosity damping parameter, which accompanies each elasticity parameter. The permanent plasticity effects (permanent deformations) are, however, not considered and have to be expressed somehow within the elasticity parameter.

- Subsequent steps

In the following, the measurement protocols of standard measurement methods and of potential alternative measurement methods are tested for the new requirements and limitations of dynamic garment simulations. At this point, two main aspects are of interest:

- (1) Are the measurements performed in a suitable bandwidth?
- (2) Are the forces and deformations applied in the right way?

Based on this knowledge, the most accurate parameters are derived and suitable measurement protocols are proposed. Correlating viscosity damping parameters are discussed later in a separate paragraph.

### 5.3.4. The tensile property in dynamic simulations

#### 5.3.4.1. FAST - KES-f tensile parameter

So far the accuracy of the FAST and KES-f tensile parameters are tested for the low force area (previous paragraph). Now their degree of accuracy for higher force areas is examined.

In static simulations the fabrics self-weight acts as a known tensile force on the garment. The bandwidth of potential tensile forces during dynamic simulations cannot be evaluated, because the loads that act on a garment during wear are unknown. For this reason, the subsequent simulation experiments are an approximation, where the parameters are tested on a typical fitting movement: the mannequin is moving the arms forward and stretches the back of the jacket.

Simulation tests are performed using FAST and KES-f parameters. During movement, each fabric is elongated to the same extent in order to demonstrate the forces that arise. For that reason the emerging forces of 100 N/m and 500 N/m (the maximum forces of FAST and KES-f measurements) are visualized with the colorscale (Figure 96) and not the fabric deformation.

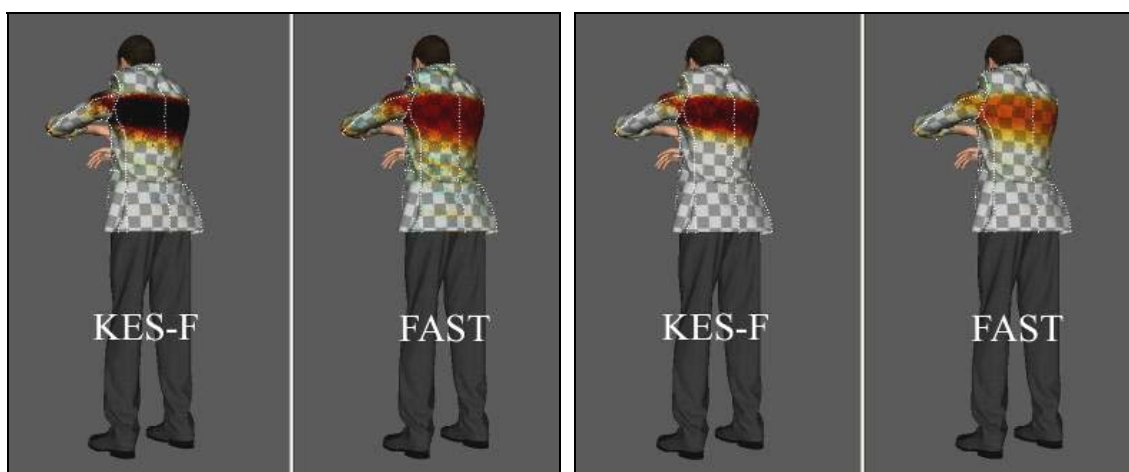
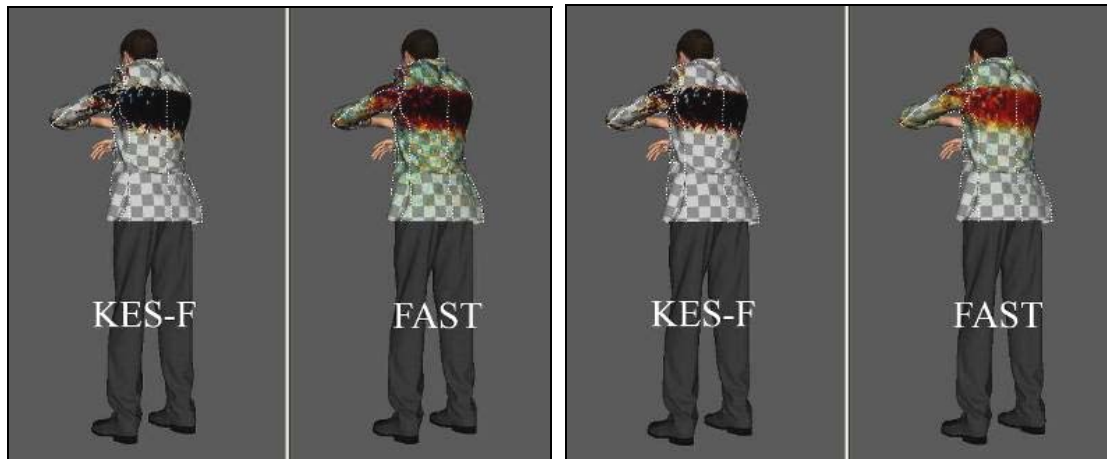


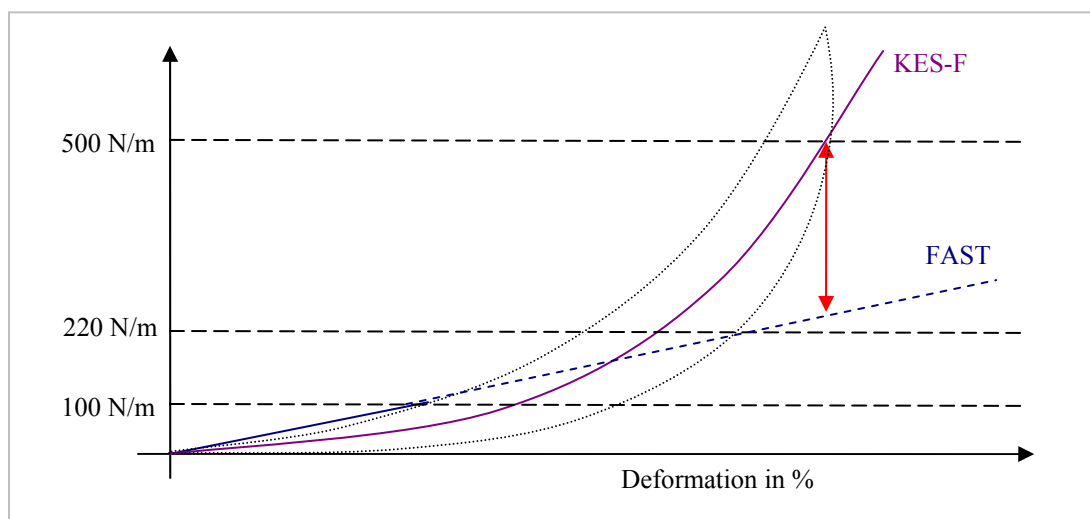
Figure 96: Fabric 05\_gabardine at 100 N/m (2 left jackets) and 500 N/m (2 right jackets)





**Figure 97: Sample 24\_satin at 100 N/m (2 left jackets) and 500 N/m (2 right jackets)**

All simulations show lower forces (lighter orange-color) and hence better comfort for the jackets simulated with the FAST parameter. Comparing both parameters, KES-f and FAST, in the higher force area (Figure 98) it becomes clear that the fitting feedback from the FAST simulation is imprecise. The linear derived parameters from FAST become more and more incorrect with increasing forces, as much lower loads are sufficient to achieve greater fabric elongations. Accordingly, we can say that the FAST tensile measurement is not suitable for the derivation of parameters for dynamic garment simulations. The KES-f tensile parameter appears at this stage to be better suited.



**Figure 98: Comparison of FAST and KES-f parameter in the higher force area**

However, the dark color in the colorscale in Figure 97 also shows that much higher loads than the maximum applied force of the KES-f measurement (500 N/m) seem to act on the garment during the fitting movement. This signifies again that regarding dynamic simulations, the KES-f measured force range is too small.

In addition, the single applied load of the KES-f method does not reflect, what happens during the wearing of garments, where the fabric is exposed to a series of elongations and relaxations. Hence, we can say that the KES-f parameter is accurate for the one specific measured load, but not for a sequence of diverse low and high loads. Therefore, additional tensile measurements are required.

#### 5.3.4.2. New measurement specification: Step tensile measurement (ITT)

Based on the previously outlined new requirements and limitations for dynamic garment simulations, a new tensile measurement is designed. The two key points for this configuration are, on the one hand, that the fabric is tested over a broader bandwidth of forces and on the other hand, that it is measured with a series of various forces.

Previous simulation experiments demonstrated that a maximum force of 500 N/m is not enough for tensile tests. Therefore, the new maximum force is doubled and set to 1,000 N/m. In addition, the new measurements are performed with five increasing force steps where, after each peak is reached, the force is completely released. The applied force steps are 200, 400, 600, 800 and 1,000 N/m with a wait phase of 120 sec. in between. The integrated wait phase should allow for the recovery of the viscous part of the fabric so that only the non-recoverable deformation is recorded by the measurement data. In doing so, plasticity effects are integrated in the subsequently derived parameter.

An alternative tensile measurement device, the more flexible Instron Tensile Tester is chosen for the new experiments. The Tensile Tester only allows a maximum sample width of 5cm. The force is applied along a sample of length 10cm. All textiles of the first and the second fabric selections are tested again.

- Measurement data

Five progressive force-deformation envelopes are obtained for each measurement cycle in weft and warp direction (see Annex D). In comparison to the standard KES-f force-deformation envelope, more information over a broader bandwidth is obtained (Figure 99).

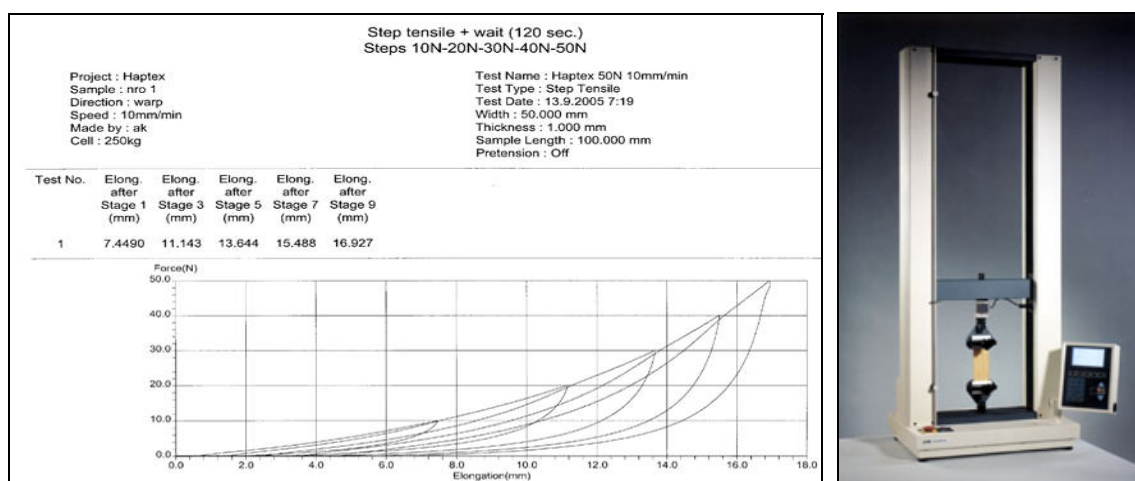
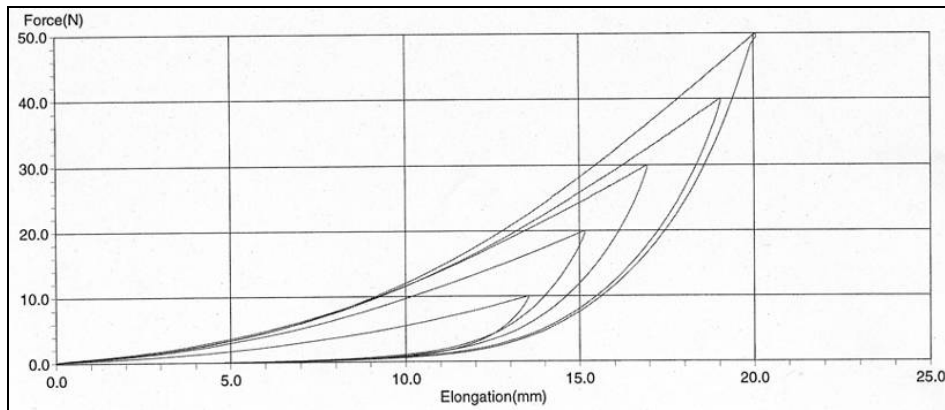


Figure 99: Example of the ITT measurement report page, Instron tensile tester

The single envelopes of each measurement cycle resemble one another and the evolution of the loops is homogenous for each measurement. The fabric's plasticity effects prevent the overlay of the single force-deformation envelopes. A completely viscous fabric material with no plasticity effects would completely recover after the release of the force and the force-deformation envelopes would look like in Figure 100. However this case does not exist in reality.



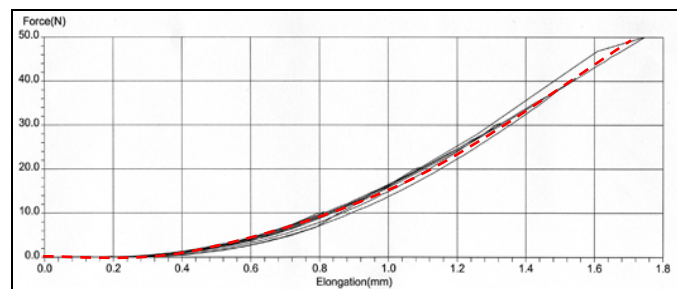
**Figure 100: Sample 01\_denim weft, recovered by hand after each load peak**

- New parameter derivation

In comparison to the single KES-f force-deformation envelope, the five progressive ITT envelopes allow a better study of the tensile hysteresis behavior and hence, a more accurate parameter derivation. The accuracy of the parameter is dependant on the dimension of the enclosed area of the hysteresis envelopes, as larger envelopes leave more space for an inaccurate interpretation of the measurement data. The measurement data reveals that the fabrics fall into four main categories of complexity of parameter derivation:

Category 1 (6 fabrics):

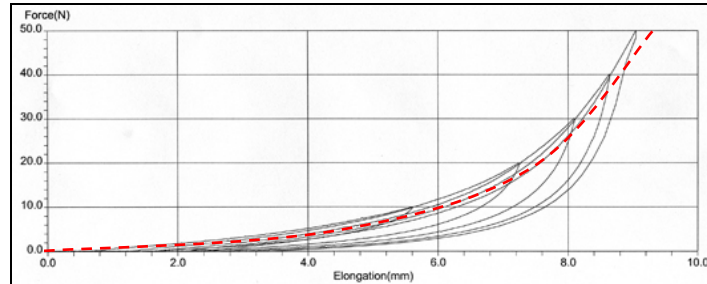
Fabrics in this category show very little hysteresis behavior. The elongation and relaxation curves are rather flat and almost overlay one another (Figure 101). This category of envelopes can be most precisely fitted with one polynomial spline. The most rigid fabrics in plain weave or satin exhibit this kind of force-deformation profile.



**Figure 101: Category 1, sample 07\_silk warp**

Category 2 (largest category, 26 fabrics):

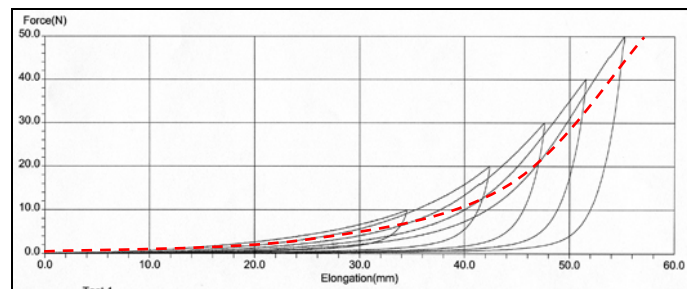
Fabrics in category 2 exhibit a medium hysteresis behavior. The measurement data of this category can still be quite accurately mathematically interpreted. Fabrics are medium elastic and contain all kinds of structures. If we assume that the fabric behavior occurs within the bandwidth of the five measured deformation curves, the inaccuracy of the derived parameter is its respective distance to one of the five elongation curves.



**Figure 102: Category 2, sample 03\_cord warp**

Category 3 (8 fabrics):

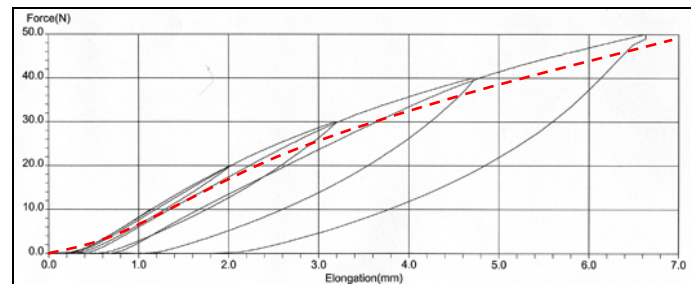
Fabrics with a large hysteresis behavior are part of this category. Fabrics of this category are the most elastic ones such as knits.



**Figure 103: Category 3, sample 16\_lurex-knit warp**

Category 4 (2 fabrics):

The particularity of this category is the decremental elongation and the incremental relaxation curve. Fabrics of category 4 possess a medium to large hysteresis behavior.



**Figure 104: Category 4, sample 26\_organza warp**

### 5.3.4.3. Comparison KES-f - ITT

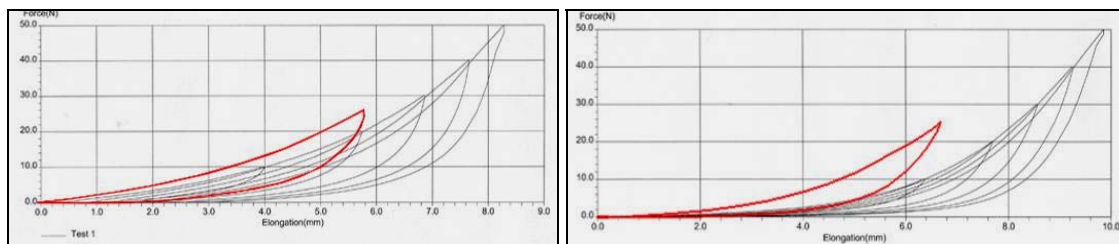
As previously stated, the KES-f parameter is accurate for its measured range, but unsuitable for parameter derivation for dynamic simulations. The broader and more precise ITT measurement should give more precise data. Next, both measurement data sets and their derived parameters are compared to see if the new, more complex ITT measurement is truly more precise or if the standard KES-f measurement returns similar data.

- Correlation of the measured data

The KES-f data can be compared with the third measurement cycle of the ITT method, as this is the first step where the maximum force of KES-f (500 N/m) is attained. 32 fabrics show a fairly good correlation, where the majority of those fabrics are in categories 1 and 2 (Figure 105 left).

	Rather good correlation	Suboptimal correlation
Category 1:	07, 09, 18, 22, 24, 29	-----
Category 2:	01, 02, 03, 04, 05, 06, 08, 09, 10, 11, 12, 13, 14, 15, 19, 23, 28, 32, 33, 34, 35, 36, 37,	30, 40, 41, 42
Category 3:	17 (warp), 20	16, 17 (weft), 21, 27, 31, 38, 39,
Category 4:	26	25

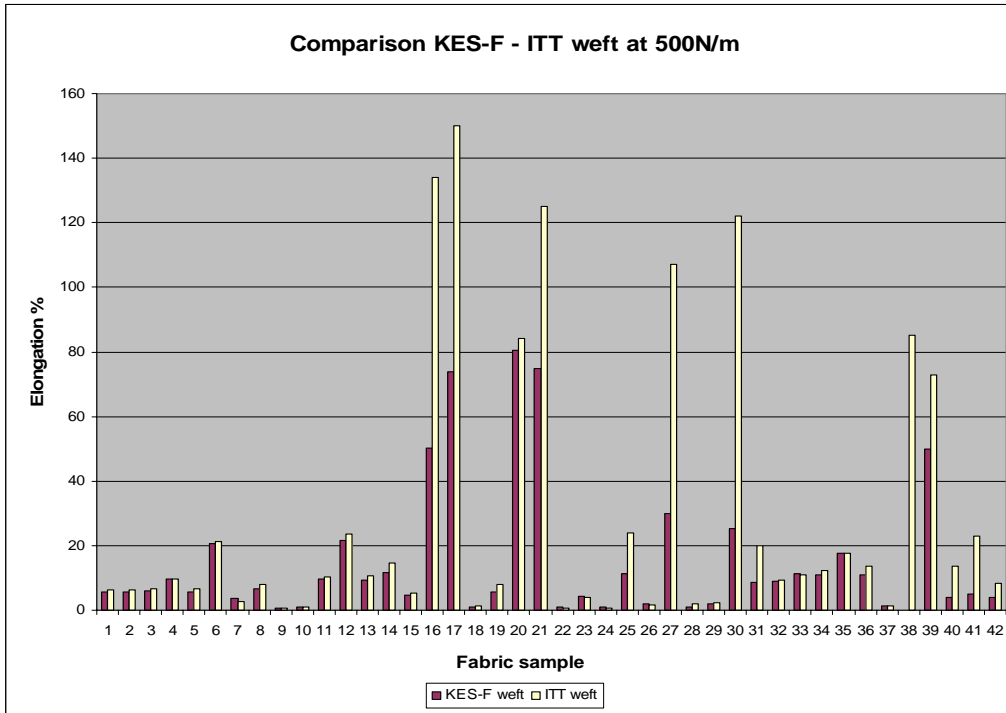
**Table 18: Correlation of KES-f and ITT**



**Figure 105: Correlation KES-f and ITT 01\_denim weft (left), and 31\_tricot-satin weft (right)**

However, even for the data with fairly good correlation, the KES-f force-deformation envelopes exhibit a slightly smaller deformation (envelope is to the left of the ITT curves). This deviation can be explained by the fact that the one load of the KES-f data is compared with the third load of ITT, where the fabric is already elongated twice from the previously applied loads. The more elastic a fabric, the greater this deviation becomes, which accounts for the less good correlation of fabrics in Category 3.

This means, however, that for fabrics in Category 3, where the KES-f and the ITT envelopes correlate the least, the derived parameter becomes increasingly inaccurate, because of greater plasticity behaviors. The following graph illustrates this suboptimal correlation for elastic fabrics.

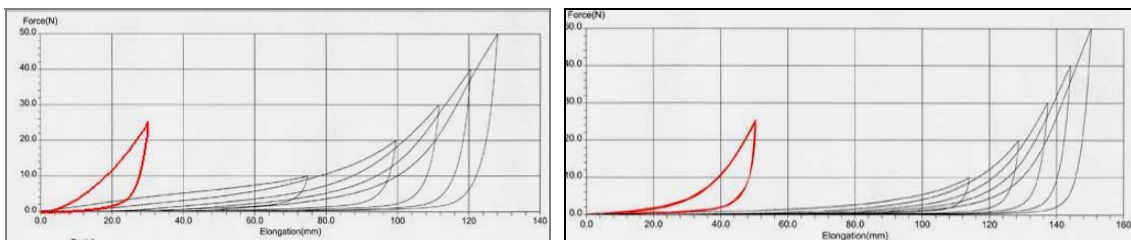


**Figure106: Comparison of KES-f and ITT data at 500N/m in weft direction**

This analysis shows that, in contrast with what we previously thought, the KES-f measurement data may also be precise enough for inelastic fabrics, where the plasticity effects are small.

- Problem of Poisson ratio

The superposition of the KES-f and ITT force-deformation profiles reveals the following additional irregularities for the three fabric samples 16\_lurex-knit, 21\_single-jersey and 27\_fleece (Figure 107): The KES-f envelope describes a disproportionately less elastic fabric than the ITT envelopes.



**Figure 107: Sample 27\_Fleece (weft), sample 16\_lurex-knit (weft)**

The search for possible error sources drew attention to the tendency of some textiles to shrink in one direction, when stretched in the other (i.e. the effect of Poisson ratio). The size of the test specimen of KES-f and ITT is not the same: KES-f = 20 cm x 5 cm and ITT = 5 cm x 10 cm. It was discovered that fabrics with a higher Poisson ratio elongate more during the ITT measurement, where much thinner test samples are used. This means that the size of the test

specimen also influences the measurement result for fabrics with a greater Poisson ratio. On the other hand, if the dimension of the test sample is important, then the KES-f sample size is the more representative one, as tensile forces act on a broader area of the textile during the wearing of a garment.

- Correlation of the derived KES-f and ITT parameters

For 69 out of 84 comparisons (42 fabrics in warp and weft direction) the KES-f parameter describes, as expected, a slightly more rigid fabric because the ITT envelope is already more elongated at the same force due to the two preceding loads (Figure 108, left). In five cases the ITT parameter describes a more rigid fabric and in only four cases, the KES-f and the ITT parameter are overlapping (Figure 108, right).

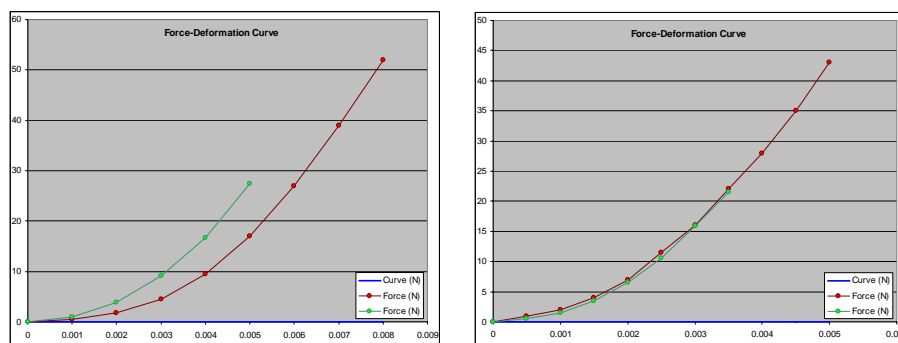


Figure 108: Example fabric 05\_gabardine warp (left), fabric 37\_woven-outdoor warp (right)

For an exact numerical comparison of the KES-f and ITT parameters, the largest divergence of both parameters below 500 N/m is compared (Figure 109).

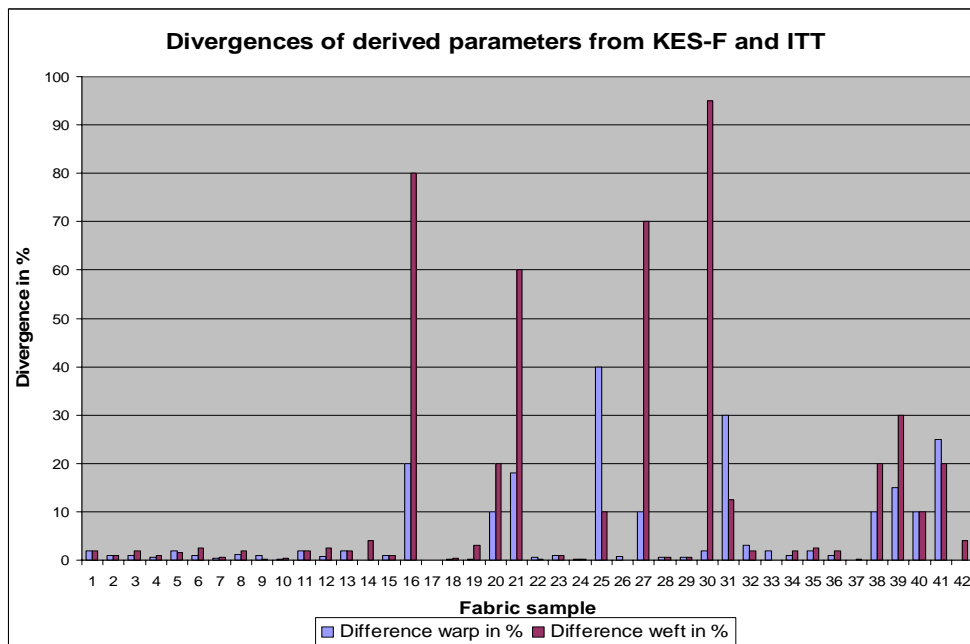


Figure 109: Differences of derived parameters from KES-f and ITT

The divergence for all fabrics is greater than 0.2%, our fixed accuracy limit for the tensile parameter. However, the divergence of 30 fabrics is rather small and below 5%. The less elastic the fabric, the smaller the divergence. For 11 fabrics (knits), the derived KES-f and ITT parameters diverge more than 10%. However, we can also assume that for forces higher than 500 N/m the parameters diverge even more and become more inaccurate.

- Simulation tests

One better correlating (36\_men-overcoat) and one poor correlating fabric parameter (21\_single-jersey) are chosen for the simulation experiments and forces of 500 N/m are visualized in orange. For the fabric with poor correlation (21\_single-jersey), the same elongation returns slightly smaller forces for the ITT parameter (Figure 110, left). As the parameter divergence between KES-f and ITT for this fabric is very high (40%), we can conclude that relatively small forces cause quite high deformations.

The simulation of the better correlating fabric parameter in contrast shows, as expected, that very similar forces occur on the fabric for the same deformation. The occurring forces are however much higher as for the elastic single-jersey fabric (Figure 110, right).



**Figure 110: Fabric 21\_single-jersey (left), Fabric 36\_men-overcoat, 500 N/m (right)**

Additional simulation experiments using some more rigid fabric parameters visualize that the occurring forces even exceed 1000 N/m (Figure 111). Hence, the upper force limit of the ITT experiment is still too low.



**Figure 111: 1000 N/m for 04\_linen, 19\_easy-care, 28\_upholstery, 36\_men-overcoat**



- Conclusion

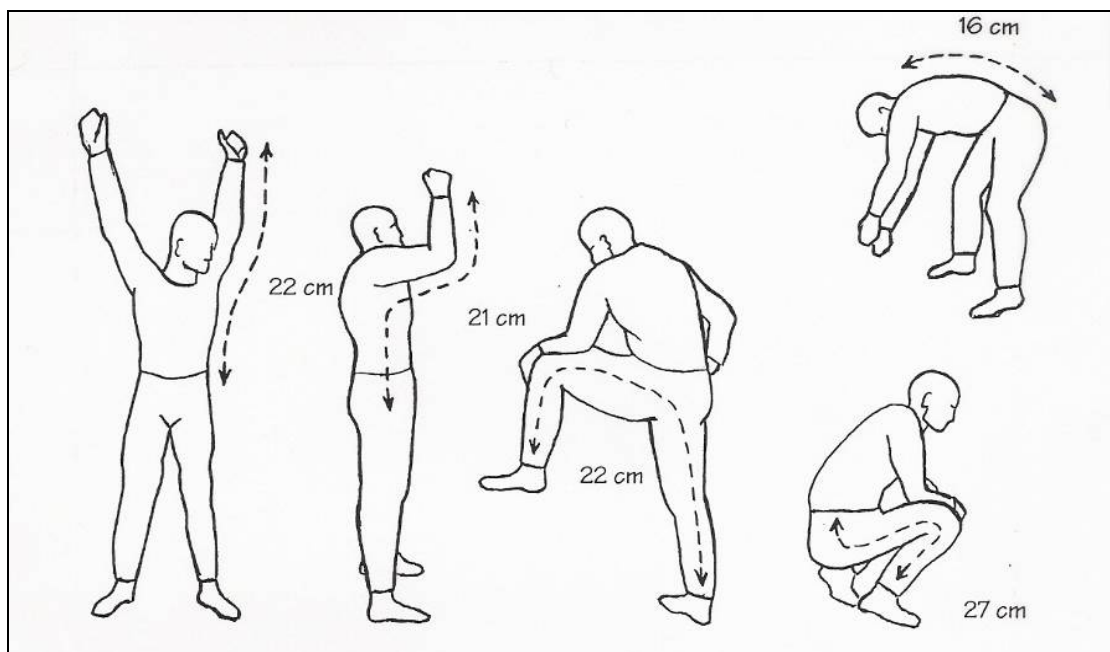
The comparison of the KES-f and the ITT parameters show a fairly good correlation for woven textiles. The correlation of more elastic knit and non-woven fabrics is suboptimal. For those cases, the ITT step tensile measurement better captures the tensile plasticity behavior over a broad bandwidth of various forces. As the elastic knit fabrics have the largest share in garment collections (70%), the ITT measurement should be chosen over the KES-f measurement.

However, the upper limit of the ITT measurement appears to be too small, as the color coded fitting feedback indicates loads above 1000 N/m for the typical fitting movement. For forces above 1000 N/m, the ITT parameter is no longer based on measured data and becomes random. Hence, an even broader bandwidth of measurement data is required.

On the other hand, the simulation experiments also demonstrate that very different forces act on the garment during the fitting movements for various textiles. Low forces are necessary to elongate elastic textiles, whereas for rigid fabrics much higher loads are needed to elongate them to the same extent. Therefore, the definition of a suitable measurement force bandwidth is particularly challenging, as the force bandwidth itself is dictated by the type of textile.

#### 5.3.4.4. Length Driven Measurement (LDM)

The definition of a valid measurement limit with hitherto applied force driven measurements is a challenging task, due to the large bandwidth of forces, the diverse range of fabric materials and the wide variety of tensile characteristics. For these reasons the next experiment will consider the force - deformation relationship from another point of view: the deformation.



**Figure 112: Several body distance changes during movements**

During wear, a garment is not endlessly elongated. Garments are designed to fit the body in a static, balanced standing position (see 5.1.1.comfort performance). When the body starts to move, the garment is deformed according to the changes in the distance between two parts of the body (= body-distance changes) (Figure 112). Constant new developments in textiles make the tensile properties potentially infinite. The scale of changing body-distances, however, is limited by the body's physiology.

The standard tensile measurement such as FAST and KES-f are force driven methods. A fabric can however also be characterized in a length driven modus, where the amount of deformation is set and the corresponding forces measured. As it is easier to identify the fabric deformations during the wearing of a garment, the length driven measurement modus seems to be advantageous for measuring the force-deformation relationship for dynamic garment simulations.

Therefore, a new length driven tensile measurement will be established. For this, the step measurement protocol will be retained, as it captures well the fabric's plasticity effects. The maximum driven length peaks are redefined. In order to determine appropriate values, the most extreme body distance-changes are studied first.

- Body-distance changes (new measurement ranges)

For the identification of typical body distance-changes, the same movements as shown in Figure 112 are measured for several people with differing body physiologies (five men size 46 - 54, five women 36 - 44). The most extreme measured body-distance changes are:

Men	Original distance	Elongation in cm	% of elongation
Lifting arm	108cm	24cm	22.2%
Lifting elbow	103cm	24cm	23.3%
Lifting leg	190cm	26cm	13.7%
Squat	115cm	27cm	26.1%
Bending back	90cm	21cm	23.3%

**Table 19: Maximum body distance-changes for men**

Women	Original distance	Elongated distance	% of elongation
Lifting arm	77cm	19cm	24.7%
Lifting elbow	77cm	13cm	16.9%
Lifting leg	145cm	20cm	13.8%
Squat	101cm	13cm	12.9%
Bending back	71cm	19cm	24.8%

**Table 20: Maximum body distance-changes for women**

The largest body-distance changes occur for men during a squat movement (26.1%), during back bending or whilst lifting up an elbow (both 23.3%). For woman, back bending (24.8%) and lifting the arm (24.7%) cause the largest body distance-changes. In summary, when the garment is following the body's movements, the resulting fabric elongations can be up to 27%. Yet, in

order to integrate a safety margin for possibly more extreme and not captured body physiologies, a maximum body distance alteration of 30% is assumed for the following tests.

Comparing the maximum body distance alteration with the previous force driven measurement data, an elongation of 30% is only reached for very elastic fabrics such as 38\_single-jersey with an applied force of 89 N/m. An elongation of 30% was never achieved during the measurement of rigid fabrics. Rigid samples such as 24\_satin could only be elongated by 1.86% at the maximum applied force of 1000 N/m.

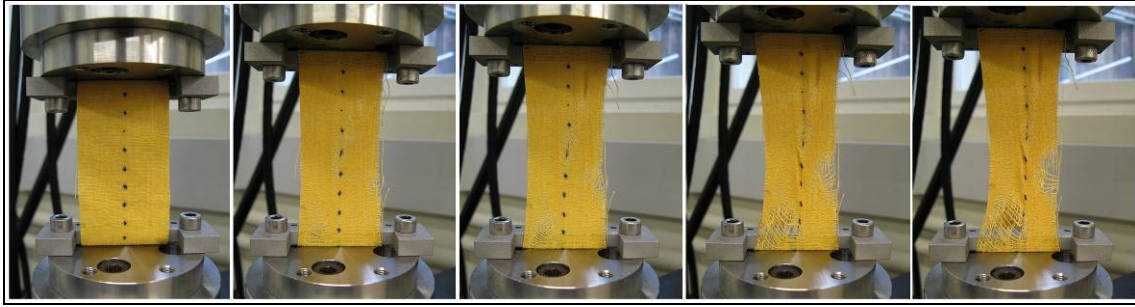
However, rigid fabric's such as sample 24\_satin would never stretch up to 30%. A tightly fitting garment made from a rigid fabric material would either restrict certain movements or cause the fabric to tear. (Therefore, for garments made out of rigid materials a comfort margin is integrated in to the 2D pattern construction). As a result, the maximum body-distance elongation of 30% cannot be used as the upper measurement limit for our new length driven experiments, as some fabrics would tear during the test. For this reason, the fabrics maximum tensile load limit should be studied first and the point of rupture of six very different fabrics is specified.

- Fabrics point of rupture

The tested fabrics are 04\_linen, 05\_gabardine, 11\_flannel, 21\_single-jersey, 24\_satin and 38\_weft-knit jersey. Another Tensile Tester is used for this experiment, where test sample size is 50mm x 100mm. During the experiment, the fabric is elongated by 100% (i.e. by 100 mm) and the breaking load recorded (Figure 113). The measurement speed is 1mm/sec. This time, three measurements are performed for the six different textiles.

Fabric sample	Measurement speed	Rupture force in /N/m	Rupture length in (%)
04_linen_1	1mm/sec. (20Hz)	9 560	15.4
04_linen_2	1mm/sec. (20Hz)	9 460	14.8
04_linen_3	1mm/sec. (20Hz)	9 420	16.1
05_gabardine_1	1mm/sec. (20Hz)	5 696	25.2
05_gabardine_2	1mm/sec. (20Hz)	5 996	23.9
05_gabardine_3	1mm/sec. (20Hz)	5 904	26.2
11_flannel_1	1mm/sec. (20Hz)	8 436	60.3
11_flannel_2	1mm/sec. (20Hz)	8 446	63.0
11_flannel_3	1mm/sec. (20Hz)	8 044	61.1
21_single-jersey	1mm/sec. (20Hz)	218	100
21_single-jersey	1mm/sec. (20Hz)	218	100
21_single-jersey	1mm/sec. (20Hz)	198	100
24_satin_1	1mm/sec. (20Hz)	19 794	28.4
24_satin_2	1mm/sec. (20Hz)	18 698	30.2
24_satin_3	1mm/sec. (20Hz)	19 134	26.4
38_weft-knit_1	1mm/sec. (20Hz)	4 364	100
38_weft-knit_2	1mm/sec. (20Hz)	3 970	100
38_weft-knit_3	1mm/sec. (20Hz)	3 484	100

**Table 21: Measurement results for the determination of the point of rupture**



**Figure 113: sample 04\_linen – measuring the point of rupture**

Once again, the determination of the fabrics point of rupture reveals the wide variety of tensile characteristics. The rupture deformation varies from 14.8% (04\_linen) to over 100% (21\_single-jersey, 38\_weft knit jersey). The rupture forces thereafter vary from 218 N/m (21\_single-jersey, fabric was not yet broken) to 19,794 N/m (24\_satin). The highest force corresponds to over 19 times more than the maximum applied force of the ITT experiment. However, the average point of rupture for three of the fabrics is below 30%:

- 15.43% for 04\_linen at 9 480 N/m
- 25.1% for 05\_gabardine at 5 865 N/m
- 28.3% for 24\_satin at 19 209 N/m

In conclusion, from this experiment we obtain the following important information:

- (1) The possible deformation range is much narrower (**0 – 30%**) than the bandwidth of potential forces (**0 – 19,794 N/m**), which can act on a garment during wear.
- (2) However, the point of rupture of fabrics can be below 30% for rigid and fragile fabrics. For those textiles, the upper measurement limit is set to a lower value of 15%. (The value is not set any lower as fabrics can actually tear during wear and this possibility has to be reflected in the measurement.)

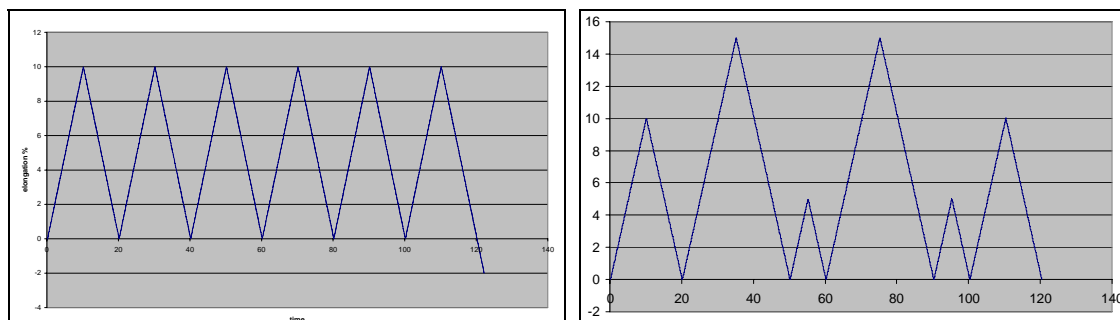
- Definition of the single measurement steps

After the definition of the new measurement limits, the single measurement steps can subsequently be defined. For comparison, the ITT measurement steps were 200, 400, 600, 800 and 1,000 N/m. This range of measurement steps captures a bandwidth of low to higher forces, but does not correspond to a natural motion sequence.

For the fitting of clothes standard reference procedure protocols are available, which suggest movements for the garment assessment on a live model: ASTM F1154 – 99a, “Standard Practices for Quality Evaluating the Comfort, Fit, Function and Integrity of Chemical-Protective Suit Ensembles” [Huck, Woodhead 34]. This protocol suggests the following motions:

- (1) Walk a distance of around 91 m (or walk on the spot for at least 3 min).
- (2) Kneel on left knee, kneel on both knees, kneel on right knee and stand (four repetitions).
- (3) Duck squat, pivot right, pivot left and stand (four repetitions).
- (4) Stand erect. With arms at sides, bend body to left and return, bend body forward and return, bend body to right and return (four repetitions).
- (5) Stand erect. Extend arms overhead in the lateral direction and then bend elbows (four repetitions). Extend arms overhead in the frontal direction and then bend elbows (four repetitions).
- (6) Stand erect. Extend arms perpendicular to sides of torso. Twist torso left and return, twist torso right and return (four repetitions).
- (7) Stand erect. Reach arms across chest completely to opposite sides (three repetitions)
- (8) Crawl on hands and knees for a distance of 6m (or crawl on the same spot for a minimum duration of 1min).

These standard fitting movements allow the derivation of typical body distance changes and thus, the derivation of fabric elongation-profiles that correspond to garment wear situations. Since the body-distances change differently for various actions, two typical elongation-profiles are derived. One typical body movement is a sequence of cyclic actions, most often used for locomotion, such as walking, running, swimming, etc. (Figure 114, left). Another typical sequence of actions is the non-cyclic motions, which are more diverse and spontaneous movements such as fitting postures (Figure 114, right).



**Figure 114: Protocol for cyclic deformations such as walking, running, etc. (left), protocol for various deformations for more spontaneous movements (right)**

The cyclic step measurement profile corresponds to the following deformations:

0 – 10% – 0 – 10% – 0 – 10% – 0 – 10% – 0 – 10% – 0 – 10% – 0

Non-cyclic step measurement profile corresponds to:

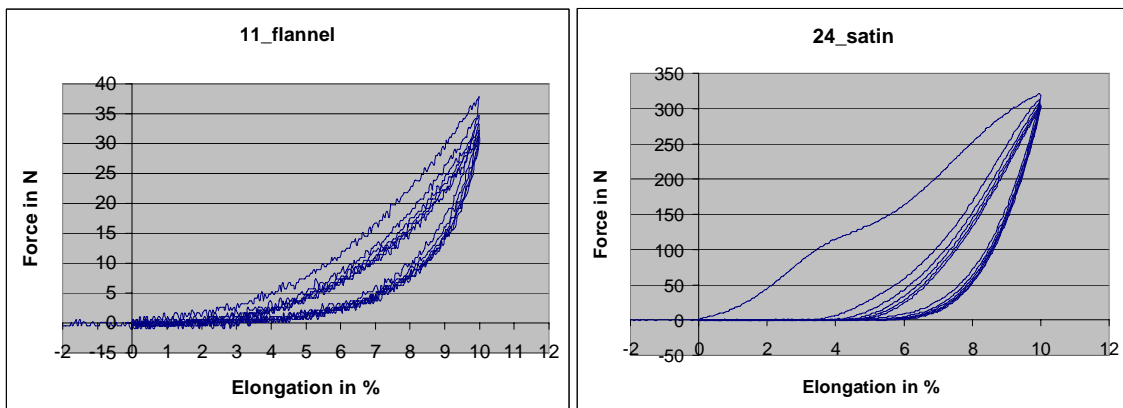
0 – 10% – 0 – 25% – 0 – 5% – 0 – 20% – 0 – 5% – 0 – 10% – 0

0 – 10% – 0 – 15% – 0 – 5% – 0 – 15% – 0 – 5% – 0 – 10% – 0 (for rigid and fragile fabrics)

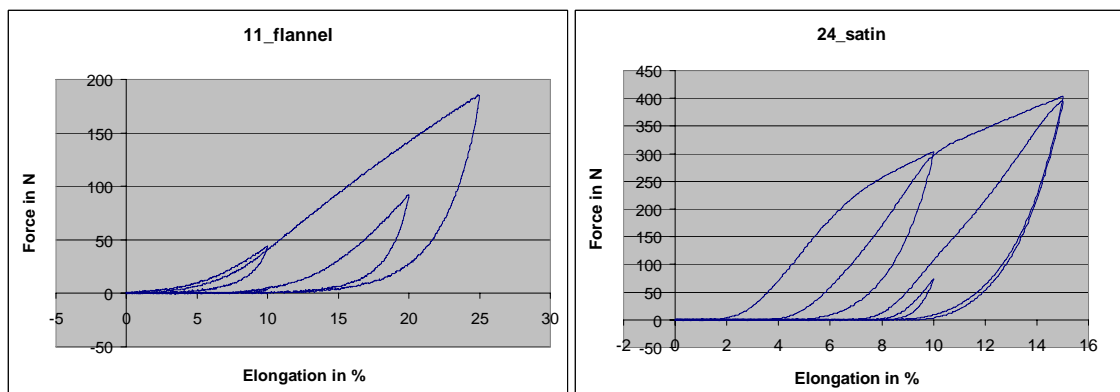
The wait phases in between each deformation are retained from the previous measurements.

- Measurement

The new measurement is performed with four different textiles regarding the tensile property: 04\_linen, 11\_flannel, 24\_satin, and 38\_weft-knit. The new cyclic step measurement returns almost overlapping force-deformation curves, as for sample 11\_flannel (Figure 115, left); only the force-deformation envelopes for sample 24\_satin return a very different first envelope, where more force is needed for the deformation (Figure 115, right). The non-cyclic measurement returns various single force-deformation curves, where the smaller deformation envelopes lie inside or overlap with the biggest deformation envelopes. However, the earlier and the later small envelopes do not overlap.



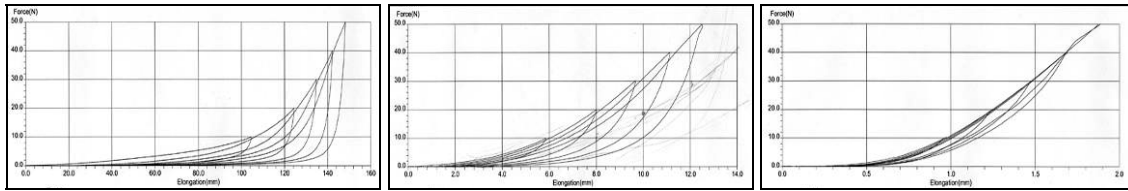
**Figure 115: 11\_flannel cyclic measurement (left), 24\_satin cyclic measurement (right)**



**Figure 116: 11\_flannel non-cyclic measurement (left), 24\_satin non-cyclic measurement data (right)**

The cyclic and non-cyclic measurement profiles show once again that very different intense forces are needed to deform various fabrics to the same extent (13 N/m for sample 38\_weft-knit, 740 N/m for 11\_flannel and 6,430 N/m for sample 24\_satin).

On the other hand, we can see that the form of the force-deformation profiles of the length-driven measurements (Figure 115 and 116) resemble one another far more than the output data of the force driven ITT experiment (Figure 117). Moreover, we can identify (even on the quite noisy data from the most elastic sample 38\_weft-knit Figure 118) that the data is captured in an area, where the fabric behavior is less non-linear (compare Figure 117, left).

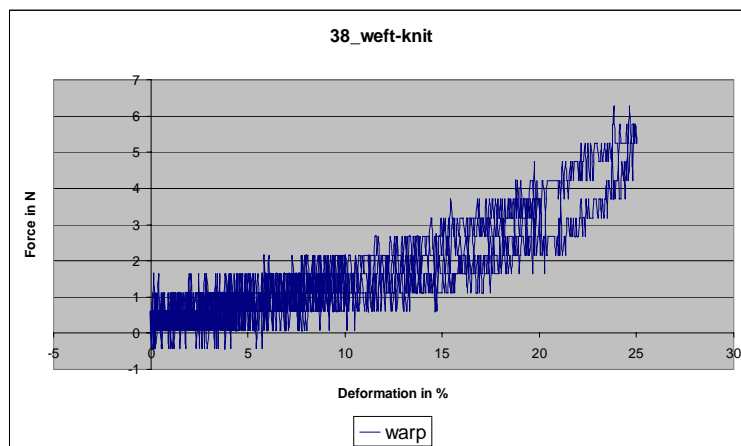


**Figure 117: ITT measurement 38\_weft-knit (left), 11\_flannel (middle), 24\_satin (right)**

Hence, even the four fabric samples possess very different tensile characteristics, however, unexpectedly their length driven fore-deformation profiles resemble. This fact could be an interesting point for future research, since derivation rules for a simplified and automated parameter derivation process could be established.

- Drawback: Noisy output data

One weak point of the new measurement is the noisy output data for the elastic fabric 38\_weft-knit (Figure 118). Other measurement devices such as KES-f and ITT are calibrated for a specific force area. Within the new, more accurate length driven measurement protocol we deal however with a much broader variety of low and high forces, which are difficult to calibrate

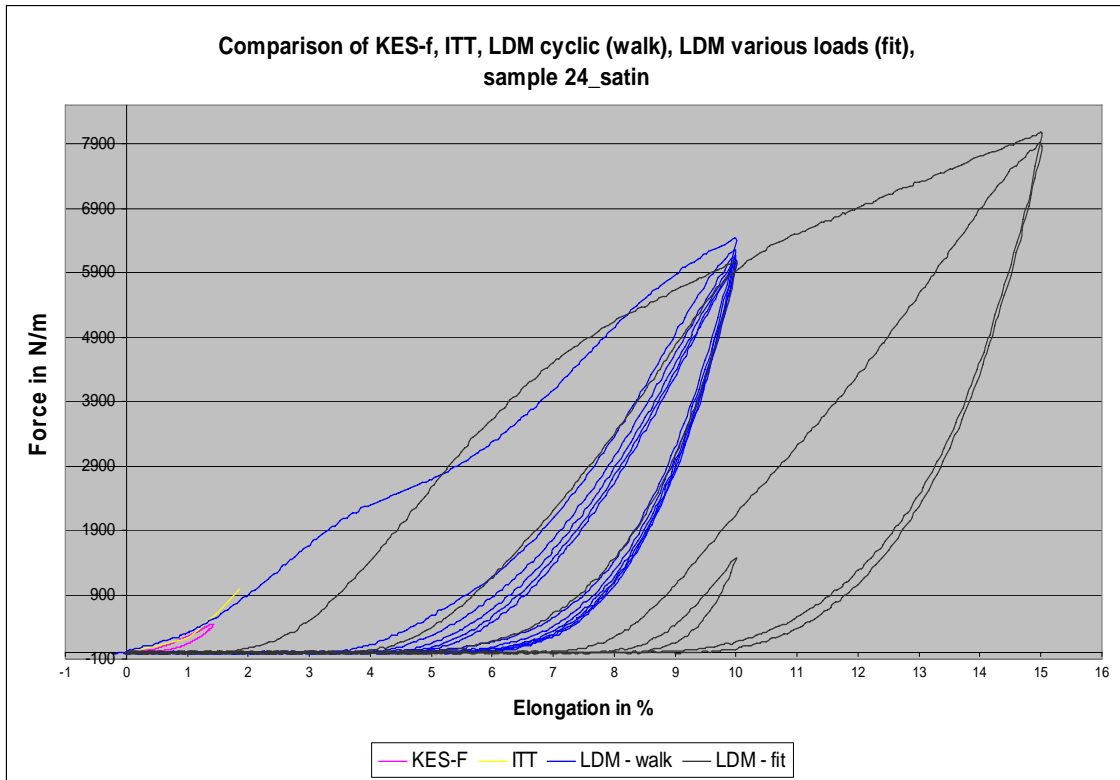


**Figure 118: 38\_weft-knit measurement with various forces**

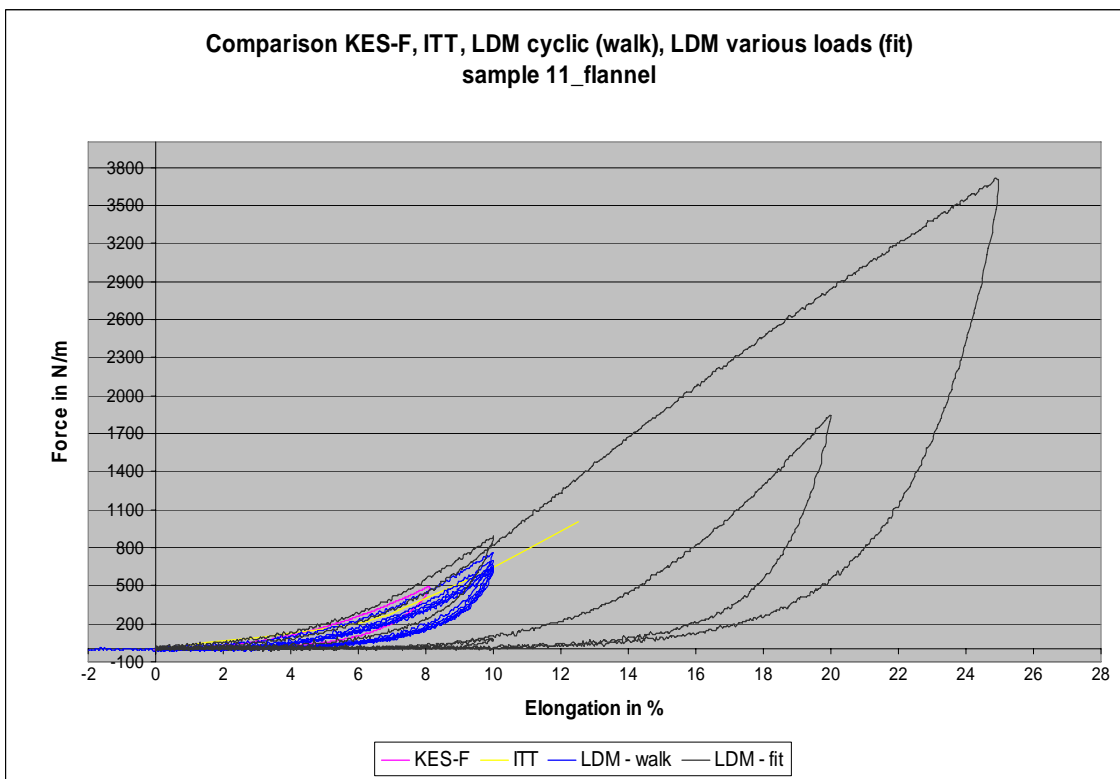
#### 5.3.4.5. Comparison KES-f – ITT – LDM

- Measurement data

The enhanced accuracy of the length driven measurements can be demonstrated by correlating the new measurements with the KES-f and ITT measurement data. For rigid fabrics, the applied force of the previous measurements was much too low (Figure 119). The fabric was thus tested in an unsuitable bandwidth. For medium elastic fabrics such as 11\_flannel, the applied forces of previous measurements correlate with the measured forces of the length driven measurements, except for the non-cyclic experiment (Figure 120). For elastic fabrics such as sample 38\_weft-knit, the previously applied forces were too high (Figure 121, left) and the force-deformation occurs in an area, where the fabric behavior is much more linear.



**Figure 119: 24\_satin comparison of measurements from KES-f, ITT and LDM**



**Figure 120: 11\_flannel comparison of measurements from KES-f, ITT and LDM**



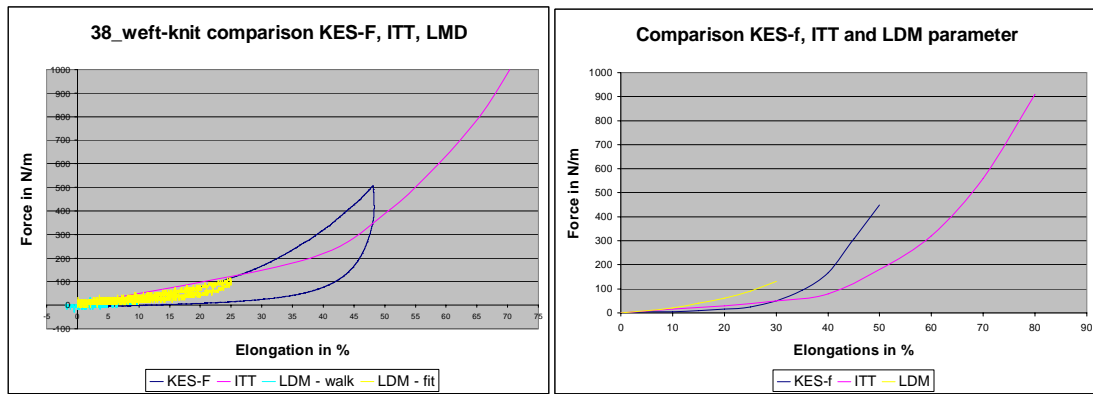


Figure 121: 38\_weft-knit (yellow) comparison of measurements (left), 38\_weft-knit parameter comparison (right)

- Parameter

The complexity of the parameter derivation is different for the cyclic and non-cyclic measurement. The overlying single force-deformation curves of the cyclic measurement allow an easier interpretation of the data. Only fabric 24\_satin shows a rather different first force-deformation curve, which correlates well with the KES-f and ITT measurement (Figure 119). For the parameter derivation, a good compromise between the first and the subsequent deformation curves needs to be found.

An accurate parameter derivation for the non-cyclic measurement is more difficult, since the different force-deformation curves do not overlap. An inaccuracy is thus inevitable as the derived parameter is an average of all deformation curves. The greatest parameter deviation occurs at the largest distance between two deformation curves. For fabric 11\_flannel (Figure 122), the greatest deviation of the parameter from the non-cyclic measurement is 2.8%. For the other three tested fabric samples, the largest observed inaccuracies are in the same range of around 3%.

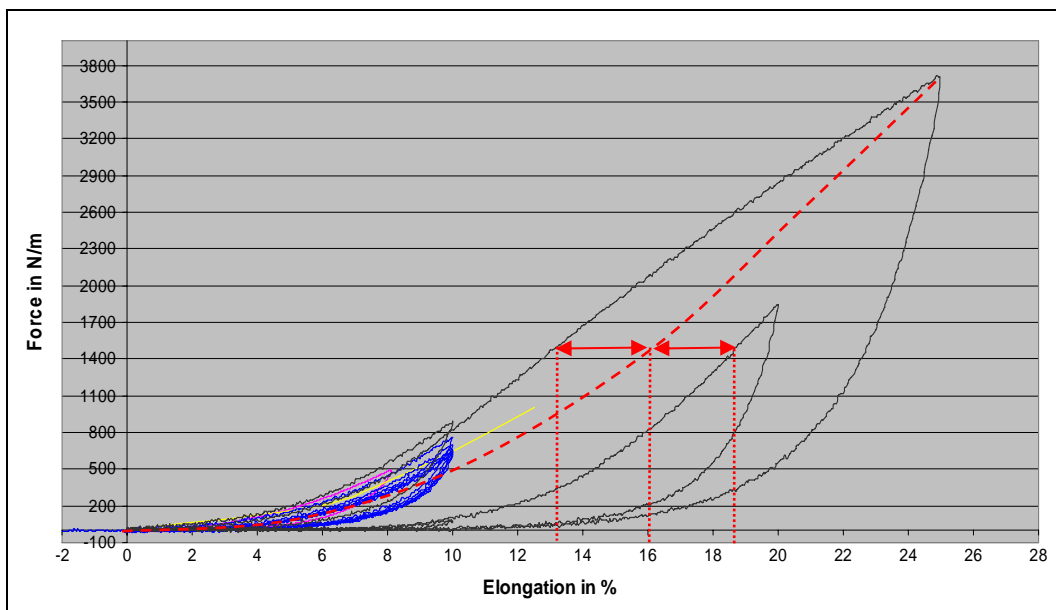


Figure 122: Non-cyclic parameter deviation from real measurement fabric 11\_flannel

At first glance, and with regards to our previously defined accuracy limit, the parameter deviation error of 3% seems to be quite high. However, considering the inaccuracies of previous parameters and considering the unlimited possibilities for fabric characterization, the new measurements capture fabric behavior quite precisely during the wearing of garments.

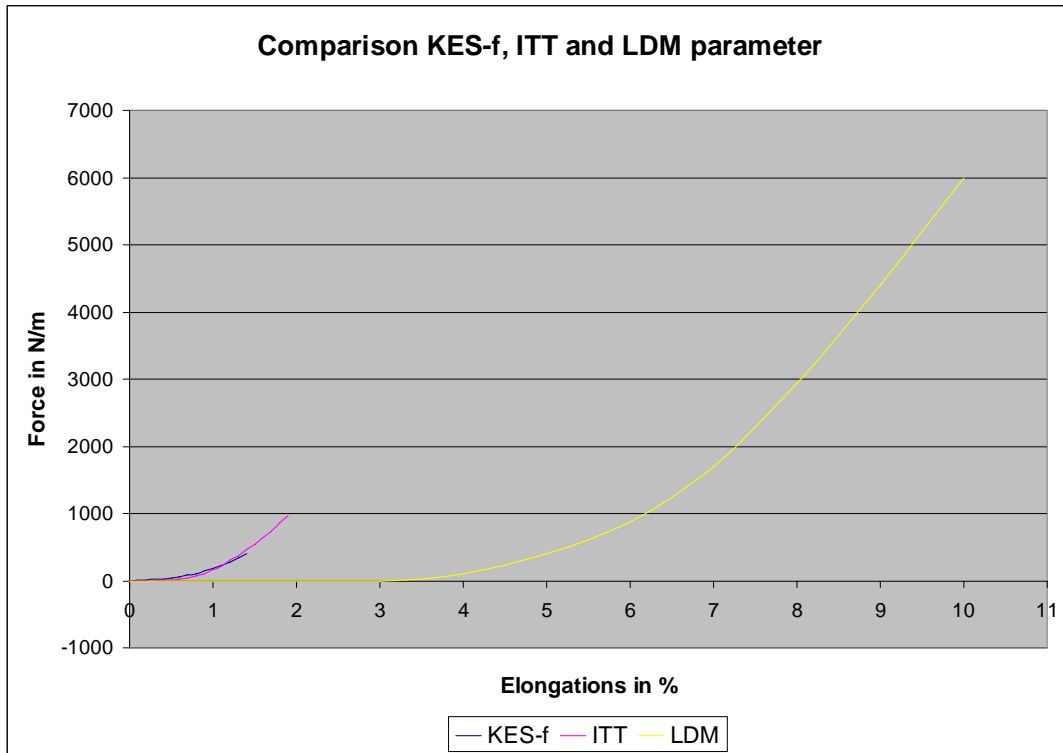


Figure 123: parameter comparison for sample 24\_satin,

- Simulation experiments

The simulation tests using the new derived parameters return more valuable fitting feedback:

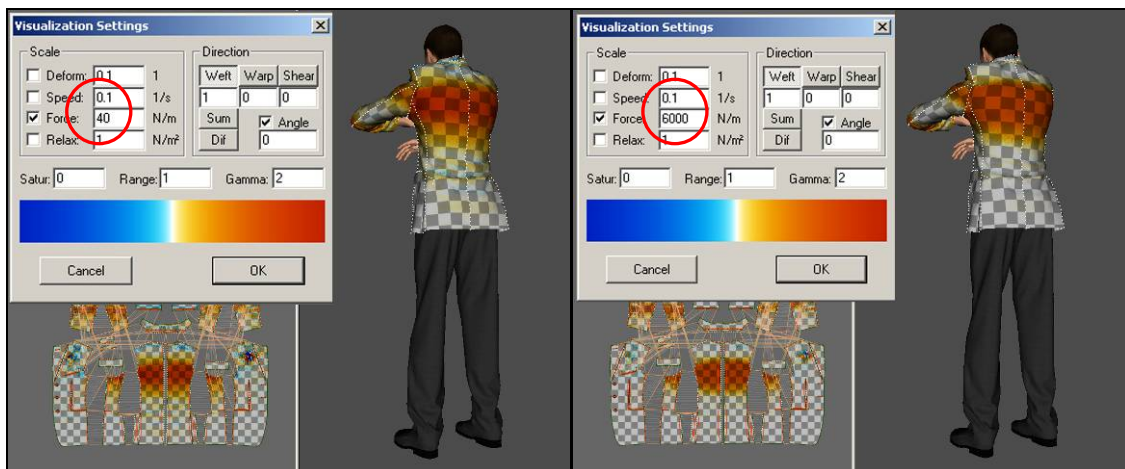


Figure 124: Fitting movement with parameters 38\_weft-knit (left), 24\_satin (right)

During the simulation with fabric parameter 38\_weft-knit, a tensile load of 40N/m is acting on the garment, whereas for fabric 24\_satin a force of 6 000 N/m is applied. Certainly the satin jacket is much less comfortable, as the person wearing it feels a much greater resistance during movement.

On the other hand, when garments such as formal suits are worn, a certain level of resistance is to be expected, since those garments are not tailored for excessive motion. As we are now able to express garment fitting by means of exact numerical data, potential future field of research could be the exploitation of the high-tech fitting data. For example, the measured fitting could be quantified by bringing it into correction with subjective user perceptions.

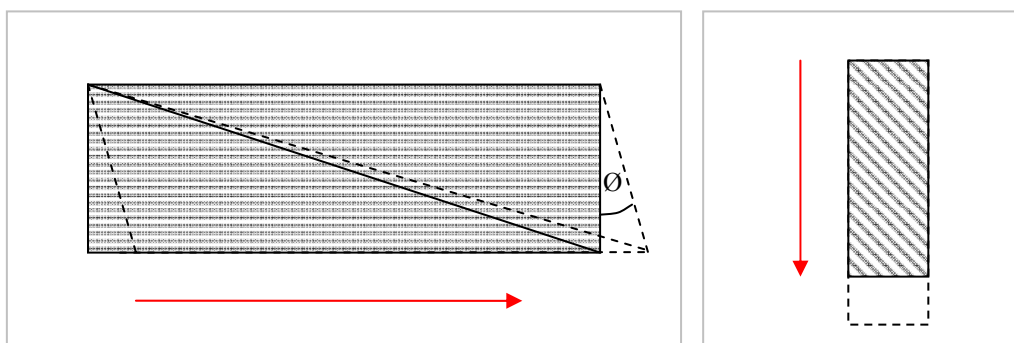
### 5.3.5. The shear property in dynamic simulations

The accuracy of standard shear measurements is tested for dynamic simulations and if necessary, a new shear measurement is designed. Within the mechanical simulation model the shear parameter is, like the tensile parameter, a measure of the fabrics 2D elongation, albeit in the diagonal fabric direction. Thus, previously obtained knowledge about the tensile parameter in dynamic simulations can be partly applied to the shear parameter.

#### 5.3.5.1. Suitability of the standard measurements

Fabrics exposed to shearing forces start to buckle at a certain point. When a fabric starts to buckle, it is not only the shear characteristic which influences the measurement result, but also the bending property. For that reason, standard shear measurement limits are designed for a force-deformation bandwidth, where fabrics usually do not buckle, so that only the shear property is assessed.

- KES-f



**Figure 125: KES-f Shear elongation scheme (left), FAST shear scheme (right)**

In contrary to the KES-f tensile test, the KES-f shear experiment is a length driven measurement, where the fabric is elongated up to  $\pm 8^\circ$  ( $\tan 8^\circ * 5 \text{ cm}$ , 3.4%). In Chapter 6.2.4.4. we deduced that during wear a fabric can be elongated by up to 30%. Thus, the measured

bandwidth of the KES-f shear experiment is too small and derived shear parameters are inaccurate outside the measured area.

- FAST

The FAST experiment is force-driven, applying a small load of 5 N/m. Corresponding deformations for the tested fabrics are:

Fabric sample	Applied force	Corresponding deformations in %
04_linen	5 N/m	17%
05_gabardine	5 N/m	16%
07_silk	5 N/m	33%
11_flannel	5 N/m	5.5%
21_jersey	5 N/m	24%
24_satin	5 N/m	17%

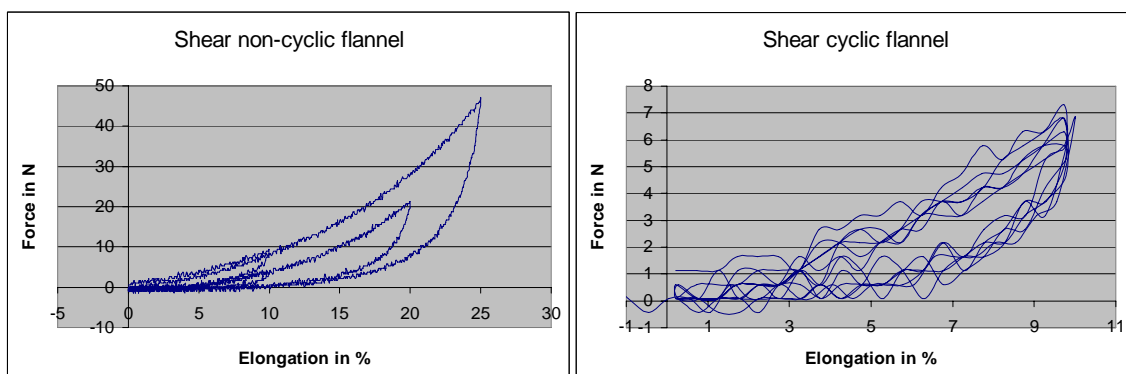
**Table 22: Shear deformations of the FAST measurement**

It appears that the measured deformations from the FAST method correspond better with garments worn in reality. However, the experiment is force-driven and does not allow an accurate control of the deformation bandwidth.

In conclusion we can say that, both, FAST and KES-f shear measurements are unsuitable for the derivation of accurate shear parameters for dynamic fabric simulations.

### 5.3.5.2. LDSM (Length Driven Shear Measurement)

For the new length driven shear measurement, the same measurement protocol as for the length driven tensile measurements is applied to the fabric samples cut in bias direction (Figure 126). The cyclic and the non-cyclic deformation sequences are applied with a rate of 1mm/sec.



**Figure 126: Non-cyclic and cyclic shear measurement for fabric 11\_flannel**

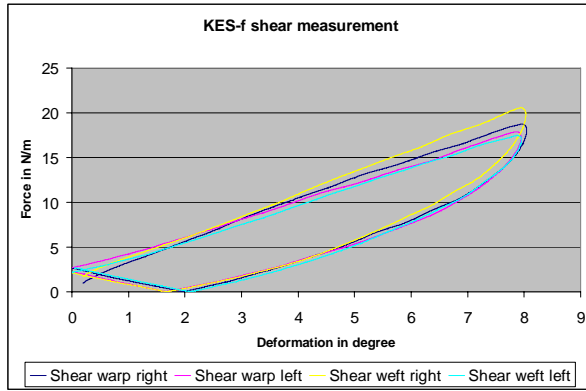


Figure 127: KES-f shear measurement for fabric 11\_flannel

Comparing the two new length driven shear force-deformation profiles with the four envelopes returned by the KES-f experiment (Figure 126, 127, 128) we can see that the actual shear behavior is more non-linear, something that was not captured by the KES-f data.

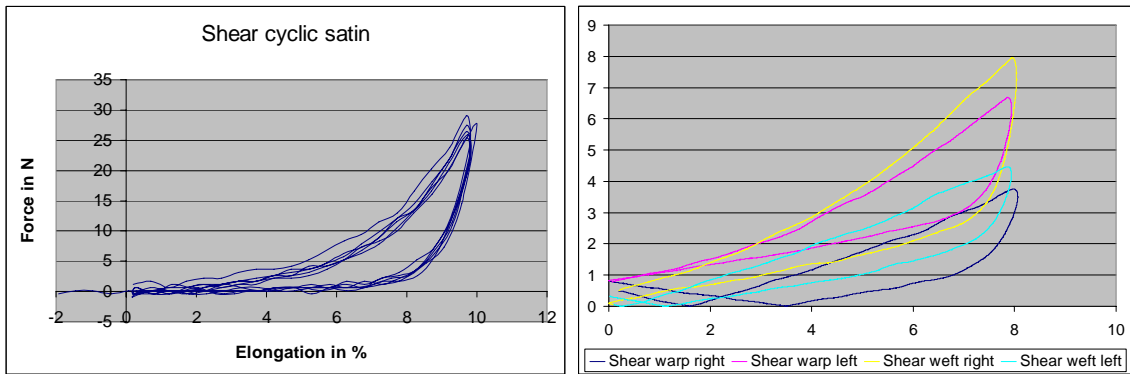


Figure 128: Cyclic shear measurements for 24\_satin (left) and 38\_weft-knit (right)

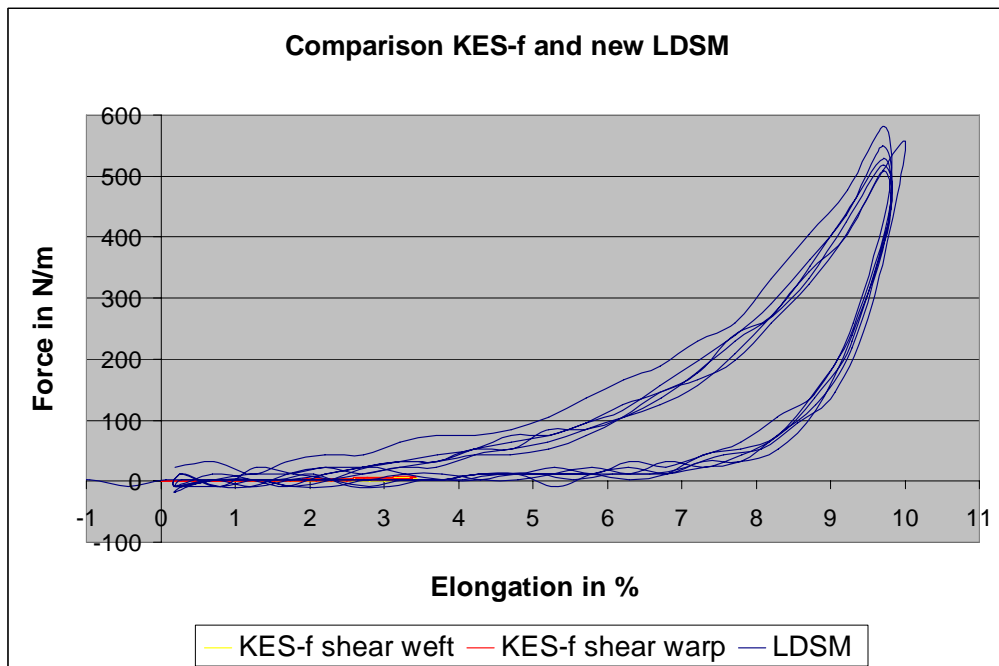
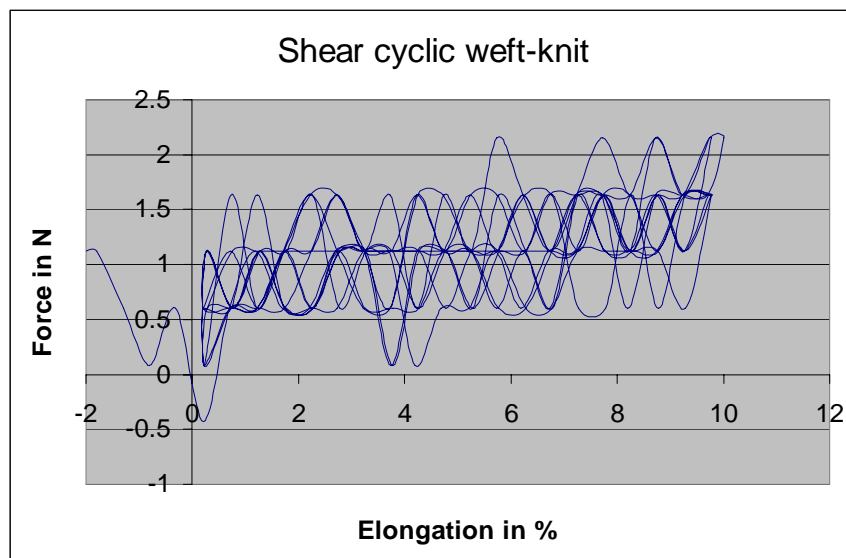


Figure 129: Superposition KES-f and LDSM shear measurement fabric 24\_satin

From the superposition of both data sets (KES-f and LDSM) we can see that the new measurement captures the shear behavior in a completely different bandwidth, which corresponds better to what actually happens when a garment is worn (Figure 129). Moreover, the linear assumption of a shear force-deformation relationship for 88% of the fabrics in our fabric selection (Chapter 4.2.1.2.) becomes insignificant, as the measurements were taken in the wrong bandwidth.

- Drawbacks

As with the tensile property, the shear measurement data of elastic fabrics, such as sample 38\_weft-knit, is quite noisy and the parameter derivation might become imprecise.



**Figure 130: noisy shear measurement data**

Additionally, fabric samples 04\_linen and 24\_satin started to buckle at an extension of 10%. However, in contrast to standard measurements, the buckling behavior in this case can be seen as a natural fabric effect and one which would occur in reality during wear. Hence, the buckling does not falsify the measurement data for our application.

- Comparing the three force direction

Woven textiles are more elastic in the bias direction. Comparing the measurement data for the three fabric directions (warp, weft and shear) we can see that generally in the shear direction lower forces are required to elongate the fabric, within our defined deformation bandwidth. Knits are equally elastic and the measurement data of the knit fabric 38\_weft-knit shows a similar force-deformation profile in all directions (Figure 131, 132).

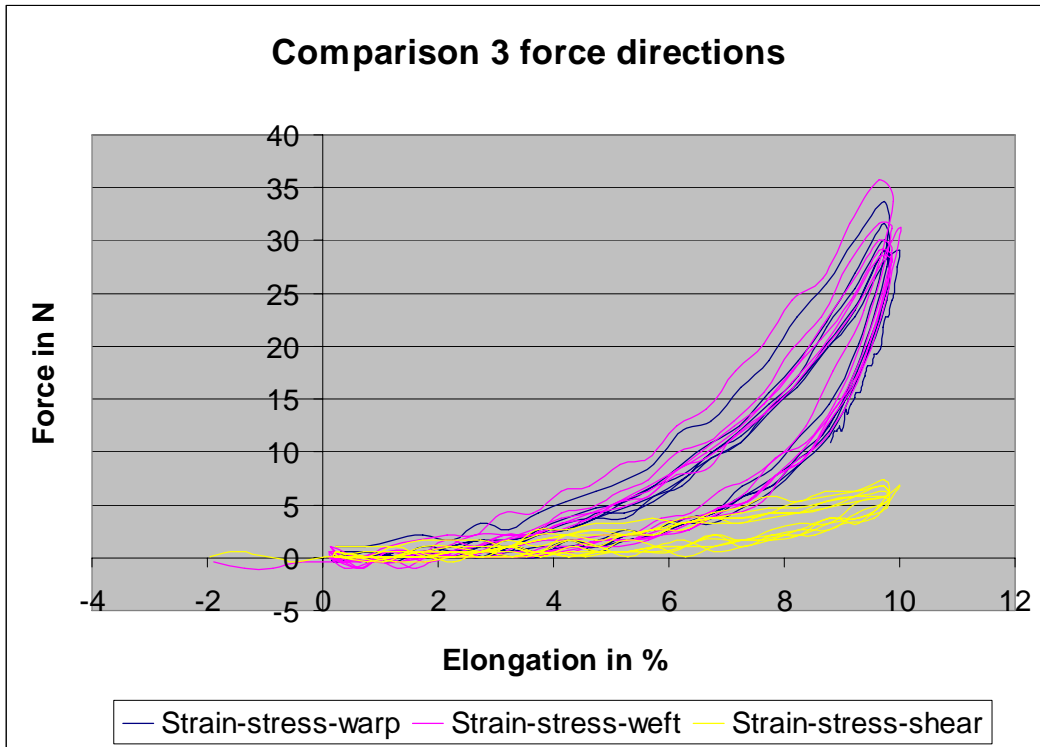


Figure 131: Comparison of the force-deformation profiles of the three simulated 2D deformation directions, fabric 11\_flannel

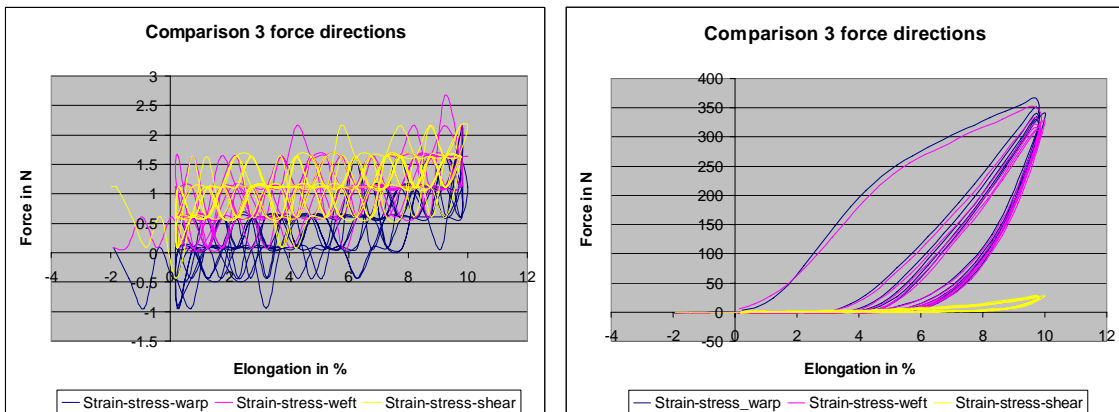


Figure 132: Three force-deformation profiles for fabric 38\_weft-knit (left) and 24\_satin (right)

In summary we can say that the LDSM derives more accurate shear parameters. The parameter is measured in the right bandwidth and one single shear parameter is easily derived from the single measurement without the necessity to evaluate four different shear behaviors, which are not reflected in the simulation system. However, we have to consider that for a more accurate simulation of shear, the various shear directions should be considered.

The parameter derivation errors for the non-cyclic measurements are within the same bandwidth as for the tensile measurement, around 3%.

### 5.3.6. The bending property in dynamic simulations

Until now, only one type of bending was examined in this work, the fabric drape in one direction (see Chapter 5.3.2.2. about bending in static simulations). These drapes arise from extra garment widths, giving the fabric enough space to bend under its own weight, with no additional, external forces.

Garments can, however, contain much smaller wrinkles. For the appearance of wrinkles, the fabric has to be somehow forced to bend more than it normally would under its own weight. This kind of bending can be based on the movements of the body. For instance the bending of the leg or the arm creates small wrinkles around the knee and on the inside of the elbow (Figure 133).



**Figure 133: wrinkles and folds during movements,**

However, small wrinkles can also be produced by fabric gatherings for aesthetic purposes (Figure 134). For these effects, the fabric is creased by forces (the seam) additional to the fabrics self-weight.



**Figure 134: Forced wrinkles on a skirt**



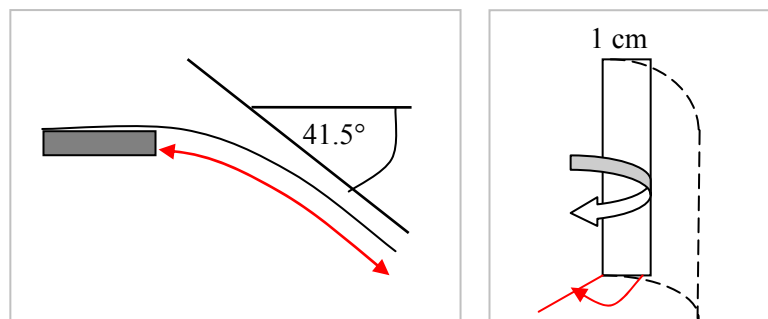
It becomes clear that with regard to the bending parameter, it is difficult to distinguish between static and dynamic simulations as both occurrences are overlapping. On the one hand, fabric drapes also appear in dynamic simulations and on the other, small wrinkles can also be part of a static garment.

The differentiation in static and dynamic simulations for the bending property should therefore be seen as the distinction between bending forces. The case where the fabric's SW acts as the only bending force on a garment is treated under static simulations, whereas the occurrence of additional bending forces is treated in the chapter about the accuracy of dynamic bending simulations. In the following, existing bending measurements are studied.

#### 5.3.6.1. Suitability of standard bending measurements for dynamic simulations

Both, FAST and KES-f are length driven measurements, as the bending angle is the driver of the experiment. This fact is important as, similar to the tensile and shear property, the bending deformation when a garment is worn (torque) is the known magnitude: A textile can only be folded by up to  $180^\circ$ . Hence the deformation area, which needs to be studied, is from  $0^\circ$  to  $180^\circ$ .

The FAST system uses the cantilever method, where the fabric is bent until an angle of  $41.5^\circ$  is reached under its SW (Figure 135, left). Hence, from this principle, the cantilever method corresponds better to static fabric drapes. The resulting bending rigidity value is based on a material deformation of up to  $41.5^\circ$ , which is not sufficient for dynamic simulations where much higher curvatures can occur.



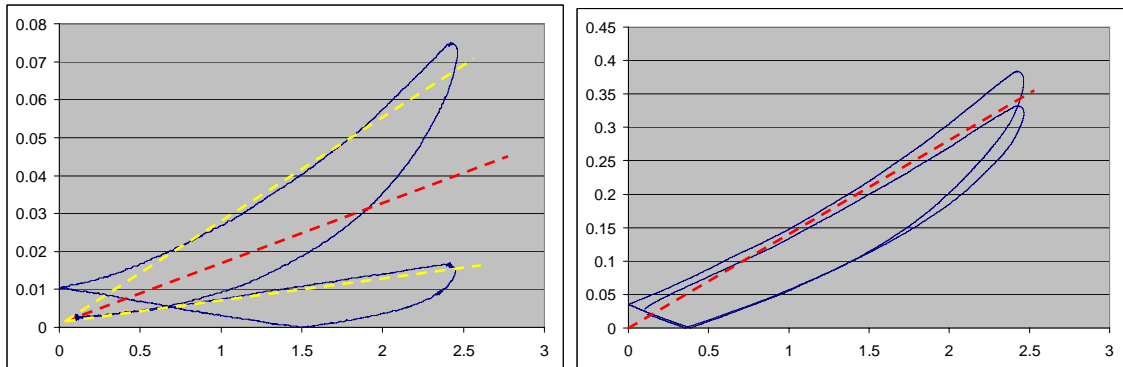
**Figure 135: FAST cantilever method, KES-f moment curvature method**

The KES-f experiment bends the fabric until an angle of  $150^\circ$  is reached and the corresponding forces are recorded (Figure 135, right). The width of the KES-f test sample measures  $1\text{ cm}$ . On the one hand, this small bending width corresponds well to the small wrinkle size, caused by body movements. On the other hand, the measurement also returns information about the momentum-curvature relationship for smaller deformations. Thus, the measurement is suitable for the derivation of parameters for static and dynamic simulations. Ideally, however, the maximum measured angle should be as close to  $180^\circ$  as possible.

In this new context, it is not surprising that the comparison of the FAST and the KES-f bending rigidity in Chapter 4.2.3 returned a suboptimal correlation.

### 5.3.6.2. Linear approach to the nonlinear bending behavior

In comparison to the tensile and shear measurement data, the bending force-deformation curves take a relatively linear course. From the curve profiles in Annex D we can see that 90% of the measurements can be accurately approximated by linear parameters (Figure 136 right). Examples with a nonlinear bending behavior are generally samples which have dissimilar front and back bending behavior. In Figure 136 the deviation of the linear parameter derivation is illustrated for two different measurements.



**Figure 136: Fabric 39\_ weft knit terry fabric (weft), 13\_plaid (warp)**

The automatic calculated bending rigidity value  $B$  is ascertained from the measurements on both fabric sides, front and back (see 2.2.2.2.) and is hence a linear approximation of both curves (red line).

For the less well correlating force-deformation curves, the combination of the front and back bending causes a greater error than the linear interpretation of the slightly nonlinear measurement data. For highly correlated curves, the error of the linear approach is negligible. Moreover, the deviation of front and back bending of up to 89% (chapter 4.3.) have to be considered during dynamic bending simulations, since the fabrics bend to a much greater extent.

### 5.3.6.3. Simulation experiments

In the previous chapters the accuracy of the bending parameter was theoretically assessed. Now, the real and virtual wrinkles are visually compared for the five fabrics with the most widely differing bending properties and with differing front and back bending deviations.

Fabric	10_jute	36_woven overcoat	05_gabardine	39_weft knit terry
<b>B</b>	Warp: 2.72 Weft: 6.47	Warp: 0.84 Weft: 0.62	Warp: 0.07 Weft: 0.06	Warp: 0.015 Weft: 0.014
<b>Deviation B front/back</b>	Warp: 15% Weft: 5%	Warp: 8% Weft: 0%	Warp: 10% Weft: 10.5%	Warp: 67% Weft: 86%

**Table 23: Various bending values of 5 fabric samples**

To achieve this, a new experiment has been designed: A fabric of size 40 cm length by 20 cm width is gathered in the middle to 10 cm in the weft direction (as occurring in skirts, blouses, etc.). The real and virtual wrinkle creation is observed.



**Figure 137: 10\_jute, real (right) and virtual (left)**



**Figure 138: 36\_woven-overcoat, real (right) and virtual (left)**



**Figure 139: 05\_gabardine, real (right) and virtual (left)**



**Figure 140: 39\_weft knit terry, real (right) and virtual (left)**

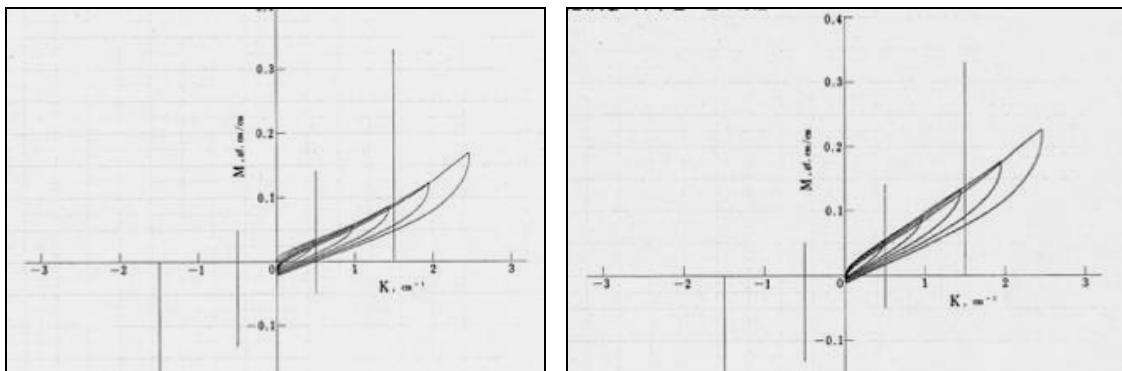
The new simulation results show a less good correlation of the real and the virtual wrinkles for fabric 39\_terry fabric (86% and 67% deviation in front and back) and fabric 05\_gabardine, as in this experiment the simplification of the bending parameter has a greater influence than during static simulation.

#### 5.3.6.4. Bending hysteresis

The tensile and shear hysteresis behavior is of special importance for dynamic simulations, as parts of the deformations are not recoverable or not immediately recoverable. As a result of this characteristic, subsequent deformations are considerably influenced by the preceding ones.

For the bending property it can be assumed that the permanently deformable part of a material due to forces of body movement is limited or takes place in the fabrics micro-structure. Even if a fabric stays partly folded after the bending process, then at the next application of force or movement, the fabric bends to another position. Given that flexibility is one of the main reasons why fabrics are used to make clothing, it can be assumed that bending deformation is generally recoverable.

For a further study of this hypothesis, alternative bending measurements have been conducted with the KES-f equipment. Ten fabric samples are bent in five progressive steps, (similar to the tensile and shear experiment) until the maximum bending angle of  $150^\circ$  is reached. Bending steps are:  $30^\circ$ ,  $60^\circ$ ,  $90^\circ$ ,  $120^\circ$  and  $150^\circ$ . For this experiment the fabric is however only in one direction (front).



**Figure 141: Step bending 36\_overcoat fabric weft (left) and warp (right)**

All ten measurements return linear progressive force-deformation envelopes, which all overlap (Figure 141). Compared with the tensile experiment, where the fabric is clamped after each measurement step in order to “remove” the non recoverable part of the fabric, the force-deformation envelopes resemble one another (see picture 100).

The bending hysteresis step measurement shows that almost no plasticity effects occur. In conclusion we can say that for bending only the viscosity plays an important role. (See Chapter 6.3.)

#### 5.3.6.5. Bending in shear direction

FAST also measures the bending property in the shear direction. For this experiment, the fabric is cut on the bias and is tested by the cantilever method. The measured values for bending in the shear direction return an average value of the warp and weft bending for all six fabrics.

### 5.3.7. Conclusion for the tensile, shear and bending parameter

Within this chapter, the accuracy of the elasticity properties has been tested for two fields of utilization, the static and the dynamic fabric simulation, what encompasses fairly different requirements. The leading question during the experiments was, if the single measurements actually represent what happens during garment wear and if thus, suitable and accurate parameters can be derived.

This question could be more easily answered for the case of static simulations, where only one force – deformation relationship and no hysteresis behavior is concerned. The KES-f and the FAST measurement data were tested to be suitable for the derivation of accurate parameters. Exceptions are fabrics showing a more nonlinear shear behavior and possessing greater densities, where the nonlinear KES-f shear parameter is more accurate. Other inaccuracies could result from the simplification of the shear and the bending property. However, simulation tests demonstrated that these simplifications can be neglected in static simulations, where only little forces are concerned.

The question of the suitability of measurements and the accuracy of the fabrics elasticity parameters was relatively more difficult to be answered for the case of dynamic simulations. Not only one, but several low and high force-deformation relationships at various frequencies can occur. Hence, the fabrics non-linear comportment as well as their hysteresis behavior become important factors.

With regards to the tensile and the shear property, the FAST and the KES-f parameter are incorrect. The FAST method only returns a linear parameter, based on a very low load. The FAST and the KES-f method measure only one force – deformation profile, which does not reflect the fabrics hysteresis behavior. Therefore, a new fabric tensile and shear measurement is designed, which represent better what happens during garment wear. The new measurement is deformation and not force driven, in order to allow an accurate control of the measurement limits (the deformations are known during garment wear). The measurement is a step measurement with several deformation peaks and wait phases in between in order to capture somehow the plasticity effects, which are otherwise not represented in the simulation (the hysteresis behavior itself is not modeled in the simulation system). The new length driven measurements finally have a small deviation error of only 3% seems to be quite high.

However, we have to consider that for a more accurate simulation of shear, the various shear directions should be considered.

With regards to the bending property, the FAST method is not suitable as it is based on the Cantilever principle, where the deformation angle is too small ( $41.5^\circ$ ). The KES-f experiment bends the fabric until an angle of  $150^\circ$ . Ideally, however, the maximum measured angle should be as close to  $180^\circ$  as possible. Moreover, the KES-f test is applied to a 1cm fabric width, what corresponds well to small wrinkles.

In comparison to the tensile and shear measurement data, the bending force-deformation curves take a relatively linear course and hence, a linear interpretation of the data is accurate. The bending hysteresis step measurements show that almost no plasticity effects occur.

## 5.4. Accuracy of the viscosity parameters for tensile, shear and bending

*Conventional theory of elasticity deals with mechanical properties of solid bodies, where, according to Hooke's law, the strain is proportional to the deformation and is independent of the deformation velocity. Conventional theory of hydromechanics deals with viscose fluids, where, according to Newton's law, the strain is proportional to the deformation velocity and independent of its size. However, in reality, there are no ideal solid bodies or fluids. In solid bodies, proportionality exists only in limited areas of deformation. In fluids, proportionality exists only for limited velocity deformations. [Gersak 04]*

Textiles are viscoelastic materials, since they show characteristics of both fluids and solids. Fabrics are not able to maintain a constant tension under a constant deformation. Tensions are gradually decreasing (relaxation). This effect is precisely the fabrics plasticity behavior (also see 6.2.3. limitations of the simulation system). The fluid characteristic of textiles allows them to retain energy during stress. After the removal of the stress, deformations are thus partly recovered (elastic recovery). This characteristic is defined as the fabrics viscosity behavior.

Typical viscosity values of various materials are:

Substance	Viscosity in Pa.s
<b>Fluids:</b>	<b>Values &lt; 10<sup>2</sup></b>
Water	0.890 (at 20°)
Corn syrup at room temperature	8
Motor Oil at room temperature	1
Canola Oil at room temperature	0.1
Air (at 18° C)	1.9 * 10 <sup>-5</sup>
<b>Solids:</b>	<b>Values &gt; 10<sup>12</sup></b>
Glass	10 <sup>40</sup>
Polypropylene	2.4 x 10 <sup>5</sup>
<b>Viscoelastic materials such as fabrics</b>	<b>Between 10<sup>2</sup> and 10<sup>12</sup></b>

**Table 24: typical viscosity values [Handbook]**

There are devices to measure the viscosity property of substances. The viscosity of fluids can be measured with a viscometer, measuring flowing speed [Handbook]. However, this method is purely designed for fluid materials and can obviously not be applied to textiles. Thus, today, no standard device exists for the characterization of the tensile, shear and bending viscosity of textiles.

#### 5.4.1. Viscosity in the applied simulation system

As already stated, in state of the art simulation systems, energy functions compute the 3D position of the vertices. The velocity dependant viscosity parameters accompany each elasticity parameter as a factor of energy damping and describe the resulting force from a given deformation speed. The viscosity parameter therefore reduces the deformation velocity.

#### 5.4.2. Existing approaches to acquire fabric damping parameters

Energy damping is an important factor for dynamic fabric simulation, since it has a significant influence on the realism of the cloth movement. Today, parameters are tuned by hand. Within previous studies, damping parameters are obtained by studying the real cloth movement and by approaching the cloth movement with simulation experiments. Therefore, a piece of cloth was fixed on a stab. The other end was pulled up and released so that the fabric is falling down. The same test was performed in real and virtual for six different fabrics. Realistic viscosity damping values were defined to be: (tensile elasticity value)  $\cdot 10^{-2}$  N.m.s., (shear elasticity value)  $\cdot 10^{-2}$  N.m.s. and (bending elasticity)  $\cdot 10^{-2}$  N.m.s.

One different approach from [Charfi 06] experimentally tried to derive suitable cloth damping parameters with the MOCAP system. Precise 3-D trajectory data of real fabrics in free fall movement were acquired and transferred to the virtual simulation.

#### 5.4.3. New approaches

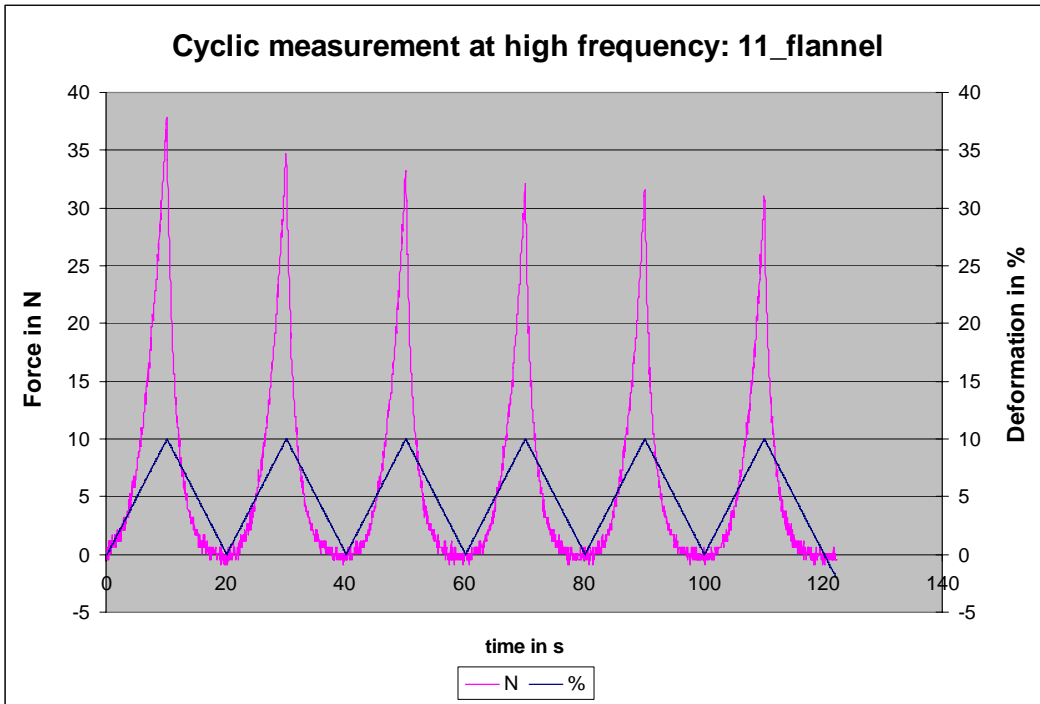
Until today, viscosity parameters are derived from elastic parameters by a multiplication of the factor  $10^{-2}$  [Venus]. This means that each elasticity behavior determines the corresponding damping parameter. This is, however, a simplified assumption, since the elastic parameter does not comprise any information about the relationship between potential recover energy and potential disappearing energy. Moreover, fabrics that retain their energy more effectively during deformation should be more damped.

##### 5.4.3.1. Measurements at high frequency and creep tests

A textile viscosity measurement would need to be able to detect the potential energy (elastic recovery energy) throughout a stress application. This is a challenging task, however, it is possible to measure the gradually decreasing energy (plasticity effect). As the fabrics plasticity and viscosity behaviors are related (total energy = dispersing energy + potential energy), the idea is to derive conclusions about viscosity from the plasticity measurements. In the following section, two different plasticity measurements are conducted.

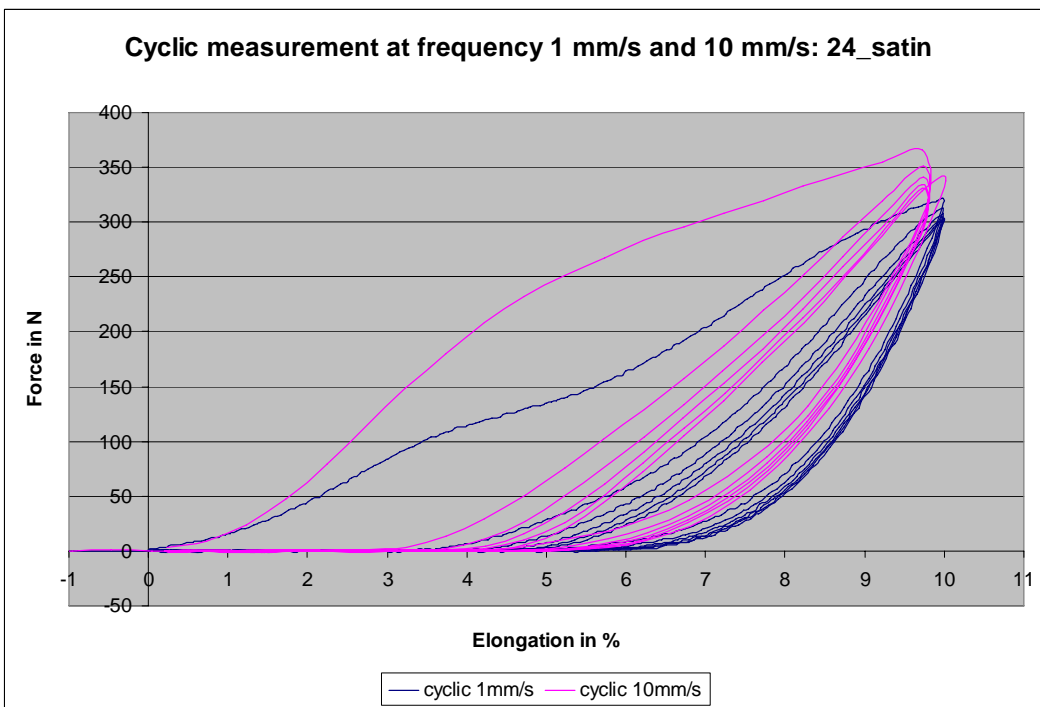
- Measurement at high frequency

For the high frequency measurement, the fabric sample is repeatedly elongated in quick succession. The energy loss over time is visible from the decreasing force peaks (Figure 142). Three fabrics with different tensile behavior are tested in the warp direction: 11\_flannel, 24\_satin and 38\_weft-knit. Six cycles of a deformation of 10% are performed. Two different measurement speeds are applied: 10mm/s and 1mm/s.



**Figure 142: Cyclic load – unload test sample 11\_flannel**

The recorded force peaks descend from 37.8 N, 34.7 N, 33.1 N, 32.1 N, 31.6 N to 30.5 N. During the gradually decreasing fabric tension, potential energy is released. Thus, less energy opposes the subsequent deformation and less force is needed to deform the fabric to the same extent.



**Figure 143: Comparison cyclic tensile test at two speeds, 1mm/s and 10mm/s for sample 24\_satin**



The superposition of the force-deformation profiles, measured at different speeds, shows that the envelopes of the faster measurement are slightly larger. Thus, during the faster experiment, less energy evaporates and greater forces are needed for the succeeding deformation.

- Creep test

During the creep test, a fabric is deformed to a specific extent and held over some time. The corresponding decreasing fabric tension is recorded. For this test fabric samples 24\_satin and 11\_flannel are elongated 10% and the very elastic fabric 38\_weft knit is elongated up to 50%. Figure 144 illustrates that most of the energy loss takes place in the first 10 seconds, followed by a slowly decreasing graph. Fabric sample 24\_satin, which is the most inelastic fabric sample, shows the most abrupt energy loss of the three samples. The more elastic fabrics tend to keep their potential energy better.

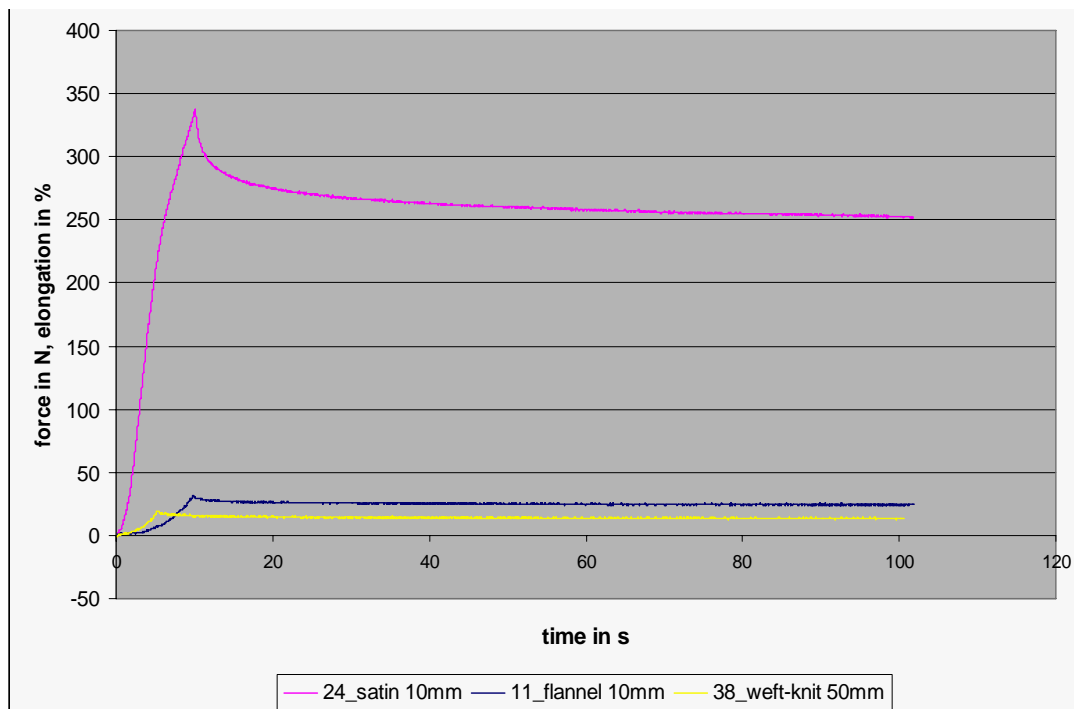
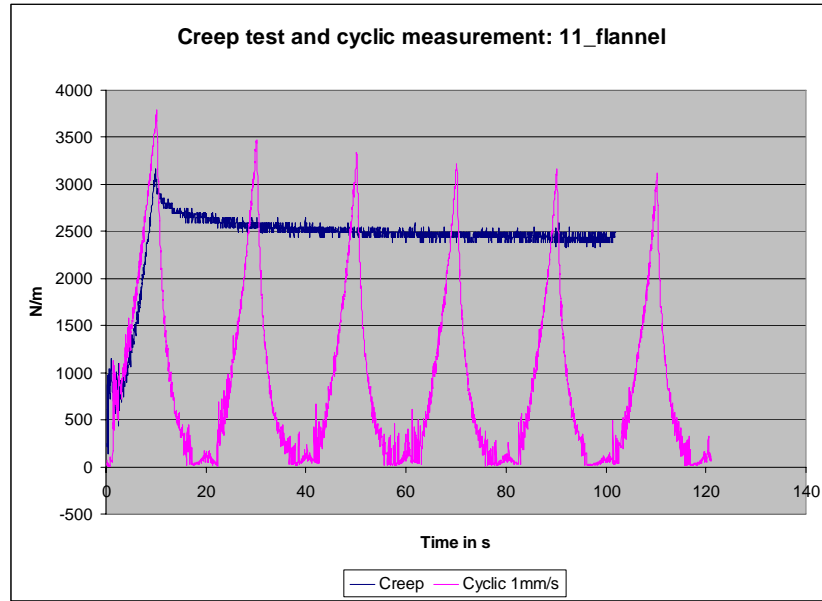


Figure 144: creep test sample 24\_satin, 11-flannel and 38\_weft knit

- Comparison

Both measurement methods illustrate the fabric's plasticity behavior for different occurrences. The measurement at a high frequency corresponds to fast cyclic movements (running), whereas the creep test records what happens to a fabric during an enduring movement (sitting). The superposition of both test data sets shows a good correlation (Figure 145). However, the energy loss during an enduring movement seems to be more abrupt than during a cyclic movement.



**Figure 145: Comparison creep test and cyclic measurement for fabric 11\_flannel**

- Conclusions for the viscosity parameter

Both tests visualize well the fabric's plasticity behavior. However, no rules for the derivation of an adequate viscosity parameter for the applied simulation system could be found, since their relationship is more complex.

#### 5.4.3.2. Elastic potential

Next, we try to use existing research on the fabrics elastic potential for a possible derivation of viscosity parameters. The elastic potential of fabrics was developed by [Gersak 04] and describes the relationship between deformational and reversible energy. It is thus a measure of the fabrics ability to recover after the removal of an applied force. Gersak defined the elastic potential for tensile (EP), shear (GP) and bending (BP) in the following way:

$$EP = WT(RT / 100)$$

$$GP = G_R \left( \theta_m - \frac{2HG}{2Gr} \right)^2 / 2, \quad G_R = G + \left( 2HG - \frac{2HG5}{5} \right)$$

$$BP = B \left( \left( K_m \frac{2HB}{2B} \right)^2 \right) / 2$$

In Figure 147, the calculated elastic potential for the first fabric selection is shown. The more elastic a fabric, the higher their elastic potential value. Hence, elastic fabrics tend to recover

better, after the removal of the force. Fabric 20\_warp-knit velour possesses the highest elastic potential, followed by 21\_single-jersey.

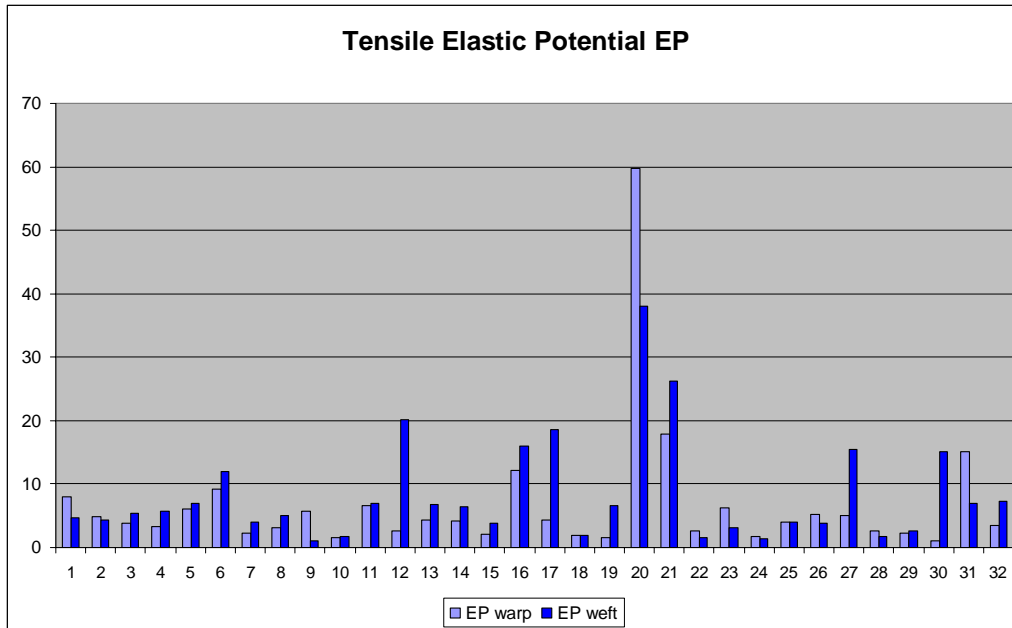


Figure 146: Elastic tensile potential EP calculated for the first fabric selection

In Figure 148, the EMP value (greatest elongation at 500gf/cm) is compared with the elastic potential value EP for the fabrics weft direction. We can see that the most elastic fabrics (17\_crepe-knit, 20\_warp-knit velour, 21-single-jersey) do not automatically possess the highest elastic potential. For example fabric 12\_denim, which elongates much less but contains elastane fibers in the weft direction, possesses a slightly higher elastic potential than fabric 17\_poly-crepe. Hence, based on Figure 148 we can say that viscosity is not proportional to the elongation itself.

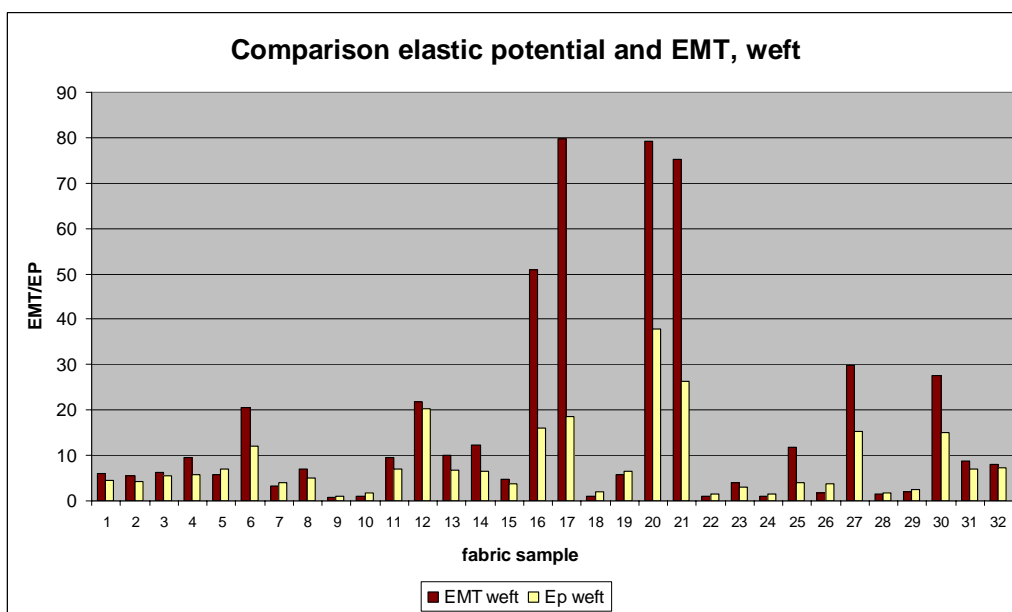
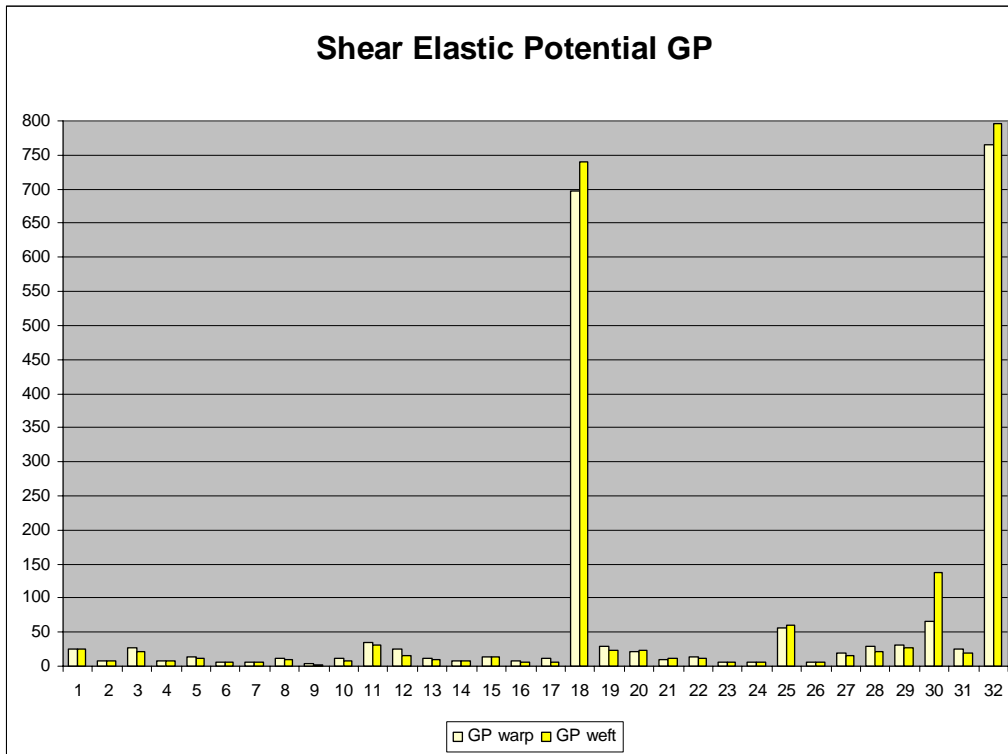


Figure 147: Comparison EP and EMT, warp

Even it is also not possible to directly derive a viscosity parameter from the elastic potential, the values have, however, been used for the fine-tuning and weighing of existing viscosity parameters.



**Figure 148: Shear elastic potential GP calculated for the first fabric selection**

- Drawbacks

The elastic potential is a simple measure in order to obtain further information about the relationship of reversible and nonreversible energy during a deformation process. The graphs are, however, based on the characteristic values of the KES-f measurements. As KES-f experiments for tensile and shear are not used for dynamic simulations, the calculation of the elastic potentials might be inaccurate for our application.

#### 5.4.3.3. New viscosity parameters

With the previous experiments it was not possible to establish a new method for the derivation of new viscosity parameters from measurements. Thus, additional simulation experiments were executed and the viscosity parameter visually assessed and defined. The tests revealed that the existing tensile and shear viscosity parameters (elastic parameters \*  $10^{-2}$ ) were too low. New viscosity parameters are defined to be: (elastic parameter) \*  $10^{-3}$  N/m.s. Additionally, the calculated elastic potential of fabrics is used for the fine-tuning and weighing of viscosity parameters.

The elastic potential for bending, however, did not return useful values. Bending viscosity parameters were therefore approximated by additional simulation experiments. Better bending viscosity values were found to be: (bending elasticity) \*  $10^{-9}$  N.m.s

#### 5.4.4. Air Viscosity (Flowing/Damping)

Real air viscosity basically depends on the temperature. For example at 15 °C real air viscosity is  $1.78 \times 10^{-5}$  kg/m.s. In the virtual simulation system no real environment and real air components are modeled and the air viscosity parameter is a simplification. The virtual air viscosity parameter is a viscous force, proportional to the speed difference between the fabric and the surrounding air, which is assumed to be still. The virtual Air Viscosity is linear, meaning that a small or a big object is falling at the same speed.

The energy damping, as described in the previous chapter is distributed between the viscosity (tensile shear and bending) and air viscosity. The air viscosity parameters are flowing and damping:

- (1) Flowing: Aerodynamic force exerted on a fabric per surface unit and per velocity unit between the fabric speed and the air speed (wind).
- (2) Damping: Normal and tangential components relative to the orientation of the fabric surface.

Existing air viscosity parameters are defined for much more elastic fabrics, with generally higher viscosity values. Hence, the Air Viscosity parameter is also adjusted with simulation experiments. New Air Viscosity values are defined to be: 0.2 (omni) and 2 (normal) N.s/m<sup>3</sup>.

#### 5.4.5. Conclusion for the viscosity parameter

As the hysteresis behavior is not modeled in state of the art simulation systems, it is difficult to derive parameters for a property, which as this does not exist in reality.

## 5.5. Friction

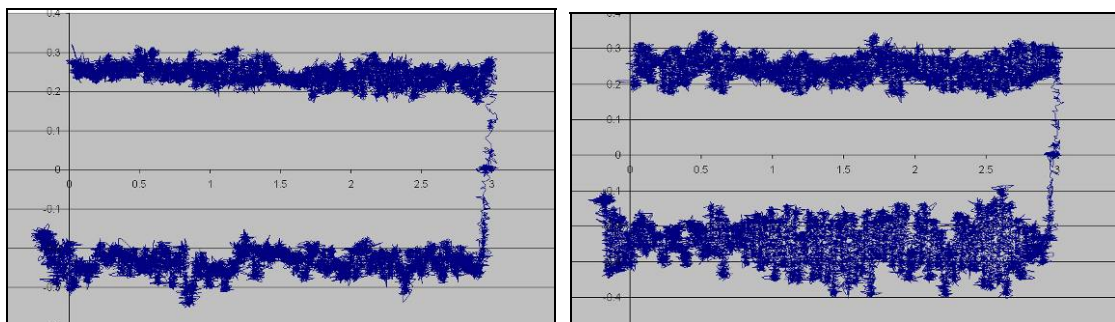
Friction is the resistance that one object encounters when moving over another. The friction property of a material is particularly difficult to define. Research and technology deals with friction as part of tribology science (Greek: to rub = tribo). Generally differentiations are made between static and dynamic friction. Static friction is the initial force at which a fabric begins to glide over a surface. Dynamic friction occurs when two objects are moving relative to each other during sliding, for example. It is similar to the angle at which a fabric continues to move over a surface with constant speed. For most materials static friction is higher than dynamic friction.

The friction parameter is relevant for static and dynamic simulations. It was, however, not treated in the previous section regarding static simulations, as at that point only elastic properties were considered. Both types of friction are discussed in this chapter.

### 5.5.1. Friction measurement

Of the standard fabric characterizations only the KES-f method measures the friction property. The measurement is conducted with a piano wire (metal loop), which slides over the fabric surface and records the resulting friction (also see 2.1.1.1). Obtained characteristic values are MIU (mean value of the coefficient of friction) and MMD (mean deviation of the coefficient of friction). Friction is measured in four directions: back and forth in warp direction, back and forth in weft direction.

The highest friction of 0.408 was observed for sample 27\_fleece and lowest of 0.103 for sample 18\_motorcyclist wear. The friction coefficient differs in the weft and warp direction. Most differences in friction in the weft and warp directions were visible for the more rough knitted fabrics (also see chapter 4.2.1.6.).



**Figure 149: Friction profile 01\_denim warp (left), weft (right)**

### 5.5.2. Friction in simulation applications

Various types of friction are considered in different applications. In the applied simulation system two kinds of friction are considered, whereas other simulation systems such as Maya or 3DSmax often consider three types:

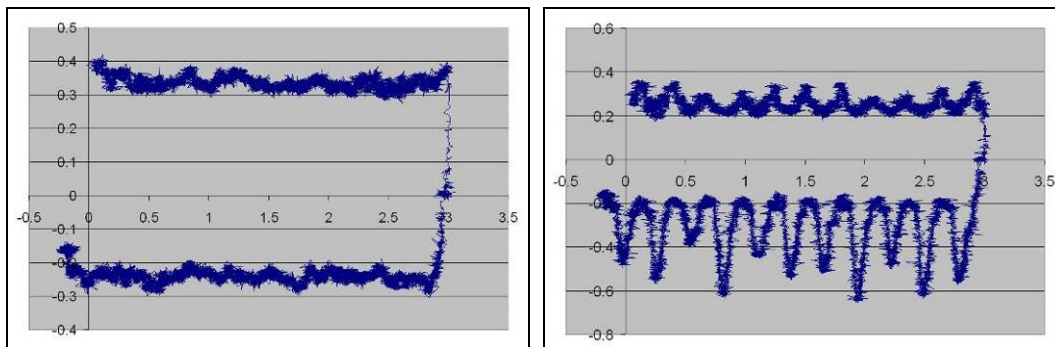
Application:	MIRALab	3DSmax	Maya
Static friction:	----	body – fabric	body – fabric
Dynamic friction:	body – fabric fabric – fabric	body – fabric fabric – fabric	body – fabric fabric – fabric

**Table 25: Various types of friction in various the simulation applications**

However, no simulation application today is capable of taking into account the friction property in different fabric directions. Hence, to obtain a friction parameter, the mean value of MIU warp and MIU weft is used.

### 5.5.3. Static and dynamic friction

For the assessment of the initial higher static friction, the empirical KES-f data is looked at in more detail. If the static friction is noticeably higher, then the measurement profiles should show a higher impulse at the beginning of the experiment.

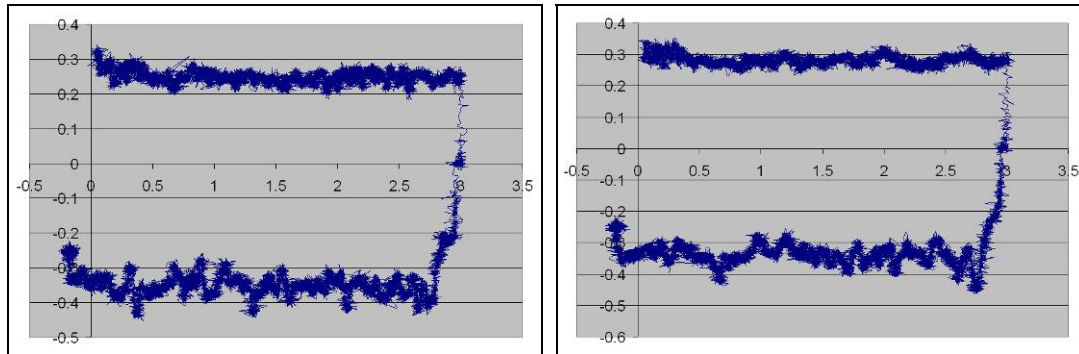


**Figure 150: Friction profile fabric 03\_cord warp (left) weft (right)**

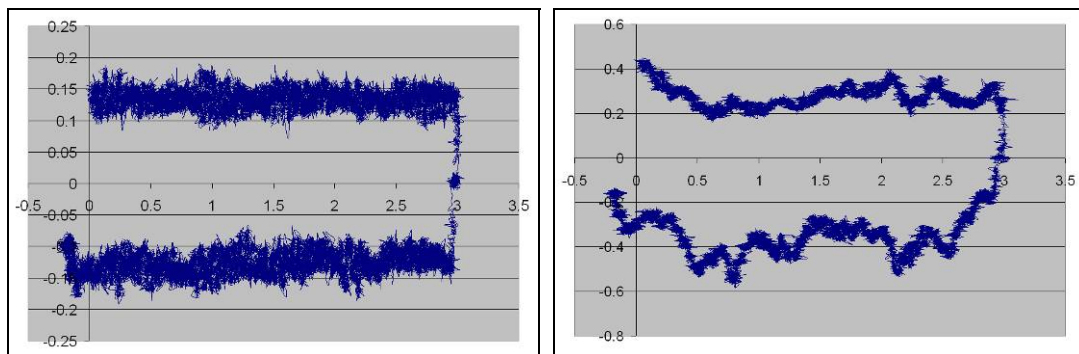
However, the friction profile of fabric 03\_cord, (where the corduroy burls are very well visible in weft direction) shows only a slightly higher initial friction measurement in warp direction (Figure 150).

Fabric 15\_velevet is a textile with a pile. From its friction profile in the pile direction (Figure 151, left) it is clearly visible that the friction against the pile is much higher than the friction in the pile direction. Although only slightly higher initial forces are detected.

Most fabrics with a more or less flat surface thereafter show a friction profile similar to fabric 05\_gabardine (Figure 152, left). The friction profiles are homogeneously straight and no significant deviation is ascertained, not even at the beginning of the measurement. The only fabric with a clearly observable higher initial friction is fabric 14\_tweed (Figure 152, right), which is a thicker and more uneven fabric with irregular burls. However, looking at the more disturbed profile, this deviation becomes marginal.



**Figure 151: Friction profile fabric 15\_velvet warp (left) weft (right)**



**Figure 152: Friction profile fabric 05\_gabrdine warp (left), 14\_tweed warp (right)**

It can therefore be concluded that no significantly higher static friction could be detected from the KES-friction measurements. Only certain fabrics, with a higher friction and an uneven surface, show slightly higher static frictions.

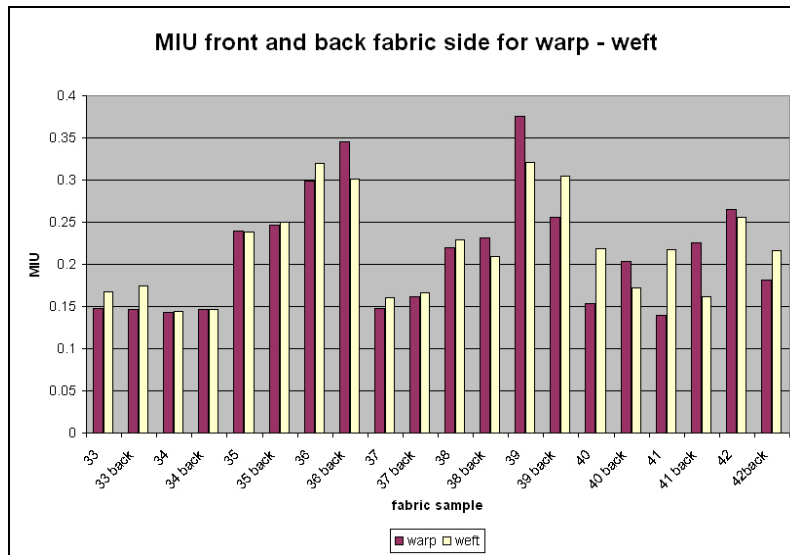
#### 5.5.4. Friction in warp and weft fabric direction

KES-f measures friction in the warp and weft direction. The difference in friction coefficients in warp and weft varies from 0 (fabric 08\_bourette-silk) to 0.15 (16\_lurex-knit, 17\_crepe-knit, 30\_tulle) (Figure 54). The difference of 0.15 constitutes a deviation of up to 50% for fabric 17\_crepe-knit. Therefore it is highly inaccurate for a simulation system's friction parameter to ignore the fabric direction.

#### 5.5.5. Friction on the front and on the back fabric side

Several textiles, with a pile (as fabric 03\_cord, 15\_velvet, 39\_weft-knit terry) or which are post-processed on the outer surface side (fabric 18\_motorcycle wear) possess different friction characteristics on each fabric side. Thus, for an accurate simulation, it would be important to consider the friction on both the front and the back fabric side. During simulations the measurement on the inner fabric side would be important for the friction between body and fabric, whereas the fabric outer side measurement would describe the friction between fabric and fabric. For a comparison of various frictions, the fabrics of the second selection are measured on both sides.





**Figure 153: MIU in weft and warp direction for the first fabric selection**

Value MIU shows homogenous friction behavior for the wool fabrics 33, 34, 35, 36 and 37. However MIU, for the more elastic fabrics, shows wider variations. Fabrics 38, 39, 41 and 42 display significant differences in outer and inner side friction. For example, 39\_weft-knit terry fabric possesses burls on its outer side, resulting in a variance of 32% between the friction coefficients of its two sides. It is clearly important to consider the friction of both sides of a fabric when constructing a virtual simulation model.

### 5.5.6. New friction experiment

A large quantity of information may be derived from the detailed KES-f friction measurements. One major criticism of the method is, however, that it is conducted using a metal wire. As already mentioned, the friction parameter is heavily influenced by the type of material involved. An experiment conducted with a metal wire can hardly be considered as a realistic approximation to the real situation, where a fabric rubs against the body or against the garment itself.

Therefore, a new friction measurement is necessary, which better imitates the real garment wear situation. For the new experiment, the friction between the fabric and the body is assessed with the skin being imitated by a piece of leather. The friction between fabric and fabric is examined by replacing the leather with a piece of fabric.

The „tilted plane” method is applied for the new test: the fabric sample is placed on a flat plane with an object of a certain weight on top. Subsequently, the plane is slowly inclined until the object begins to slide. The tangent of the tilting angle is the friction angle and is related to the coefficient of friction  $\mu$  ( $\mu = \tan\theta$  [Tribo]).



Figure 154: Scheme of friction evaluation [Tribol]

The experiment is conducted with two different settings: Firstly using a box weighing 100g and secondly 500g. The measurement of each weight is recorded as a control measure. Both experiments should return the same friction coefficient.

The test fabrics are not ironed beforehand in order to imitate real wear situations, where fabrics are slightly uneven. The test “fabric to skin” is performed with the inner side of the fabric and the test “fabric to fabric” with the outer fabric side. Both tests, “fabric to skin” and “fabric to fabric” are performed in the warp and weft fabric directions. The experiment “fabric to fabric” is additionally performed for warp against weft fabric direction. Fabrics with a pile are tested in the pile and against the pile direction. All 22 fabrics of the first fabric selection are tested. Each fabric is tested four times and the average value is taken as the friction coefficient. (Complete test results see Annex E)

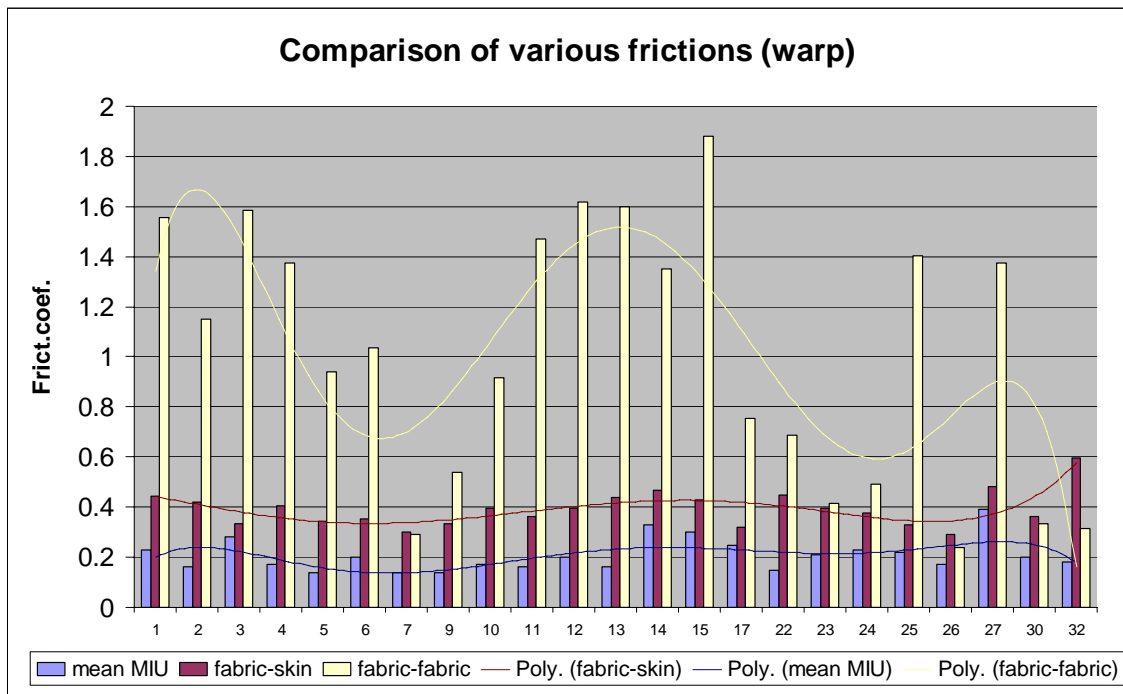


Figure 155: Comparison of three obtained friction parameters

Comparing the three data sets (KES-f, “fabric to skin”, “fabric to fabric”) the KES-f data returns the lowest friction coefficients. The experiment “fabric to fabric” returns the highest values for cotton, wool and fabrics with a pile. The trendlines of the three data sets show correlation between the KES-f and the “fabric to skin” measurement.

A fairly significant static friction was observed during the new experiments, especially during the “fabric to fabric” test. In addition, decreasing friction was observed during the four measurement cycles, as the fibers were probably oriented in the same direction after the first test. This, however, corresponds to what happens during real life garment wear.

In summary, the KES-f friction measurement is precise, but not suitable for a use in virtual simulations, as the resistance created by the metal wire is too low. Measurements with a piece of leather as contact material better imitate real garment wear situations (although it is not possible to imitate the skin moisture). A second measurement for the specification of the “fabric to fabric” friction is absolutely necessary, as completely different frictions occur, when a fabric rubs against itself. The friction “fabric to skin” should be measured on the fabric inner side and the “fabric to fabric” friction on the fabric outer side. For better precision, measurements should be conducted in both the warp and weft fabric directions. Also the static friction needs to be determined for the higher “fabric to fabric” friction.

## 5.6. New fabric measurement specifications

In order to summarize the obtained knowledge from the previous investigations, the suitable fabric measurements for static and dynamic simulation are listed once more in this paragraph (together with the single steps which led to the new characterization protocols).

### 5.6.1. Suitable measurements for static simulations

KES-f and FAST tensile parameters are accurate enough for static simulations. KES-f and FAST shear parameters are accurate enough as well for fabrics exhibiting linear shear behavior. For fabrics with a fairly nonlinear shear behavior, inaccuracies might occur for textiles with greater densities. In this case the nonlinear KES-f shear parameter should be used.

KES-f and FAST bending measurements return the bending rigidity as linear fabric description which is sufficient accurate. However, the simulation of bending generally comprises inaccuracies from the simplification of the bending behavior, by not considering the front and the back bending, in the simulation application. The fabric's hysteresis behavior is not relevant for static simulations. In summary, the standard measurement methods are suitable for the derivation of fabric parameters for static simulations.

<b>Static simulation:</b>	<b>FAST</b>	<b>KES-f</b>
Tensile	accurate	accurate
Shear	accurate (for linear shear behavior)	accurate
Bending	accurate	accurate

**Table 26: Suitability of standard measurement methods**

### 5.6.2. Suitable measurements for dynamic simulations

For dynamic garment simulations, the FAST measurement method is not suited for the derivation of parameters. From the KES-f experiments only the bending measurement was sufficient accurate. For the derivation of tensile and shear parameters, the new developed length driven measurement methods (LDM, LDSM) are better suited. The tilted plane method returned better friction parameters.

<b>Dynamic simulations:</b>	<b>FAST</b>	<b>KES-f</b>	<b>LDM</b>	<b>Tilted plane</b>
Tensile	not accurate	not accurate	<b>accurate</b>	----
Shear	not accurate	not accurate	<b>accurate</b>	----
Bending	not accurate	<b>accurate</b>	----	----
Friction	----	not accurate	----	<b>accurate</b>

**Table 27: Suitability of various measuring methods**

- Conclusion for tensile

The FAST tensile data is not suited as the measurement is limited to one low applied load. The KES-f tensile measurement, even returning a nonlinear force-deformation envelope, is not suited. On the one hand, the maximum load is too low and on the other hand, the solely applied load does not represent what happens during wearing of garments.

The ITT step tensile test captures more information over a broader bandwidth of various forces and corresponds better to what happens during garment wear. The applied step measurement constitutes an improved recording of the fabric’s plasticity behavior. However, the measurement is force driven and thus, not suited.

The new designed length driven step tensile measurement is finally suited for the derivation of accurate tensile and shear parameters. The single measurement steps and measurements limits were defined according to various body movements and according to the body-distance changes. Two deformation profiles were established, one for repetitive movements such as walking and one for non-cyclic movements such as fitting postures. A wait phase of 120 seconds in-between each measurement, for the fabric recovery, is integrated.

The preferable specimen size is 20cm width by 10cm length. As most tensile testing devices only allow a width of 10cm and in order to save costly fabric specimen, a sample size of 10cm x 10cm can be taken as well. The velocity of 1mm/sec. returns sufficient accurate information, avoiding large data sets.

<b>Tensile measurement specification</b>	
<b>Sample size</b>	Preferably 20 cm x 10 cm (10 cm x 10 cm would be satisfactory as well)*
<b>Point of rupture</b>	The point of rupture needs to be tested on a smaller fabric sample (5 x 10cm)
<b>Applied deformation</b>	Cyclic step measurement profile: 0 – 10% – 0 – 10% – 0 – 10% – 0 – 10% – 0 – 10% – 0 – 10% – 0
	Non-cyclic step measurement profile: A) 0 – 10% – 0 – 25% – 0 – 5% – 0 – 20% – 0 – 5% – 0 – 10% – 0 B) 0 – 10% – 0 – 15% – 0 – 5% – 0 – 15% - 0 – 5% – 0 – 10% – 0 * (*The non-cyclic profile B should be applied to fabrics with a point of rupture lower than 30%)
<b>Wait phases</b>	120 seconds
<b>Speed</b>	1 mm/second

**Table 28: Tensile measurement specification**

\* In the deformation direction, additional fixation length needs to be added.

- Conclusion for shear

FAST and KES-f shear measurements are not suited for the derivation of accurate shear parameters for dynamic fabric simulations. The FAST measurement only returns linear data and is a force-driven experiment. The KES-f shear measurement is length driven, however the maximum applied deformation is too low (~ 3.4%).

A length driven step shear measurement, applying the same deformation profile as for the tensile measurement, is better suited. As state of the art simulation systems only consider one shear direction, the measurement is taken on a bias cut fabric sample (45°). Fabrics are generally fairly more elastic in shear direction; thus no point of rupture is detected for this measurement. Moreover, the deformation profile for more elastic fabrics is applied.

<b>Shear measurement specification</b>	
<b>Sample size</b>	Bias cut fabric sample, preferably 20 cm x 10 cm (10 cm x 10 cm would be satisfactory as well)*
<b>Applied deformation</b>	Cyclic step measurement profile: 0 – 10% – 0 – 10% – 0 – 10% – 0 – 10% – 0 – 10% – 0 – 10% – 0
	Non-cyclic step measurement profile: 0 – 10% – 0 – 25% – 0 – 5% – 0 – 20% – 0 – 5% – 0 – 10% – 0
<b>Wait phases</b>	120 seconds
<b>Speed</b>	1 mm/second

**Table 29: Shear measurement specification**

\* In the deformation direction, additional fixation length needs to be added.

- Conclusion for bending

FAST and KES-f bending measurements are length driven. The FAST bending measurement is however not suited for dynamic fabric simulations, as the returned bending rigidity value is based on a too low deformation. The KES-f bending test is better suited as it captures the moment – curvature relationship up to an angle of 150°. For bending, no step measurement is necessary, as plasticity effects are small.

<b>Bending measurement specification (see 2.2.2.2) [KAW80]</b>	
<b>Sample size</b>	20 cm x 1 cm
<b>Applied deformation</b>	0 – 150°
<b>Speed (curvature change rate)</b>	The is 0.50 cm-1 /sec.

**Table 30: Bending measurement specification**

- Conclusion for friction

The FAST standard does not measure the friction property. The KES-f friction measurement is not suited for a parameter derivation for virtual simulations as the resistance, created by the metal wire, is too low. Measurements with a piece of leather, for the imitation of the skin as contact material, are closer to reality. A second measurement for the specification of the friction between fabric and fabric is important, as completely different frictions take place, when the material collides with itself. The “body to fabric” friction should be measured on the inner fabric side and the “fabric to fabric” friction on the outer fabric side. Measurements should be conducted in both fabric directions warp and weft. Also the static friction should be determined, as this value can differ considerably for the “fabric to fabric” friction. The tilted plane method is simple and satisfactory.

<b>Friction measurement specification</b>	
<b>Sample size</b>	Ideally 40cm x 20cm for the fixed fabric on the plane, 20cm x 20cm for the fabric around the box. If fabric samples are limited: 20cm x 10cm for the fixed fabric on the plane, 10 cm x 10 cm for the fabric around the box.
<b>Sliding box</b>	Weight: 500g, sliding box size ca.10 cm x 10 cm x 5 cm,
<b>Size of the plane</b>	40 cm x 20 cm, fixed on one side of the bottom,

**Table 31: Friction measurement specification**

# Chapter 6

## Validation

### 6.1. Experiment description

Subsequently, the newly derived parameters are validated within an applied example. An entire garment prototyping process is performed, comparing the real procedures with the virtual simulated ones. Additional experiments, respectively to each topic, are added for garment details which cannot be shown on the prototyping example.

For the prototyping experiment the real mannequin is scanned with a body scanner to obtain an accurate virtual 3D body model. From the scan, exact body measurements are obtained, which are used for the construction of a real “made to measure” 2D pattern and dress. For the corresponding virtual dress, the real 2D pattern is digitized and imported to the simulation system. Inside the simulation system, the dress is virtually tailored using the new derived fabric parameters. Afterwards, both the real and the virtual fitting procedures (comfort performance and utility performance) are performed in parallel and are compared.

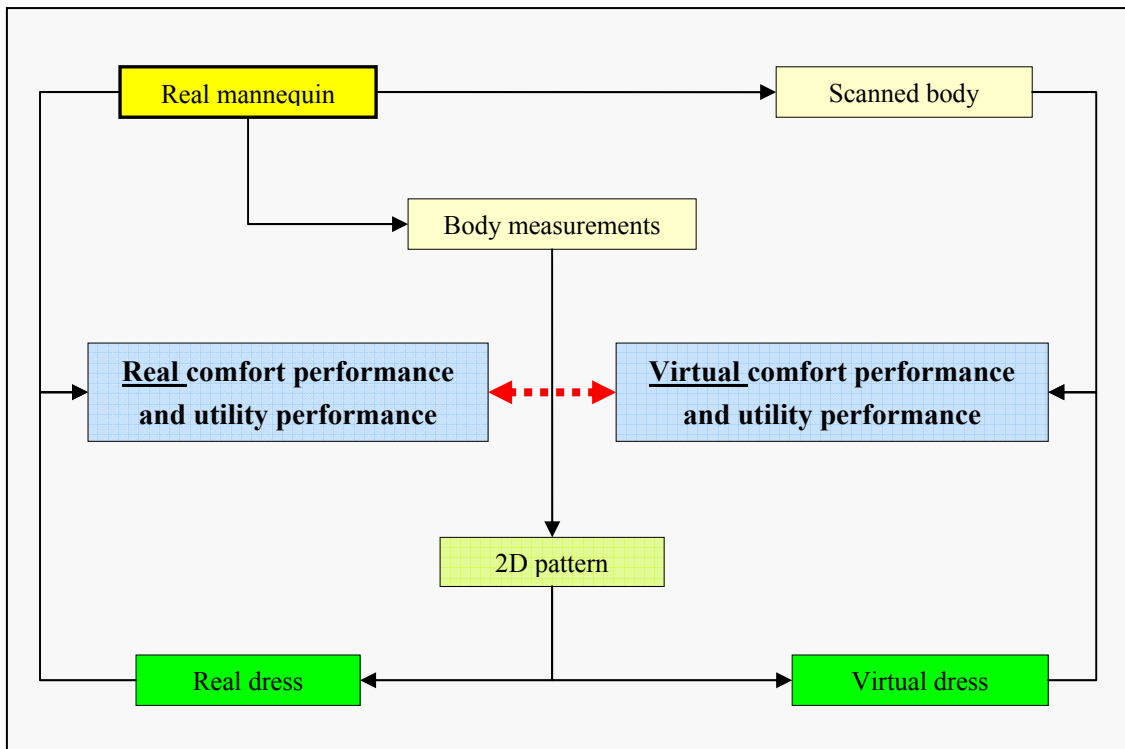


Figure 156: Pipeline of validation experiment



## 6.2. Comparison of real and virtual garment prototyping processes

### 6.2.1. Real and virtual mannequin

A female mannequin is chosen for the prototyping experiment. The person is scanned with a body scanner, wearing underwear and shoes (Figure 157). As the underwear and shoes are influencing the body silhouette and posture, the same underwear and shoes are worn later on during the real fitting process.

- Error margin

According to the information of the scanner company [human solutions], an error margin of 1mm might be included within the scan data. However, taking into account the body dimensions (Figure 158) and our accuracy scheme of 0.2% (0.7%), this error is not significant.



**Figure 157: Scanning process of the real mannequin (left), virtual mannequin (right)**

### 6.2.2. 2D pattern

The body scanner automatically returns a predefined set of body measurements. Therefrom, the most important for the 2D pattern construction are retained. Out of this data, a simple, straight and close fitted dress is designed, customized for the mannequin's body. For this, a standard 2D pattern construction method is applied [Müller & Sohn].

The dress is constructed as simple as possible, in order to avoid unnecessary seams, which would additionally influence the garment appearance. The influence of seams on the fabric's

mechanics and the garment's appearance is however not tested within this study and is thus avoided.

Body height	158 cm
Bust circumference	89 cm
Waist circumference	69 cm
Hip circumference	98 cm
Leg length (waist to ankle)	93 cm
Skirt length (waist to below knee)	61 cm
Arm length (outer shoulder to wrist)	53 cm
Shoulder width	11 cm
Back length (cervical vertebra to waist)	37 cm
Front length 1	26 .5 cm
Front length 2	44 cm
Seat raise	24 cm

**Table 32: Mannequin's body measurements**

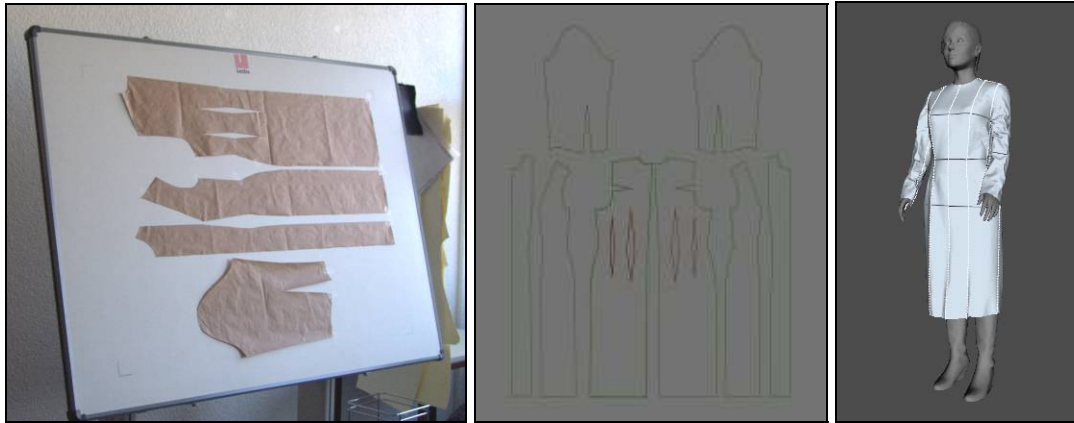
### 6.2.3. Real and virtual dresses

The real dress, is tailored out of a simple cotton material (02\_shirt –cotton), using the previously designed 2D pattern.



**Figure 158: 2D pattern and sewing of the real dress**

Before the assembly of the virtual dress, the 2D pattern needs to be digitized. For this step, the 2D paper pattern is fixed on a digitalization board and scanned with a particular device (Figure 159, left). Applying this process, exactly the same 2D pattern is obtained within the CAD software (Figure 159, center). Now the 2D pattern data can be exchanged with the simulation system and the virtual dress be tailored (Figure 159, right)



**Figure 159: Digitalization process (left), digitized 2D pattern (center), virtual dress (right)**

- Error margin

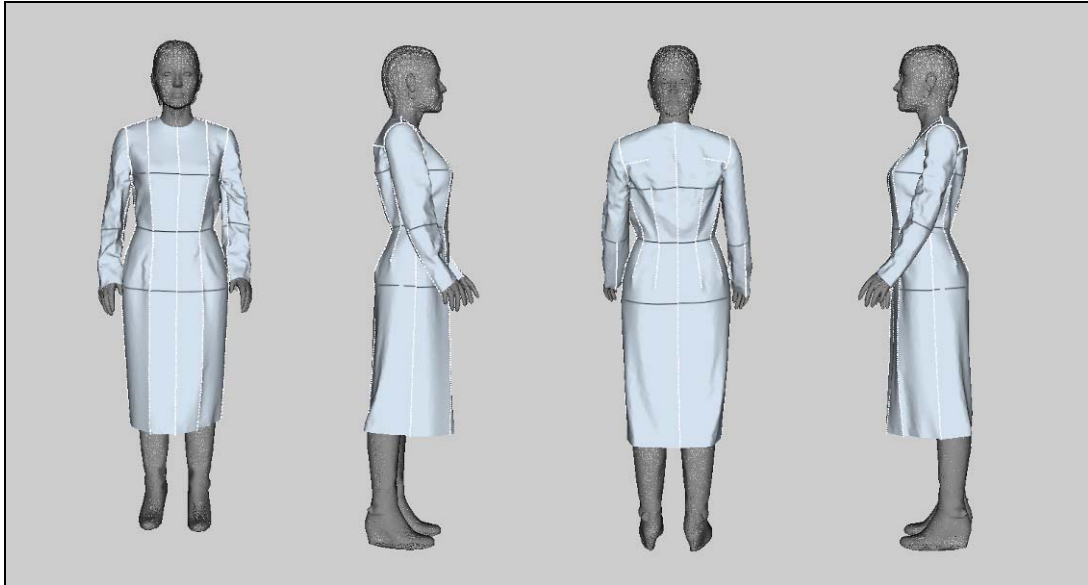
During the 2D pattern design on paper an error margin of 1 mm is unavoidable, due to the used tools. During the real sewing process the margin of error should not be above 1mm for an experienced tailor. The virtual sewing is 100% accurate. However, the digitalization process of the 2D pattern adds another margin of error of ca.1mm. Thus, all together around 3mm error margin (1mm body scan, 2mm garment tailoring) should be taken into consideration during a fitting process (real and virtual).

#### 6.2.4. Comparison real and virtual comfort performance (static simulation)

During comfort performance, the correlation of the garment and the static body is tested, based on four elements of fit: Grain, set, line and balance (see Chapter 5.1.1.). Thus, these four elements are examined on the real and the virtual prototype.



**Figure 160: Real comfort performance**



**Figure 161: Virtual comfort performance**

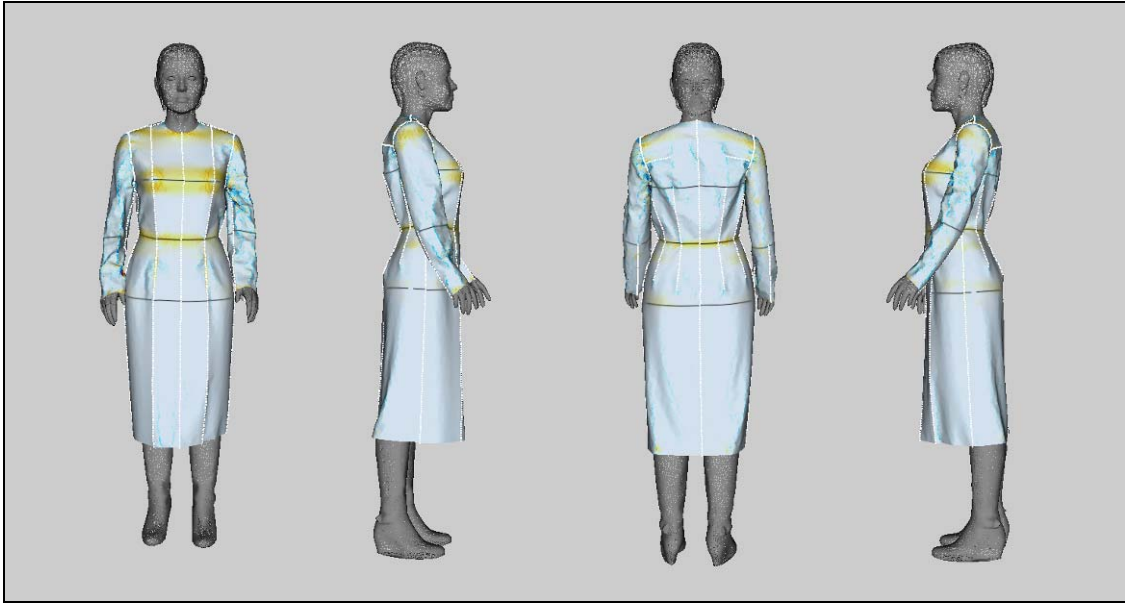
The fit element “grain” is the equal and symmetric appearance of the garment in horizontal and vertical fabric direction. A good “grain” could be stated for the real and the virtual garment prototype of our experiment (Figure 160, 161). On the real prototype, the evaluated vertical lines are the seam lines. On the virtual prototype, the vertical seam lines are visualized in the form of a white dotted line. The horizontal bust, waist and hip lines are visualized with black lines on both, the virtual and the real sample.

The fit element “set” refers to a smooth fit with no undesirable wrinkles. This aspect can also be positively approved for the real and the virtual prototype.

The fit element “line” is related to the design and follows the silhouette and circumference lines of the body. Both prototypes exhibit the same garment lines, for example around the collar, the hem or the sleeve length.

The fourth fit element, the garment’s “balance”, can also be observed in the same way for the real and the virtual prototype. Both garments appear symmetrical from side to side and front to back.

Recapitulatory, we can say that the comfort performance can be performed in the same way on the real and on the virtual garment prototype, although the virtual prototype returns more precise numerical fitting data. In Figure 162, the tensile deformations in the fabrics weft direction are visualized within a scale of 1%. The virtual fitting data reveals that the dress is slightly tight in the bust and in the shoulder area. However, the deformations are fairly below 1% and no 2D pattern alteration is necessary.



**Figure 162: Comfort fitting**

- Additional validation experiment: Fabric drape

The tested dress has a straight cut and is fitted close to the body in order to be able to assess well the tensile property. Consequently, no fabric drapes and folds can be observed and compared on this garment sample. The fabric drape is thus validated with an additional experiment, where the fabric is draped over a sphere, which is fixed on a stick (Figure 163). Three textiles with different bending and shear properties are tested with this experiment: 36\_overcoat fabric, 38\_single-jersey and 41\_warp-knit jersey.



**Figure 163: Fabric 38\_single-jersey: real and virtual drape (left), fabric 36\_overcoat fabric: real and virtual drape (right)**



**Figure 164: Fabric 41\_warp-knit: real and virtual drape**

This experiment returns a fairly good correlation for the real and the virtual fabric drape for samples 38\_single-jersey and 36\_overcoat fabric. The drapes of fabric 41\_warp-knit show a medium good correlation (the virtual drape shows a greater amount of folds). Fabric 41\_warp-knit is also the textile with the largest deviation for the front and the back bending measurement (89% warp). However despite this divergence, the fabric color still gives the impression of a similar textile.

- Additional validation experiment: Scanned fabric drapes

For a better comparison of the real and virtual fabric drapes, the scan test method is applied next. For this experiment, 10 fabric drapes are scanned with the body scanner and compared with the virtual simulated counterpart.

This method does however not deliver any useful result. The scanner calibration for bodies is not suitable for the scanning of fabrics, as the fold depth disappears within the closed polygonal mesh (Figure 165, right). Also the superposition of the scanner raw data (point cloud, Figure 165, center) and the simulated drape in a separate viewer, does not return any significant result, as the point clouds are too blurred.



**Figure 165: Comparison virtual simulation (left), scanned real fabric as point-cloud (center), scanned real fabric as polygons (right)**

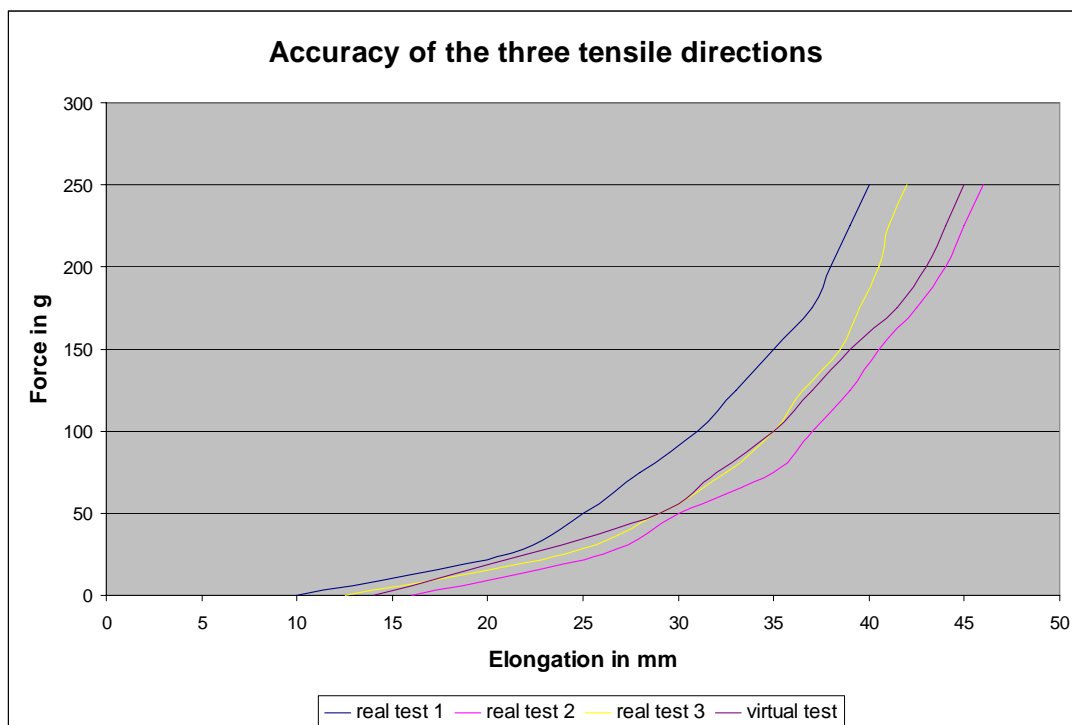
- Additional validation experiment: Accuracy test for the three tensile elasticity directions weft, warp and shear

It rarely occurs that a garment is just elongated in one fabric direction. Therefore, another experiment is set up, where the interaction between the three tensile elasticity directions is assessed. For this test, the real sample 39\_weft-knit terry fabric is fixed in a round support (Figure 166, left). In the following, several progressive loads are applied to the middle of the fabric: 25g, 50g, 75g, 100g, 125g, 150g, 175g, 200g, 225g and 250g. For each of the applied loads, the 3D deformation of the fabric is measured. The real test is conducted three times.

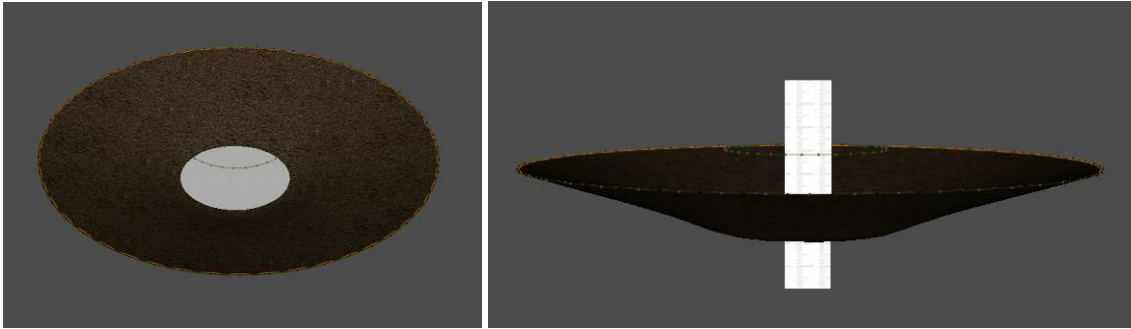


**Figure 166: Set up of the real experiment**

The same experiment is recreated in the virtual simulation system, where the round fabric is fixed in space (Figure 168). The progressive loads are applied in the form of an additional small round piece of fabric, where the density parameter is progressively augmented.



**Figure 167: Diagram illustrating the real and the virtual force – deformation relationship**



**Figure 168: Virtually recreated experiment**

The simulation experiment showed a good correlation of the real and the virtual experiment (Figure 167). The virtual deformations lie within the data-set of the real experiment.

### 6.2.5. Comparison real and virtual utility performance (dynamic simulation)

In order to make a garment truly comfortable, it also requires an adequate freedom of movement. The extent of ease of movement depends on the respective use of the garment (also see Chapter 5.1.2.). In chapter 6.2.4.4. (page 108), the standard movements for fitting procedures are outlined. For this validation experiment, five of the eight movements are recorded with the Vicon Motion Tracking System. One duck squat movement is replaced with a simpler squat movement. During recording, the mannequin is wearing the same shoes (Figure 169).



**Figure 169: Vicon Motion Tracking**

- (1) Walk a distance of around 91 m. (The 91m are reduced to our tracking space)
- (2) Stand erect. With arms at sides, bend body to left and return, bend body forward and return, bend body to right and return.
- (3) Stand erect. Extend arms overhead in the lateral direction and then bend.



- (4) Stand erect. Extend arms perpendicular to sides of torso. Twist torso left and return, twist torso right and return.
- (5) Stand erect. Reach arms across chest completely to opposite sides.
- (6) Simple squat.

During dynamic simulations, the garment follows the movement of the mannequin. Different fabrics should behave differently for each action and return and different fitting feedback (freedom of movement). Thus, garments out of various fabrics are tailored for this experiment: Two dresses (05\_gabardine, 24\_satin) and four skirts (11\_flannel, 38\_weft-knit, 04\_linen, 39\_weft-knit terry fabric). The two tight skirts are based on the 2D pattern of the dress. The two wide skirts are simply gatherings of a rectangle fabric, fixed with a belt.

In the following, the real garment behavior is directly compared with the virtual simulation. For each dress one or several movements are chosen.



**Figure 170: Virtual skirt 38\_weft-knit jersey**



**Figure 171: Virtual skirt 38\_weft-knit jersey**



Figure 172: Virtual skirt 04\_linen



Figure 173: Virtual skirt 39\_weft-knit terry fabric



Figure 174: Virtual skirt 11\_flannel



Figure 175: Real and virtual dress 24\_satin

- Error margin

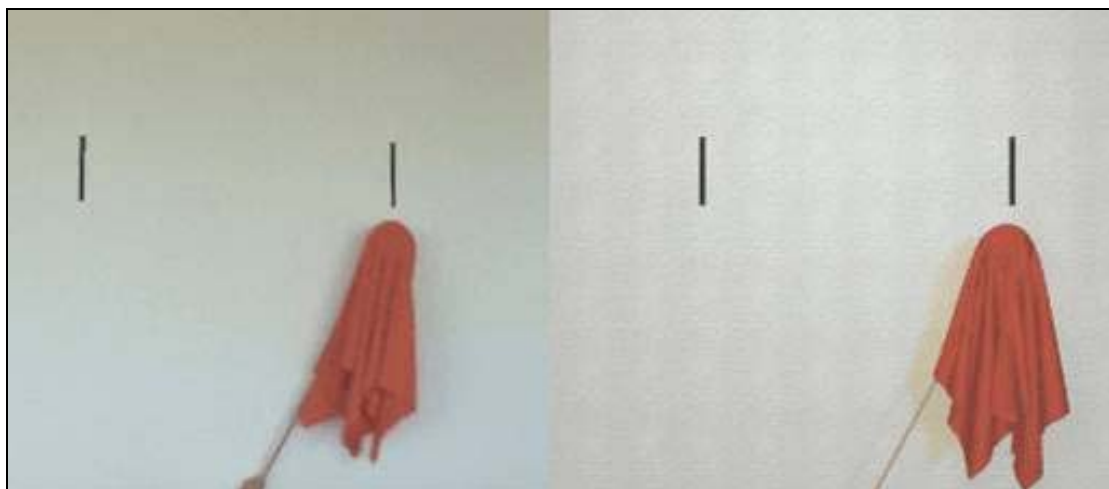
During dynamic simulation important additional error margins influence the simulation result. These additional error margins are basically related to the body animation. When the virtual body is animated, several procedures are applied, which add each of them some kind of inaccuracy to the virtual moving clone. Among them, the three main factors are:

- (1) Today, body animations are mainly obtained with Motion Tracking Systems. The body movement is recorded with infrared cameras that capture reflecting markers, which are placed on significant parts of the body. However, due to instabilities of the markers during the recording, the obtained movement data is not 100% accurate. Inaccuracies of up to 4 cm [Leardini 05] can be comprised, what corresponds to one entire garment size step.
- (2) For the body animation, the 3D mesh needs to be attached to a virtual Skelton. The dimension of the virtual Skelton is, however, again based on the imprecise motion capturing data.
- (3) In order to finally animate the 3D body, the mesh has to be attached to the virtual Skeleton. This so called skinning process is made by hand and therefore, comprises additional inaccuracies.

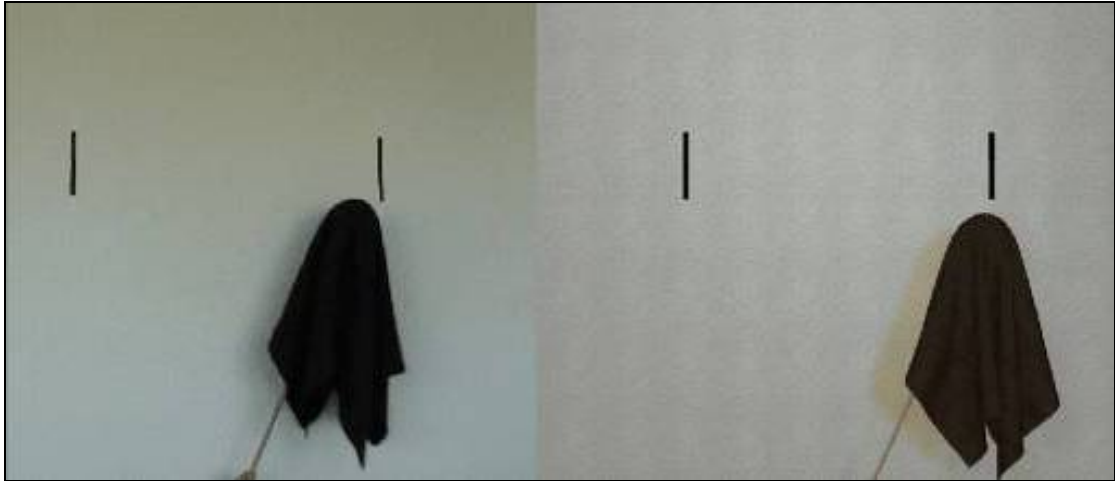
Thus, dynamic garment simulations on virtual mannequins are today precise from the fabric mechanics point of view, but not from the side of the body animations.

- Additional validation experiment: Moving fabric drape on an animated sphere

As the virtually animated body is not accurate, an additional experiment for the validation of the fabric drapes during dynamic simulation is performed. For this test, the same fabric drapes from the previous static experiment is taken. This time, the sphere on the stick is moved to the left and to the right. The same experiment is virtually recreated and compared to the real fabric movement. The comparison of the real and the virtual experiment returned a good correlation.

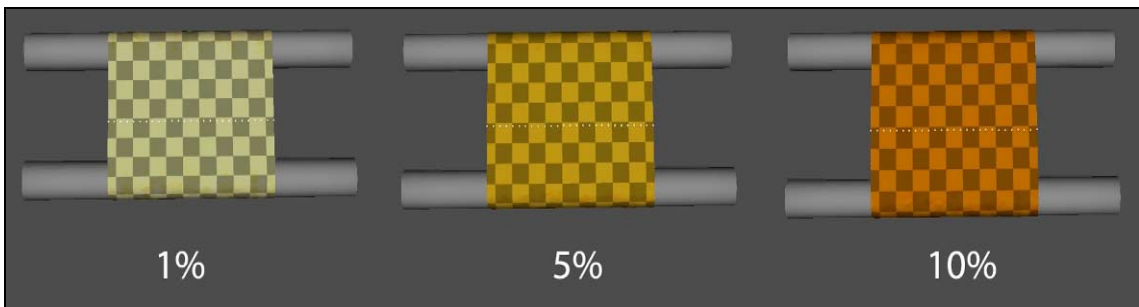


**Figure 176: Fabric 38\_ weft-knit on a moving sphere, left real fabric, right virtual simulation**



**Figure 177: Fabric 36\_overcoat fabric on a moving sphere, left real fabric, right virtual simulation**

- Additional validation experiment: Fabric around two cylinders which move apart  
 For an additional validation of the tensile parameter in dynamic simulations, three fabrics are elongated with two cylinders that move apart. Fabrics are deformed progressively 1%, 5% and 10% and corresponding forces are visualized. For all tested fabrics, the color-coded visualized force range corresponds to what was measured during the tensile test previously.



**Figure 178: Fabric 11\_flannel around two cylinders that move apart**

### 6.2.6. Summary of impreciseness and related error sources

In the following, all impressions which occur and accumulate in the case study are summed up, brought into correlation and discussed more in detail. In summary we can say that inaccuracies result from the fabrics side (including the fabric measurement, the parameter derivation, as well as limitations from the simulation system), during the 2D pattern creation, during the creation of the virtual mannequin and the body animation.

<i>Error margins</i>	<b>Comfort performance</b>	<b>Utility performance</b>
<u>Fabrics:</u>		
<b>Tensile and shear (page 116)</b>	-	Up to ~ 3 %
<b>Bending (loop length test, page 93)</b>	Up to ~ 3 %	Up to ~ 3 %
<b>Friction</b>	-	-
<b>Viscosity</b>	Further studies are needed	Further studies are needed
<u>2D pattern:</u>		
<b>Pattern digitalization</b>	~ 0.16 %*	~ 0.16 %*
<u>Virtual mannequin:</u>		
<b>Body scanning</b>	~ 0.16 %*	~ 0.16 %*
<b>Skeleton attachment</b>	~ 7 %	~ 7 %
<u>Body animation:</u>		
<b>Motion tracking</b>		~ 7 %
<b>Summary</b>	<i>Up to ~ 10.35% dimension Up to 3% bending</i>	<i>Up to ~ 17.35% dimension Up to 3% bending</i>

**Table 33: Summary of error margins, \*calculated with a waist girth of 60cm**

- Inaccuracies from the virtual mannequin

In table 34 we can see that most of the inaccuracies of virtual garment simulations are related to the virtual body. Even for the comfort performance, the scanned body needs to be attached to a virtual skeleton in order to be able to animate the body to the standard fitting pose (Figure 157, Figure 160). During utility performance, the imprecise body animations add another amount of inaccuracy to the garment simulation.

- Impressions of the fabric properties

Regarding fabric properties, the simplification of the bending property (considering no back and front bending) adds most of the inaccuracy. This error is, however, less observable as the bending property is visual assessed. In contrary, it is much more difficult to judge the simulation results for the viscosity properties. An evaluation is visually made upon simulation experiments. The comparison of the real and virtual fabric behavior, however, returns a satisfactory result for the viscosity characteristics.

## 6.3. Experiments with new derived parameters for other applications

### 6.3.1. Accurate simulation for robotic driven sewing processes

Within the European project Leapfrog [Leapfrog 08], garment simulations are exploited for automatic sewing processes. The virtually simulated jacket serves for the adjustment of the sewing mould and the positioning of the robot. In reality, the single fabric pieces are placed on the mould in a way, so that no creases or folds occur on the textile surface.

In order to be able to simulate the jacket previously in the same way, new fabric properties need to be developed, based on the fabric measurements. For this, the tensile parameter has to be kept, so that the jacket deforms to the right extent. The bending parameter, however, needs to be changed to a much stiffer material. The applied parameter alterations are based on the previous study on bending: realistic bending measurements limits are finally known and could be adjusted with suitable values. [Leapfrog 08]



**Figure 179: Jacket for the Leapfrog project [Leapfrog 08]**

# Chapter 7

## Conclusion

### 7.1. Contribution

This work has studied the accuracy of fabric properties in virtual simulations, mainly in the framework of the European project HAPTEX [haptex 07] with the intention of making such computation applications more accurate and explicit for important garment development and manufacturing processes.

The study has been performed by means of a broad selection of 42 very different fabric test samples which were chosen in two cycles, according to three defined selection criteria: the raw material, the planar structure and the fabrics dimension. The fabric selection was measured using existing standard fabric characterization methods such as FAST and KES-f in order to identify mechanical and physical behavior properties of the textiles.

Existing measurement methods were compared and evaluated according their suitability for static and dynamic virtual garment simulation. For those measurements which were found to be unsuitable, new methods have been developed, which better replicate real life garment wear. Using a broad range of fabric materials, this study has also refined the computation system's requirements and proposed improvements and refinements for the integration of parameters.

Finally the newly derived parameters and the measurement method derivation processes have been empirically tested. A prototyping process has been developed and parallel tested to compare both the real and virtual processes. It was demonstrated that typical garment assessments such as comfort and utility performance can be accurately simulated in the virtual world. Moreover, additional important numerical fitting data attested to better performance in the virtual process.

Separate validation experiments have been successfully conducted for various details. Parameters have also been tested for future robotic driven sewing processes. Besides, new areas of research have been outlined.

In summary, this study provided the important deeper knowledge for accurate dynamic garment simulation, in particular for the simulation of RT textiles for touching them, as it needs to be very precise. The new measurement specifications should lead, in the long term, to the establishment of new measurement standards, which are designed for virtual simulation processes.



Summary of advantages of virtual prototyping processes:

	Traditional prototyping and fitting	Virtual prototyping and fitting
<b>Time</b>	<ul style="list-style-type: none"> <li>- Preparation time for a real garment prototype: <b>1-8 hours</b> (depending on the garment style).</li> <li>- For each modification/correction, a new garment sample is produced: <b>1-8 hours</b>.</li> </ul>	<ul style="list-style-type: none"> <li>- Preparation time for a virtual garment prototype: same time, <b>1-8 hours</b>.</li> <li>- For each modification/correction, the edited 2D pattern is directly re-simulated in 3D: <b>no additional time is needed</b>.</li> </ul>
<i>For one garment up to 5 prototypes are needed. Hence, virtual prototyping methods could save up to 36 working hours per garment.</i>		
<b>Precision</b>	<ul style="list-style-type: none"> <li>- Real garments prototypes are <b>visually</b> evaluated.</li> <li>- Real garments are mainly assessed in the <b>base size</b>.</li> <li>- Real garments are mainly assessed in <b>static postures</b>.</li> </ul>	<ul style="list-style-type: none"> <li>- Virtual simulation systems return <b>precise numerical fitting data</b>.</li> <li>- Virtually, <b>all garment sizes can be tested</b> without additional costs and time.</li> <li>- Virtual garments can be tested precisely with <b>all kinds of movements</b>.</li> </ul>
<i>As the virtual prototyping returns more and more precise fitting information, less prototyping cycles are needed.</i>		
<b>Cost</b>	<ul style="list-style-type: none"> <li>- Cheap development costs are strongly dependant on <b>cheap labor</b>.</li> <li>- <b>High shipping and travel costs</b> to low wage countries</li> </ul>	<ul style="list-style-type: none"> <li>- Development <b>costs are reduced by technological means</b> (fewer prototypes are made in less time).</li> <li>- Less expenses for goods shipping or travels are needed.</li> </ul>
<b>Versatility</b>	<ul style="list-style-type: none"> <li>- Each change requires a new expensive garment sample.</li> <li>- Only <b>one garment sample is available</b> for the evaluation process.</li> <li>- No integration with PDM/PLM solutions is possible</li> </ul>	<ul style="list-style-type: none"> <li>- Modifications can be executed with <b>one mouse click</b>.</li> <li>- A virtual garment sample can be <b>endlessly copied</b> and easily sent to other manufacturing places.</li> <li>- The digital garment sampling can be easily integrated into PDM/PLM solutions.</li> </ul>
<b>Ecology</b>	<ul style="list-style-type: none"> <li>- Waste of resources and energy.</li> </ul>	<ul style="list-style-type: none"> <li>- Protection of resource materials, such as fabrics.</li> <li>- No waste of resources for shipping of goods or travels.</li> </ul>

**Table 34: Key factors for real and virtual garment prototyping**

## 7.2. Limitations and future research

### 7.2.1. Rheology aspects

This work has highlighted the fact that the rheological aspects, particularly of the tensile and shear parameters, are of great importance to dynamic simulations. Without the integration of the hysteresis behavior, the dynamic simulation of these parameters will remain an approximation.

### 7.2.2. Automation of parameter derivation processes

The force-deformation envelopes of the new length driven measurements resembled one another, even for textiles with very different elasticity characteristics. This leads to the assumption that, if deformed to the same extent, fabrics might possess proportionally similar tensile hysteresis behavior. If dependency rules could be established, then parameter derivation could be automated, reducing or eliminating the time consuming fabric measurement process.

### 7.2.3. Accuracy of body deformations in dynamic simulations

To achieve an accurate dynamic garment simulation it is necessary, not only to make a precise simulation of the cloth used, but also to achieve a precise dynamic body simulation, including all its deformations. Today it is possible to make an accurate virtual simulation of a static body. During animation the 3D body is moved by the skeleton, to which he is attached. This simplified attachment does not, however, correspond to the complexity of a real human body, where a myriad of muscles interact and define the body's dimension during movement.

For accurate dynamic garment simulation however, the virtual body deformation must correspond with defined accuracy limits in order to guarantee precise computations. However, this topic has yet to be widely investigated and further research is required.

### 7.2.4. Quantification and exploitation of numerical fitting data

Until today, garment fitting has depended upon the subjective perception of the tailor/designer and the mannequin. New virtual fitting methods, which are accurate for both comfort and utility performance, give feedback about a garment's fit not only visually but also in the form of precise numerical data.

The availability of these new precise high-tech fitting statistics present further avenues of research. For example the subjectively perceived interaction between the body and the garment could be objectively measured and quantified for various groups of customers. Hence, factors such as fitting preferences or typical misfits could be better studied and optimized.

### 7.2.5. Parameters for extreme wearing situations

The aim of this work was the investigation of the accuracy of fabric simulations for usual garment wearing situations (assessed within the fitting movements). However, some garments have to be able to resist particularly extreme situations, where the cloth is deformed by disproportionately higher stresses. The investigation of these particular cases would be an

interesting field of research and is of particular importance to the protection and sports clothing sectors.

#### 7.2.6. Fabric performance

It would also be interesting to integrate fabric performance processes into garment simulation applications. This would necessitate the discovery of a way to virtually imitate complex manufacturing procedures such as formability, sewing or ironing.

#### 7.2.7. Simulation of additional fabric characteristics

The accurate virtual reproduction of mechanical and physical fabric parameters constitutes one part of a complete virtual imitation of the real textile with all its components. In a next step it would be interesting to simulate additional aspects and in particular to combine them in one simulation application, in order to be able to perform each computation upon demand. This possibility would be interesting for an integration in PDM/PLM (FLM) solutions, as all garment aspects could be simulated and predicted within one application, as for example the abrasion or the aging of textiles.

- Physiological properties

For the visualization and simulation of an optimal thermo regulation between the skin and the fabric it would be interesting to integrate physiological fabric aspects such as thermal or hygral properties. In doing so, the comfort of sports clothing, the skin hydration or the fabric breathability could be imitated.

- Aging and abrasion properties

The simulation of the abrasion and the aging of fabrics would be an interesting aspect for simulation.

- UV protection properties

The UVP factor of a garment is a new standard, describing the UV protection offered by the garment. By integrating this parameter into virtual simulations, the risk factor for certain body parts which exposed to the sun, could be calculated for several actions, for example for different sports.

#### 7.2.8. Fabric appearance

Other aspects such as the appearance of fabrics on screen constitute additional topics of research, for example the much appreciated characteristic sheen of linen. However, it is important to accurately visualize these typical effects in order to be able to identify different materials. These effects also include transparency and material irregularities.

## Bibliography:

- [AATCC 02] AATCC Technical Manual 2002, [www.aatcc.org](http://www.aatcc.org)
- [Abbott 51] Abbott N. J., "The Measurement of Stiffness in Textile Fabrics", Textile Research Journal, Sage, Vol. 21, 1951, pp. 435-444
- [Adidas] [www.adidas.com](http://www.adidas.com)
- [Adler 04] Adler U., "Structural change - The dominant feature in the economic development of the German textile and clothing industries", Journal of Fashion Marketing and Management, Emerald, Vol. 8, No. 3, 2004, pp. 300 – 319
- [Ask 05] Askeland D. R., Pradeep P. Phulé, "The Science & Engineering of Materials", 5th edition, Thomson-Engineering, ISBN 0534553966, 2005
- [Assyst/Bullmer] [www.assyst.com](http://www.assyst.com)
- [Autodesk] [www.autodesk.com](http://www.autodesk.com)
- [Baraff 98] Baraff D., Witkin A., "Large Steps in Cloth Simulation", Computer Graphics (SIGGRAPH'98 proceedings), Addison-Wesley, 32, 1998, pp. 106-117
- [Behery 06] Behery H. M., "Effects of mechanical and physical properties on fabric hand", Woodhead publishing in textiles, ISBN 1 85573 918 6, 2006, pp. 203
- [Behre 61] Behre B., "Mechanical Properties of Textile Fabrics Part I: Shearing", Textile Research Journal, Sage, Vol. 31, No.2, 1961, pp. 87-93
- [Boss] [www.boss.com](http://www.boss.com)
- [Bottino 01] Bottino A., Laurentini A., Scalabrin S., "Quantitatively comparing virtual and real draping of clothes", International Conferences in Central Europe on Computer Graphics, Visualization and Computer Vision, 2001, WSCG, pp. 63-70
- [Breen 94] Breen D., House D., Wozny M., "Predicting the Drape of Woven Cloth Using Interacting Particles", Proceedings of the 21st annual conference on Computer graphics and interactive techniques, ISBN 0-89791-667-0, 1994, pp. 365-372
- [Browzwear] [www.browzwear.com](http://www.browzwear.com)

- [Carignan 92] Carignan M., Yang Y., Magnenat-Thalmann N., Thalmann D., "Dressing Animated Synthetic Actors with Complex Deformable Clothes", Computer Graphics (Siggraph'92 proceedings), Addison-Wesley, 26(2), 1992
- [C-Design] [www.c-design.com](http://www.c-design.com)
- [Charfi 06] Charfi H., Gagalowicz A., R. Brun, "Measurement of Viscosity Damping Parameters of Fabric Related to a Non-linear Textile Model", Textile Research Journal, Sage, Vol. 76, No. 10, 2006, pp 787-790
- [Choi 02] Choi K.J., Ko H.S., "Stable but Responsive Cloth", Computer Graphics (SIGGRAPH'02 proceedings), Addison Wesley, 2002.
- [ClothReyes] [www.clothreyes.com](http://www.clothreyes.com)
- [ClothFX] [www.3ds.com](http://www.3ds.com)
- [Collier 91] Collier J.R., Collier B.J., O'Toole G., Sargand S.M., "Drape prediction by means of finite element analysis", Journal of the Textile Institute, Taylor & Francis, Vol. 82, No.1, 1991, pp. 96-107
- [Cooper 60] Cooper D.N.E., "The Stiffness of Woven Textile", Journal of the Textile Institute, Taylor & Francis, Vol. 51, 1960, pp. T317-T335
- [CSIRO] <http://www.csiro.au/solutions/ps26n.html>
- [Cusick 61] Cusick G.E., "The resistance of fabrics to shearing forces", Journal of the Textile Institute, Taylor & Francis, Vol. 52, 1961, pp. 395-406
- [Cusick 65] Cusick G.E., "The dependence of fabric drape on bending and shear stiffness", Journal of the Textile Institute, Taylor & Francis, Vol. 56, 1965, pp. T596-T606
- [Cusick 68] Cusick G.E. "The measurement of fabric drape", Journal of the Textile Institute, Taylor & Francis, Vol. 59, 1968, pp. 253-260
- [Dahlberg 61] Dahlberg B., "Mechanical Properties of Textile Fabrics, Part II: Buckling," Textile Research Journal, Sage, Vol. 31, No.2, 1961, pp. 94-99
- [Dew 03] Dewangshu D., „Retail @ the speed of fashion part I + II, Zara Case study“, [www.3isite.com](http://www.3isite.com), 2003
- [Ebe 96] Eberhardt B., Weber A., Strasser W., "A Fast, Flexible, Particle-System Model for Cloth Draping", Computer Graphics in Textiles and Apparel, (IEEE Computer Graphics and Applications), IEEE Press, 1996. pp. 52-59,

- [Ebe 97] Eberhardt B., Weber A., “Modeling the draping behavior of woven cloth”, MapleTech, Birkhäuser, Volume 4, Issue 2, 1997, pp. 25 - 31
- [Ebe 99] Eberhardt B., Weber A., “A particle system approach to knitted textiles”, Computers & Graphics, Elsevier, Volume 23, issue 4, 1999, pp. 599-605
- [Eischen 96] Eischen J.W., Deng S., Clapp T.G., “Finite-Element Modeling and Control of Flexible Fabric Parts”, IEEE Computer Graphics and Applications, special issue on Computer Graphics in Textiles and Apparel, Vol. 16 (5), 1996, pp. 71-80
- [Elder 84] Elder H.M., Fisher S., Armstrong K., Hutchison, “Fabric softness, handle and compression”, Journal of the Textile Institute, Taylor & Francis, Vol.75, 1984, No.1, pp. 37-46
- [Elder 84-2] Elder H.M., Fisher S., Armstrong K., Hutchison, “Fabric stiffness, handle and flexion”, Journal of the Textile Institute, Taylor & Francis, Vol.75, 1984, No. 2, pp. 99-106
- [Elder 85] Elder H.M., Fisher S., Hutchison G., Beattie, “A psychological scale for fabric stiffness”, Journal of the Textile Institute, Taylor & Francis, Vol. 76, 1985, No. 6, pp. 442-449
- [EN ISO 03] EN ISO 8388, “Knitted fabrics, Types, Vocabulary”, European committee for standardization, 2003
- [Fan 05] Fan J., Yu W., Hunter L., “Clothing appearance and fit: Science and technology”, Woodhead publishing in textiles, ISBN 1 85573 745 0, pp. 90-95
- [FAST 94] De Boos A., Tester D., “FAST – Fabric Assurance by Simple Testing”, Textile and Fiber Technology, Report No. WT92.02, ISBN 0 643 06025 1, 1994
- [FAST 95] Minazio P. G., “FAST – Fabric Assurance by Simple Testing”, International Journal of Clothing Science and Technology, Emerald, Vol. 7, No. 2/3, 1995
- [Fibers] <http://www.twd-fibres.de/>
- [Gersak 02] Gersak J., “Development of the system for qualitative prediction of garments appearance quality”, International Journal of Clothing Science and Technology, Emerald, Vol. 14, No. 3/4, 2002, pp. 169 – 180

- [Gersak 04] Gersak J., "Study of relationship between fabric elastic potential and garment appearance quality", *International Journal of Clothing Science and Technology*, Emerald, Vol. 16, No. 1/2, 2004, pp. 238-251
- [Gersak 05] Gersak J., Sajn D., Bukosek V., „A study of the relaxation phenomena in the fabrics containing elastane yarns“, *International Journal of Clothing Science and Technology*, Emerald, Vol. 17, No. 3/4, 2005, pp. 188-199
- [Gersak 07] Gersak J., Pavlinic D. Z., "Objective evaluation of garment appearance", proceedings of the 5th IMCEP 2007, University of Maribor, October 2007, pp. 35 - 42
- [Goldenthal 07] Goldenthal R., Harmon D., Fattal R., Bercovier R., Grinspun E., "Efficient Simulation of Inextensible Cloth", *ACM Siggraph 2007*, digital library, papers, ISSN: 0730-0301 2007
- [Grosberg 66] Grosberg P., Swani N. M., "The Mechanical Properties of Woven Fabrics," *Textile Research Journal*, Sage, Vol. 36, 1966, pp. 338-345
- [Grosberg 66-2] Grosberg P., Abbot G.M., "Measurement of fabric stiffness and hysteresis in bending", *Textile Research Journal*, Sage, Vol. 36, 1966, pp. 338-345
- [Guercini 04] Guercini S., "International competitive change and strategic behavior of Italian textile-apparel firms", *Journal of Fashion Marketing and Management*, Emerald, Vol. 8 No. 3, 2004, pp. 320-339
- [Haptex 07] <http://haptex.miralab.unige.ch>
- [Hatch 93] Hatch, L. K., "Textile Science", West Publishing Company, Minneapolis, USA, ISBN 0-314-90471-9, 1993
- [Havok] [www.havok.com](http://www.havok.com)
- [Hohenstein] <http://www.hohenstein.de/>
- [Hui 03] Hui, C. L., Ng S. F., "Theoretical Analysis of Tension and Pressure Decay of a Tubular Elastic fabric", *Textile Research Journal*, Sage, Vol. 73, 2003, pp. 268-272
- [Hui 04] Hui C. L., "Neural Network Prediction of Human Psychological Perceptions of Fabric Hand", *Textile Research Journal*, Sage, Vol. 74, 2004

- [Hui 07] Hui C. L., Keith C.C., Yeung K. W., Frency S.F, “ Application of artificial neural networks to the prediction of sewing performance of fabrics”, International Journal of Clothing Science and Technology, Emerald, Vol. 19, No. 5, 2007, pp. 291-318
- [human solutions] <http://www.human-solutions.com>
- [Instron 06] <http://www.instron.us>
- [Isshi 57] Isshi T., "Bending tester for fibers, yarns and fabrics", Journal of the Textile Machinery Society of Japan, Journal@rchive, online ISSN: 1881-1159, print ISSN: 0040-5043, Vol. 3 No.2, 1957, pp. 48-52
- [Jevsnik 2005] Jevsnik S., “The advance engineering methods to plan the behavior of fused panel”, International Journal of Clothing Science and Technology, Emerald, Vol.17, No. 3-4, 2005, pp. 161-170
- [Jones 04] Jones R.M., Hayes S.G., “The UK clothing industry - Extinction or evolution?”, Journal of Fashion Marketing and Management, Emerald, Vol. 8, No. 3, 2004, pp. 262-278
- [Kang 02] Kang Y. M., Cho H. G., “Bi-layered Approximate Integration for Rapid and Plausible Animation of Virtual Cloth with Realistic Wrinkles”, Computer Animation 2000 proceedings, IEEE Computer Society, 2002
- [Kaw 80] Kawabata S., “The standardization and analysis of hand evaluation” (2nd Edition). The hand evaluation and standardization committee, The Textile Machinery Society of Japan, Osaka, 1980
- [Kaw 89] Kawabata S., Niwa M., “Fabric performance in clothing and clothing manufacture”, Journal of the Textile Institute, Taylor & Francis, Vol.80, No. 1, 1989, pp. 19
- [Kaw Niwa 98] Kawabata S., Niwa M., “Influence of fiber process parameters on product performance”, Proceedings Fiber to Finished Fabrics, Fiber Science/Dyeing & Finishing Groups Joint Conference, The Textile Institute, Taylor & Francis, Dec. 1998, 1.
- [Keckeisen 04] Keckeisen K., Feurer M., Wacker M., “Tailor Tools for Interactive Design of Clothing in Virtual Environments”, Proceedings of ACM VRST, 2004, pp.182 -185
- [Kenkare 05] Kenkare N., May-Plumlee T., “Evaluation of drape characteristics in fabrics”, International Journal of Clothing Science and Technology, Emerald, Vol. 17, No. 2, 2005, pp. 109-123



- [Lafleur 91] B. Lafleur, N. Magnenat-Thalmann, D. Thalmann, "Cloth Animation with Self-Collision Detection", IBIP conference on Modeling in Computer Graphics proceedings, Springer-Verlag, 1991
- [Lam 06] Lam Po Tang S., Stylios G., "An overview of smart technologies for clothing design and engineering", International Journal of Clothing Science and Technology, Emerald, Vol. 18, No. 2, 2006, pp. 108-128
- [LaRedoute] [www.laredoute.fr](http://www.laredoute.fr)
- [Leardini 05] Leardini A., Chiari L., Della Croce U., Cappozzo A., "Human movement analysis using stereophotogrammetry. Part 3. Soft tissue artifact assessment and compensation", Gait & Posture, Elsevier, pp. 212–225, 2005
- [Leapfrog 08] [www.leapfrog-eu.org](http://www.leapfrog-eu.org)
- [Lectra] [www.lectra.com](http://www.lectra.com)
- [Leung 00] Leung, "Draping performance of fabrics for 3D garment simulation", 29th Textile Symposium, Mt Fuji, 2000, pp.169 – 175
- [Lindberg 61] J. Lindberg and B. Dahlberg, "Mechanical Properties of Textile Fabrics, Part III: Shearing and Buckling of Various Commercial Fabrics," Textile Research Journal, Sage, Vol. 31, No. 2, 1961, pp. 99-122
- [Livesey 64] R. G. Livesey, J. D. Owen, "Cloth stiffness and hysteresis in bending", Journal of the Textile Institute, Taylor & Francis, Vol. 55, 1964, No 10
- [Li 40] Li Y., "The Science of Clothing Comfort", Journal of the Textile Institute, Taylor & Francis, Textile Progress, Vol. 31, 1940, No.1/2,
- [Loschek 94] Loschek I., "Reclams Mode und Kostümllexikon", Philipp Reclam jun. GmbH & Co., Stuttgart 1994 ISBN 3-15-010403-3
- [Luible 07] Luible C., Magnenat-Thalmann N., "Suitability of standard fabric characterization experiments for a use in virtual simulations", AUTEX conference, Tampere, 2007
- [Lycra] [http://heritage.dupont.com/touchpoints/tp\\_1962/overview.shtml](http://heritage.dupont.com/touchpoints/tp_1962/overview.shtml)
- [Mae 05] Mäkinen M., Meinander H., Luible C., Magnenat-Thalmann N., "Influence of Physical Parameters on Fabric Hand", Proceedings of Workshop on Haptic and Tactile Perception of Deformable Objects, Hanover, 2005
- [Mango] [www.mango.com](http://www.mango.com)

- [Maklewska 07] Maklewska E., Nawrocki A., Kowalski K., Andrzejewska E., Kuzanski W., "New measuring device for estimating the pressure under compression garments", *International Journal of Clothing Science and Technology*, Emerald, Vol. 19, No. 3/4, 2007, pp. 215-221
- [Matrix] [www.matrixone.com](http://www.matrixone.com)
- [Metzger 03] Metzger J., Kimmerle S., Etmuss O., "Hierarchical Techniques in Collision Detection for Cloth Animation", *Journal of WSCG*, digital library, Volume 11, No. 1, ISSN 1213-6972, 2003
- [Müller & Sohn] <http://www.mms-schule.de/>
- [MVM] [www.myvirtualmodel.com](http://www.myvirtualmodel.com)
- [Nike] [www.nike.com](http://www.nike.com)
- [Optitex] [www.optitex.com](http://www.optitex.com)
- [Pavlinic 03] Pavlinic D., Gersak J., "Investigation of the relation between fabric mechanical properties and behavior", *International Journal of Clothing Science and Technology*, Emerald, Vol. 15, No. 3/4, 2003, pp. 231-240
- [Peak] [www.peak-performance.com](http://www.peak-performance.com)
- [Peirce 30] Peirce F. T., "The Handle of Cloth as a Measurable Quantity", *Journal of the Textile Institute*, Taylor & Francis, Vol. 21, 1930, pp. 377-416
- [Peirce 37] Peirce F.T., "The geometry of cloth structure", *Journal of the Textile Institute*, Taylor & Francis, Vol. 28, 1937, pp. T45-T96
- [Postle 83] Postle R., "Objective evaluation of the mechanical properties and performance of fabrics and clothing", in *Objective evaluation of apparel fabrics*, Proceedings 2nd Australian-Japan Symposium, Melbourne, 1983, The Textile Machinery Society of Japan, J-stage, Osaka, 1983
- [Provatidis 04] Provatidis C.G., Vassiliadis S. G., "On the performance of the geometrical models of fabrics for use in computational mechanical analysis", *International Journal of Clothing Science and Technology*, Emerald, Vol. 16, No. 5, 2004, pp. 434-444
- [Provatidis 05] Provatidis C. G., Vassiliadis S. G., Anastasiadou E. A., "Contact mechanics in two-dimensional finite element modeling of fabrics", *International Journal of Clothing Science and Technology*, Emerald, Vol. 17, No. 1, 2005, pp. 29-40

- [Provot 95] Provot X., "Deformation constraints in a mass-spring model to describe rigid cloth behavior", Proceedings of the Graphics Interface Conference, 1995, pp. 147-154
- [Reflexstock] [www.reflexstock.com](http://www.reflexstock.com), royalty free images
- [Roberts 04] Roberts W., B. Beil, "Fibrous assemblies: modeling/computer simulation of compressional behavior", International Journal of Clothing Science and Technology, Emerald, Vol. 16, No. 1/2, 2004, pp. 108-118
- [Romberg 04] Romberg O., Hinrichs N., „Keine Panik vor der Mechanik“, Vieweg Verlag/Springer Science und Business Media, ISBN 3-528-33132-1, pp. 10
- [Runtime] [www.runtimegeox.com](http://www.runtimegeox.com)
- [San] Hunt M. C., "Fashion's changing face", The San Diego Union-Tribune web-site, February 5, 2006
- [Shishoo 05] Shishoo R., "Textiles in sports", Woodhead Publishing in Textiles, ISBN 1 1-85573-922-4, 2005, pp. 7
- [Spiegel 07] <http://www.spiegel.de/auto/aktuell/0,1518,461956,00.html>
- [Stylios 04] Stylios G., Editorial, Research Register, International Journal of Clothing Science and Technology, Emerald, Vol. 16, No. 6, 2004, pp. 4-5
- [Stylios 05] Stylios G., "New measurement technologies for textiles and clothing", International Journal of Clothing Science and Technology, Emerald, Vol. 17, No. 3/4, 2005, pp. 135-149
- [Syflex] [www.syflex.biz](http://www.syflex.biz)
- [Taplin 04] Taplin I.M., Winerton J., "The European clothing industry-Meeting the competitive challenge", Journal of Fashion Marketing and Management, Emerald, Vol. 8, No. 3, 2004, pp. 256-261
- [Terz 87] Platt J., Barr A., "Elastically Deformable Models", Computer & Graphics, Elsevier, Volume 21, Nr.4, 1987
- [TER 88] Terzopoulos D., Fleischer K., "Modeling Inelastic Deformation: Viscoelasticity, Plasticity, Fracture", Computer Graphics (SIGGRAPH'98 proceedings), Addison-Wesley, 22, 1988, pp. 269-278
- [Tribo] <http://www.tribology-abc.com/abc/friction.htm>

- [Thom 06] Thomaszewski B., Wacker M., “Bending Models for thin Flexible Objects”, WSCG Short Communication Proceedings, 9(1), 2006.
- [Volino 00] P. Volino, N. Magnenat-Thalmann, “Virtual Clothing”, Springer, ISBN 3-540-67600-7, 2000
- [Volino 00-2] P. Volino, N. Magnenat-Thalmann, “Implementing fast cloth simulation with collision response”, Proceedings of the conference on Computer Graphics, (CGI 00), 2000, pp. 257-268
- [Volino 05] P. Volino, N. Magnenat-Thalmann, "Accurate Garment Prototyping and Simulation", Computer-Aided Design & Applications, CAD Solutions, Vol. 2, No. 1-4, 2005, pp. 645-654
- [Volino 06] P. Volino, N. Magnenat-Thalmann, “Simple Linear Bending Stiffness in Particle Systems”, SIGGRAPH-Eurographics Symposium on Computer Animation 2006 proceeding, 2006, pp. 101-105
- [VTO] A. Divivier, Dr. R. Triebel, A. Ebert, Prof. Dr. H. Hagen, C. Gross, A. Fuhrmann, Dr. V. Luckas, Prof. Dr.-Ing J.L. Encarnação, E. Kirchdörfer, M. Rupp, S. Vieth, S. Kimmerle, M. Keckeisen, Dr. M. Wacker, Prof. Dr. W. Strasser, Mirko Sattler, Ralf Sarlette, Prof. Dr. R. Klein, „Virtual Try-On – Topics in Realistic, Individualized Dressing in Virtual Reality“, [www.hohenstein.de](http://www.hohenstein.de)
- [Wiwo 08] <http://www.wiwo.de/handelsblatt/elektronik-sorgt-fuer-komfort-266762/>
- [Wpd] [www.wikipedia.com](http://www.wikipedia.com)
- [Yang 91] Yang Y., Magnenat-Thalmann N., “Techniques for Cloth Animation, New trends in Animation and Visualization”, book published by John Wiley & Sons Ltd, ISBN 0-471-93020-2, 1991, pp. 242 - 256
- [Zegna] [www.zegna.com](http://www.zegna.com)
- [Zhou 98] Zhou N., Ghosh T.K., “On-line measurement of fabric bending behavior: background, need and potential solutions”, International Journal of Clothing Science and Technology, Emerald, Vol. 10, No. 2, 1998, pp. 143-156

## **Publications resulting from research on haptex project:**

C. Luible, N. Magnenat-Thalmann. The simulation of cloth using accurate physical parameters. CGIM 2008, Innsbruck/Austria.

C. Luible, M. Varheenmaa, N. Magnenat-Thalmann, H. Meinander. Subjective fabric evaluation. Proceedings of the Haptex 07 workshop, Hanover, October 2007.

C. Luible, P. Volino, N. Magnenat-Thalmann. High Fashion in Equations. International Conference on Computer Graphics and Interactive Techniques, ACM Siggraph 2007 sketches, San Diego, Article Nr. 36

C. Luible, N. Magnenat-Thalmann. Suitability of standard fabric characterization experiments for the use in virtual simulations. Proceedings of the AUTEX conference, Tampere/Finland, June 2007

M. Mäkinen, C. Luible, H. Meinander, N. Magnenat-Thalmann. Influence of Physical Parameters on Fabric Hand. Proc. of the Workshop on Haptic and Tactile Perception of Deformable Objects, Hanover (HAPTEX'05), pp. 8-16, December 2005.

## **Related publications:**

N. Magnenat-Thalmann, C. Luible, P. Volino, E. Lyard, "From Measured Fabric to the Simulation of Cloth", 12th IEEE Inter. Conference on Emerging Technologies and Factory Automation, Patras/Greece, 2007

P. Volino, P. Davy, U. Bonanni, C. Luible, N. Magnenat-Thalmann, M. Mäkinen, H. Meinander, "From Measured Physical Parameters to the Haptic Feeling of Fabric. The Visual Computer, Springer Berlin/Heidelberg, vol. 23, no. 2, pp. 133–142. February 2007.

N. Magnenat Thalmann, F. Dellas, C. Luible and P. Volino, "From Roman Garment to Haute-Couture with the Fashionizer Platform", Virtual Systems and Multi Media, Japan, November 2004.

D. Protopsaltou, M. Arevalo, C. Luible, N. Magnenat-Thalmann "A body and garment creation method for an Internet based virtual fitting room", Computer Graphics International Conference Proceedings, Springer Verlag, pp 105-122, July 2002

## Annex A: Technical terms

<b>Base size:</b>	Regarding the range of sizes, in which a garment is produced, the base size is the one in which a garment is prototyped.
<b>Bending elasticity:</b>	The required couple to bend unit width of fabric to unit curvature is called bending.
<b>Bending length:</b>	Bending length is the length of a fabric that will bend under its own weight to a certain angle.
<b>Bending rigidity:</b>	Bending rigidity is a fabrics resistance to bending.
<b>Body cathexis:</b>	Satisfaction with body appearance and its separate parts is termed as body cathexis. It is therefore an evaluation o body image and self concept.
<b>CAD/CAM:</b>	Computer Aided Design/Computer Aided Manufacturing
<b>Density:</b>	Density describes the mass per surface unit of a fabric in $g/m^2$ .
<b>Elasticity:</b>	Elasticity is the recoverable part of a material after the release of an applied load. Inside the simulation system, elasticity can also describe an internal force, resulting from a given geometrical deformation.
<b>Elasticity modulus:</b>	The elasticity modulus is a linear mathematical description of a materials elastic deformation behavior. The elasticity modulus is defined as the slope of a force-deformation curve.
<b>Flexural rigidity:</b>	See bending rigidity.
<b>Formability:</b>	Formability is the possible compression of a fabric until no buckling occurs (Bending rigidity * Extensibility).
<b>Friction:</b>	Friction is the ratio between the maximum tangential contact force and the normal pressure force between two surfaces in contact.
<b>Friction coefficient:</b>	The friction coefficient is the magnitude of the friction force.
<b>Fusing:</b>	Fusing is a permanently fixed, second fabric layer in parts of a garment (for example collars or belts) to make those parts more rigid.

<b>Grading:</b>	The method of deriving various garment sizes out of the base size is called grading.
<b>Gravity:</b>	Nominal acceleration of objects left at rest = $9.81 \text{ m.s}^{-2}$ .
<b>Hysteresis:</b>	Hysteresis is the characteristic of a material to not go back immediately or to not return completely to the initial state after the release of an applied force.
<b>Interlining:</b>	Interlining is a non-fixed second fabric layer inside the garment.
<b>Marker:</b>	The description of how to cut out all 2D pattern pieces out of the fabric with the least material loss is called marker.
<b>Orthonormal:</b>	Two vectors in an inner product space are orthonormal ( $= 0$ ), if the two vectors are orthogonal.
<b>PDM/PLM:</b>	Product data management/Product lifecycle management. The product data management solution provides tools to control the access, the structure and the management of all technical data related to a product development process. The product life cycle management solution thereafter brings together all information from the first idea of the product until its disposal.
<b>Plasticity:</b>	Plasticity is the tendency of a material to undergo permanent deformation under load.
<b>Poisson coefficient:</b>	The Poisson coefficient of a material describes its tendency to deform in one direction if elongated in the other direction.
<b>Relaxation shrinkage:</b>	Relaxation shrinkage is the irreversible change in dimension that occurs when a fabric is relaxed with steam or water.
<b>Resilience:</b>	The resilience characteristic describes to which degree a fabric property recovers after the release of the force.
<b>Seam pucker:</b>	Seam pucker is the occurrence of unwanted small fabric wrinkles at a garment's seam.
<b>Stiffness:</b>	See bending rigidity.

**Shear elasticity:** Shear can be described as required force to change the angle between intersecting threads of a fabric.

**Shear modulus:** The shear modulus is defined as the ratio of shear stress to the shear strain and is thus a linear description of the parameter.

**Shear rigidity:** Shear rigidity is the fabrics resistance to shearing.

**Strain:** Strain is the geometrical expression of a deformation and is hence a change of shape, caused by stress. In its most general form, the strain is a symmetric tensor. During testing of a material sample, the force-deformation curve is a graphical representation of the relationship between stress, derived from measuring the applied load on the sample and strain, derived from measuring the deformation of the sample, for example the elongation. The form of the curve is material dependant.

**Stress:** Stress is a measure of the average amount of force, which is exerted per unit surface area. It is a measure of the total internal forces, acting across a fabric surface, resulting from an external applied force. Stress cannot be measured but derived from measurements of strain and knowledge of elastic material properties. Stress is expressed as:

$$\sigma = \frac{F}{A}$$

Where  $\sigma$  is the average stress and F is the acting force over the area A.

**Surface resolution:** Surface resolution is the accuracy of a virtual surface and is related to the applied amount of polygons.

**Tensile elasticity:** Tensile elasticity is the measurement of the fabric elongation elasticity, which is the force value per length unit exerted for a given percentage of geometric deformation.

**Tensile resilience:** This property describes to which degree the fabric recovers, after the release of the force.

**Viscosity:** Viscosity can be described as internal forces and frictions of material resulting from a given deformation speed, which are responsible that the material does not recover immediately after the release of an applied load.

#### **Aerodynamic**

**Viscosity:** Aerodynamic viscosity is an input parameter, decomposed into a normal component, which acts orthogonally to the fabric surface



orientation and a tangential component, which acts along the parallel direction. The tangential component illustrates the friction between the fabric and the air masses, whereas the normal component illustrates the forces resulting from impermeable fabric surfaces.

## Annex B: Fabric selection

Sample	Description	Fiber content	Structure	Weight g/m <sup>2</sup>	Thickness mm
<b>1<sup>st</sup> set of measurements:</b>					
1.	Denim	100% CO	twill	380	1,60
2.	Shirt cotton	100% CO	combined twill	120	0,61
3.	Cord	100% CO	velveteen	330	1,76
4.	Linen	100% LI	plain weave	250	1,09
5.	Gabardine	100% WO	twill	175	0,55
6.	Crepe	100% WO	plain weave	145	0,93
7.	Silk	100% SE	plain weave	15	0,10
8.	Natural silk (bourette)	100% SE	plain weave	150	0,80
9.	Wild silk (tussah)	100% SE	plain weave	80	0,44
10.	Jute	100% JU	plain weave	300	1,44
11.	Flannel	80% WO 20% PES	twill	290	1,53
12.	Denim	62% PES 35% CO 3% EL	twill	275	1,13
13.	Plaid	35% PES 35% AF 30% WO	twill	270	1,14
14.	Tweed	66% AF 14% WO 10% PES 10% CMD	combined twill	270	3,90
15.	Velvet	92% CO 8% CMD	velvet	300	1,88
16.	Lurex knit	70% PES 30% PA	held stitch knit	215	2,94
17.	Crepe-jersey	85% PES 15% EL	rib knit	135	0,73
18.	Woven motorcyclist wear fabric, coated	72% PA 28% PU	plain weave	90	0,39
19.	Woven easy care fabric	65% PES 35% CO	twill	180	0,57
20.	Warp knitted velour fabric	90% PA 10% EL	warp knit velour	235	1,56
21.	Weft knitted plain fabric	98% CLY	single jersey	172	1,21

		2% EL			
22.	Taffeta	100% CA	plain weave	125	0,33
23.	Crepe	100% PES	plain weave	85	0,25
24.	Satin	100% PES	sateen	125	0,30
25.	Felt	100% PES	Non woven	155	1,25
26.	Organza	100% PES	plain weave	25	0,16
27.	Fleece	100% PES	weft terry knit	250	3,99
28.	Woven upholstery	100% PES	woven Jacquard	600	2,38
29.	Woven outdoor leisure wear fabric	100% PES	plain weave	90	0,20
30.	Tulle	100% PA	warp knitted tulle	10	0,30
31.	Warp knitted tricot-satin	100% PA	warp knitted tricot-satin	100	0,40
32.	leather	100% Leather	-----	815	1,68
<b>2<sup>nd</sup> set of measurements:</b>					
33.	Men's woven suit fabric	60% WO 38% PES 3% EL	plain weave	195	0.57
34.	Men's woven suit fabric	100% WO	herringbone	232	0.83
35.	Men's woven overcoat fabric	80% WO 20% PA	Plain weave	324	2.64
36.	Men's woven overcoat fabric	59% CO 25% PAN 11% WO 5% PES	twill	460	3.23
37.	Woven outdoor leisurewear fabric	100% PES	Plain weave	198	0.26
38.	Weft knitted jersey fabric	48% CO 48% CMD 4% EL	Weft knitted	208	1.09
39.	Weft knitted terry fabric	55% CV 45% PES	Weft knitted	288	1.69
40.	Warp knitted jersey- based fabric	100% PES	Warp knitted	154	0.51
41.	Warp knitted mesh fabric	100% PES	Warp knitted	128	0.51
42.	Brushed knitted fabric	100 PES	Brushed knitted	215	0.98

## Annex C: 16 KES-f characteristic fabric hand values

FB01 KES-F **tensile** characteristic values:

Sample	LT warp	LT weft	WT warp	WT weft	RT warp	RT weft	EMT warp	EMT weft
1	0.771	0.762	22.60	11.33	35.07	40.84	11.727	5.949
2	0.629	0.644	9.23	9.03	52.03	48.48	5.874	5.608
3	0.684	0.684	7.45	10.90	50.36	49.80	4.416	6.382
4	0.606	0.633	6.63	15.25	48.68	37.23	4.376	9.634
5	0.739	0.727	8.53	10.43	70.68	67.16	4.614	5.741
6	0.548	0.458	15.75	23.40	57.94	51.28	11.485	20.447
7	0.854	0.749	3.00	6.25	74.33	64.47	1.404	3.339
8	0.686	0.601	5.78	10.38	54.55	48.67	3.372	6.913
9	0.825	0.981	10.45	1.70	55.53	58.87	5.071	0.700
10	0.905	0.971	2.63	2.88	61.10	60.30	1.439	0.963
11	0.654	0.62	13.60	14.63	48.17	47.18	8.313	9.442
12	0.759	0.62	5.53	33.95	46.61	59.58	2.917	21.916
13	0.71	0.575	8.45	14.25	52.36	47.54	4.760	9.931
14	0.591	0.55	7.95	16.88	52.83	38.51	5.385	12.296
15	0.833	0.623	3.90	7.23	54.49	53.29	1.878	4.640
16	0.471	0.447	34.8	56.75	34.92	28.10	29.538	50.778
17	2.185	1.922	6.60	38.30	65.15	48.52	12.083	79.714
18	0.992	1.023	2.75	2.78	70.93	71.27	1.112	1.085
19	0.859	0.86	2.60	12.45	60.58	52.81	1.219	5.790
20	0.553	0.525	118.8	104.00	50.33	36.50	85.877	79.182
21	0.417	0.434	48.75	81.65	36.82	32.21	46.733	75.229
22	0.981	0.935	4.53	2.28	58.57	71.42	1.846	0.974
23	0.563	0.561	9.45	5.55	66.93	56.35	6.713	3.967
24	0.822	0.952	2.85	2.48	59.67	59.09	1.389	1.051
25	0.97	1.002	21.75	29.28	18.63	13.59	8.967	11.683
26	0.978	1.013	7.20	4.75	73.08	79.64	2.948	1.874
27	0.605	0.744	11.00	55.68	46.37	27.62	7.274	29.932
28	0.783	0.786	5.65	2.88	44.69	60.16	2.899	1.557
29	0.784	0.866	3.88	4.075	59.99	63.83	1.977	1.882
30	0.961	1.096	1.65	37.55	66.73	40.15	1.381	27.459
31	0.753	0.65	32.45	14.15	46.31	49.30	17.248	8.709
32	0.844	0.903	7.28	18.28	48.43	39.99	3.461	8.066

FB01 KES-F shear characteristic value:

Sample	G warp	G weft	2HG warp	2HG weft	2HG5 warp	2HG5 weft
1	1.822	1.750	2.456	1.940	6.058	5.712
2	0.367	0.321	0.258	0.196	0.665	0.538
3	1.525	1.365	2.537	2.200	4.565	4.307
4	0.403	0.333	0.070	0.020	0.699	0.559
5	0.588	0.545	0.197	0.129	0.993	0.827
6	0.260	0.241	0.141	0.194	0.340	0.307
7	0.179	0.179	-0.171	-0.156	-0.026	-0.053
8	0.733	0.597	0.647	0.654	2.197	1.862
9	1.383	1.429	9.594	9.366	11.828	12.223
10	2.516	2.203	2.995	2.584	12.127	10.918
11	2.127	1.996	4.527	4.341	7.025	6.984
12	1.438	1.043	2.017	0.818	4.093	2.981
13	0.660	0.586	0.785	0.806	1.790	1.790
14	0.409	0.380	0.861	0.976	1.099	1.002
15	1.013	1.015	1.199	1.570	3.409	3.680
16	0.360	0.306	0.771	1.025	0.812	0.996
17	0.449	0.280	0.592	0.703	0.673	0.650
18	27.195	28.266	24.297	22.119	36.674	34.527
19	2.095	1.938	1.427	1.409	6.547	6.705
20	0.715	0.803	0.639	0.875	0.568	0.856
21	0.356	0.464	0.359	0.479	0.491	0.637
22	2.292	2.478	10.225	9.466	14.645	15.499
23	0.211	0.197	0.002	-0.134	0.190	0.029
24	0.522	0.412	0.343	0.121	1.927	1.297
25	3.576	3.053	4.468	5.140	11.057	8.000
26	0.184	0.176	-0.131	-0.148	-0.023	-0.057
27	0.973	0.920	2.923	3.058	3.234	3.631
28	3.107	2.809	6.665	5.051	14.064	12.930
29	2.315	2.328	1.832	1.270	7.451	7.837
30	2.240	5.421	2.147	9.574	1.622	9.672
31	1.296	0.907	2.881	1.233	3.748	2.010
32	30.998	31.582	54.661	55.478	57.774	56.374
33	0.718	0.764	0.23	0.287	1.411	1.405
34	0.65	0.499	0.701	0.552	1.595	1.224
35	0.613	0.667	0.835	1.427	1.374	1.917
36	0.536	0.514	0.580	0.838	0.821	1.052
37	2.357	2.285	3.515	2.583	8.732	8.659
38	0.838	0.968	1.362	1.555	1.818	1.627
39	0.488	0.459	1.169	0.784	1.271	0.999
40	2.057	1.593	5.906	3.692	7.341	5.607
41	2.567	2.538	4.047	3.785	6.174	5.311
42	2.410	2.121	5.975	3.184	7.864	5.265

FB02 KES-F bending characteristic values:

<b>Sample</b>	<b>B warp</b>	<b>B weft</b>	<b>2HB warp</b>	<b>2HB weft</b>
1	0.395	0.171	0.283	0.159
2	0.057	0.033	0.041	0.029
3	0.180	0.125	0.181	0.120
4	0.279	0.181	0.127	0.096
5	0.073	0.063	0.018	0.017
6	0.065	0.049	0.025	0.020
7	0.014	0.007	0.006	0.004
8	0.040	0.040	0.032	0.031
9	0.015	0.183	0.069	0.416
10	2.725	6.479	1.715	6.249
11	0.288	0.190	0.257	0.176
12	0.255	0.107	0.230	0.052
13	0.128	0.089	0.081	0.055
14	--	--	--	--
15	0.225	0.112	0.215	0.119
16	0.081	0.061	0.093	0.057
17	0.012	0.002	0.027	0.005
18	1.197	1.222	0.424	0.405
19	0.219	0.090	0.179	0.068
20	0.021	0.029	0.022	0.031
21	0.007	0.010	0.010	0.010
22	0.085	0.059	0.127	0.348
23	0.016	0.007	0.004	0.003
24	0.134	0.215	0.062	0.097
25	0.159	0.363	0.096	0.244
26	0.048	0.055	0.008	0.009
27	--	--	--	--
28	0.643	0.699	0.571	0.608
29	0.027	0.046	0.015	0.032
30	0.276	0.019	0.093	0.009
31	0.004	0.003	0.005	0.005
32	3.964	2.154	3.245	1.839
33	0.054	0.054	0.0176	0.0193
34	0.143	0.096	0.071	0.040
35	0.268	0.129	0.228	0.118
36	0.843	0.622	0.632	0.423
37	0.026	0.105	0.022	0.063
38	0.028	0.025	0.030	0.033
39	0.015	0.014	0.015	0.014
40	0.022	0.049	0.017	0.036
41	0.020	0.027	0.012	0.019
42	0.017	0.061	0.015	0.041

**FB03 KES-F compression characteristic values:**

<b>Sample</b>	<b>LC</b>	<b>WC</b>	<b>RC</b>	<b>T0</b>	<b>Tm</b>
1	0.355	0.457	39.73	1.60	1.09
2	0.322	0.217	42.64	0.61	0.34
3	0.418	0.728	44.23	1.76	1.07
4	0.359	0.448	36.42	1.09	0.57
5	0.291	0.116	64.07	0.55	0.39
6	0.413	0.288	61.92	0.93	0.59
7	0.421	0.024	93.75	0.10	0.09
8	0.350	0.196	51.05	0.80	0.54
9	0.232	0.138	51.15	0.44	0.21
10	0.459	0.338	53.91	1.44	1.12
11	0.375	0.453	61.23	1.53	1.04
12	0.345	0.341	41.02	1.13	0.72
13	0.360	0.296	59.61	1.14	0.80
14	0.509	1.056	51.89	3.90	1.83
15	0.433	0.264	42.23	1.88	1.62
16	0.467	1.679	52.56	2.94	1.49
17	0.501	0.177	51.58	0.73	0.58
18	0.243	0.028	90.87	0.39	0.35
19	0.261	0.136	45.98	0.57	0.35
20	0.404	0.619	48.09	1.56	0.94
21	0.35	0.539	40.78	1.21	0.58
22	0.564	0.04	64.41	0.33	0.28
23	0.478	0.042	59.03	0.25	0.21
24	0.434	0.043	67.32	0.30	0.26
25	0.496	0.401	62.56	1.25	0.90
26	0.251	0.033		0.16	0.12
27	0.635	1.256	49.85	3.99	2.38
28	0.580	1.006	37.43	2.38	1.62
29	0.289	0.040	85.00	0.20	0.15
30	0.453	0.046	87.03	0.30	0.26
31	0.407	0.073	52.05	0.40	0.33
32	2.395	0.232	47.42	1.68	1.59
33	0.418	0.097	57.61	0.57	0.47
34	0.402	0.209	58.85	0.83	0.62
35	0.419	1.212	51.09	2.64	1.49
36	0.540	1.307	44.34	3.23	2.26
37	0.294	0.059	73.79	0.26	0.18
38	0.357	0.422	37.56	1.09	0.62
39	0.474	0.640	45.36	1.69	1.15
40	0.543	0.098	53.08	0.51	0.44
41	0.453	0.114	44.30	0.51	0.40
42	0.560	0.359	48.32	0.98	0.69

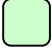







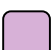
FB04 KES-F surface **roughness** and **friction** characteristic values:

Sample	MIU warp	MIU weft	MMD warp	MMD weft	SMD warp	SMD weft
1	0.217	0.234	0.015	0.029	4.138	9.735
2	0.149	0.179	0.019	0.020	5.938	4.570
3	0.284	0.274	0.009	0.020	4.083	24.815
4	0.166	0.177	0.022	0.027	11.040	9.055
5	0.146	0.128	0.020	0.011	5.325	2.860
6	0.181	0.225	0.022	0.042	9.438	9.553
7	0.137	0.140	0.015	0.013	2.815	1.855
8	0.168	0.169	0.027	0.034	16.530	13.450
9	0.140	0.146	0.045	0.020	8.528	4.675
10	0.171	0.163	0.034	0.032	16.050	10.600
11	0.159	0.165	0.011	0.012	3.000	3.115
12	0.187	0.207	0.013	0.020	3.315	8.243
13	0.159	0.158	0.013	0.012	4.705	4.658
14	0.321	0.341	0.015	0.020	3.890	6.358
15	0.300	0.293	0.013	0.011	7.455	4.963
16	0.277	0.419	0.013	0.019	4.038	10.448
17	0.190	0.304	0.019	0.020	4.555	13.425
18	0.103	0.115	0.036	0.051	12.190	5.605
19	0.143	0.153	0.010	0.048	1.818	4.293
20	0.283	0.230	0.012	0.009	4.705	2.698
21	0.220	0.231	0.014	0.010	6.293	4.313
22	0.145	0.157	0.036	0.021	10.663	2.605
23	0.187	0.234	0.018	0.017	4.253	2.838
24	0.188	0.265	0.005	0.015	0.421	2.233
25	0.217	0.213	0.012	0.013	4.273	3.318
26	0.178	0.170	0.035	0.034	4.080	6.630
27	0.408	0.364	0.010	0.009	1.765	1.780
28	0.305	0.300	0.024	0.018	16.960	7.763
28 back	0.260	0.292	0.016	0.031	6.670	12.683
29	0.145	0.142	0.043	0.015	3.858	1.335
30	0.132	0.262	0.021	0.038	7.125	18.848
31	0.200	0.143	0.022	0.011	9.218	10.123
32	0.182	0.187	0.009	0.009	1.785	1.473
33	0.148	0.167	0.026	0.022	7.92	6.69
33 back	0.147	0.174	0.025	0.022	8.03	6.78
34	0.143	0.144	0.011	0.013	5.12	6.52
34 back	0.146	0.147	0.014	0.015	5.92	6.13
35	0.240	0.238	0.016	0.014	6.31	5.91
35 back	0.246	0.250	0.016	0.016	5.83	5.45
36	0.299	0.320	0.026	0.029	14.51	12.13
36 back	0.345	0.301	0.043	0.034	17.17	14.15
37	0.148	0.161	0.038	0.017	3.23	1.26


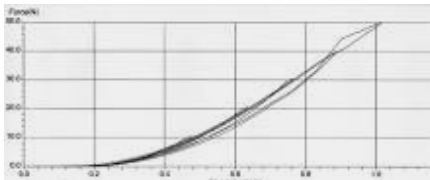
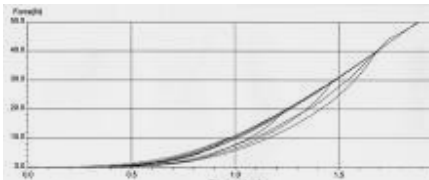
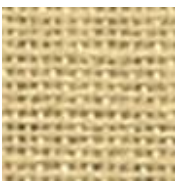
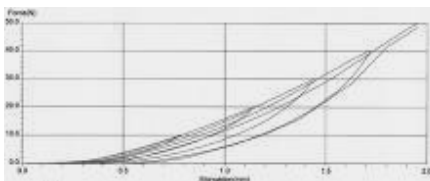
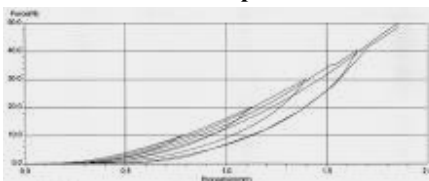



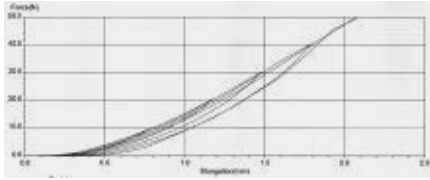
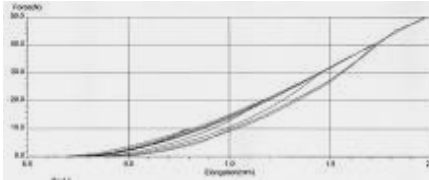

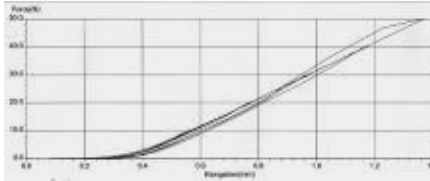
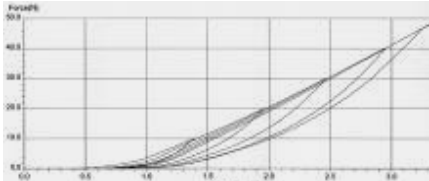
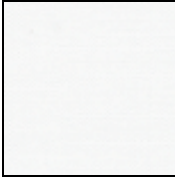
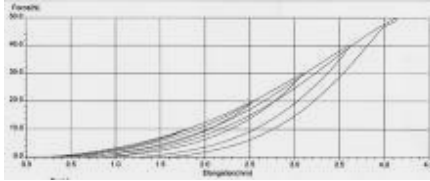
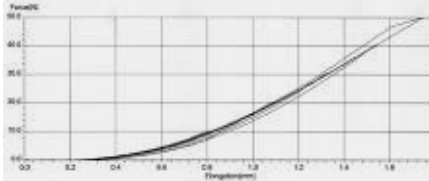

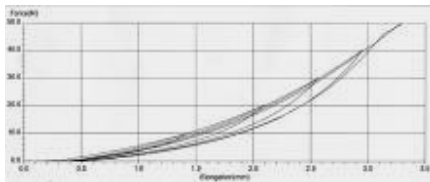
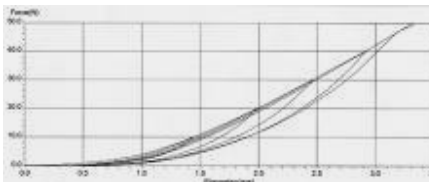

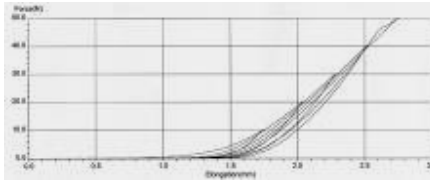
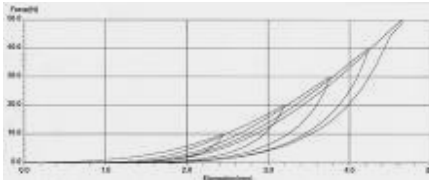

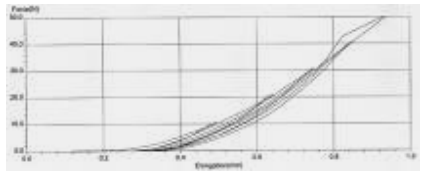
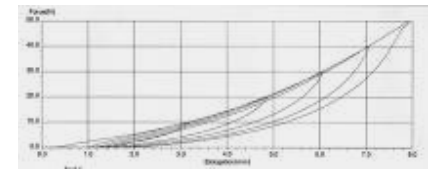
<b>37 back</b>	0.162	0.166	0.031	0.011	3.27	1.15
<b>38</b>	0.220	0.229	0.013	0.012	6.05	2.82
<b>38 back</b>	0.231	0.209	0.016	0.012	5.66	6.31
<b>39</b>	0.376	0.321	0.025	0.026	10.57	11.47
<b>39 back</b>	0.256	0.305	0.016	0.027	6.18	10.80
<b>40</b>	0.153	0.219	0.013	0.029	5.72	8.98
<b>40 back</b>	0.204	0.172	0.045	0.021	18.61	3.56
<b>41</b>	0.139	0.217	0.015	0.025	4.54	9.21
<b>41 back</b>	0.226	0.162	0.043	0.020	10.84	5.21
<b>42</b>	0.265	0.256	0.009	0.016	3.08	7.44
<b>42back</b>	0.181	0.216	0.010	0.025	3.10	12.44

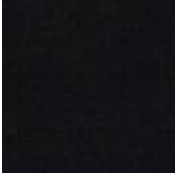
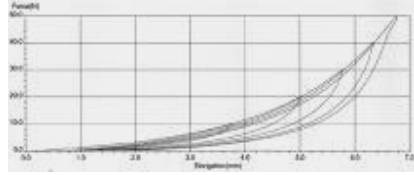
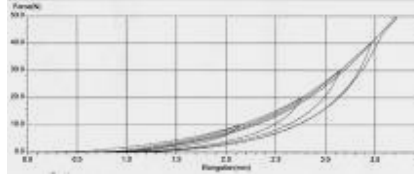

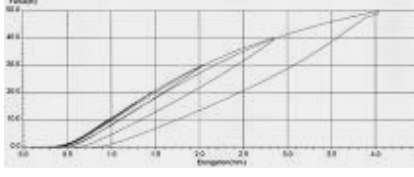
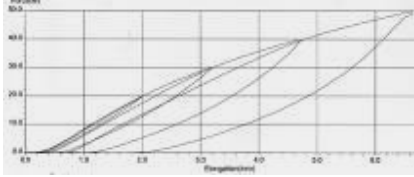

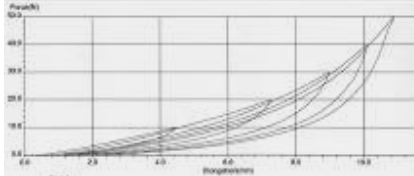
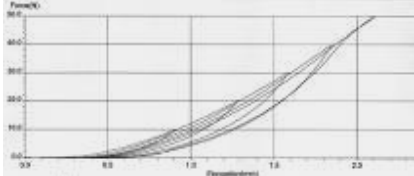

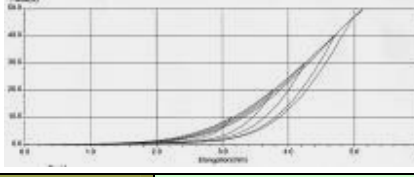
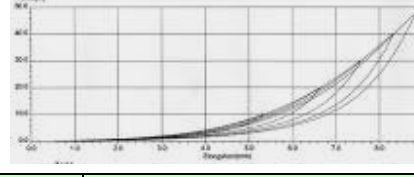

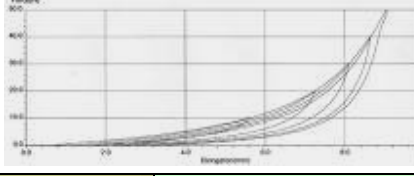
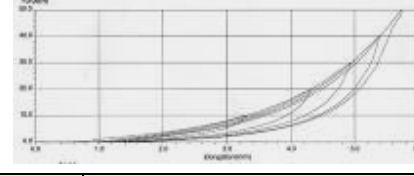

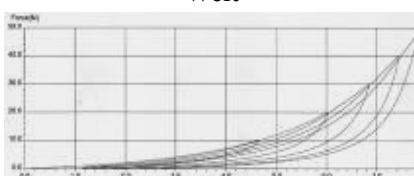
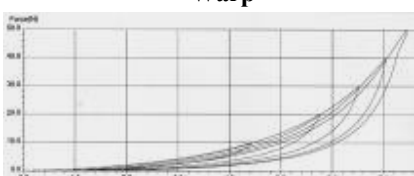
## Annex D: Elasticity force-deformation envelopes

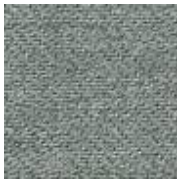
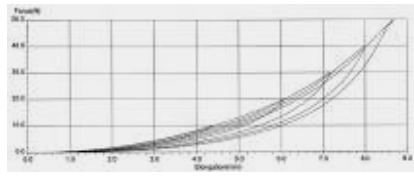
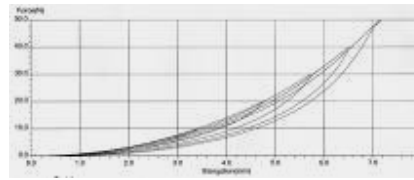

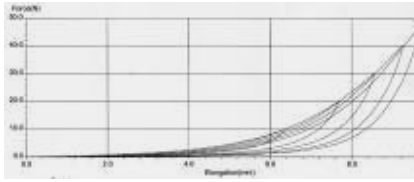
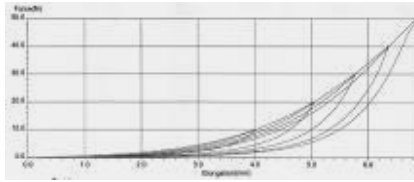
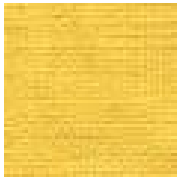
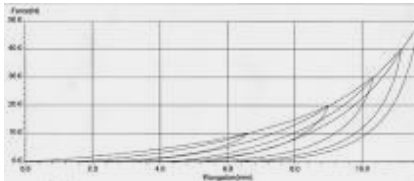
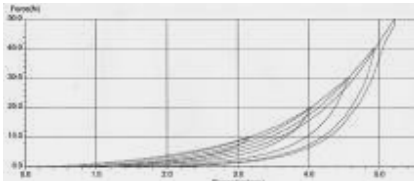

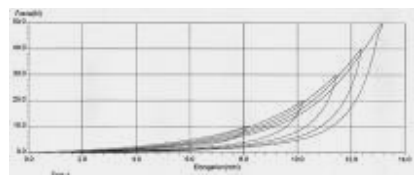
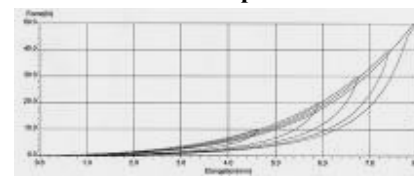

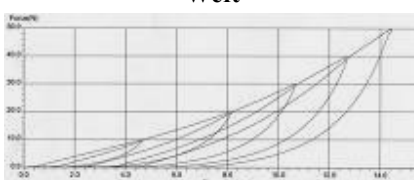
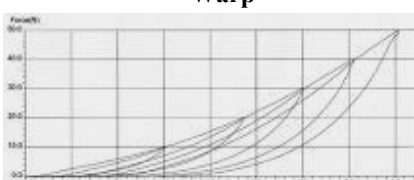
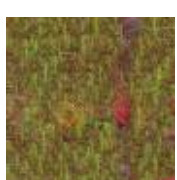
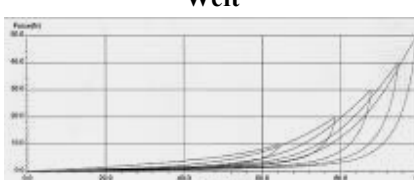
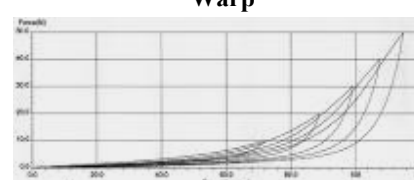
	Fabrics based on natural fibers
	Fabrics based on man made fibers
	Fabrics based on blended fibers (natural and man made)
	Skin (Leather)
	Structure: satin/Jacquard
	Structure: plain weave
	Structure: twill
	Structure: Velvet/velveteen
	Structure: Knit


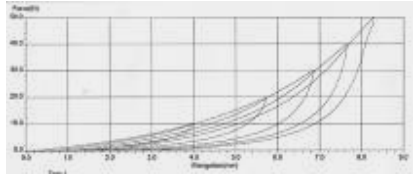
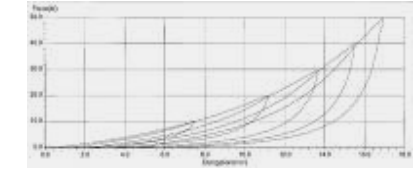

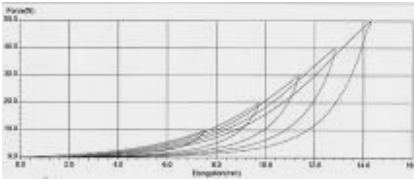
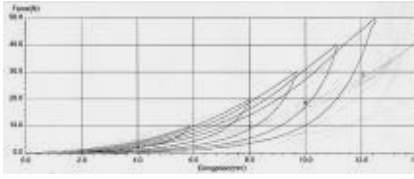

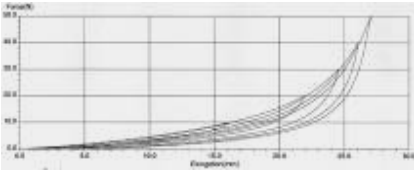
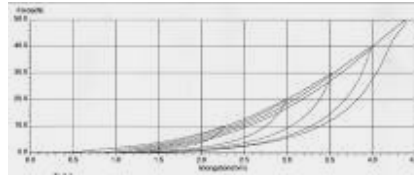

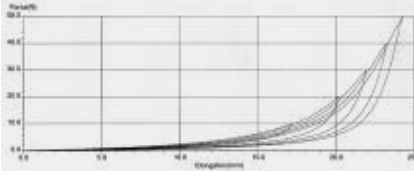
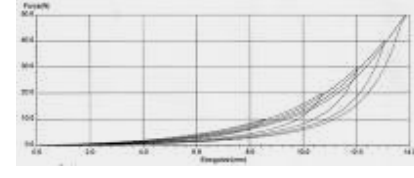

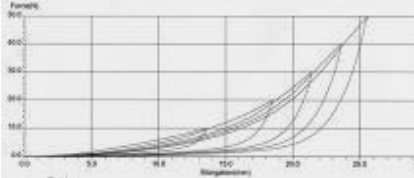
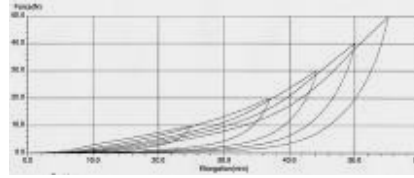

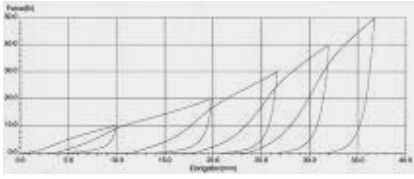
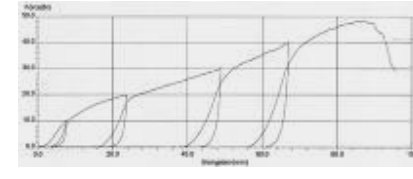
ITT step tensile measurements 1<sup>st</sup> fabric selection: (order from most rigid to most elastic)


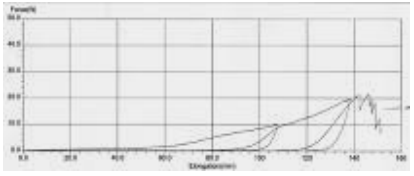
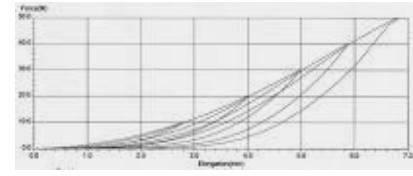
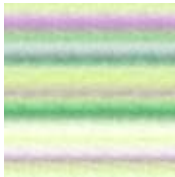
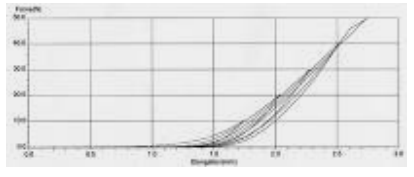
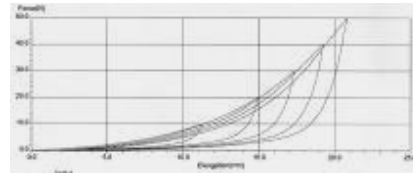

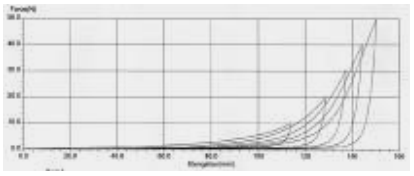
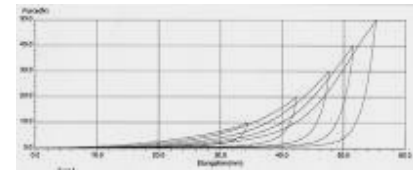

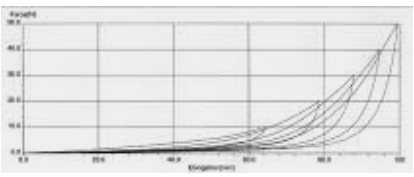
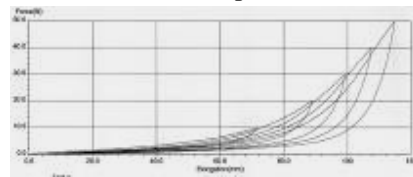

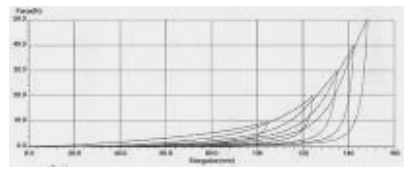
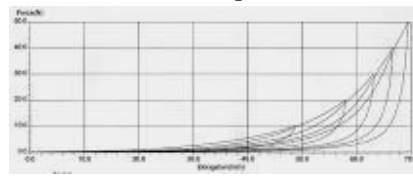

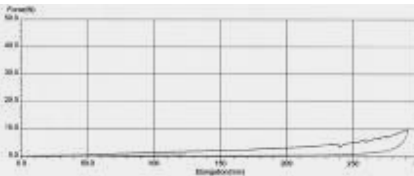
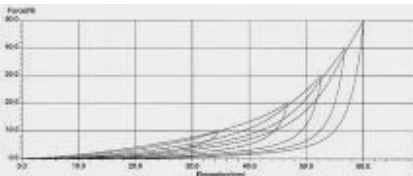
Sample	Structure	Max- elongation Weft in mm	Max Elongation Warp in mm
24_Satin	satin	1.02	1.86
	<b>Weft</b>		<b>Warp</b>
			
10_Jute	plain weave	1.94	1.83
	<b>Weft</b>		<b>Warp</b>
			

18_Woven motorcyclist	plain weave	2.06	1.96	
	<b>Weft</b>		<b>Warp</b>	
22_Taffeta	plain weave	1.36	3.39	
	<b>Weft</b>		<b>Warp</b>	
7_Silk	plain weave	4.11	1.74	
	<b>Weft</b>		<b>Warp</b>	
29_Woven outdoor leisure	plain weave	3.28	3.31	
	<b>Weft</b>		<b>Warp</b>	
28_upholstery	Jacquard	2.73	4.63	
	<b>Weft</b>		<b>Warp</b>	
9_Wild silk (dupion)	plain weave	0.94	7.91	
	<b>Weft</b>		<b>War</b>	


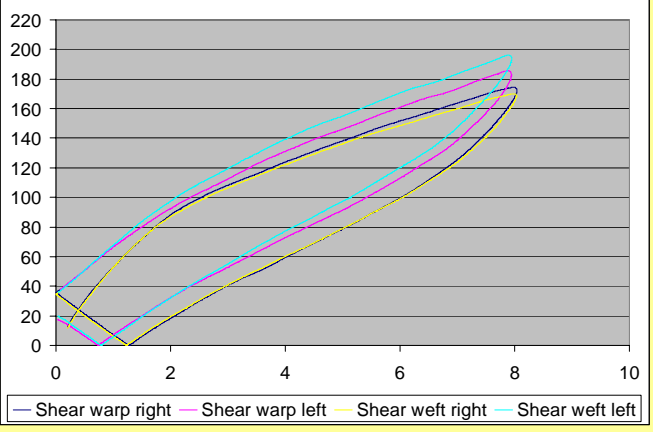

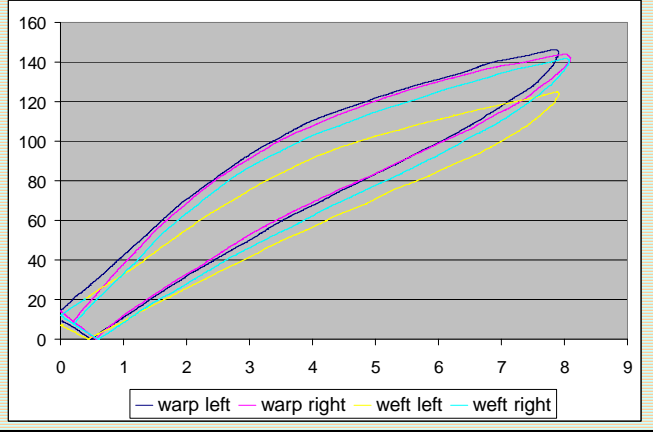

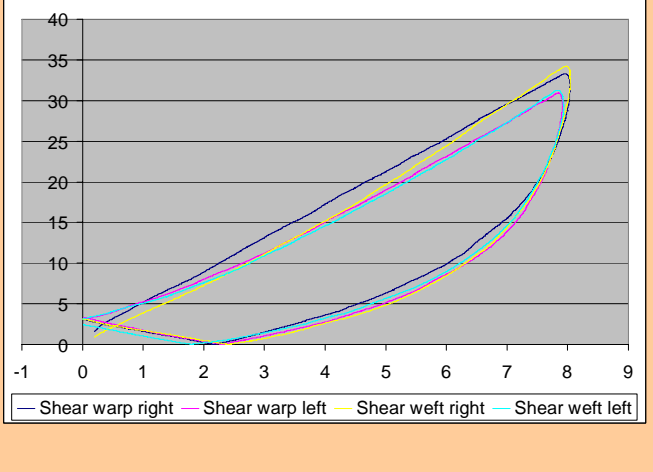
15_Velvet	velvet	6.76	3.70	
	<b>Weft</b>		<b>Warp</b>	
26_Organza	plain weave	4.02	6.62	
	<b>Weft</b>		<b>Warp</b>	
19_Woven easy care fabric	twill	10.87	2.10	
	<b>Weft</b>		<b>Warp</b>	
23_Crepe	plain weave	5.12	8.96	
	<b>Weft</b>		<b>Warp</b>	
3_Cord	velveteen	9.04	5.72	
	<b>Weft</b>		<b>Warp</b>	
2_Shirt cotton	combined twill	7.90	7.43	
	<b>Weft</b>		<b>Warp</b>	

5_Gabardine	twill	8.64	7.14	
	<b>Weft</b>		<b>Warp</b>	
8_Natural silk (bourette)	plain weave	9.84	6.85	
	<b>Weft</b>		<b>Warp</b>	
4_Linen	plain weave	11.74	5.21	
	<b>Weft</b>		<b>Warp</b>	
13_Plaid	twill	13.132	7.93	
	<b>Weft</b>		<b>Warp</b>	
32_Leather	-----	14.422	8.06	
	<b>Weft</b>		<b>Warp</b>	
14_Tweed	combined twill	17.90	6.19	
	<b>Weft</b>		<b>Warp</b>	


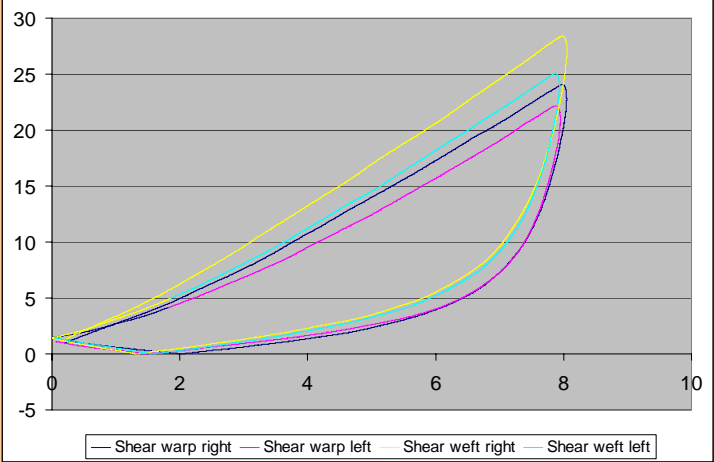

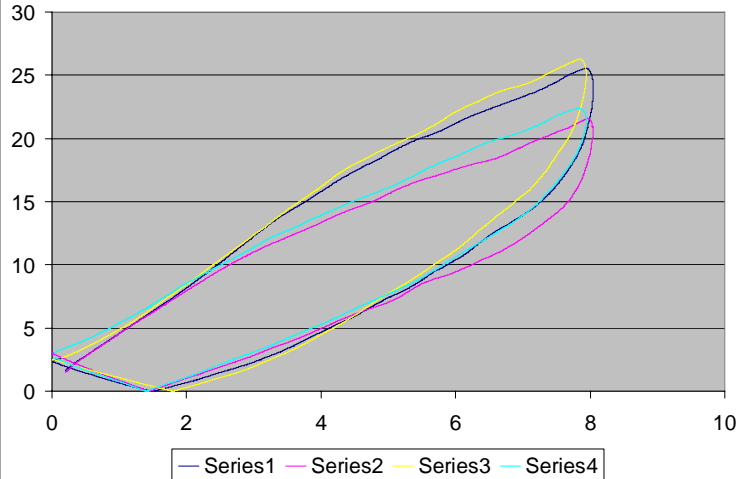

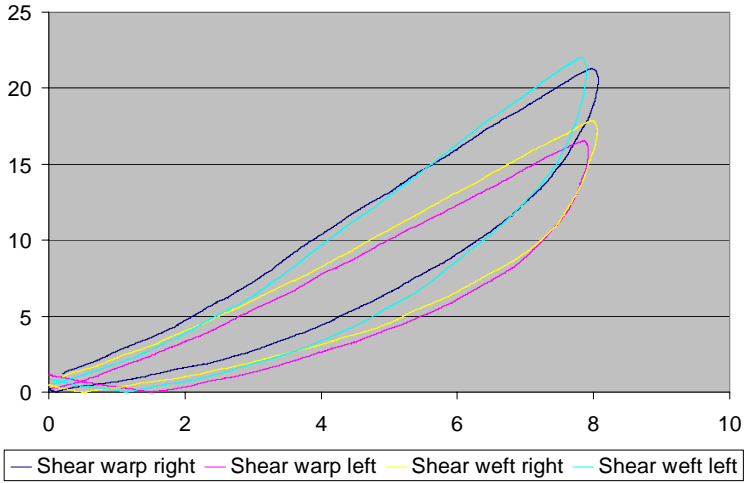
1_Denim	twill	8.28	16.93	
	<b>Weft</b>		<b>Warp</b>	
11_Flannel	twill	14.27	12.50	
	<b>Weft</b>		<b>Warp</b>	
12_Denim	twill	27.04	4.37	
	<b>Weft</b>		<b>Warp</b>	
6_Crepe	plain weave	24.22	13.83	
	<b>Weft</b>		<b>Warp</b>	
31_Warp knitted tricot- satin	warp knitted tricot-satin	25.54	55.15	
	<b>Weft</b>		<b>Warp</b>	
25_Felt	Non woven	36.74	broken	
	<b>Weft</b>		<b>Warp</b>	


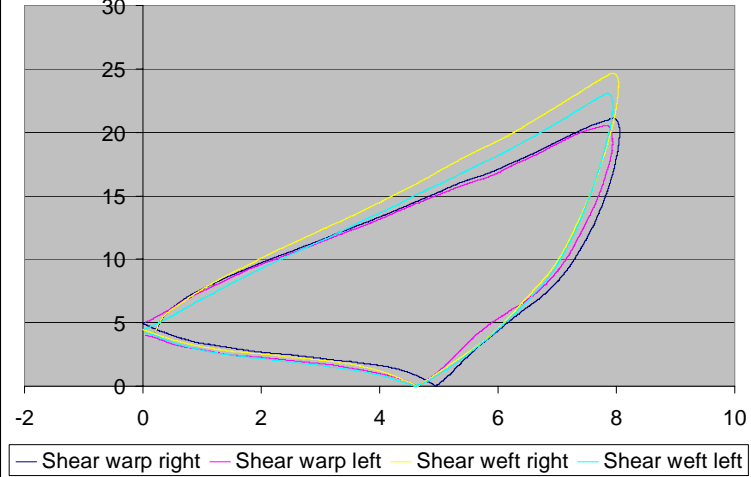

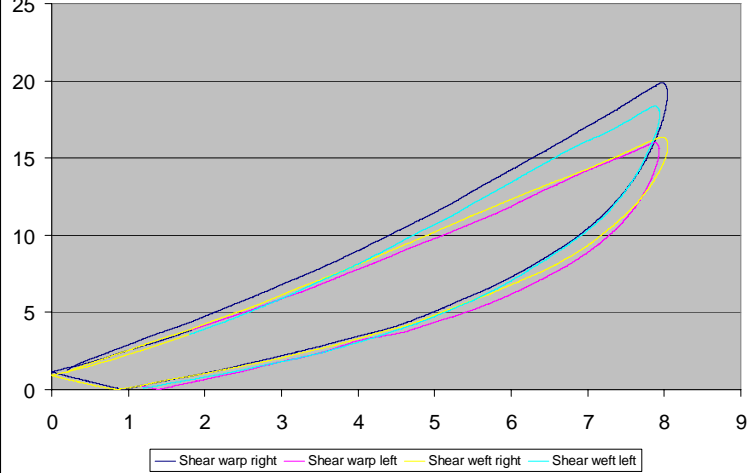
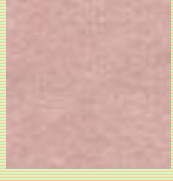
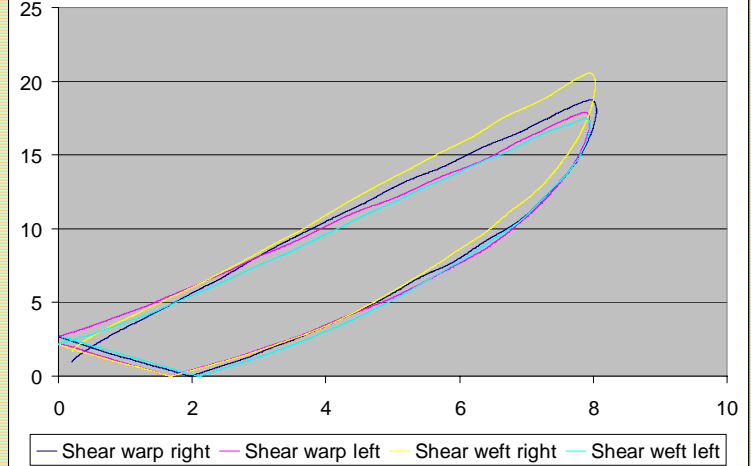
30_Tulle	warp knit tulle	broken	6.77
	<b>Weft</b>	<b>Warp</b>	
			
27_Fleece	weft knit	128.00	20.81
	<b>Weft</b>	<b>Warp</b>	
			
16_Lurex knit	held stitch knit	150.31	55.22
	<b>Weft</b>	<b>Warp</b>	
			
20_Warp knitted velour	warp knit velour	99.45	114.81
	<b>Weft</b>	<b>Warp</b>	
			
21_Weft knitted plain fabric	single jersey	148.19	69.49
	<b>Weft</b>	<b>Warp</b>	
			
17_Crepe-jersey	rib knit	broken	60.07
	<b>Weft</b>	<b>Warp</b>	
			

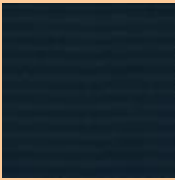
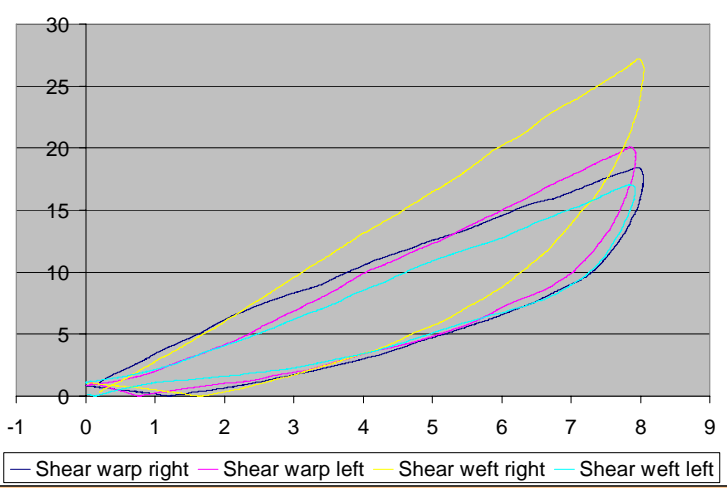

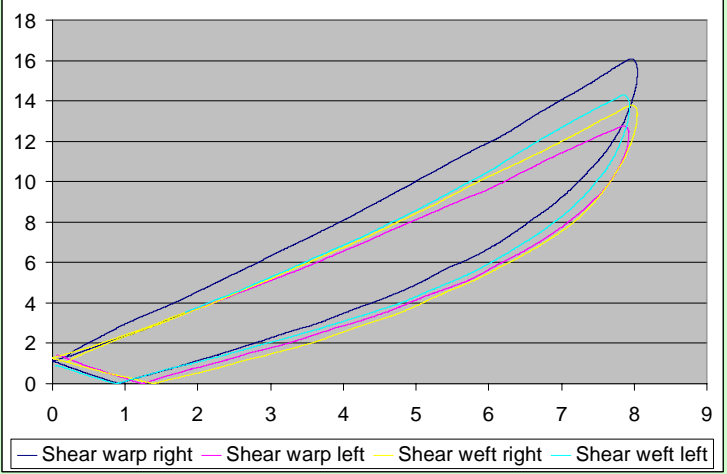
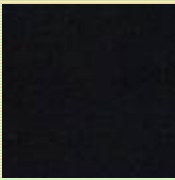
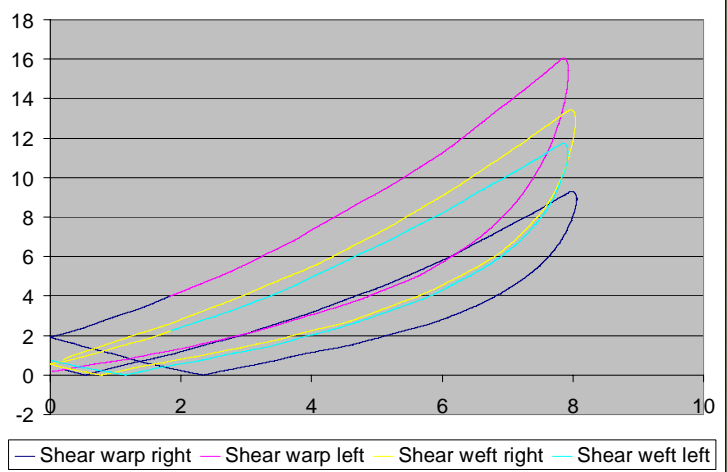
KES-f shear measurements 1<sup>st</sup> and 2<sup>nd</sup> fabric selection: (order 1<sup>st</sup> selection from most rigid to most elastic)

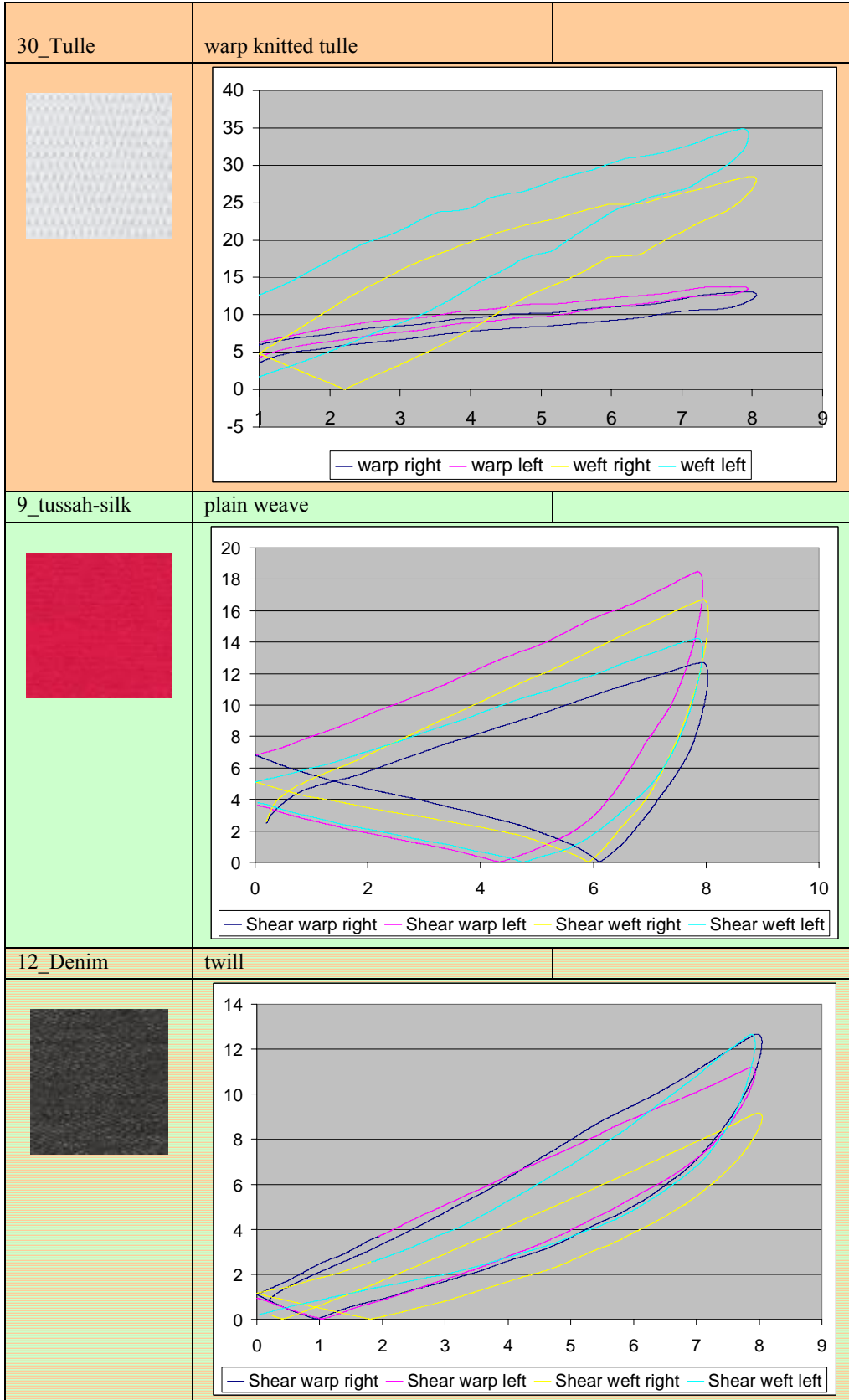
32_Leather	-----	
		
18_Woven motorcyclist	plain weave	
		
28_Woven upholstery	woven Jacquard	
		


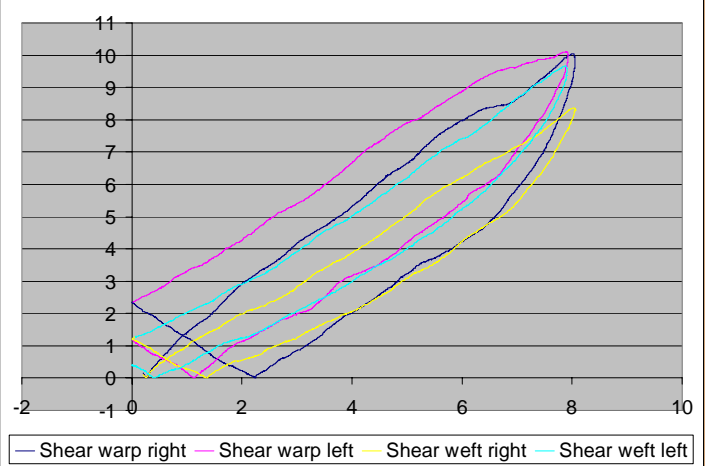
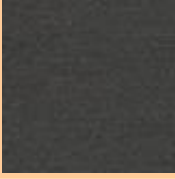
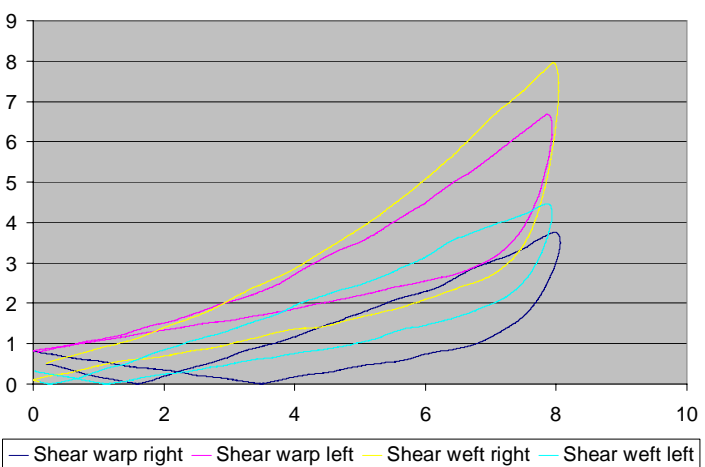

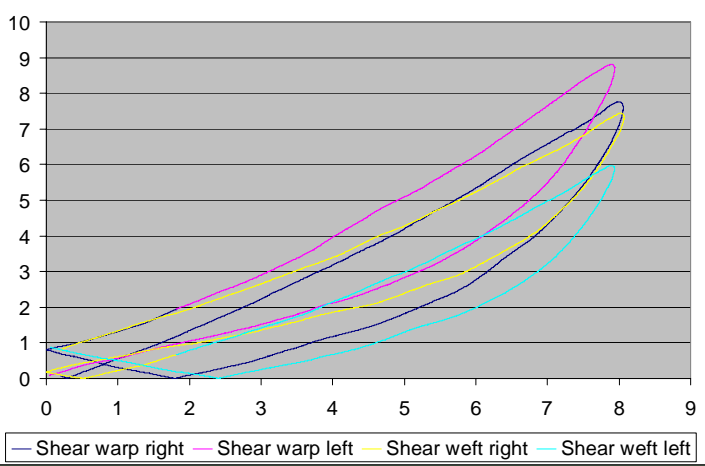


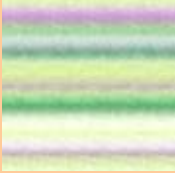
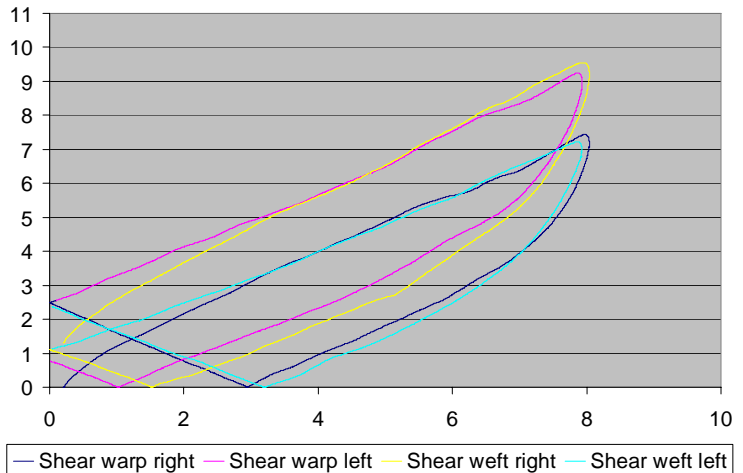

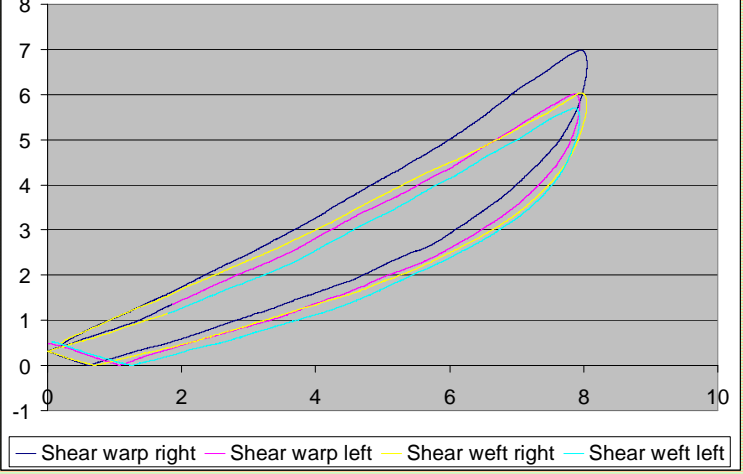

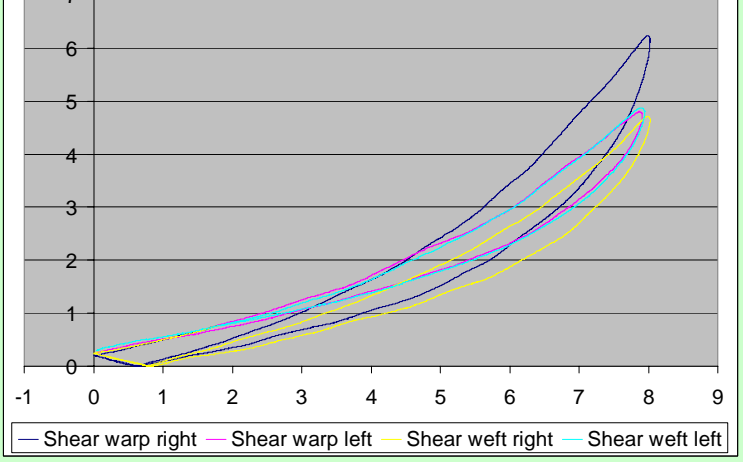
		
<p>25_Felt</p>	<p>Non woven</p>	
		
<p>19_Woven easy care fabric</p>	<p>twill</p>	
		


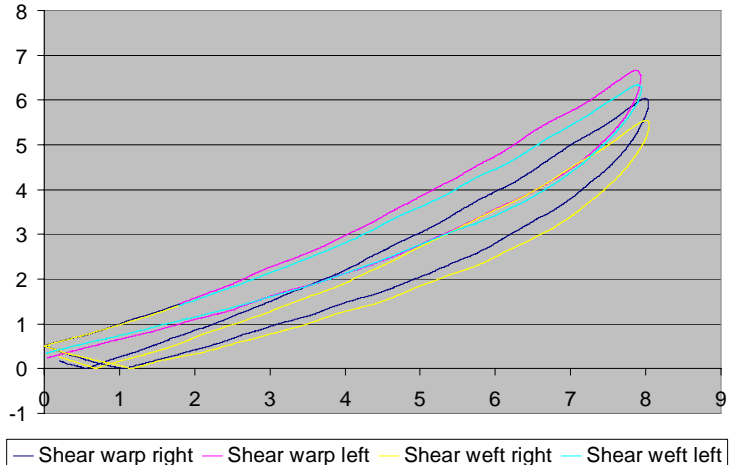

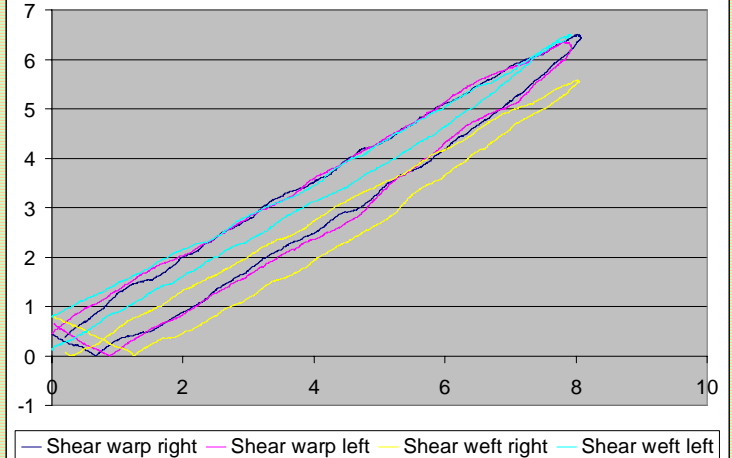

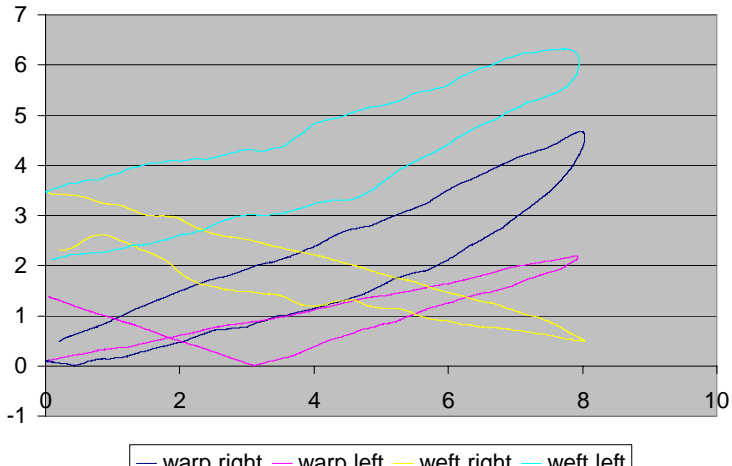
22_Taffeta	plain weave	
	 <p>— Shear warp right — Shear warp left — Shear weft right — Shear weft left</p>	
1_Denim	twill	
	 <p>— Shear warp right — Shear warp left — Shear weft right — Shear weft left</p>	
11_Flannel	twill	
	 <p>— Shear warp right — Shear warp left — Shear weft right — Shear weft left</p>	


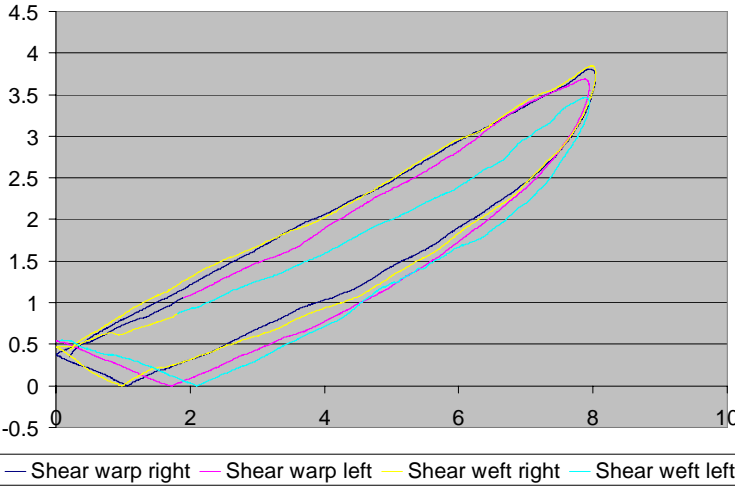

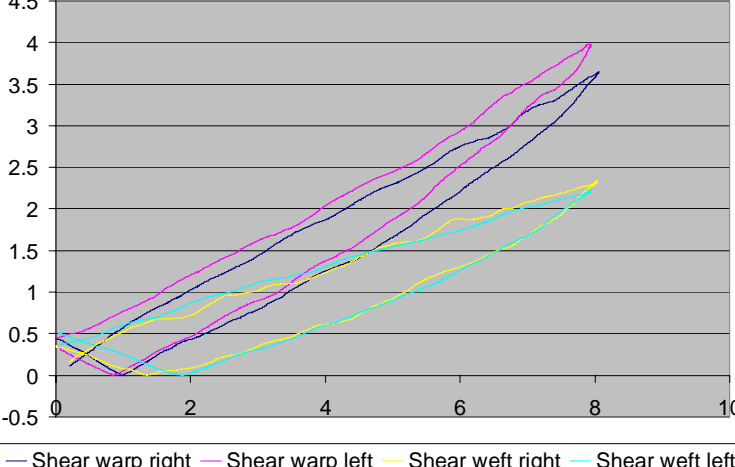

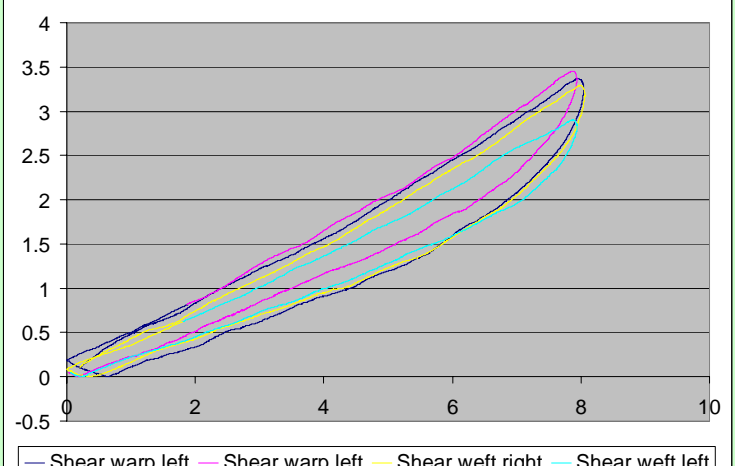
<p>29_Woven outdoor leisure</p>	<p>plain weave</p>	
		
<p>3_Cord</p>	<p>velveteen</p>	
		
<p>15_Velvet</p>	<p>velvet</p>	
		




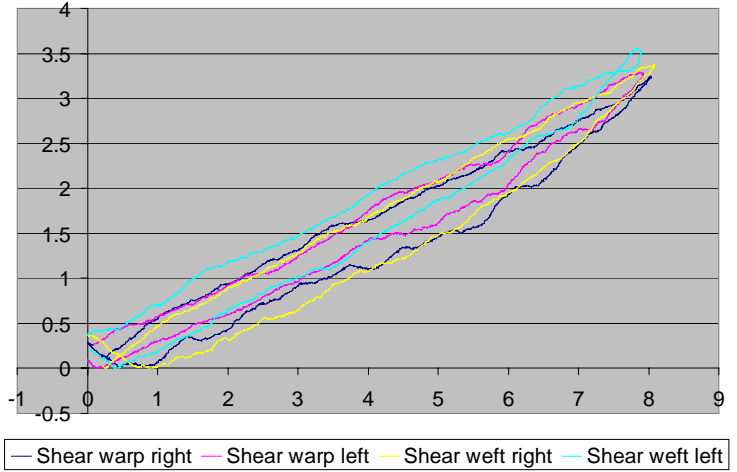

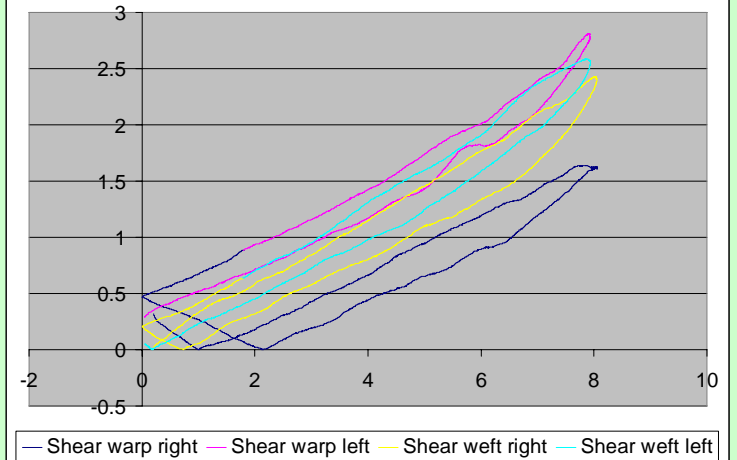

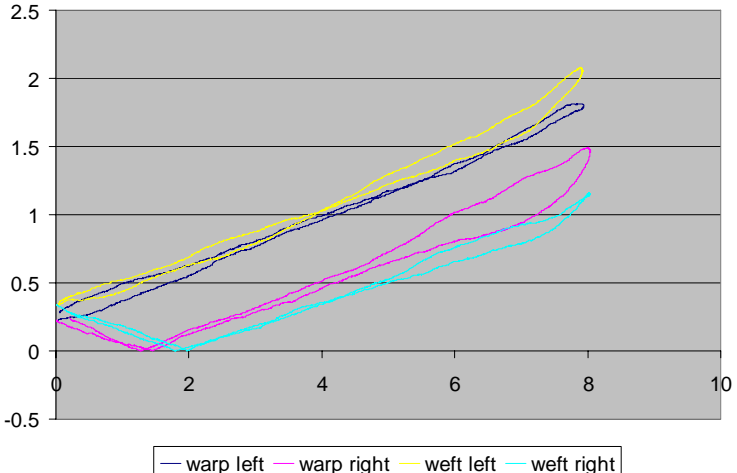
31_Warp knit tricot-satin	warp knitted tricot-satin	
		
24_Satin	satin	
		
8_Natural silk (bourette)	plain weave	
		


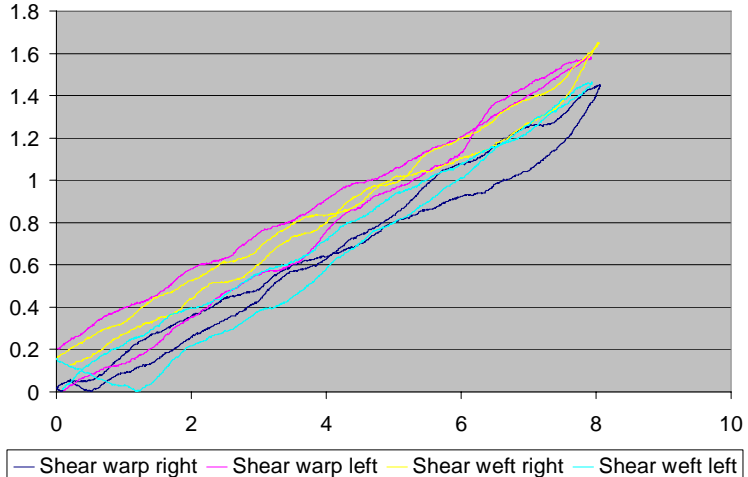

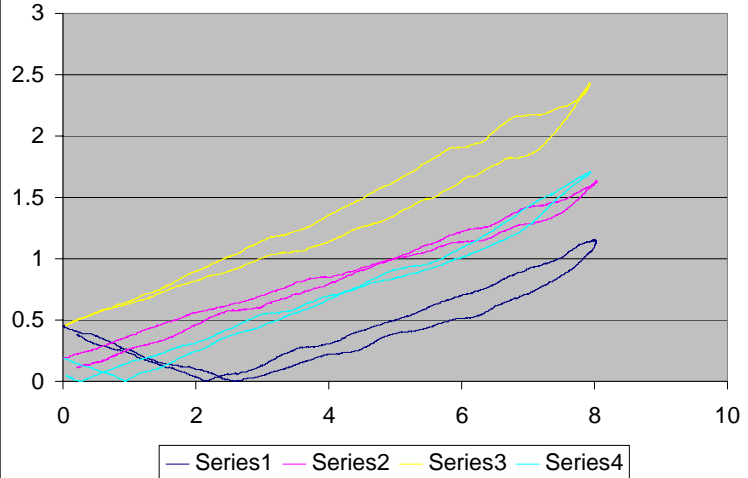

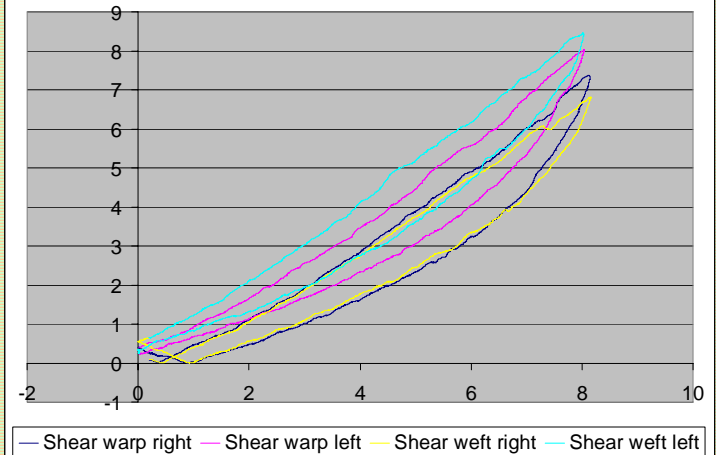
27_Fleece	weft knit	
		
13_Plaid	twill	
		
4_Linen	plain weave	
		


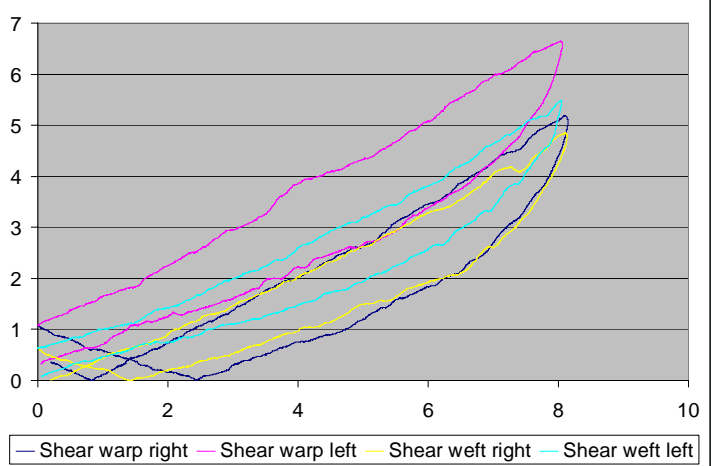
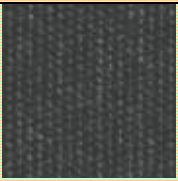
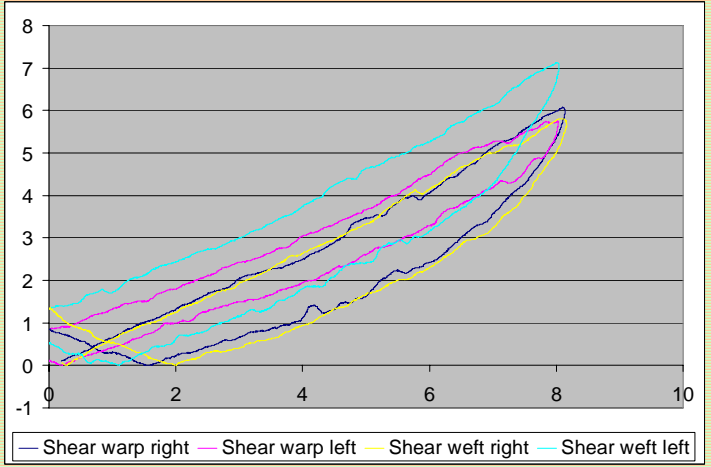

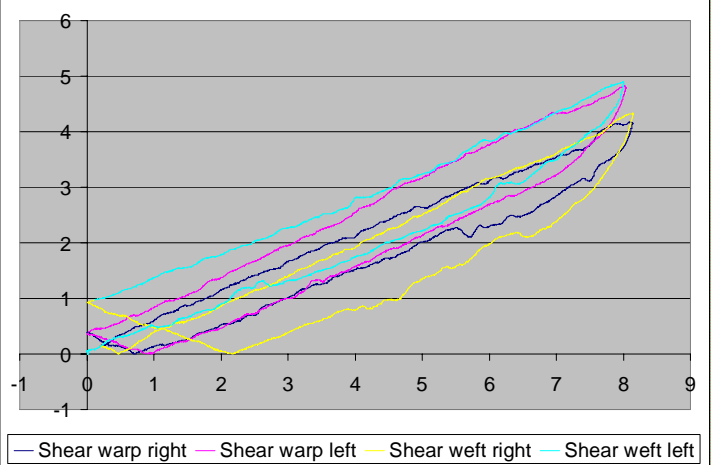
5_Gabardine	twill	
		
20_Warp knitted velour	warp knit velour	
		
16_Lurex knit	held stitch knit	
		


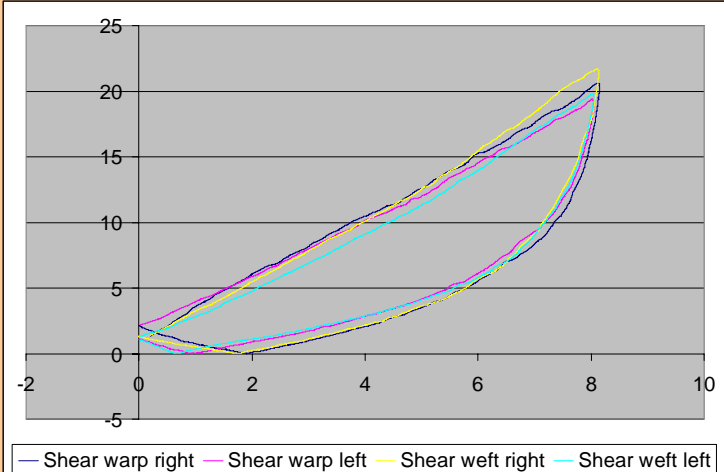

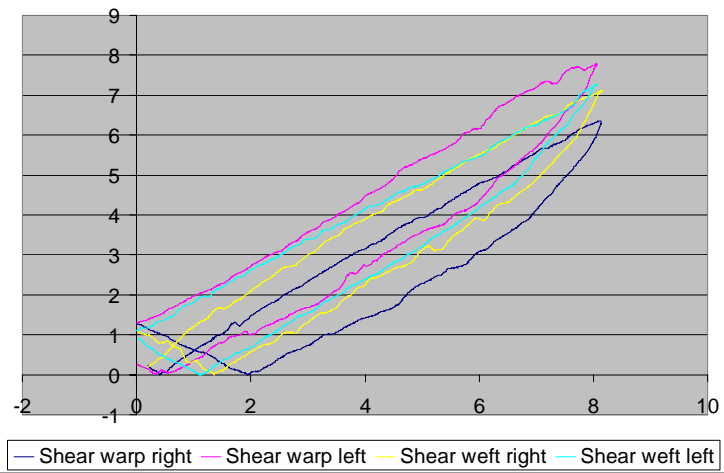

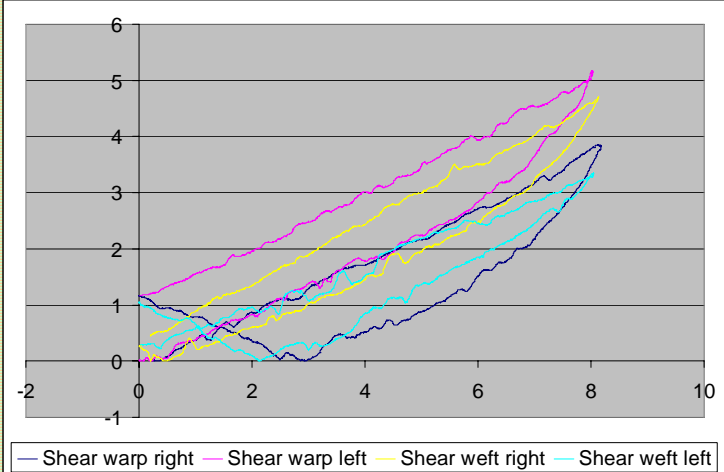
14_Tweed	combined twill	
		
17_Crepe-jersey	rib knit	
		
2_Shirt cotton	combined twill	
		


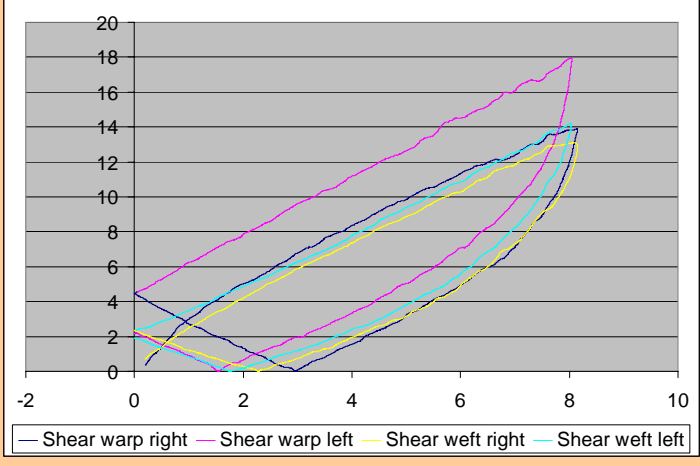
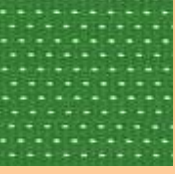
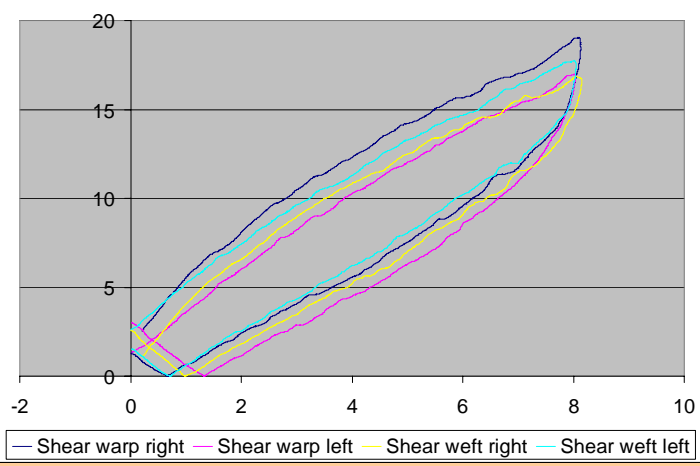

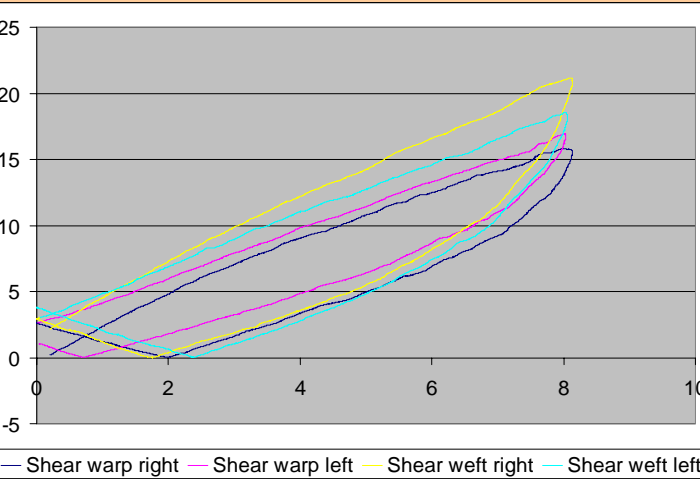


21_Weft knitted plain fabric	single jersey	
		
6_Crepe	plain weave	
		
7_Silk	plain weave	
		


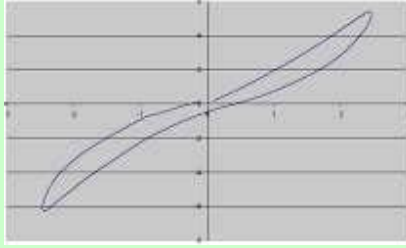
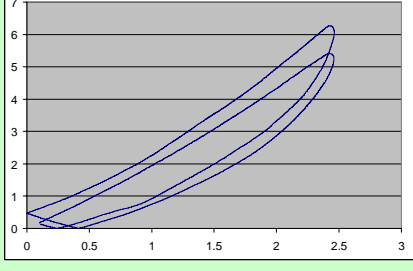
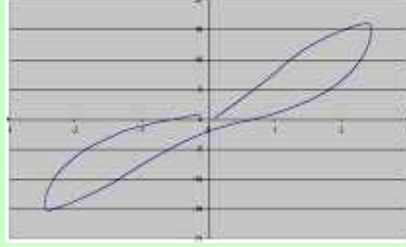
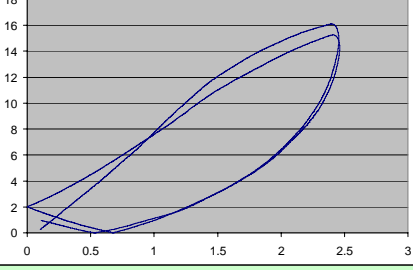

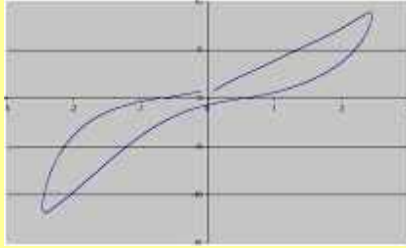
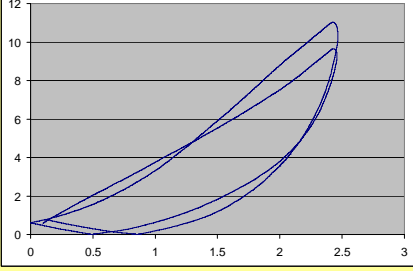
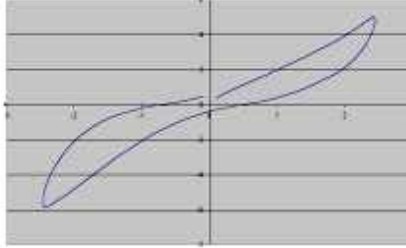
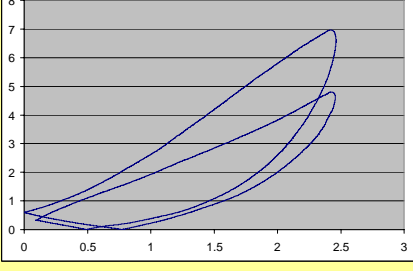
26_ Organza	plain weave	
		
23_ Crepe	plain weave	
		
33_ Men's woven suit	plain weave	
		

34_ Men's woven suit	herringbone	
		
35_ Men's woven overc.	Plain weave	
		
36_ Men's woven overc.	twill	
		

<p>37_Woven outdoor leisure</p>	<p>Plain weave</p>	
		
<p>38_Weft knit</p>	<p>Weft knitted</p>	
		
<p>39_Weft knitted terry</p>	<p>Weft knitted</p>	
		

40_Warp knitted jersey	Warp knitted	
		
41_Warp knitted mesh	Warp knitted	
		
42_Brushed knitted fabric	Brushed knitted	
		

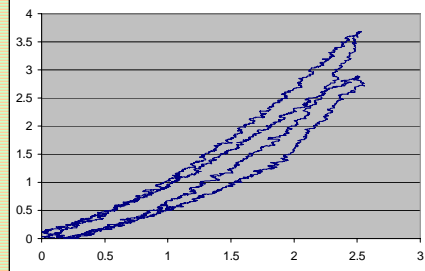
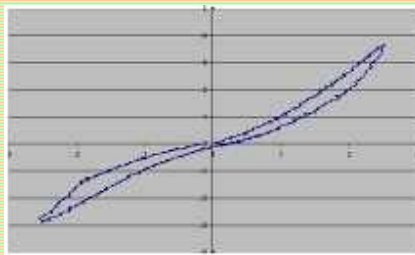
KES-f bending measurements 1<sup>st</sup> and 2<sup>nd</sup> fabric selection: (order 1<sup>st</sup> selection from most rigid to most elastic)

10_jute		Superposed curves front/back bending
	<p><b>Warp</b></p> 	
	<p><b>Weft</b></p> 	
32_leather		
	<p><b>Warp</b></p> 	
	<p><b>Weft</b></p> 	

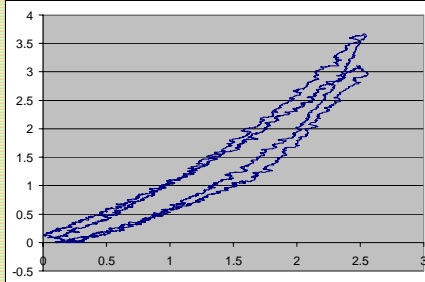
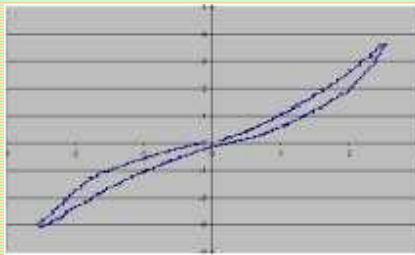
18\_Motorcycle wear fabric



Warp



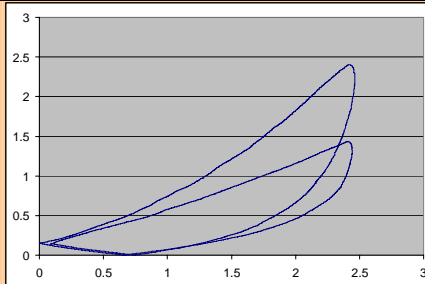
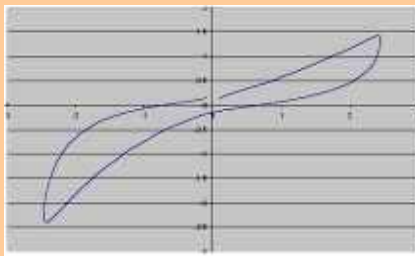
Weft



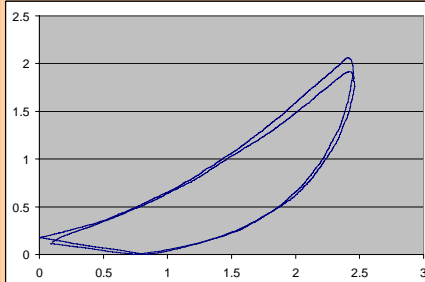
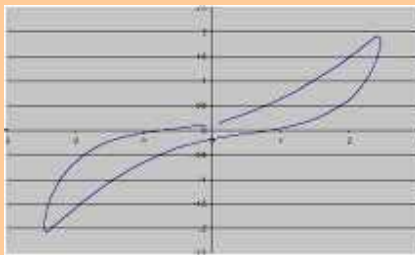
28\_Woven upholstery



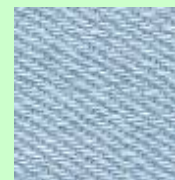
Warp



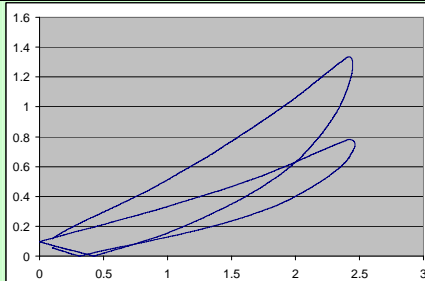
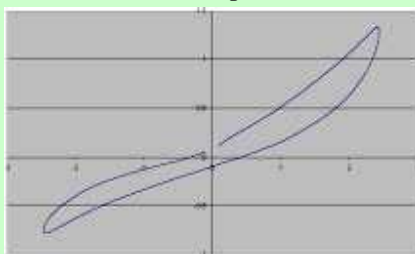
Weft

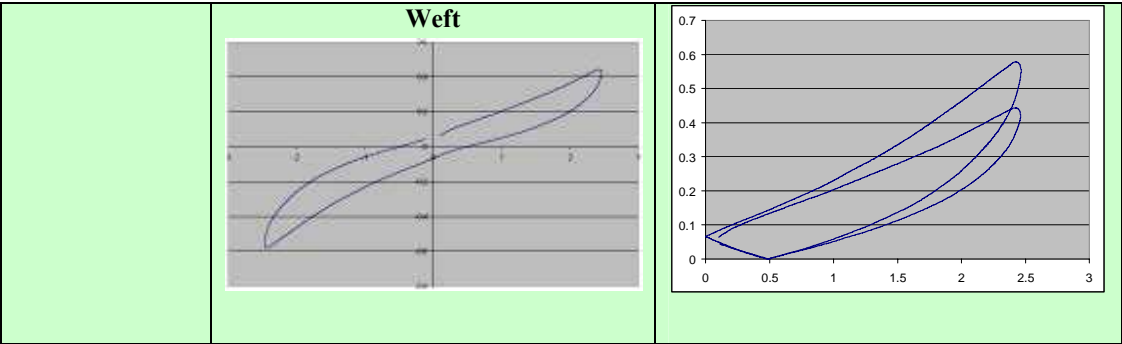


01\_denim

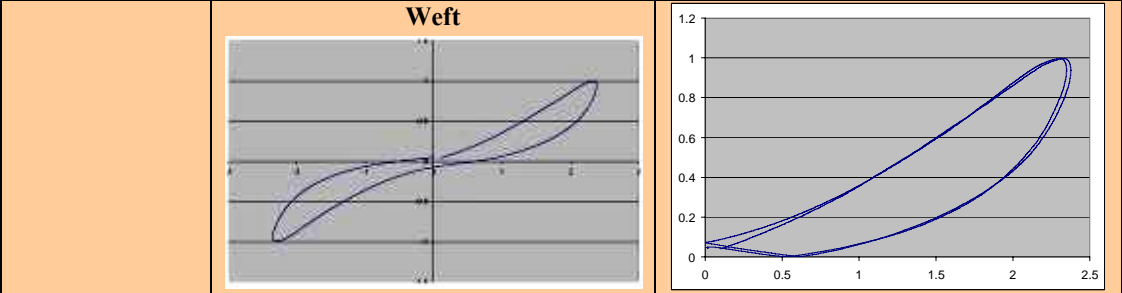
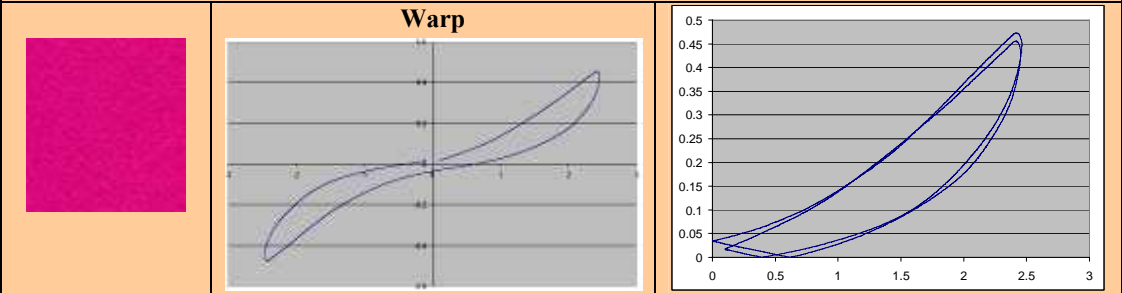


Warp

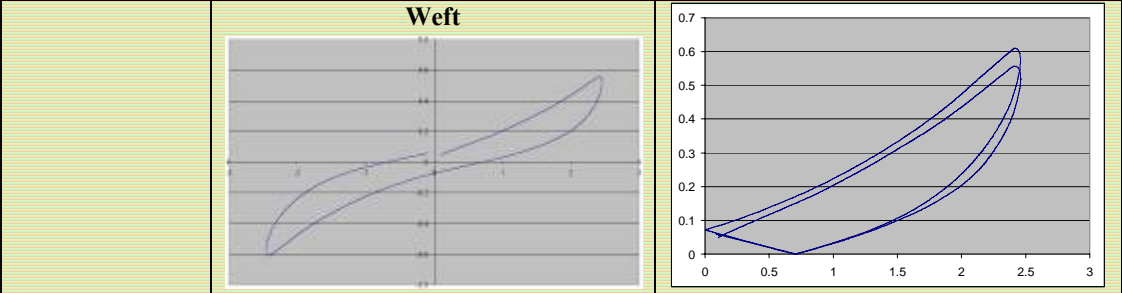
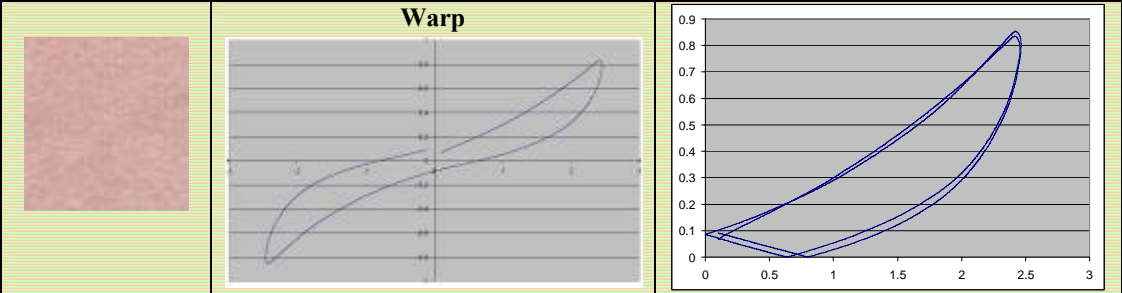




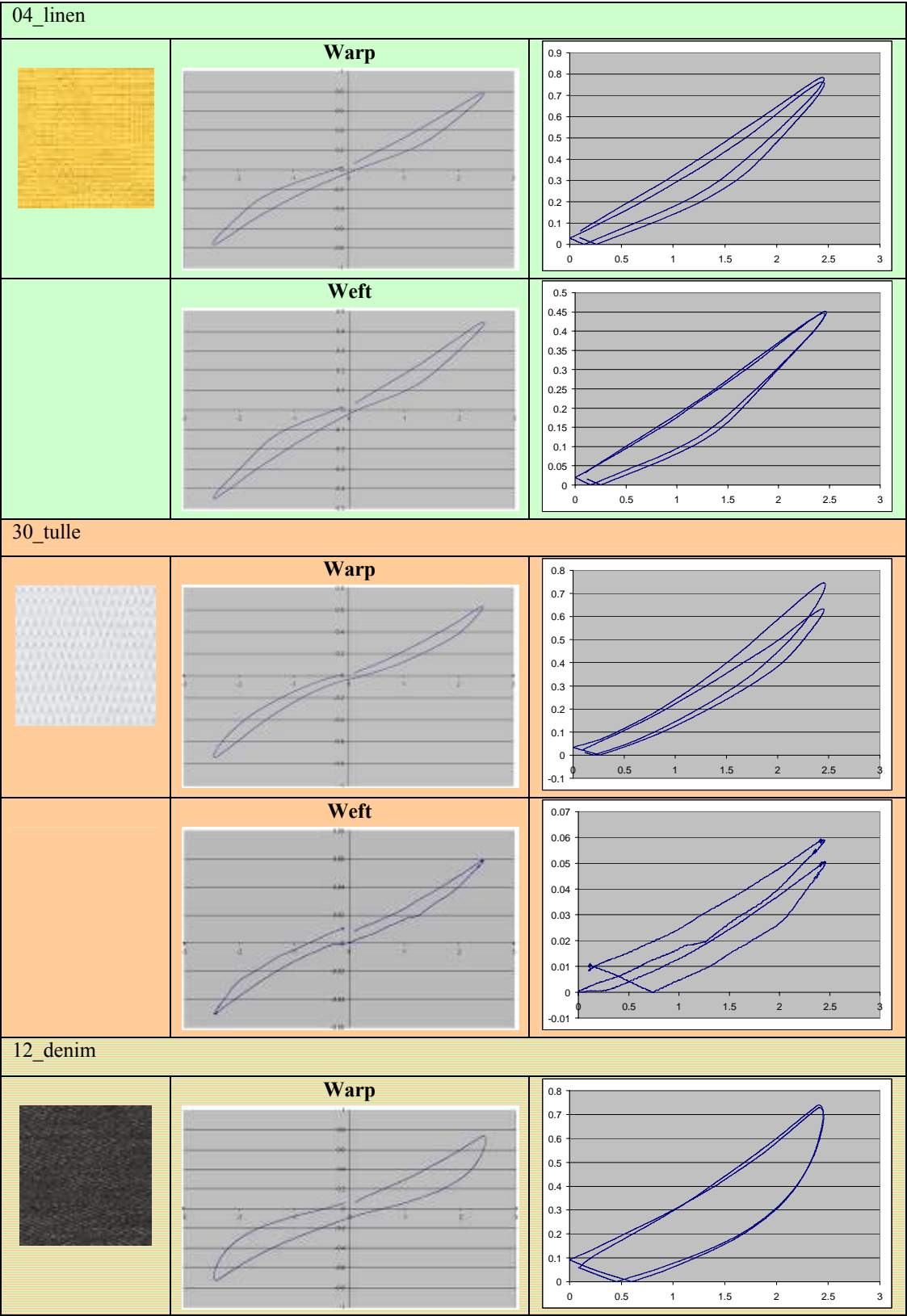
25\_felt

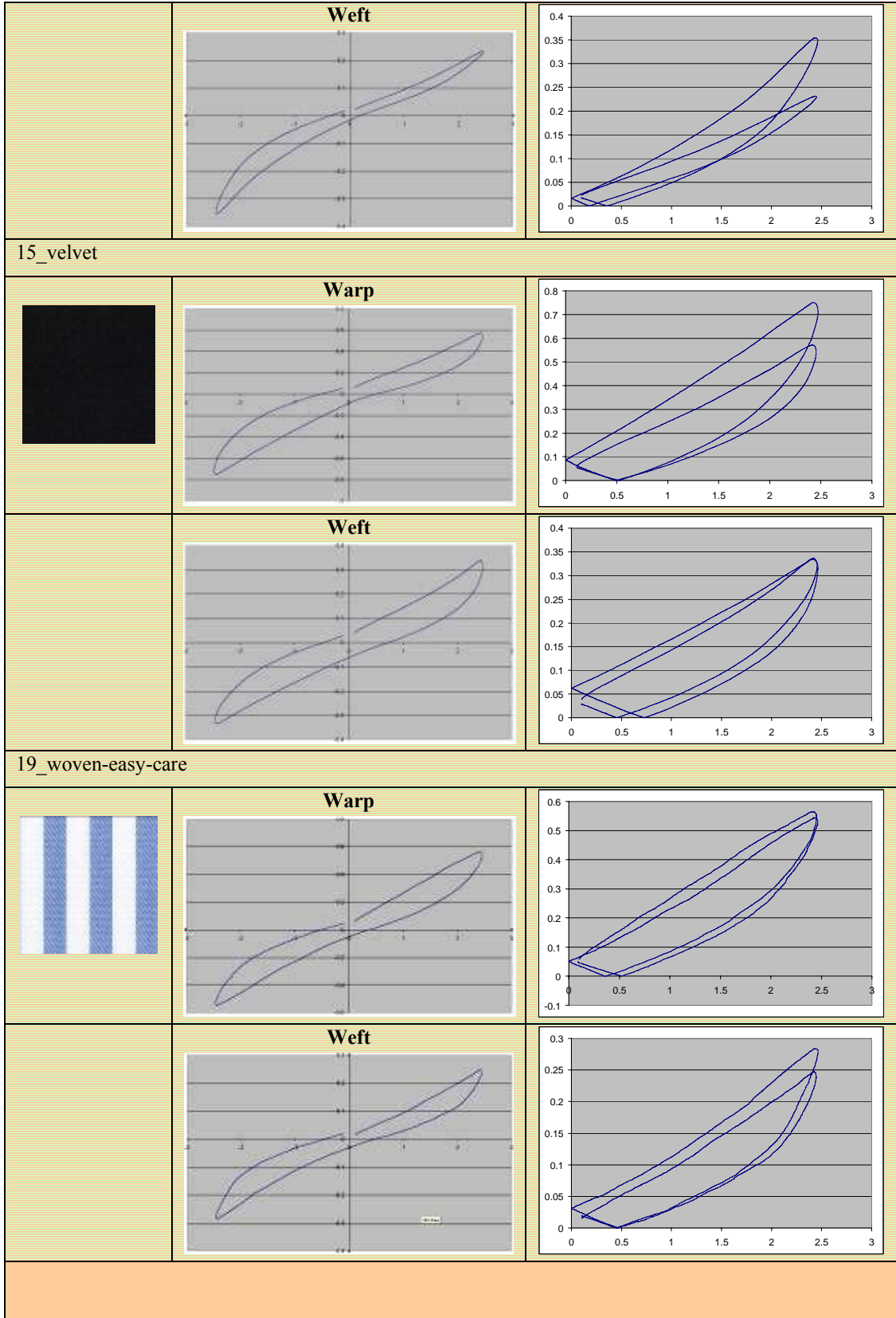



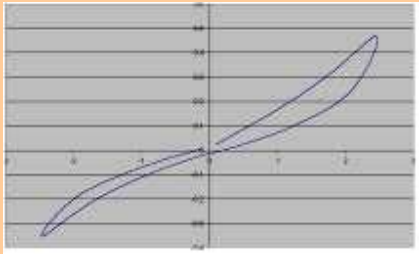
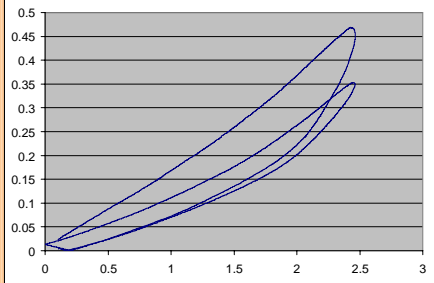

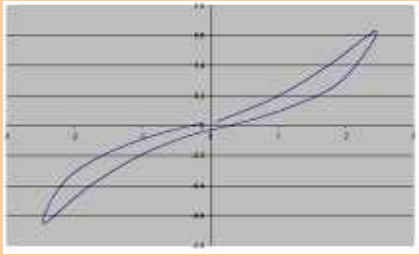
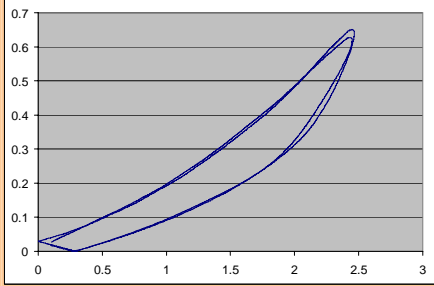

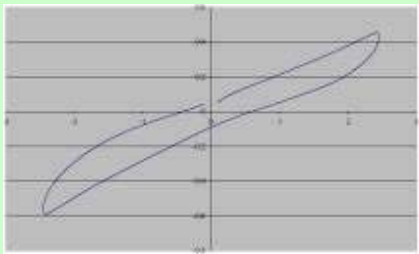
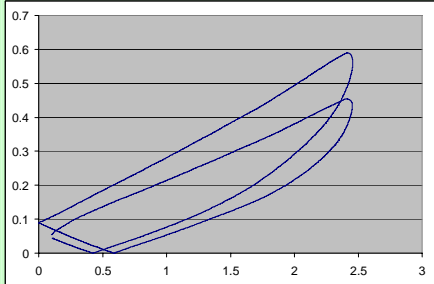

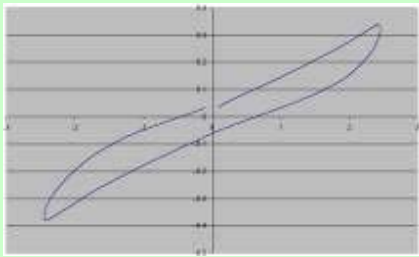
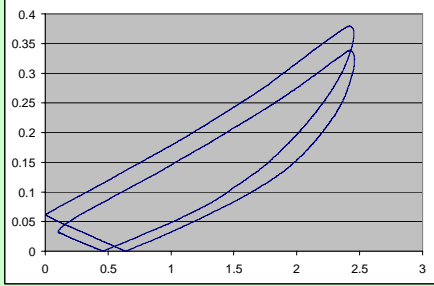

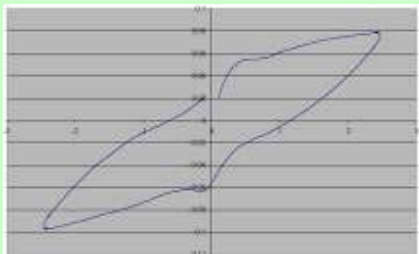
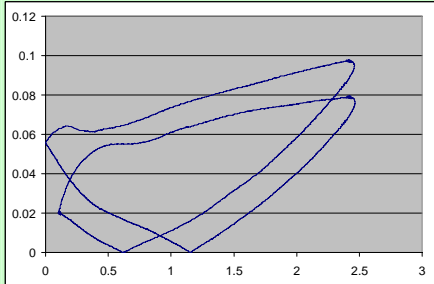
11\_flannel

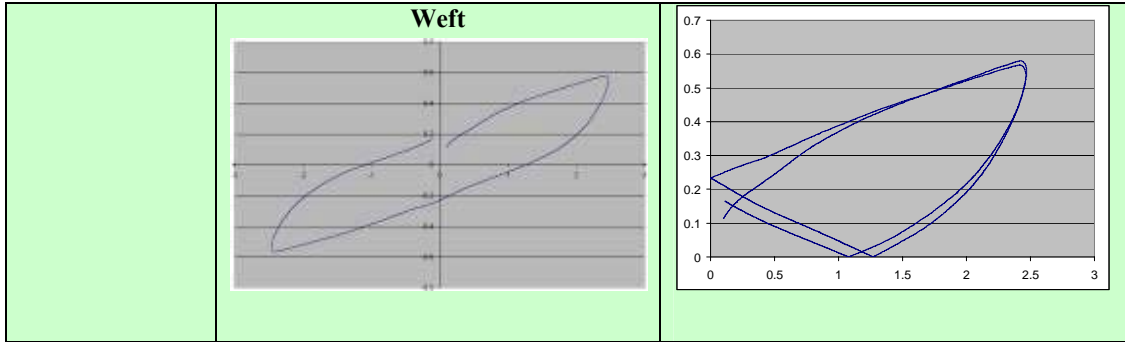




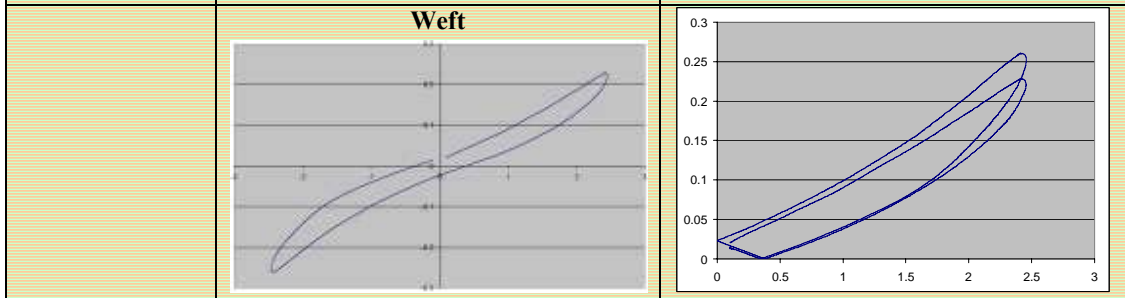
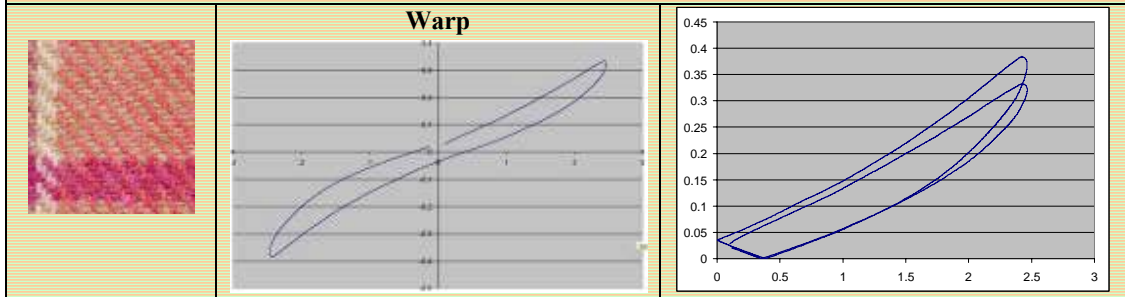




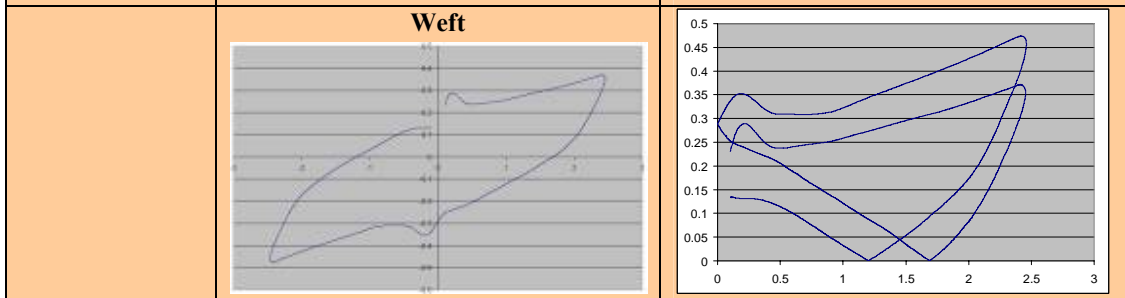
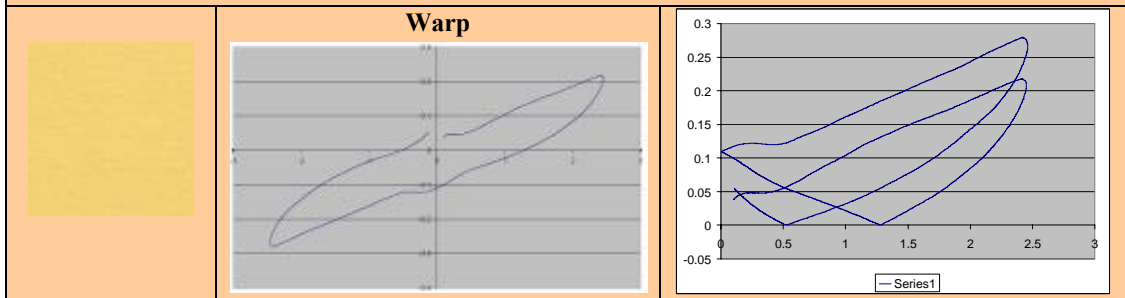
24_satin		
	<p><b>Warp</b></p> 	
	<p><b>Weft</b></p> 	
03_cord		
	<p><b>Warp</b></p> 	
	<p><b>Weft</b></p> 	
09_tussah-silk		
	<p><b>Warp</b></p> 	



13\_plaid



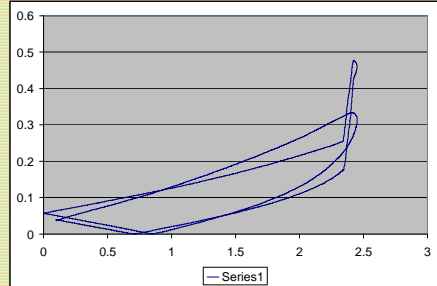
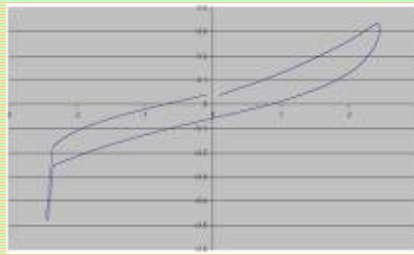
22\_taffeta



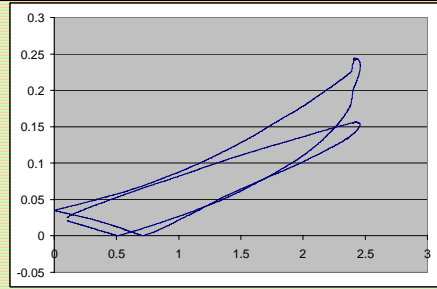
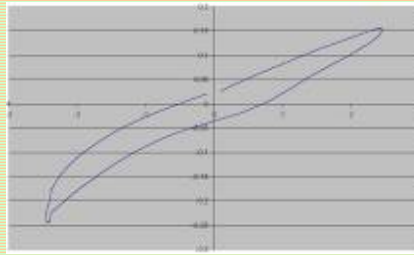
16\_lurex-knit



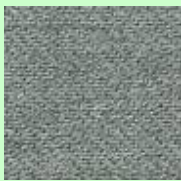
Warp



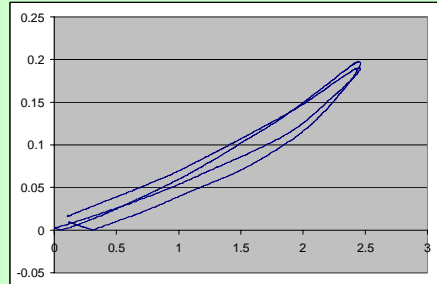
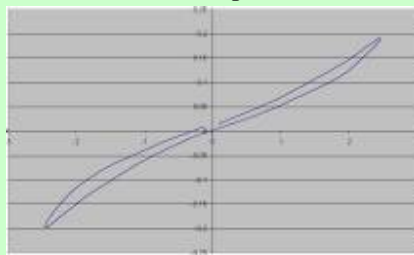
Weft



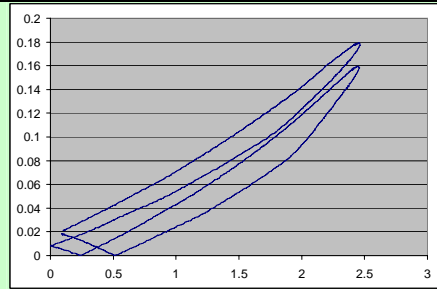
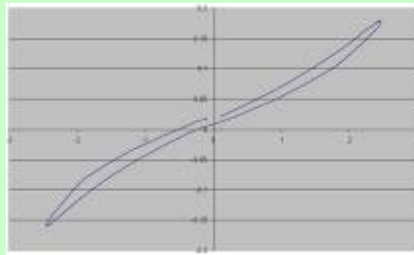
05\_gabardine



Warp



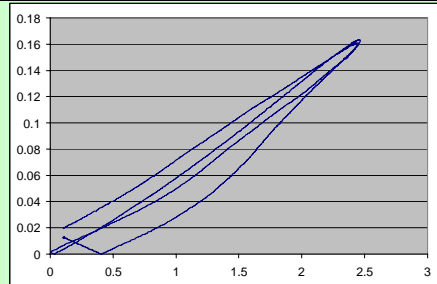
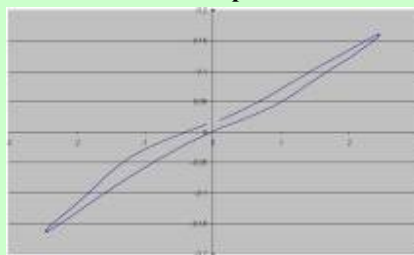
Weft

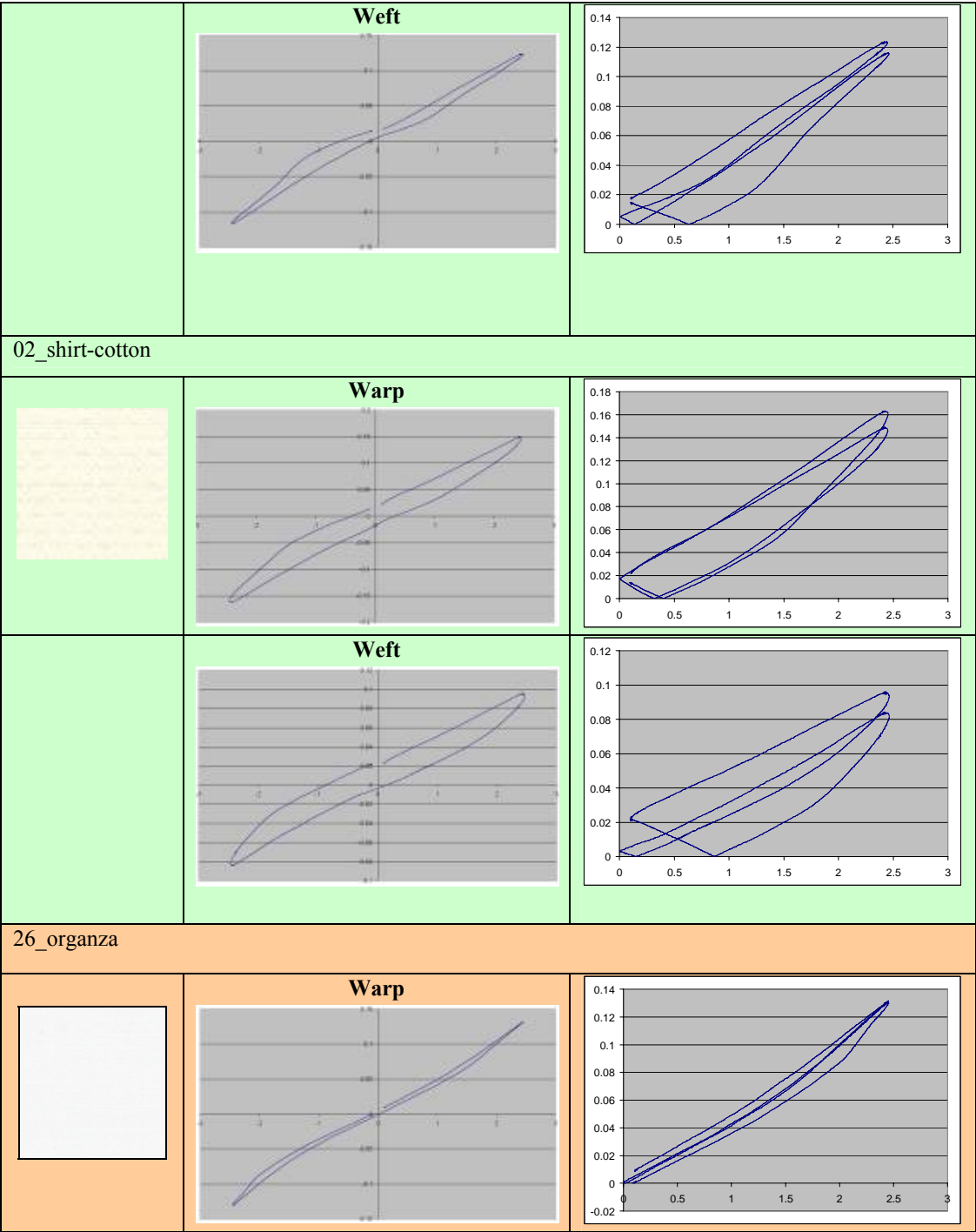


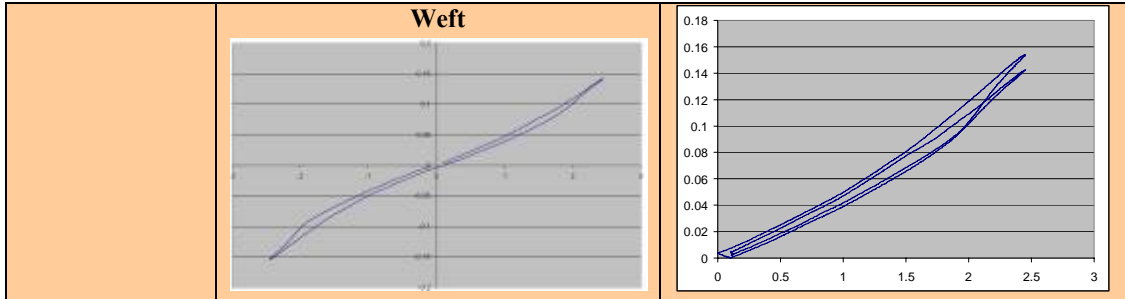
06\_wool-crepe



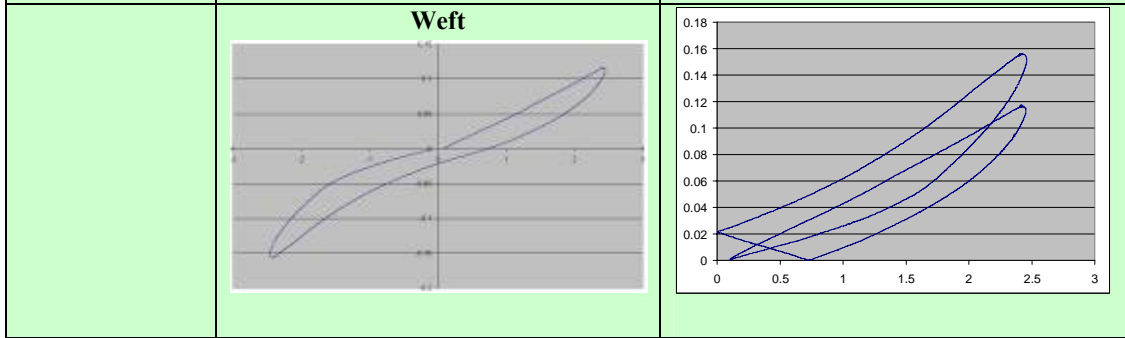
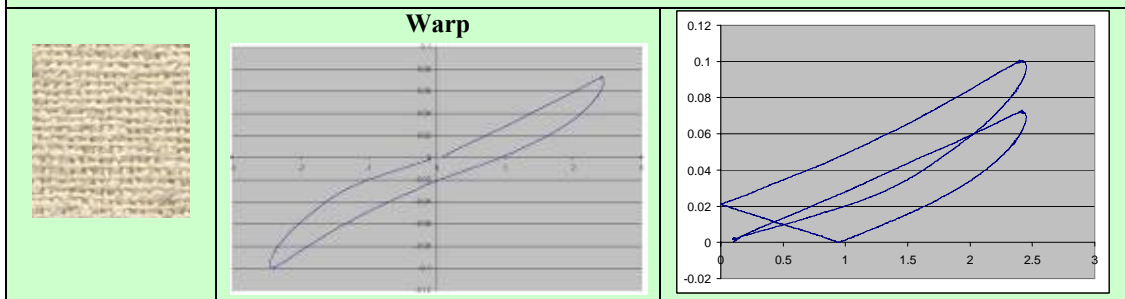
Warp



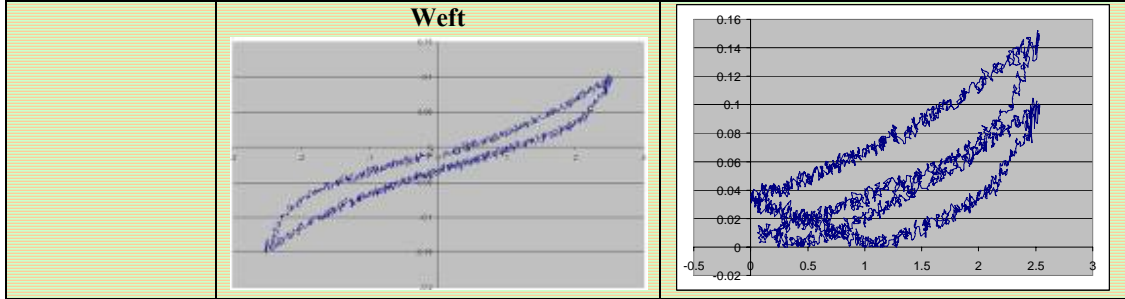
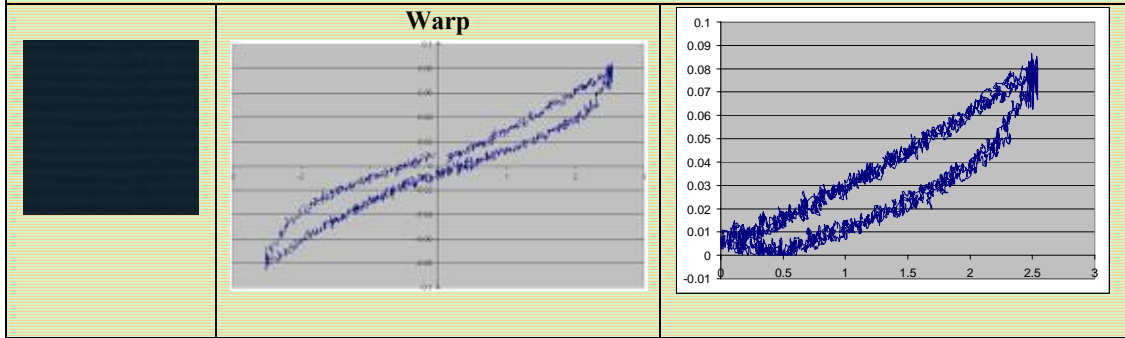


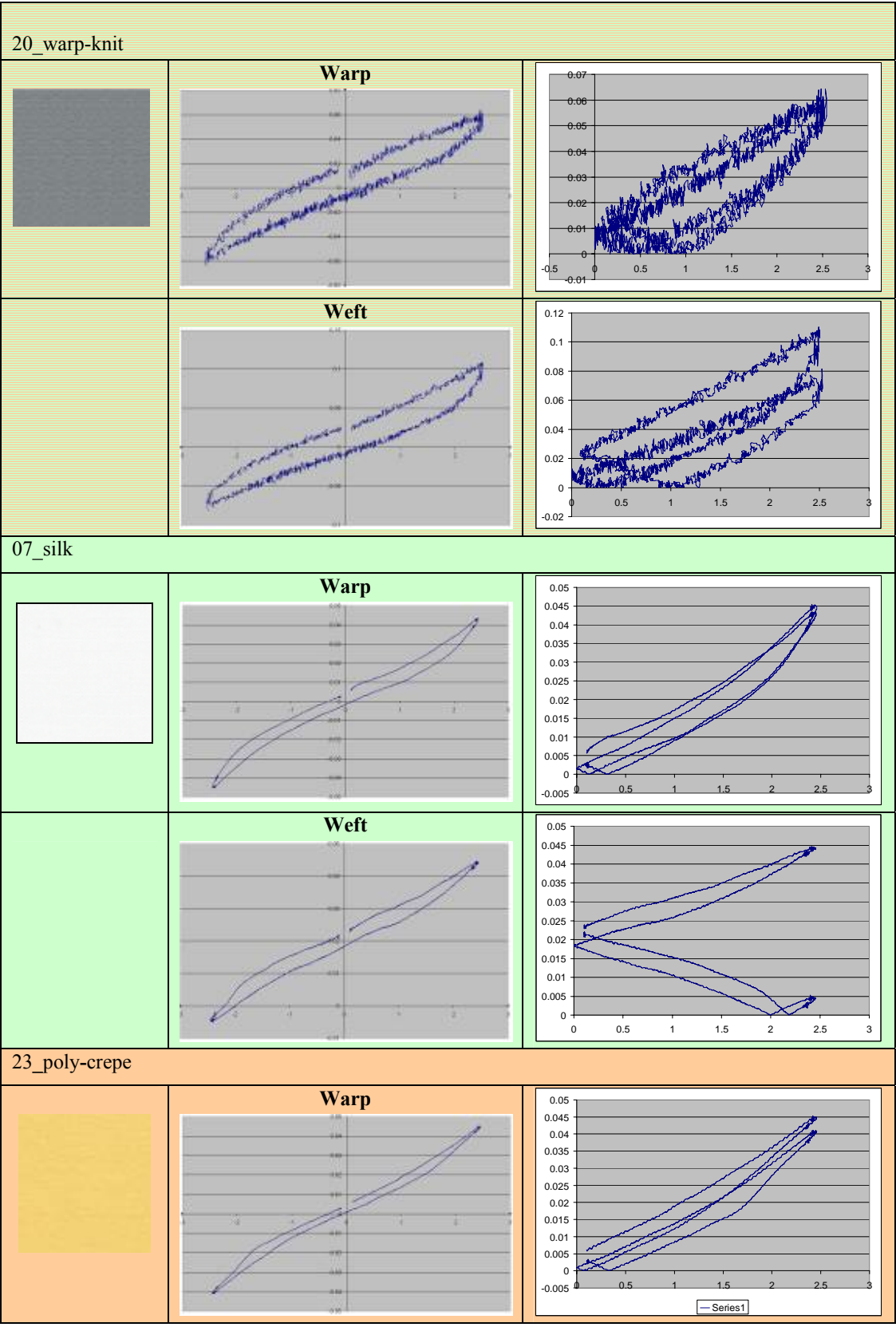


08\_bourette-silk

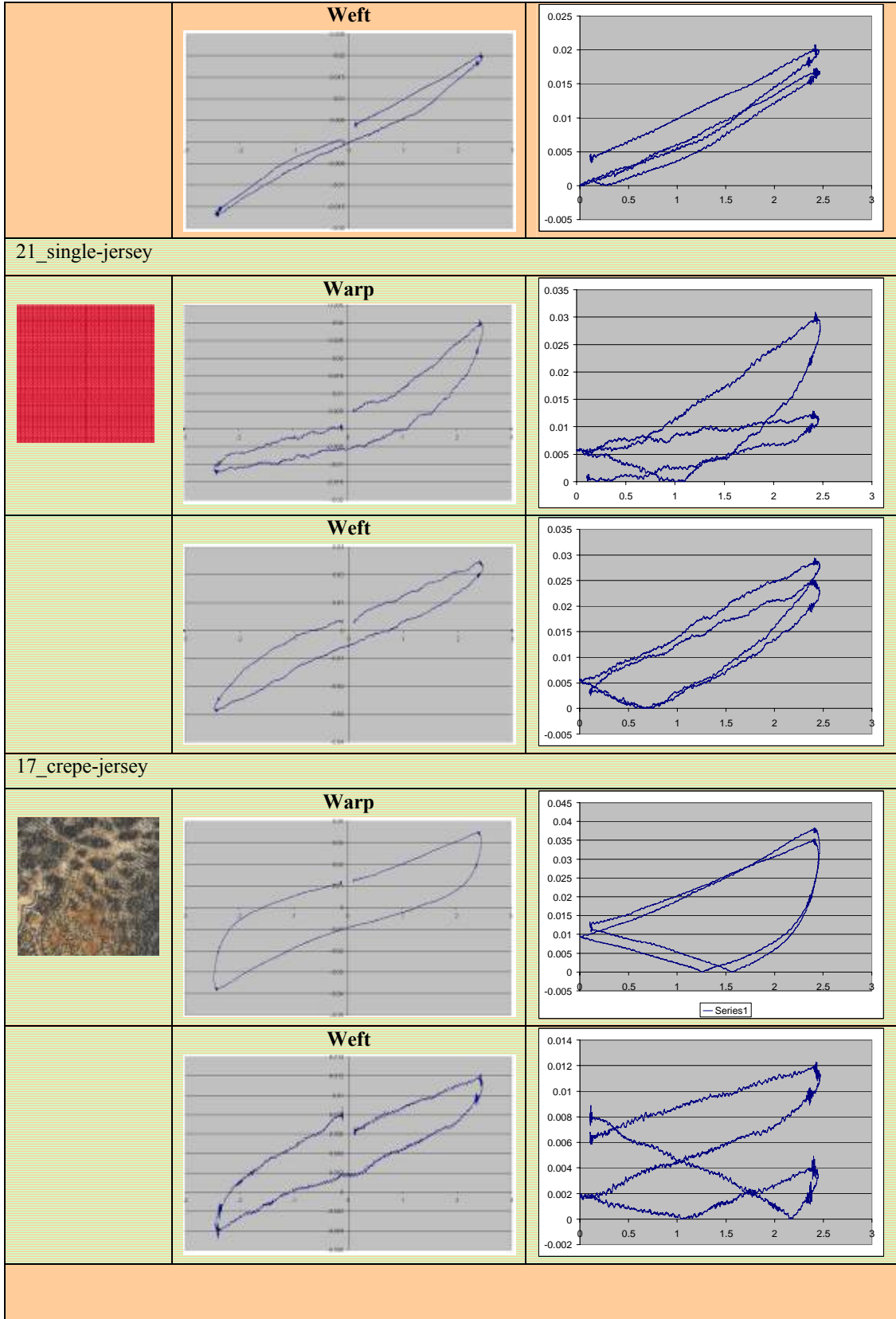


29\_woven-outdoor-leisure wear

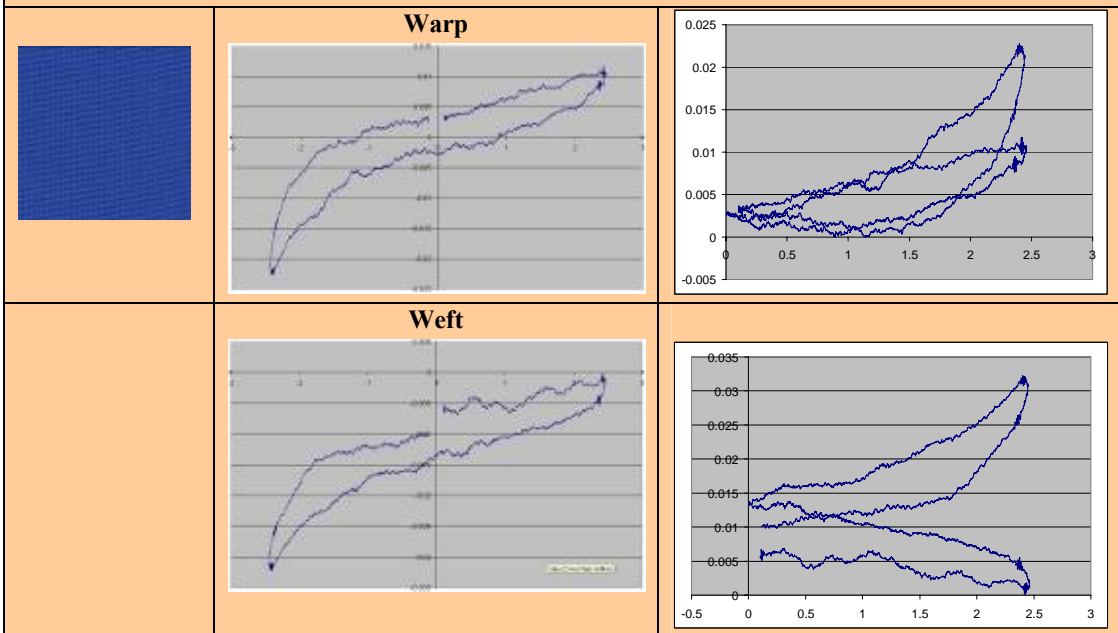




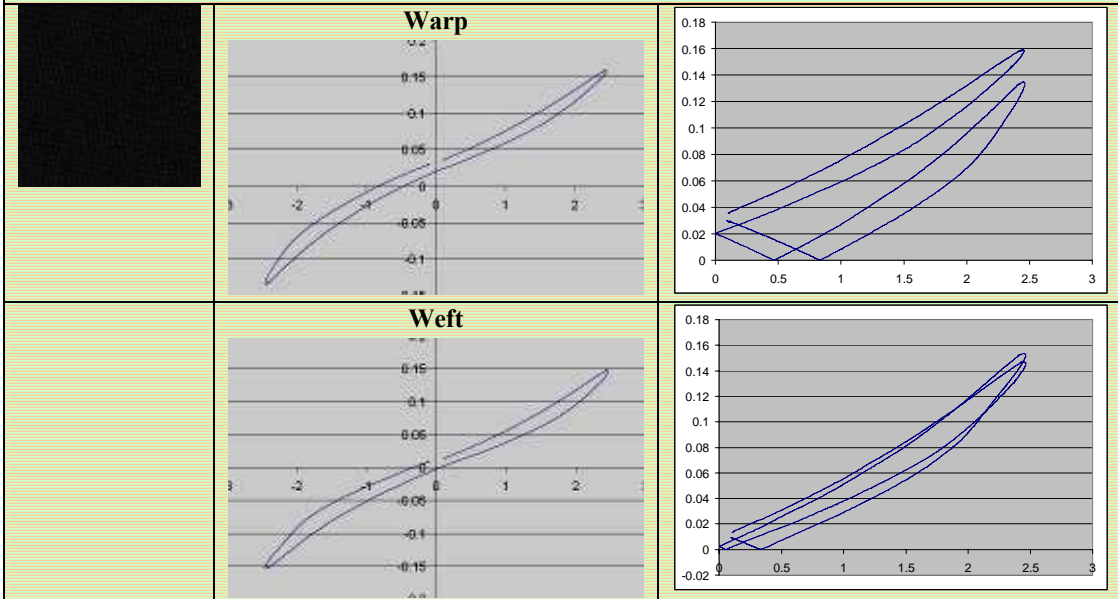




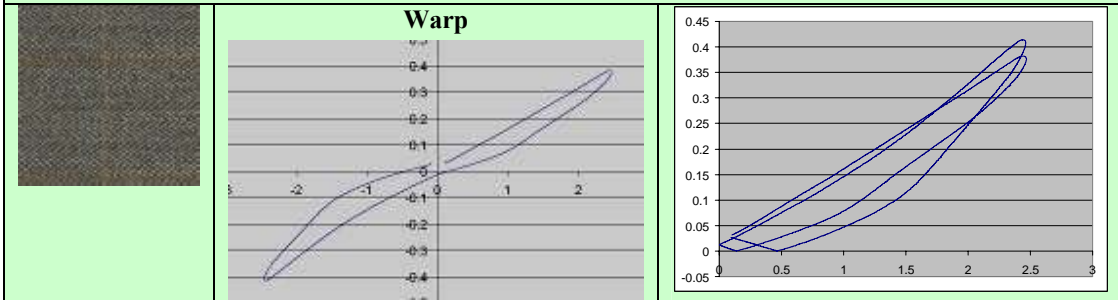
31\_warp-knit tricot satin

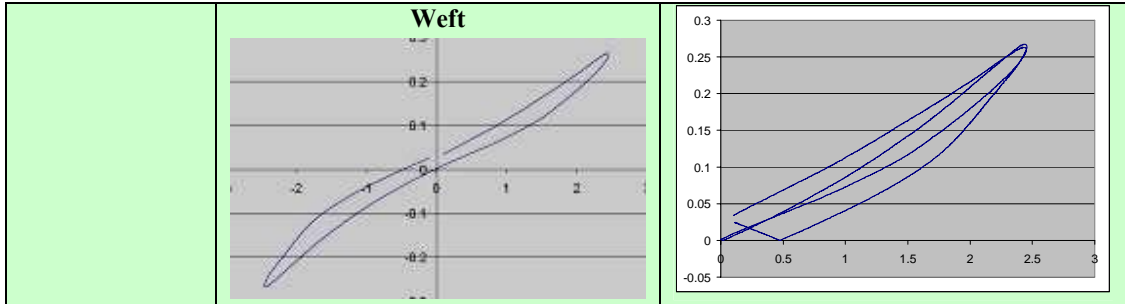


33\_Men's woven suit fabric

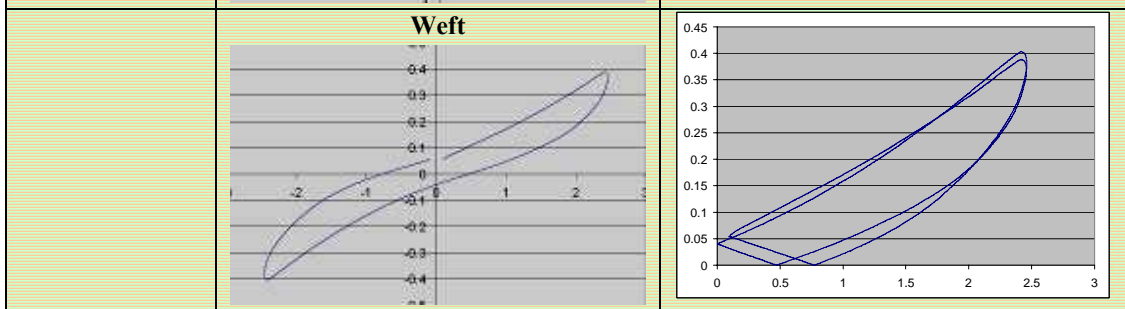
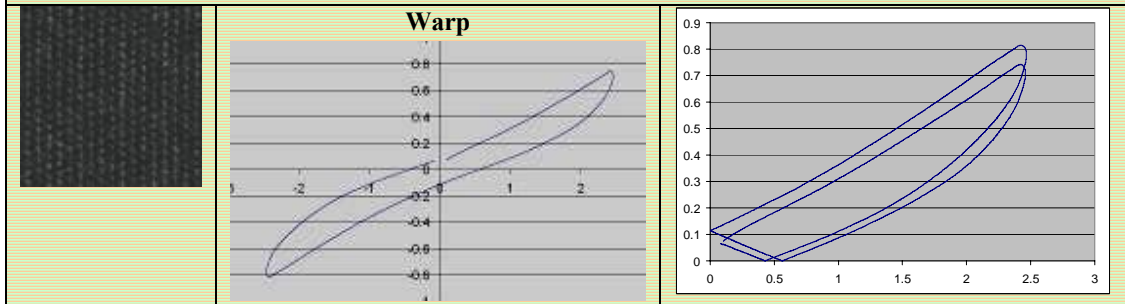


34\_Men's woven suit fabric

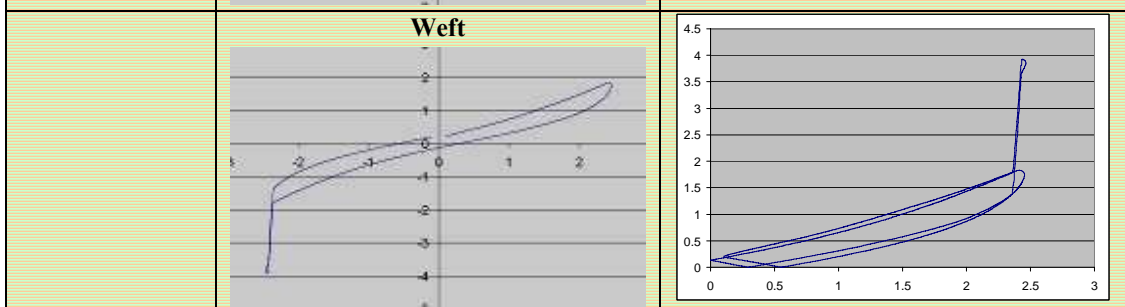
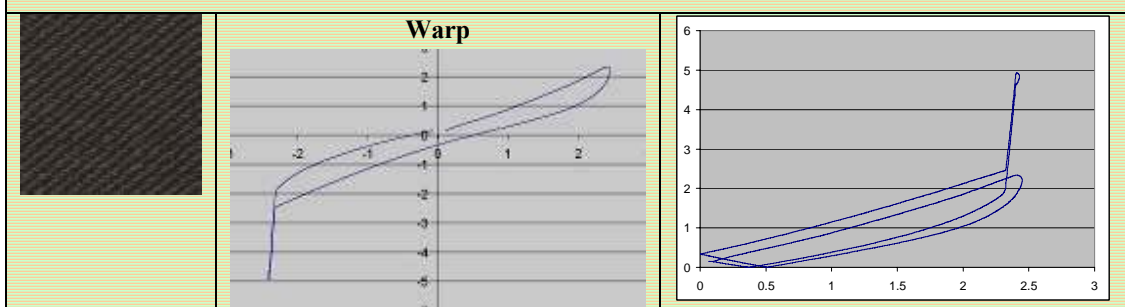




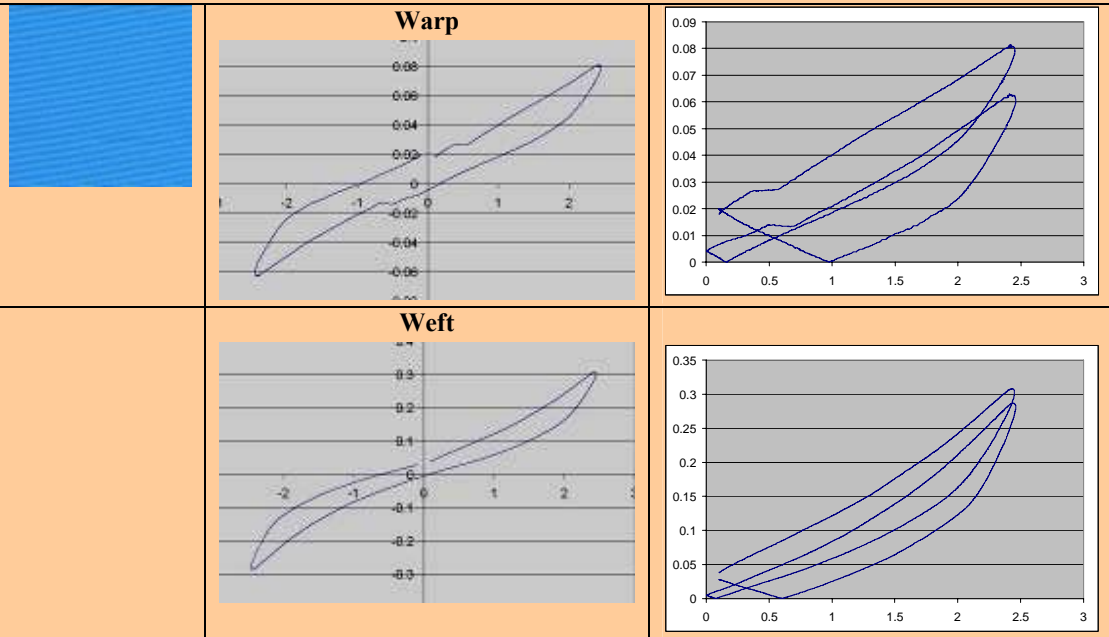
35\_Men's woven overcoat fabric



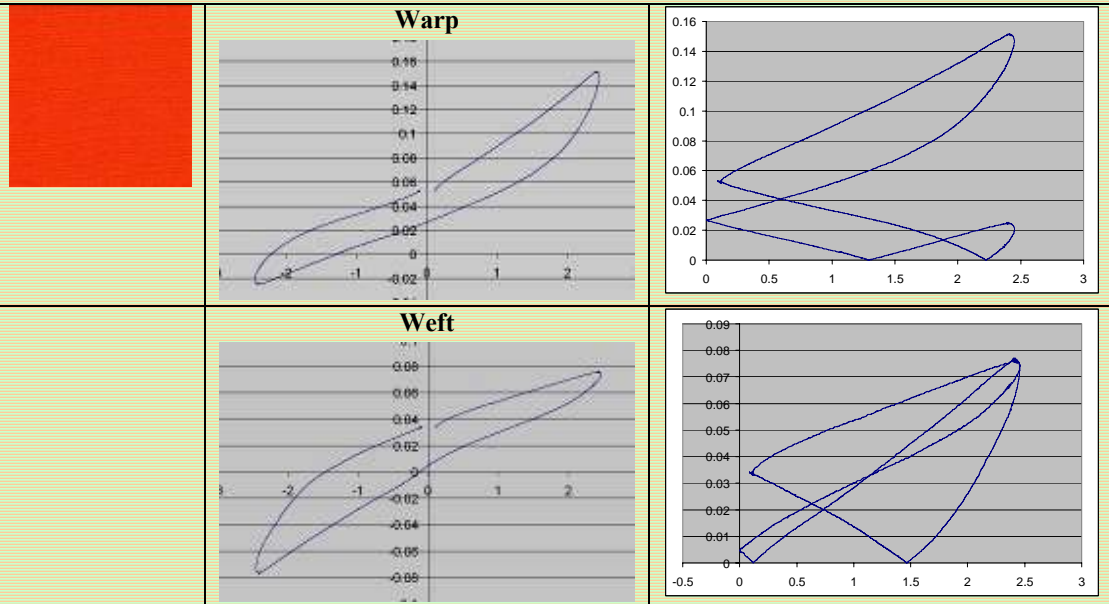
36\_Men's woven overcoat fabric



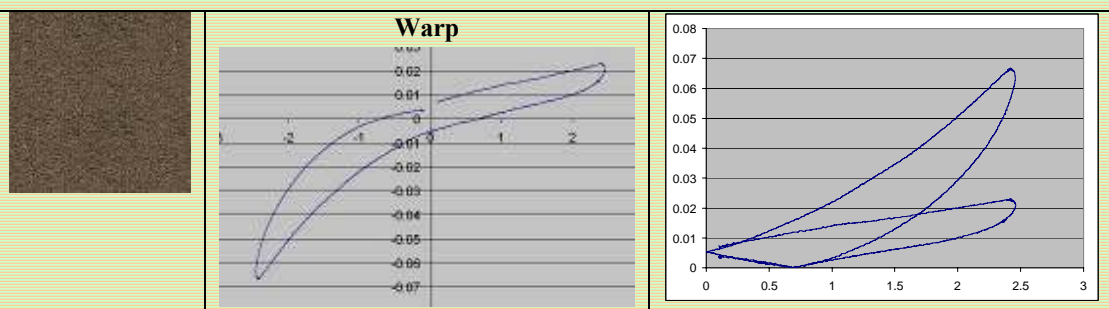
37\_ Woven outdoor leisurewear fabric

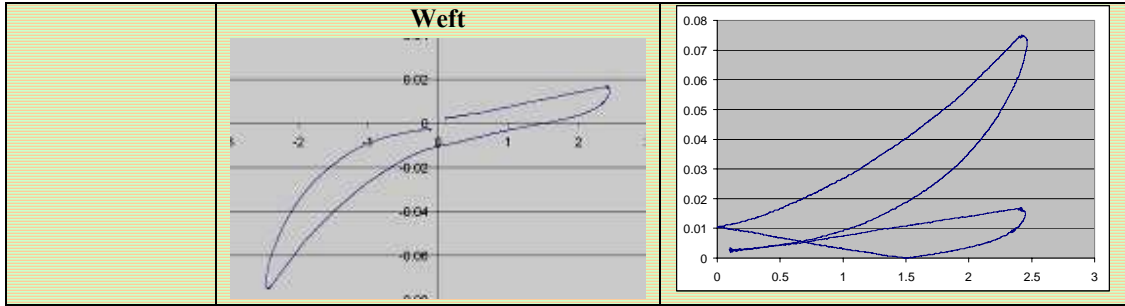


38\_ Weft knitted jersey fabric

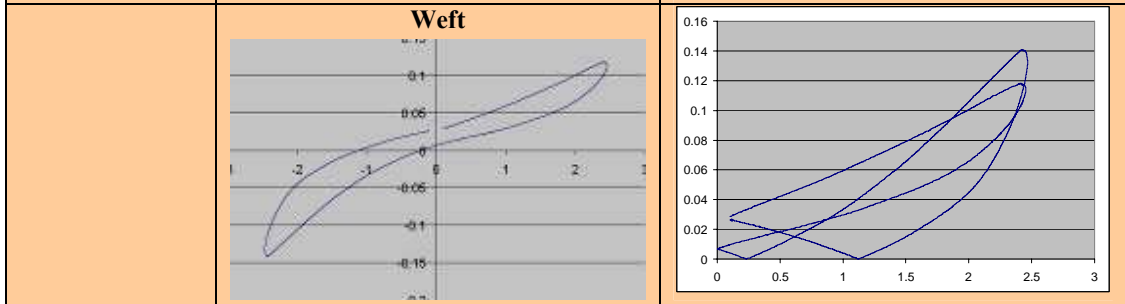
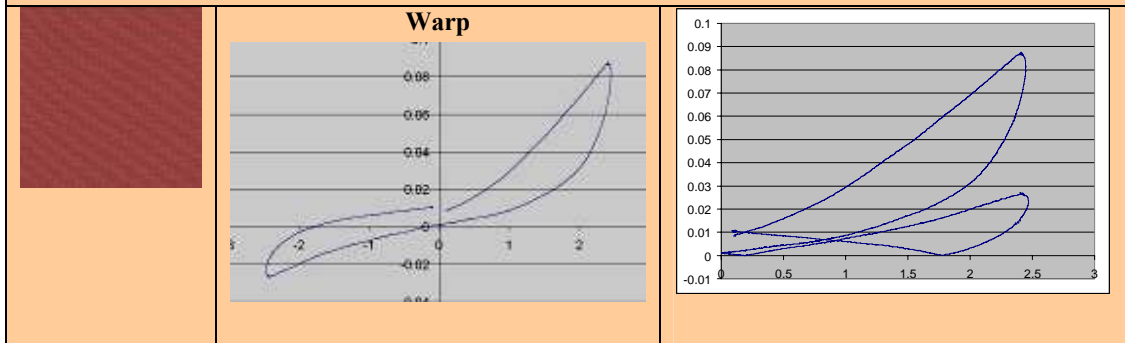


39\_ Weft knitted terry fabric

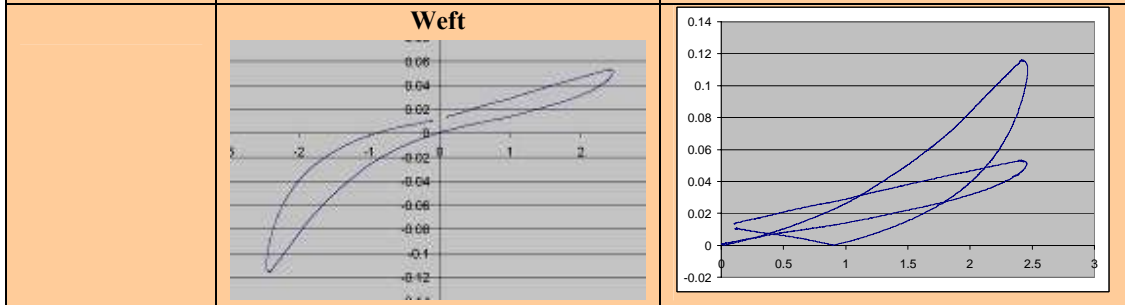
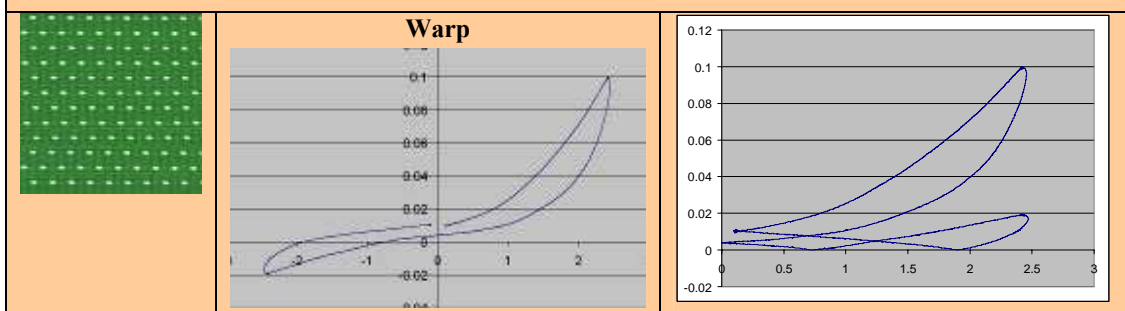


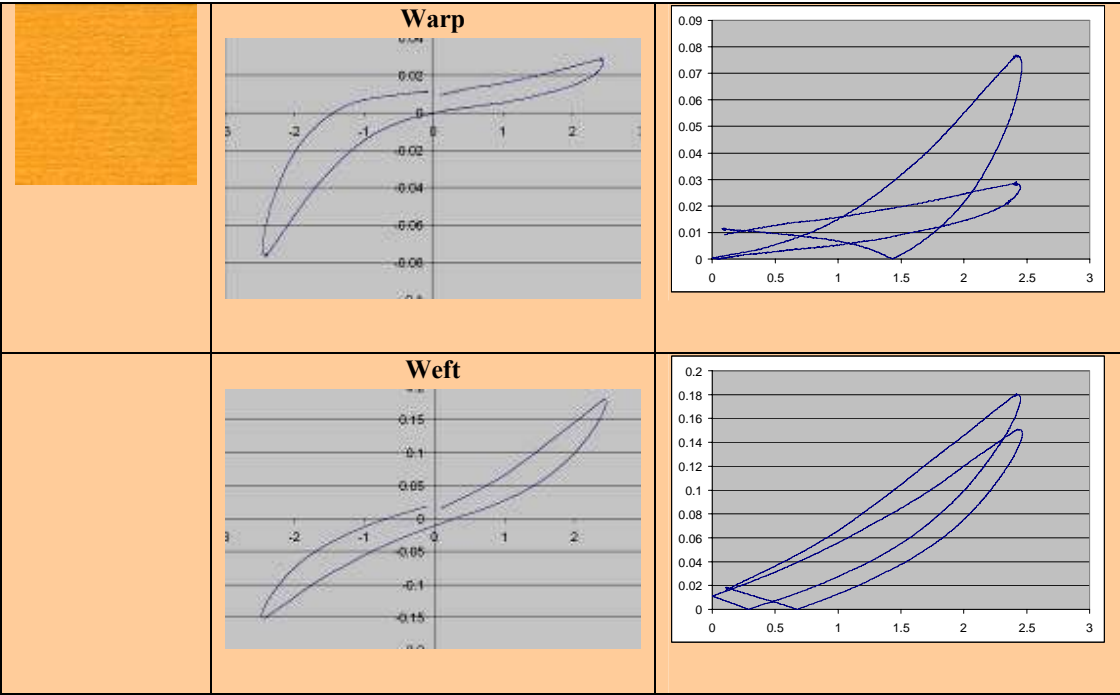


40\_Warp knitted jersey-based fabric



41\_Warp knitted mesh fabric





## Annex E: Alternative friction tests:

Experiment „fabric-fabric“:

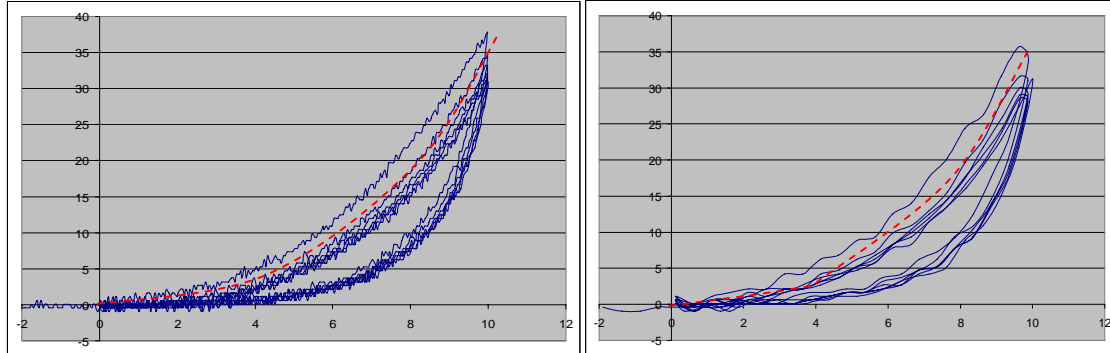
Fabric.	Fabric-fabric (outside):					Average	Warp-Weft 500g (degree °)			
	Test 1	Test 2	Test 3	Test 4	Warp-Warp 500g (degree °)		Test 1	Test 2	Test 3	Test 4
1	57	60	57	55	57.25	59	56	56	54	
2	53	49	47	47	49	47	45	44	46	
3	58	58	57	58	57.75	58	57	56	56	
4	57	53	53	53	54					
5	44	43	42	44	43.25	46	46	45	43	
6	46	not enough fabric			46					
7	15	17	16	17	16.25	21	20	17	18	
8	not enough fabric									
9	30	29	29	25	28.25	22	22	23	22	
10	50	41	40	39	42.5	39	37	37	37	
11	59	56	54	54	55.75					
12	62	59	58	54	58.25					
13	60	58	57	57	58					
14	56	54	52	52	53.5					
15	62	62	with stroke		62	65	65	against stroke		
16	not enough fabric									
17	37	37			37					
22	35	34			34.5					
23	22	23			22.5					
24	27	27	25	26	26.25					
25	56	53			54.5					
26	13	14			13.5					
27	55	53			54					
30	19	18			18.5					
32	20	18	16	16	17.5					

Experiment „fabric-skin“:

Fabric	Fabric-skin (inside):					-	Warp 500g (degree °)					-	Weft 100g (degree °)					-	Weft 500g (degree °)					-
	Test 1	Test 2	Test 3	Test 4	Warp 100g (degree °)		Test 1	Test 2	Test 3	Test 4	Test 1		Test 2	Test 3	Test 4	Test 1	Test 2		Test 3	Test 4	Test 1	Test 2	Test 3	
1	28	27	27	27	27.25	26	24	23	23	24	28	28	28	28	28	25	24	24	24	24.25				
2	21	21	23	23	22	23	23	22	23	22.75	22	23	22.5	22.5	22.5	24	23	23	23	23.25				
3	28	27	27	28	27.5	18	18	18	20	18.5	28	28	28	28	28	18	18	20	18	18.5				
4	24	26	26	25	25.25	22	22	22	22	22	26	26	26	26	26	23	22	22	22	22.25				
5	25	25	24	25	24.75	19	19	19	19	19	25	24	24	23	24	19	19	19	19	19				
6	23	23	22	23	22.75	20	19	20	19	19.5	24	23	22	23	23	21	21	20	20	20.5				
7	20	21	22	21	21	16	18	17	16	16.75	22	22	21	21	21.5	18	19	18	17	18				
8	23	23	22	23	22.75	23	22	21	22	22	25	27	25	27	26	22	23	23	20	22				
9	19	19	21	18	19.25	17	19	18	20	18.5	19	20	21	20	20	20	20	22	20	20.5				
10	25	22	22	23	23	21	22	22	21	21.5	25	23	22	22	23	21	21	20	20	20.5				
11	25	25	25	25	25	20	20	20	20	20	27	24	25	24	25	20	20	20	20	20				
12	25	24	24	23	24	22	21	22	21	21.5	25	24	24	23	24	22	20	22	21	21.25				
13	24	24	23	24	23.75	25	24	23	23	23.75	24	24	24	24	24	23	23	22	22	22.5				
14	22	21	22	21	21.5	25	25	25	25	25	26	25	25	25	25.25	27	27	27	27	27				
15	31	31	31	30	30.75	24	23	23	23	23.25	24	23	22	21	22.5	22	22	22	21	21.75				
16	23	23	23	23	23	21	21	21	22	21.25	24	22	23	22	22.75	21	19	19	19	19.5				
17	20	21	20	20	20.25	18	18	17	18	17.75	19	18	17	17	17.75	19	18	18	18	18.25				
22	23	23	23	24	23.25	24	24	25	24	24.25	23	23	23	22	22.75	20	21	22	24	21.75				
23	18	18	22	21	19.75	22	22	21	21	21.5	25	27	23	25	25	25	24	23	21	23.25				
24	17	17	16	18	17	21	21	20	21	20.75	22	24	22	20	22	17	17	17	17	17				
25	19	19	19	19	19	18	19	18	18	18.25	Uniform, no waeve, warp only													
26	17	17	15	14	15.75	15	17	17	16	16.25	18	17	17	17	17.25	17	19	18	19	18.25				
27	30	28	29	28	28.75	25	26	26	26	25.75	31	29	28	28	29	31	29	29	29	29.5				
30	19	19	18	18	18.5	19	20	21	20	20	20	22	21	20	20.75	23	23	23	23	23				
32	33	31	32	32	32	33	30	30	30	30.75	31	29	32	29	30.25	32	30	31	30	30.75				

## Annex F: Parameter derivation example fabric 11\_flannel

- Tensile



Cyclic strain-stress curve warp

Cyclic strain-stress curve weft

For the derivation of the non-linear tensile property, the strain-stress data is fitted with a polynomial spline. Parameters for weft and warp direction are derived (Figure 1/2). During the parameter derivation process, it is important that the units of the measured data are converted to match the units of the computation system:

**N, mm** → **N/m**

Resulting mathematical description for the tensile parameter sample 11\_flannel:

Weft	Warp
500 N/m	1500 N/m
Polynomial curve order 3/number 1: offset > 0.02 Polynom 42.000	Polynomial curve order 3/number 1: offset > 0.04 Polynom 67.000
Polynomial curve order 3/number 2: offset > 0.07 Polynom 130.000	Polynomial curve order 3/number 2: offset > 0.1 Polynom -60.000

- Shear

KES-f returns the shear rigidity  $G$  as characteristic value. However, the standard value  $G$  is different from the definition of shear modulus. If the shear strain is taken instead of the shear angle for defining  $G$ , the values is equal to shear modulus and can be taken as linear input parameter. [Kaw 80]



$$\text{Shear modulus} = (\text{shear force } F_s \text{ (gf/cm)}) / (\text{shear strain} = \tan\theta)$$

The relation between the two values of G defined by  $\tan \theta$  and by  $\theta$  degree is:

$$G(\tan \theta) = 57.3 G(\theta \text{ degree})$$

For the fabric 11\_flannel the mean value of G ( $\tan \theta$ ) weft and warp can be taken as linear description for static garment simulations.

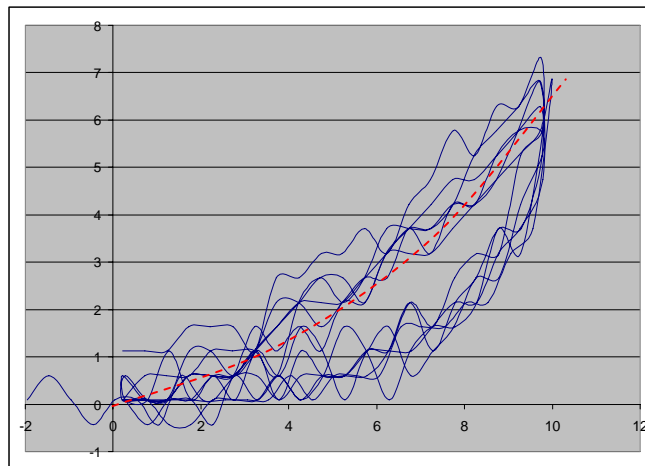
KES-f characteristic values for SHEAR								
Sample	G	G	G ( $\tan \theta$ )	G ( $\tan \theta$ )	2HG	2HG	2HG5	2HG5
11_flannel	warp	weft	warp	weft	warp	weft	warp	weft
	2.127	1.996	121.88	114.37	4.527	4.341	7.025	6.984

The nonlinear shear behavior, similar to the tensile parameter, is fitted with a polynomial spline. During the parameter derivation process, it is again important to convert the units to ones of the computation system:

N, mm

→

N/m



Shear strain-stress curves

Resulting mathematical description for the shear parameter sample 01\_denim:

KES-f Shear rigidity (linear)	LDSM shear parameter (nonlinear)
118.13 N/m (Mean value of weft and warp G ( $\tan \theta$ ))	240 N/m
	Polynomial curve order 3/number 1: offset > 0.01 Polynom 11.000

- Bending

In the computation system, the bending property is linear modeled. Thus, a simple mathematical interpretation for the bending behavior is sufficient. KES-f returns the bending rigidity as characteristic value. This measure is similar to the shear rigidity a description of the slope between two major points of the measured data; consequently it is suited to be directly taken as linear bending characteristic.

KES-f characteristic values for BENDING				
Sample 11_flannel	B warp	B weft	2HB warp	2HB weft
	0,288	0,190	0,257	0,176

During the parameter derivation process, the units need to be converted as following:

**Torque gf cm/cm, radian 1/cm (KES-f) → N.m (Simulation system)**

Conversion:

100 g = 1N, 1g = N/100 → values on y-axis / 100

1/cm \* 1/100 = 1/m → values on x-axis / 100,

→ Input parameter = B \* 10<sup>-4</sup>

Mathematical description of the tensile parameter (green line):

Weft	Warp
28.8 μ N.m	19 μ N.m

- Thickness

The characteristic fabric hand value T0 = 1.6mm is taken as thickness property.

KES-f characteristic values for COMPRESSION							
Sample 11_flannel	LC	WC	RC	T0	Tm		
	0,375	0,453	61.23	1,53	1,04		

- Friction

The characteristic value MIU, the mean value of the coefficient of friction, can be taken as input parameter. At this, the mean value of weft and warp direction is taken.

New friction measurements			
Sample 11_flannel	Fabric - fabric	Fabric - body	
	1.47	0.36	

KES-f fabric input parameter for sample 11\_flannel:

Elasticity N/m		
Weft	Warp	Shear
500 N/m	1500 N/m	240 N/m
Polynomial curve order 3/number 1: offset > 0.02 Polynom 42.000	Polynomial curve order 3/number 1: offset > 0.04 Polynom 67.000	Polynomial curve order 3/number 1: offset > 0.01 Polynom 11.000
Polynomial curve order 3/number 2: offset > 0.07 Polynom 130.000	Polynomial curve order 3/number 2: offset > 0.1 Polynom -60.000	

Bending N.m 10 <sup>-6</sup>		Thickness (mm)	Weight (g)	Friction coefficient	
Weft	Warp				
28.8	19	1.53	290	1.47 (f-f)	0.36 (f-b)

## Annex G: Linear derived fabric input parameters

01_Denim, 100% CO, twill, 380g/m <sup>2</sup> , 1.60 mm					
Elasticity N/m			Bending N.m 10 <sup>-6</sup>		Friction coefficient
Weft	Warp	Shear	Weft	Warp	0.44 (f-b)
3000 N/m	1800 N/m	102 N/m	17.1	39.5	1.55 (f-f)

02_Shirt cotton, 100% CO, combined twill, 120 g/m <sup>2</sup> , 0.61 mm					
Elasticity N/m			Bending N.m 10 <sup>-6</sup>		Friction coefficient
Weft	Warp	Shear	Weft	Warp	0.41 (f-b)
3000 N/m	2000 N/m	20 N/m	3.3	5.7	1.15 (f-f)

03_Cord, 100% CO, velveteen, 330 g/m <sup>2</sup> , 1.76 mm					
Elasticity N/m			Bending N.m 10 <sup>-6</sup>		Friction coefficient
Weft	Warp	Shear	Weft	Warp	0.33 (f-b)
2000 N/m	3000 N/m	82 N/m	12.5	18	1.58 (f-f)

04_Linen, 100% LI, plain weave, 250 g/m <sup>2</sup> , 1.09 mm					
Elasticity N/m			Bending N.m 10 <sup>-6</sup>		Friction coefficient
Weft	Warp	Shear	Weft	Warp	0.40 (f-b)
2000 N/m	3000 N/m	21 N/m	18.1	27.9	1.37 (f-f)

05_Gabardine, 100% WO, twill, 175 g/m <sup>2</sup> , 0.55 mm					
Elasticity N/m			Bending N.m 10 <sup>-6</sup>		Friction coefficient
Weft	Warp	Shear	Weft	Warp	0.34 (f-b)
2500 N/m	3000 N/m	32 N/m	6.3	7.3	0.95 (f-f)

06_Wool-crepe, 100% WO, plain weave, 145 g/m <sup>2</sup> , 0.93 mm					
Elasticity N/m			Bending N.m 10 <sup>-6</sup>		Friction coefficient
Weft	Warp	Shear	Weft	Warp	0.35 (f-b)
600 N/m	1300 N/m	14.3 N/m	4.9	6.5	1.06 (f-f)

07_Mulberry-silk, 100% SE, plain weave, 15 g/m <sup>2</sup> , 0.10 mm					
Elasticity N/m			Bending N.m 10 <sup>-6</sup>		Friction coefficient
Weft	Warp	Shear	Weft	Warp	0.30 (f-b)
4500 N/m	6000 N/m	10 N/m	0.7	1.4	0.29 (f-f)

08_Bourette-silk, 100% SE, plain weave, 150 g/m <sup>2</sup> , 0.80 mm					
Elasticity N/m			Bending N.m 10 <sup>-6</sup>		Friction coefficient
Weft	Warp	Shear	Weft	Warp	0.40 (f-b)
1500 N/m	1500 N/m	38 N/m	4	4	

09_Tussah-silk100% SE plain weave 80 g/m <sup>2</sup> 0.44					
Elasticity N/m			Bending N.m 10 <sup>-6</sup>		Friction coefficient
Weft	Warp	Shear	Weft	Warp	0.33 (f-b)
10000 N/m	4500 N/m	80 N/m	1.83	1.5	0.54 (f-f)

10_Jute, 100% JU, plain weave, 300 g/m <sup>2</sup> , 1.44 mm					
Elasticity N/m			Bending N.m 10 <sup>-6</sup>		Friction coefficient
Weft	Warp	Shear	Weft	Warp	0.39 (f-b)
12000 N/m	13000 N/m	135 N/m	647	272	0.91 (f-f)

11_Flannel, 80% WO, 20% PES, twill, 290 g/m <sup>2</sup> , 1.53 mm					
Elasticity N/m			Bending N.m 10 <sup>-6</sup>		Friction coefficient
Weft	Warp	Shear	Weft	Warp	0.36 (f-b)
800 N/m	1400 N/m	118 N/m	19	28.8	1.47 (f-f)

12_Denim, 62% PES, 35% CO, 3% EL twill , 275 g/m <sup>2</sup> , 1.13 mm					
Elasticity N/m			Bending N.m 10 <sup>-6</sup>		Friction coefficient
Weft	Warp	Shear	Weft	Warp	0.39 (f-b)
400 N/m	4000 N/m	71 N/m	10.7	25.5	1.62 (f-f)

13_Plaid, 35% PES, 35% AF, 30% WO, twill, 270 g/m <sup>2</sup> , 1.14 mm					
Elasticity N/m			Bending N.m 10 <sup>-6</sup>		Friction coefficient
Weft	Warp	Shear	Weft	Warp	0.44 (f-b)
800 N/m	1500 N/m	35 N/m	8.9	12.8	1.60 (f-f)

14_Tweed, 66% AF, 14% WO, 10% PES, 10% CMD, combined twill, 270 g/m <sup>2</sup> , 3.90 mm					
Elasticity N/m			Bending N.m 10 <sup>-6</sup>		Friction coefficient
Weft	Warp	Shear	Weft	Warp	0.46 (f-b)
300 N/m	1000 N/m	22 N/m	Too thick for KES-F	Too thick for KES-F	1.35 (f-f)

15_Velvet, 92% CO, 8% CMD, velvet, 300 g/m <sup>2</sup> , 1.88 mm					
Elasticity N/m			Bending N.m 10 <sup>-6</sup>		Friction coefficient
Weft	Warp	Shear	Weft	Warp	0.43 (f-b)
1000 N/m	2000 N/m	58 N/m	11.2	22.5	1.88 (f-f)

16_Lurex-knit, 70% PES, 30% PA, held stitch knit, 215 g/m <sup>2</sup> , 2.94 mm					
Elasticity N/m			Bending N.m 10 <sup>-6</sup>		Friction coefficient
Weft	Warp	Shear	Weft	Warp	0.38 (f-b)
40 N/m	180 N/m	19 N/m	6.1	8.1	

17_Crepe-jersey, 85% PES, 15% EL, rib knit, 135 g/m <sup>2</sup> , 0.73 mm					
Elasticity N/m			Bending N.m 10 <sup>-6</sup>		Friction coefficient
Weft	Warp	Shear	Weft	Warp	0.32 (f-b)
6 N/m	240 N/m	20.8 N/m	0.2	1.2	0.75 (f-f)

18_Motorcycle wear fabric, 72% PA, 28% PU, plain weave, 90 g/m <sup>2</sup> , 0.39 mm					
Elasticity N/m			Bending N.m 10 <sup>-6</sup>		Friction coefficient
Weft	Warp	Shear	Weft	Warp	
1000 N/m	2000 N/m	1588.9 N/m	122.2	119.7	

19_Woven-easy-care, 65% PES, 35% CO, twill, 180 g/m <sup>2</sup> , 0.57 mm					
Elasticity N/m			Bending N.m 10 <sup>-6</sup>		Friction coefficient
Weft	Warp	Shear	Weft	Warp	
1300 N/m	4000 N/m	115 N/m	9	21.9	

20_Warp-knitted-velour, 90% PA, 10% EL, warp knit velour, 235 g/m <sup>2</sup> , 1.56 mm					
Elasticity N/m			Bending N.m 10 <sup>-6</sup>		Friction coefficient
Weft	Warp	Shear	Weft	Warp	
70 N/m	80 N/m	43 N/m	2.9	2.1	

21_Single-jersey, 98% CLY, 2% EL, single jersey, 172 g/m <sup>2</sup> , 1.21 mm					
Elasticity N/m			Bending N.m 10 <sup>-6</sup>		Friction coefficient
Weft	Warp	Shear	Weft	Warp	
50 N/m	120 N/m	23 N/m	1	0.7	

22_ Taffeta, 100% CA, plain weave, 125 g/m <sup>2</sup> , 0.33 mm					
Elasticity N/m			Bending N.m 10 <sup>-6</sup>		Friction coefficient
Weft	Warp	Shear	Weft	0.69	0.45 (f-b)
10000 N/m	4000 N/m	136 N/m	5.9	8.5	0.68 (f-f)

23_ Ployester-crepe, 100% PES plain weave, 85 g/m <sup>2</sup> , 0.25 mm					
Elasticity N/m			Bending N.m 10 <sup>-6</sup>		Friction coefficient
Weft	Warp	Shear	Weft	Warp	0.39 (f-b)
1000 N/m	600 N/m	11 N/m	0.7	1.6	0.41 (f-f)

24_ Satin, 100% PES, sateen, 125 g/m <sup>2</sup> , 0.30 mm					
Elasticity N/m			Bending N.m 10 <sup>-6</sup>		Friction coefficient
Weft	Warp	Shear	Weft	Warp	0.38 (f-b)
10000 N/m	4000 N/m	26.7 N/m	21.5	13.4	0.49 (f-f)

25_ Felt, 100% PES, Non woven, 155 g/m <sup>2</sup> , 1.25 mm					
Elasticity N/m			Bending N.m 10 <sup>-6</sup>		Friction coefficient
Weft	Warp	Shear	Weft	Warp	0.33 (f-b)
1000 N/m	860 N/m	189.9 N/m	36.3	15.9	1.40 (f-f)

26_ Organze, 100% PES, plain weave, 25 g/m <sup>2</sup> , 0.16 mm					
Elasticity N/m			Bending N.m 10 <sup>-6</sup>		Friction coefficient
Weft	Warp	Shear	Weft	Warp	0.29 (f-b)
4000 N/m	3600 N/m	10.3 N/m	5.5	4.8	0.24 (f-f)

27_ Fleece, 100% PES, weft terry knit, 250 g/m <sup>2</sup> , 3.99 mm					
Elasticity N/m			Bending N.m 10 <sup>-6</sup>		Friction coefficient
Weft	Warp	Shear	Weft	Warp	0.48 (f-b)
130 N/m	500 N/m	54.2 N/m	Too thick for KES-F	Too thick for KES-F	1.38 (f-f)

28_ Woven-Upholstery, 100% PES, woven Jacquard, 600 g/m <sup>2</sup> , 2.38 mm					
Elasticity N/m			Bending N.m 10 <sup>-6</sup>		Friction coefficient
Weft	Warp	Shear	Weft	Warp	
3000 N/m	1000 N/m	169.4 N/m	69.9	64.3	

29_ Woven outdoor leisure wear fabric, 100% PES, plain weave, 90 g/m <sup>2</sup> , 0.20 mm					
Elasticity N/m			Bending N.m 10 <sup>-6</sup>		Friction coefficient
Weft	Warp	Shear	Weft	Warp	
5000 N/m	4000 N/m	133 N/m	4.6	2.7	

30_ Tulle, 100% PA, warp knitted tulle, 10 g/m <sup>2</sup> , 0.30 mm					
Elasticity N/m			Bending N.m 10 <sup>-6</sup>		Friction coefficient
Weft	Warp	Shear	Weft	Warp	0.36 (f-b)
35 N/m	3000 N/m	219.5 N/m	1.9	27.6	0.33 (f-f)

31_ Warp knitted tricot-satin, 100% PA , warp knitted tricot-satin, 100 g/m <sup>2</sup> , 0.40 mm					
Elasticity N/m			Bending N.m 10 <sup>-6</sup>		Friction coefficient
Weft	Warp	Shear	Weft	Warp	
700 N/m	450 N/m	63 N/m	0.3	0.4	

32_ Leather, 100% Leather, 815 g/m <sup>2</sup> , 1,68 mm					
Elasticity N/m			Bending N.m 10 <sup>-6</sup>		Friction coefficient
Weft	Warp	Shear	Weft	Warp	0.59 (f-b)
2400 N/m	3000 N/m	1792.9 N/m	215.4	396.4	0.32 (f-f)

33_ Men's woven suit fabric, 60% WO, 38% PES, 3% EL, plain weave, 195 g/m <sup>2</sup> , 0,57 mm					
Elasticity N/m			Bending N.m 10 <sup>-6</sup>		Friction coefficient
Weft	Warp	Shear	Weft	Warp	0.47 (f-b)
2000 N/m	400 N/m	42.5 N/m	5.4	5.4	1.35 (f-f)

34_ Men's woven suit fabric, 100% WO, herringbone, 232 g/m <sup>2</sup> , 0,82 mm					
Elasticity N/m			Bending N.m 10 <sup>-6</sup>		Friction coefficient
Weft	Warp	Shear	Weft	Warp	0.42 (f-b)
400 N/m	2000 N/m	32.9 N/m	9.6	14.3	1.47 (f-f)

35_ Men's woven overcoat fabric, 80% WO, 20% PA, Plain weave, 324 g/m <sup>2</sup> , 2,64 mm					
Elasticity N/m			Bending N.m 10 <sup>-6</sup>		Friction coefficient
Weft	Warp	Shear	Weft	Warp	0.41 (f-b)
400 N/m	1200 N/m	36.7 N/m	12.9	26.8	1.57 (f-f)



36_ Men's woven overcoat fabric, 59% CO, 25% PAN, 11% WO, 5% PES, twill, 460 g/m <sup>2</sup>					
Elasticity N/m			Bending N.m 10 <sup>-6</sup>		Friction coefficient
Weft	Warp	Shear	Weft	Warp	0.46 (f-b)
300 N/m	600 N/m	30 N/m	62.2	84.3	1.62 (f-f)

37_ Woven outdoor leisurewear fabric, 100% PES, Plain weave, 98 g/m <sup>2</sup>					
Elasticity N/m			Bending N.m 10 <sup>-6</sup>		Friction coefficient
Weft	Warp	Shear	Weft	Warp	0.44 (f-b)
1000 N/m	400 N/m	132.7 N/m	10.5	2.6	0.55 (f-f)

38_ Weft knitted jersey fabric, 48% CO, 48% CMD, 4% EL, Weft knitted, 208 g/m <sup>2</sup>					
Elasticity N/m			Bending N.m 10 <sup>-6</sup>		Friction coefficient
Weft	Warp	Shear	Weft	Warp	0.34 (f-b)
50 N/m	150 N/m	51.7 N/m	2.5	2.8	0.94 (f-f)

39_ Weft knitted terry fabric, 55% CV, 45% PES, Weft knitted, 288 g/m <sup>2</sup>					
Elasticity N/m			Bending N.m 10 <sup>-6</sup>		Friction coefficient
Weft	Warp	Shear	Weft	Warp	0.42 (f-b)
70 N/m	80 N/m	27.13 N/m	1.4	1.5	1.62 (f-f)

40_ Warp knitted jersey-based fabric, 100% PES, Warp knitted, 154 g/m <sup>2</sup>					
Elasticity N/m			Bending N.m 10 <sup>-6</sup>		Friction coefficient
Weft	Warp	Shear	Weft	Warp	0.37 (f-b)
600 N/m	500 N/m	104.5 N/m	4.9	2.2	1.23 (f-f)

41_ Warp knitted mesh fabric, 100% PES, Warp knitted, 128 g/m <sup>2</sup>					
Elasticity N/m			Bending N.m 10 <sup>-6</sup>		Friction coefficient
Weft	Warp	Shear	Weft	Warp	0.32 (f-b)
500 N/m	320 N/m	146.3 N/m	2.7	2	0.82 (f-f)

42_ Brushed knitted fabric, 100% PES, Brushed knitted fabric, 215 g/m <sup>2</sup>					
Elasticity N/m			Bending N.m 10 <sup>-6</sup>		Friction coefficient
Weft	Warp	Shear	Weft	Warp	0.35 (f-b)
2000 N/m	500 N/m	129.8 N/m	6.1	1.7	1.42 (f-f)

Nonlinear descriptions: Polynomial splines suited for the applied simulation system:

Tensile	Weft	Warp	Shear
01_Denim	$1.5 * 10^3$ $20 * 10^{-3} / 95 * 10^3$ $54 * 10^{-3} / 290 * 10^3$	$0.9 * 10^3$ $30 * 10^{-3} / 18 * 10^3$ $90 * 10^{-3} / 22 * 10^3$ $130 * 10^{-3} / 52 * 10^3$	$0.09 * 10^3$ $50 * 10^{-3} / 600$
02_Shirt cotton	$1.5 * 10^3$ $10 * 10^{-3} / 45 * 10^3$ $45 * 10^{-3} / 340 * 10^3$	$0.4 * 10^3$ $10 * 10^{-3} / 70 * 10^3$ $40 * 10^{-3} / 340 * 10^3$	$0.016 * 10^3$ $0 / 40$
03_Cord	<b>600</b> $20 * 10^{-3} / 60 * 10^3$ $60 * 10^{-3} / 400 * 10^3$ $80 * 10^{-3} / 3.6 * 10^6$	<b>200</b> $5 * 10^{-3} / 150 * 10^3$ $35 * 10^{-3} / 700 * 10^3$	<b>80</b> $50 * 10^{-3} / 400$
04_Linen	$1 * 10^3$ $40 * 10^{-3} / 50 * 10^3$ $80 * 10^{-3} / 230 * 10^3$	$1 * 10^3$ $10 * 10^{-3} / 140 * 10^3$ $30 * 10^{-3} / 1 * 10^6$	$0.008 * 10^3$ $20 * 10^{-3} / 300$
05_Gabardine	$0.2 * 10^3$ $8 * 10^{-3} / 95 * 10^3$ $50 * 10^{-3} / 138 * 10^3$	$1 * 10^3$ $10 * 10^{-3} / 150 * 10^3$ $26 * 10^{-3} / 80 * 10^3$	$0.012 * 10^3$ $0 / 200$
06_Crepe wool	<b>200</b> $60 * 10^{-3} / 5 * 10^3$ $150 * 10^{-3} / 40 * 10^3$ $200 * 10^{-3} / 150 * 10^3$	<b>500</b> $10 * 10^{-3} / 12 * 10^3$ $80 * 10^{-3} / 155 * 10^3$	<b>12</b> $0 / 30$
07_Silk	$1.8 * 10^3$ $4 * 10^{-3} / 330 * 10^3$ $12.5 * 10^{-3} / 440 * 10^3$	$1 * 10^3$ $1.6 * 10^{-3} / 2.8 * 10^6$ $3 * 10^{-3} / 1.7 * 10^6$	$0.012 * 10^3$
08_Natural Silk	<b>300</b> $30 * 10^{-3} / 70 * 10^3$ $60 * 10^{-3} / 250 * 10^3$	<b>500</b> $10 * 10^{-3} / 70 * 10^3$ $32 * 10^{-3} / 360 * 10^3$	<b>16</b> $0 / 230$
09_Wild silk	$1 * 10^3$ $2.5 * 10^{-3} / 21 * 10^6$	$0.05 * 10^3$ $4 * 10^{-3} / 140 * 10^3$ $50 * 10^{-3} / 80 * 10^3$	$0.06 * 10^3$ $0 / 100$
10_Jute	$1 * 10^3$ $2 * 10^{-3} / 2.95 * 10^6$	$1 * 10^3$ $2 * 10^{-3} / 3.3 * 10^6$	$0.06 * 10^3$ $0 / 750$
11_Flannel	<b>500</b> $20 * 10^{-3} / 42 * 10^3$ $70 * 10^{-3} / 130 * 10^3$	<b>1500</b> $40 * 10^{-3} / 67 * 10^3$ $100 * 10^{-3} / -60 * 10^3$	<b>240</b> $10 * 10^{-3} / 11 * 10^3$
12_Denim	<b>200</b> $50 * 10^{-3} / 8 * 10^3$	<b>700</b> $5 * 10^{-3} / 280 * 10^3$	<b>50</b> $0 / 200$

	$220 \cdot 10^{-3} / 120 \cdot 10^3$	$20 \cdot 10^{-3} / 680 \cdot 10^3$	
13_Plaid	$0.6 \cdot 10^3$ $40 \cdot 10^{-3} / 30 \cdot 10^3$ $80 \cdot 10^{-3} / 160 \cdot 10^3$	$1 \cdot 10^3$ $20 \cdot 10^{-3} / 115 \cdot 10^3$ $50 \cdot 10^{-3} / 350 \cdot 10^3$	$0.028 \cdot 10^3$ 0/110
14_Tweed	70 $60 \cdot 10^{-3} / 29 \cdot 10^3$ $115 \cdot 10^{-3} / 95 \cdot 10^3$	800 $20 \cdot 10^{-3} / 350 \cdot 10^3$ $40 \cdot 10^{-3} / 500 \cdot 10^3$	20 0/30
15_Velvet	300 $10 \cdot 10^{-3} / 110 \cdot 10^3$ $30 \cdot 10^{-3} / 290 \cdot 10^3$	300 $3 \cdot 10^{-3} / 50 \cdot 10^3$ $7.5 \cdot 10^{-3} / 550 \cdot 10^3$ $20 \cdot 10^{-3} / 1 \cdot 10^6$	50 $50 \cdot 10^3 / 550$
16_Lurex knit	20 $600 \cdot 10^{-3} / 140$ 1 / 900 $1.25 / 4 \cdot 10^3$	50 $120 \cdot 10^{-3} / 1.3 \cdot 10^3$ $400 \cdot 10^{-3} / 18 \cdot 10^3$	19 0/80
17_Crepe-jersey	1 (broken) $500 \cdot 10^{-3} / 8$ 2 / 19 2.5 / 190	200 $200 \cdot 10^{-3} / 1.4 \cdot 10^3$ $400 \cdot 10^{-3} / 7 \cdot 10^3$	25
18_Woven motorcycle	1000 $3 \cdot 10^{-3} / 5.6 \cdot 10^6$ $7 \cdot 10^{-3} / -4.4 \cdot 10^6$	1000 $3 \cdot 10^{-3} / 5.6 \cdot 10^6$ $7 \cdot 10^{-3} / -3.9 \cdot 10^6$	1100
19_Woven easy care	$0.9 \cdot 10^3$ $10 \cdot 10^{-3} / 46 \cdot 10^3$ $70 \cdot 10^{-3} / 170 \cdot 10^3$	$1 \cdot 10^3$ $2.5 \cdot 10^{-3} / 2.7 \cdot 10^6$	$0.07 \cdot 10^3$ 0/500
20_Warp knitted velour	70 $400 \cdot 10^{-3} / 800$ $700 \cdot 10^{-3} / 4 \cdot 10^3$	50 $200 \cdot 10^{-3} / 200$ $500 \cdot 10^{-3} / 400$ $750 \cdot 10^{-3} / 2 \cdot 10^3$	42
21_Weft knitted plain (single-jersey)	17 $40 \cdot 10^{-3} / 50$ $800 \cdot 10^{-3} / 450$ $1.2 / 4 \cdot 10^3$	70 $100 \cdot 10^{-3} / 200$ $400 \cdot 10^{-3} / 3.5 \cdot 10^3$ $550 \cdot 10^{-3} / 15 \cdot 10^3$	22
22_Taffeta	$1 \cdot 10^3$ $1.5 \cdot 10^{-3} / 6 \cdot 10^6$ $2.5 \cdot 10^{-3} / 23 \cdot 10^6$ $4 \cdot 10^{-3} / -22 \cdot 10^6$	$0.5 \cdot 10^3$ $4 \cdot 10^{-3} / 4.4 \cdot 10^6$	$0.14 \cdot 10^3$
23_Crepe Poly	300 $10 \cdot 10^{-3} / 130 \cdot 10^3$ $25 \cdot 10^{-3} / 990 \cdot 10^3$	10 $10 \cdot 10^{-3} / 58 \cdot 10^3$ $41 \cdot 10^{-3} / 200 \cdot 10^3$	11
24_Satin	600 $30 \cdot 10^{-3} / 0.9 \cdot 10^6$	9000 $20 \cdot 10^{-3} / 0.66 \cdot 10^6$	280 $30 \cdot 10^{-3} / 44 \cdot 10^3$

		$60 \cdot 10^{-3} / -0.82 \cdot 10^6$	$70 \cdot 10^{-3} / 550 \cdot 10^3$
25_Felt	900 $50 \cdot 10^{-3} / 4.5 \cdot 10^3$	860 (broken)	165
26_Organza	0 $1 \cdot 10^{-3} / 1.9 \cdot 10^6$ $10 \cdot 10^{-3} / -2.17 \cdot 10^6$	$3.6 \cdot 10^3$ $2 \cdot 10^{-3} / 380 \cdot 10^3$ $15 \cdot 10^{-3} / -379 \cdot 10^3$	$0.01 \cdot 10^3$
27_Fleece	100 $300 \cdot 10^{-3} / 250$ $800 \cdot 10^{-3} / 1.7 \cdot 10^3$	450 $75 \cdot 10^{-3} / 31 \cdot 10^3$ $150 \cdot 10^{-3} / 50 \cdot 10^3$	50
28_Woven upholstery	100 $12 \cdot 10^{-3} / 4.4 \cdot 10^6$	200 $10 \cdot 10^{-3} / 520 \cdot 10^3$ $25 \cdot 10^{-3} / 280 \cdot 10^3$	160 $50 \cdot 10^{-3} / 700$
29_Woven outdoor	800 $1.7 \cdot 10^{-3} / 910 \cdot 10^3$	10 $4 \cdot 10^{-3} / 1.25 \cdot 10^6$ $20 \cdot 10^{-3} / -700 \cdot 10^3$	100 $50 \cdot 10^{-3} / 380$
30_Tulle	$0.027 \cdot 10^3$ (broken) $400 \cdot 10^{-3} / 120$ 1/480	$1.2 \cdot 10^3$ $10 \cdot 10^{-3} / 120 \cdot 10^3$ $20 \cdot 10^{-3} / 190 \cdot 10^3$	$0.3 \cdot 10^3$ $0 / -3 \cdot 10^3$ $30 \cdot 10^{-3} / 1 \cdot 10^3$ $50 \cdot 10^{-3} / 2.1 \cdot 10^3$
31_Warp knit tric. Sat.	400 $50 \cdot 10^{-3} / 5 \cdot 10^3$ $160 \cdot 10^{-3} / 52 \cdot 10^3$	300 $80 \cdot 10^{-3} / 1.1 \cdot 10^3$ $300 \cdot 10^{-3} / 6 \cdot 10^3$	65
32_Leather	$2 \cdot 10^3$ $60 \cdot 10^{-3} / 70 \cdot 10^3$	$0.9 \cdot 10^3$ $5 \cdot 10^{-3} / 105 \cdot 10^3$ $40 \cdot 10^{-3} / 80 \cdot 10^3$	$1.2 \cdot 10^3$
33_Men's woven suit fabric	$2 \cdot 10^3$ $20 \cdot 10^{-3} / 18 \cdot 10^3$ $80 \cdot 10^{-3} / 70 \cdot 10^3$	400 $80 \cdot 10^{-3} / 15 \cdot 10^3$ $160 \cdot 10^{-3} / 24 \cdot 10^3$	20 0/180
34_Men's woven suit fabric	400 $30 \cdot 10^{-3} / 20 \cdot 10^3$ $100 \cdot 10^{-3} / 85 \cdot 10^3$	$2 \cdot 10^3$ $20 \cdot 10^{-3} / 170 \cdot 10^3$ $50 \cdot 10^{-3} / 180 \cdot 10^3$	14 0/100
35_Men's woven overcoat fabric	400 $75 \cdot 10^{-3} / 13 \cdot 10^3$	$1.2 \cdot 10^3$ $28 \cdot 10^{-3} / 130 \cdot 10^3$	20 0/110
36_Men's woven overcoat fabric	300 $50 \cdot 10^{-3} / 18 \cdot 10^3$ $120 \cdot 10^{-3} / 90 \cdot 10^3$	600 $30 \cdot 10^{-3} / 50 \cdot 10^3$ $70 \cdot 10^{-3} / 210 \cdot 10^3$	25 0/10
37_Woven outdoor	$10 \cdot 10^3$ $2.5 \cdot 10^{-3} / 1.6 \cdot 10^6$	$4 \cdot 10^3$ $8 \cdot 10^{-3} / 340 \cdot 10^3$	60 0/380
38_Weft knitted jersey	60 $600 \cdot 10^{-3} / 180$	100 $300 \cdot 10^{-3} / 580$	45
39_Weft	70	80	25

knitted terry	$550 \cdot 10^{-3} / 420$	$300 \cdot 10^{-3} / 940$	
40_Warp knitted jersey- based fabric	<b>600</b> $80 \cdot 10^{-3} / 40 \cdot 10^3$ $150 \cdot 10^{-3} / 80 \cdot 10^3$	<b>500</b> $40 \cdot 10^{-3} / 13 \cdot 10^3$ $120 \cdot 10^{-3} / 40 \cdot 10^3$	<b>90</b>
41_Warp knitted mesh fabric	<b>500</b> $100 \cdot 10^{-3} / 4 \cdot 10^3$ $200 \cdot 10^{-3} / 3.8 \cdot 10^3$	<b>320</b> $150 \cdot 10^{-3} / 3.2 \cdot 10^3$ $280 \cdot 10^{-3} / 10 \cdot 10^3$	<b>120</b>
42_Brushed knitted fabric	<b><math>2 \cdot 10^3</math></b> $25 \cdot 10^{-3} / 64 \cdot 10^3$	<b>500</b> $50 \cdot 10^{-3} / 1.2 \cdot 10^3$	<b>100</b> 0/180

Default fabric parameter:

Elasticity N/m		
Weft	Warp	Shear
2800 N/m	2500 N/m	60 N/m

Bending N.m		Thickness (mm)	Weight (g)	Friction (coeff.)
Weft	Warp			
8	11	2	185	0.15

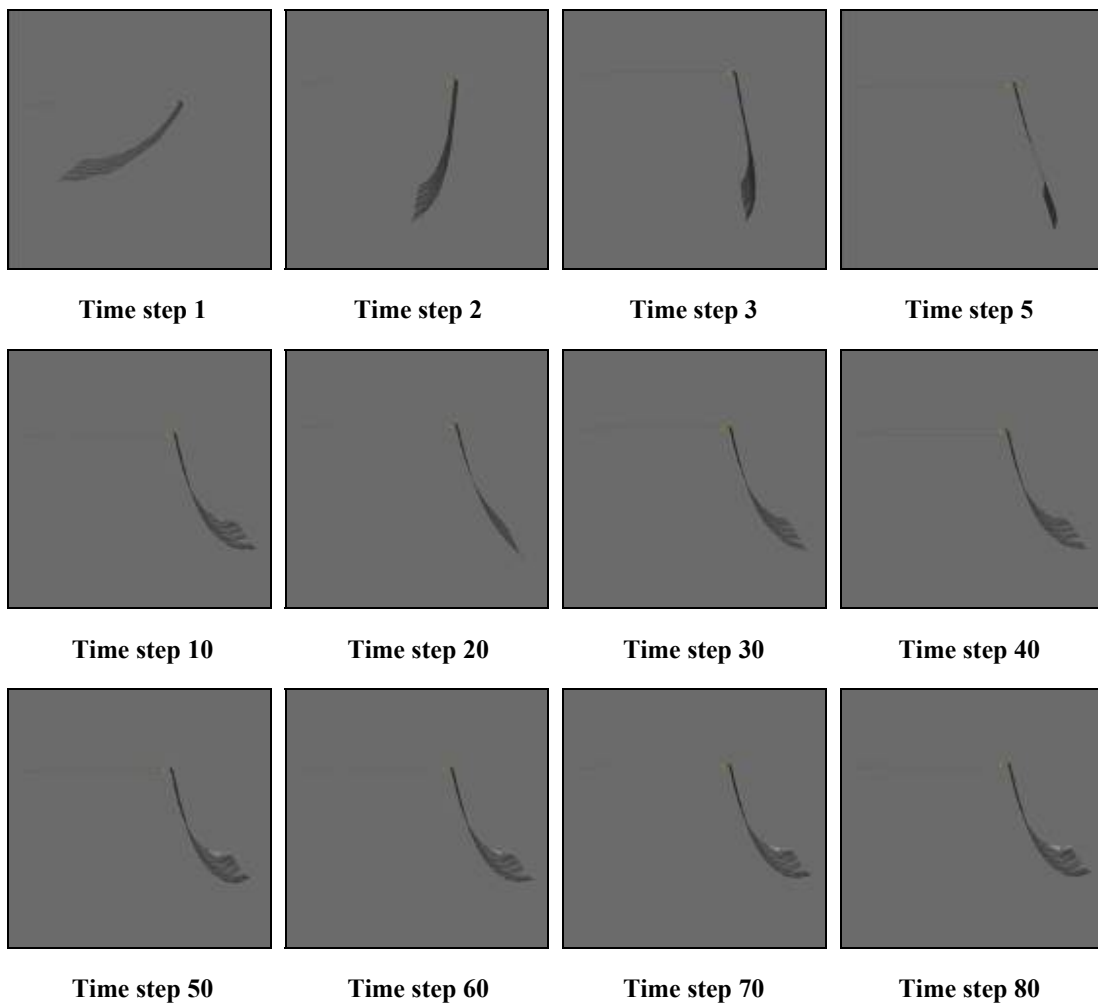
Parameter	New measurements smallest	New measurements highest	Old measurement smallest	Old measurement highest
Tensile				
Warp	80 (20_knit velour)	6000 (07_silk)	6.5 (silk)	50 (linen)
Weft	50 (21_weft knit)	10.000 (09_wild silk, 22_taffeta, 24_satin)	isotropic assumption	isotropic assumption
Shear	10 (26_organza)	1100 (18_woven motorcycle fabric)	3.5	25
Bending				
Warp	$0.4^{-6}$ (31_warp knit tricot)	$110^{-6}$ (18_woven motorcycle fabric)	$0.8^{-6}$ (cotton, cupro)	$18^{-6}$ (linen)
Weft	$0.22^{-6}$ (31_warp knit tricot)	$110^{-6}$ (18_woven motorcycle fabric)	isotropic assumption	isotropic assumption
Density	15 (07_silk)	600 (28_upholstery)	85 (silk)	327 (tencel)

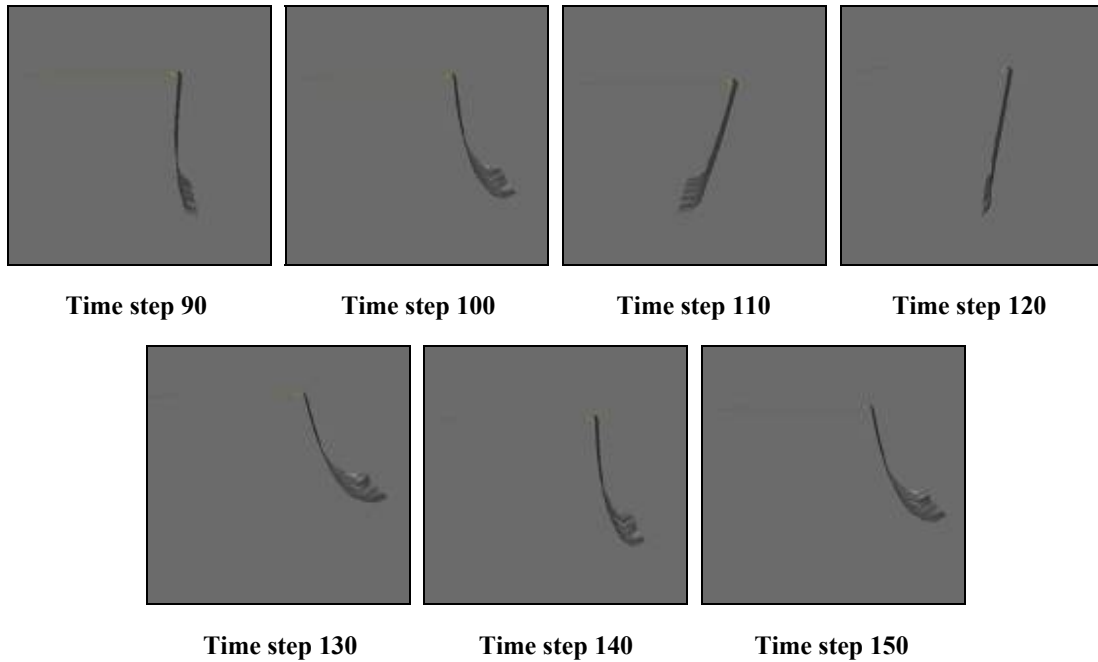
## Annex H: Simulation settings

### Simulation setting “Time step”:

Simple linear fabric parameters need fewer timesteps in order to simulate a piece a cloth up to a certain distance or deformation. Complex nonlinear fabric parameters need more calculation time for the same distance or deformation. Therefore the timestep parameter needs to be re-adjusted for the new fabric parameters.

For the experiment, a horizontal piece of fabric is released so that it simulates into a vertical position. The fabric is simulated 10 frames. The pictures below illustrate that from a certain number of timesteps on, the fabric simulates to the same extent, what is the searched position. For the fabric below only little difference is visible between a timestep value of 10 and 80. In order to reduce computation time, the lowest possible timestep is searched.





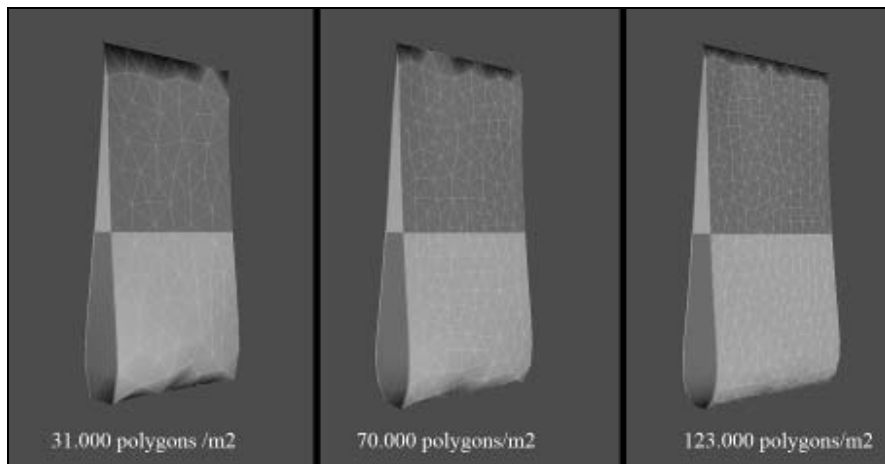
The same experiment is executed with all new fabric parameters. For the more elastic fabric, a low number of 10 timesteps was sufficient. For more rigid fabric, a timestep of 30-50 was necessary. In order to have the same value for all fabrics, 50 is taken as new timestep parameter. (As we saw from the experiments, a higher number is no problem for the more elastic fabric, as the simulation returns the same result until a value of 80)

### Fabric resolution:

The literature often emphasizes the accuracy of the mechanical model. The major causes of inaccuracy, however, are rather found in the surface discretization [Volino 00]. For an accurate simulation of the fabric behaviour, in particular of the bending characteristic, it is important that the virtual surface contains a minimum of triangles. Regarding bending, the size of the polygon defines the smallest possible wrinkle. The setting “Accuracy” of the simulation system describes the fabric resolution. This parameter defines the amount of triangles per surface.

For the following simulation test, the fabric with the smallest bending rigidity value (sample 39\_weft-knit terry fabric) is taken and simulated with the loop test method. Several accuracy values are tried out to determine the necessary fabric resolution. The applied resolutions correspond to the following amount of triangles per m<sup>2</sup>:

- Accuracy 100 = 31.000 polygons / m<sup>2</sup>
- Accuracy 150 = 69.200 polygons / m<sup>2</sup>
- Accuracy 160 = 78.900 polygons / m<sup>2</sup>
- Accuracy 170 = 88.400 polygons / m<sup>2</sup>
- Accuracy 200 = 123.600 polygons / m<sup>2</sup>



The picture of the loop test shows that a minimum amount of 70.000 polygons is necessary for an accurate bending simulation. On the other hand, the loop test is a static simulation and during dynamic simulation the fold might be smaller and higher amounts of triangles are needed. But it would be impossible to compute an elastic fabric as 39\_weft-knit terry fabric until it is completely folded. The computation of that amount of polygons would be too slow. A fabric resolution of up to 150 000 polygons per m<sup>2</sup> is therefore taken as an upper limit for dynamic simulations. For more rigid fabric lower values are sufficient. The loop test is however a good test to approach the fabric resolution.

## Annex I: Remarks

The Kawabata standard recommends to measure very elastic fabrics with a smaller jaw length of 2.5cm. The smaller jaw length was used for fabrics 16\_lurex-knit, 17\_crepe-jersey, 20\_warp-knit, 21\_single-jersey, 30\_tulle, 38\_weft-knit-jersey, 39\_weft-knit terry. Hence, we have to consider that those textiles are characterized with a smaller specimen. However, the elongations are expressed in % and so no conversion is necessary for the measurement data.



## Annex J: List of Figures

Figure 1: Different branches of the clothing and textile industry [Mango], [Fibers], (Miralab – University of Geneva)

Figure 2: Four examples of realistic virtual garments (Miralab – University of Geneva)

Figure 3: Virtual prototyping of men suits visualizing numerical fitting data (Miralab-University of Geneva), real men suits [Zegna]

Figure 4: Numerical fitting data while running in Weft-direction, Warp direction (Miralab-University of Geneva)

Figure 5: Low technological sketches and garment description (Miralab-University of Geneva)

Figure 6: Corresponding virtual 3D garment, used as visual language (Miralab-University of Geneva)

Figure 7: Virtual try on of men suits in various colors (Miralab-University of Geneva)

Figure 8: Two aspects of accuracy in virtual simulations

Figure 9: Scheme on influencing factors [Mae 05]

Figure 10: Subjective fabric assessment, Objective measurement device [Instron 06]

Figure 11: Group 1: Cantilever principle (left) and loop method (middle), Group 2: moment – curvature method (right)

Figure 12: Angle force method (left), Shear seen as Cantilever (middle), Shear in 45° (right)

Figure 13: Scheme of measuring tensile, tensile hysteresis envelope [Kaw 80]

Figure 14: Scheme of measuring shear, shear hysteresis envelope [Kaw 80]

Figure 15: Scheme of bending, bending hysteresis envelope [Kaw 80]

Figure 16: SiroFAST bending measurement machine [CSIRO 07]

Figure 17: KES-f shear elongation scheme (left), FAST shear deformation scheme (right)

Figure 18: FAST cantilever method, KES-f moment curvature method

Figure 19: KES-f tensile measurement report page for fabric single-jersey

Figure 20: Photo drapemeter [Kenkare 05], Scheme drapemeter, Output picture [Kenkare 05]

Figure 21: Spring-mass model by [Provot 95]

Figure 22: Three ways of creating bending stiffness in a triangle mesh: Crossover springs (top), forces along normals (bottom), and forces as weighted sums of vertex positions (right) [Volino 06]

Figure 23: Virtual garment examples, (Miralab – University of Geneva)

Figure 24: Workflow

Figure 25: Cotton plant [Fibers] (left), scheme twill [Loschek 94] (middle), denim fabric (left)

Figure 26: Real fitting processes [San], [Reflexstock]

Figure 27: Traditional fabric manufacturing processes a) wool shearing, b) fiber spinning-wheel, c) weaving. Today the manufacturing is more automated

Figure 28: Fabric selection criteria (detailed fabrics selection list can be found in Annex B)

Figure 29: Fiber shares in the two fabric selection cycles

Figure 30: EMT warp and weft for the first fabric selection cycle

Figure 31: Tensile force-deformation curve 07\_silk,

Figure 32: Force-deform. curve 16\_Lurex-knit

Figure 33: Tensile force-deformation curve 01\_denim,

Figure 34: Force-deformation curve 25\_felt

Figure 35: Tensile resilience

Figure 36: Shear rigidity values G

Figure 37: Ratio (tensile elongation weft/warp) and (G weft/warp)

Figure 38: Shear force-deformation curve 21\_single-jersey (knit),

Figure 39: 09\_wild-silk (plain),

Figure 40: Shear force-deformation curve 02 shirt cotton (plain)

Figure 41: Sample 24\_satin (satin)

Figure 42: Hysteresis of shear force at 5°

Figure 43: Sample 01\_denim (warp)

Figure 44: Sample 01\_denim (weft)

Figure 45: Four shear force-deformation curves sample 24\_satin (left) and 11\_flannel (right)

Figure 46: Bending rigidity of the measured samples in KES-f system

Figure 47: Hysteresis of bending moment

Figure 48: Sample 03\_cord,

Figure 49: Sample 28\_woven upholstery fabric

Figure 50: Sample 18\_woven motorcycle fabric,

Figure 51: Sample 17\_crepe-jersey

Figure 52: Four bending force-deformation curves for fabric 01\_denim (left) and 24\_satin (right)

Figure 53: Thickness first fabric selection cycle

Figure 54: Fabric weight

Figure 55: MIU in weft and warp direction for the first fabric selection

Figure 56: MIU in weft and warp direction for the second fabric selection

Figure 57: Simulated cotton fabric with three different simulation applications: MIRALab's in-house software, 3ds max 9 (ClothFX), Maya 8.5 (MayaCloth)

Figure 57: Simulated cotton fabric with MIRALab's in-house simulation application,

Figure 58: 3ds max 9 (ClothFX) simulation application

Figure 59: Maya 8.5 (MayaCloth)

Figure 60: A triangle element deformed in 3D [Volino 05]

Figure 61: Scheme of the applied bending model [Volino 06]

Figure 62: Ratio of EMT (max elongation) and B (Bending stiffness)

Figure 63: Input parameter box of the used simulation system

Figure 64: Four measured KES-f shear force-deformation envelopes for fabric 28\_upholstery fabric (left)

Figure 65: 30\_tulle (right)

Figure 66: Force deviation in % for the four measured shear directions

Figure 67: Good and bad correlating front and back bending force-deformation envelopes sample 28\_upholstery fabric (warp left, weft right)

Figure 68: Measurement deviation for fabrics front and back bending for warp and weft measurements

Figure 69: Deviation according to fabric structures in comparison with the bending rigidity B (warp direction)

Figure 70: Fabric performance [Reflexstock], [Fan 04]

Figure 71: comfort performance [San], [Reflexstock]

Figure 72: utility performance [Reflexstock]

Figure 73: 2D Pattern misfit and related folds [Reflexstock]

Figure 74: 2D pattern construction with base lines

Figure 75: Garment showing base lines

Figure 76: Scheme for the tensile parameter evaluation

Figure 77: Hanging cloth (left),

Figure 78: Stretch fitting posture movement

Figure 79: Bending loop test method

Figure 80: Former cotton parameter (left) and new linear derived FAST cotton parameter (right)

Figure 81: Linear derived data from FAST, Non-linear interpreted data from KES-f

Figure 82: Colorscale

Figure 83: Tensile deformations under the fabric SW for sample 21\_single-jersey (left) and 11\_flannel (right), deformation scale 0.2% in warp direction

Figure 84: Scheme – inaccuracies of FAST tensile parameters

Figure 85: 2D and 3D view of simulated hanging rectangle, visualizing fabric elongations of 0.1% (accuracy limit) in shear direction. 24\_satin (left) and 21\_single-jersey (right)

Figure 86: Shear forces, fabrics SW and FAST tensile forces - scheme

Figure 87: Elongations of 0.2% in shear direction using nonlinear KES-f parameter and linear FAST parameter, 04\_linen (left) and 05\_gabardine (right).

Figure 88: Comparison of real warp front and back bending

Figure 89: Comparison of real weft front and back bending

Figure 90: Comparison average real and virtual loop length in warp direction

Figure 91: Comparison average real and virtual loop length in weft direction

Figure 92: Comparison KES-f, FAST and average real front and back bending

Figure 93: Real bending loop front, KES-f bending loop, FAST bending loop

Figure 94: Loop length test 10\_jute real (right) and virtual (left)

Figure 95: Six deformation cycles of 10% elongation. Less and less force is needed for the same deformation, as the fabric does not fully recover from previous load.

Figure 96: Fabric 05\_gabardine at 100 N/m (2 left jackets) and 500 N/m (2 right jackets)

Figure 97: Sample 24\_satin at 100 N/m (2 left jackets) and 500 N/m (2 right jackets)

Figure 98: Comparison of FAST and KES-f parameter in the higher force area

Figure 99: Example of the ITT measurement report page, Instron tensile tester

Figure 100: Sample 01\_denim weft, recovered by hand after each load peak

Figure 101: Category 1, sample 07\_silk warp

Figure 102: Category 2, sample 03\_cord warp

Figure 103: Category 3, sample 16\_lurex-knit warp

Figure 104: Category 4, sample 26\_organza warp

Figure 105: Correlation KES-f and ITT 01\_denim weft (left), and 31\_tricot-satin weft (right)

Figure 106: Comparison of KES-f and ITT data at 500N/m in weft direction

Figure 107: Sample 27\_Fleece (weft), sample 16\_lurex-knit (weft)

Figure 108: Example fabric 05\_gabardine warp (left), fabric 37\_woven-outdoor warp (right)

Figure 109: Differences of derived parameters from KES-f and ITT

Figure 110: Fabric 21\_single-jersey (left), Fabric 36\_men-overcoat, 500 N/m (right)

Figure 111: 1000 N/m for 04\_linen, 19\_easy-care, 28\_upholstery, 36\_men-overcoat

Figure 112: Several body distance changes during movements

Figure 113: sample 04\_linen – measuring the point of rupture

Figure 114: Protocol for cyclic deformations such as walking, running, etc. (left), protocol for various deformations for more spontaneous movements (right)

Figure 115: 11\_flannel cyclic measurement (left), 24\_satin cyclic measurement (right)

Figure 116: 11\_flannel non-cyclic measurement (left), 24\_satin non-cyclic measurement data (right)

Figure 117: ITT measurement 38\_weft-knit (left), 11\_flannel (middle), 24\_satin (right)

Figure 118: 38\_weft-knit measurement with various forces

Figure 119: 24\_satin comparison of measurements from KES-f, ITT and LDM

Figure 120: 11\_flannel comparison of measurements from KES-f, ITT and LDM

Figure 121: 38\_weft-knit (yellow) comparison of measurements (left), 38\_weft-knit parameter comparison (right)

Figure 122: Non-cyclic parameter deviation from real measurement fabric 11\_flannel

Figure 123: parameter comparison for sample 24\_satin,

Figure 124: Fitting movement with parameters 38\_weft-knit (left), 24\_satin (right)

Figure 125: KES-f Shear elongation scheme (left), FAST shear scheme (right)

Figure 126: Non-cyclic and cyclic shear measurement for fabric 11\_flannel

Figure 127: KES-f shear measurement for fabric 11\_flannel

Figure 128: Cyclic shear measurements for 24\_satin (left) and 38\_weft-knit (right)

Figure 129: Superposition KES-f and LDSM shear measurement fabric 24\_satin

Figure 130: noisy shear measurement data

Figure 131: Comparison of the force-deformation profiles of the three simulated 2D deformation directions, fabric 11\_flannel

Figure 132: Three force-deformation profiles for fabric 38\_weft-knit (left) and 24\_satin (right)

Figure 133: wrinkles and folds during movements,  
 Figure 134: Forced wrinkles on a skirt  
 Figure 135: FAST cantilever method, KES-f moment curvature method  
 Figure 136: Fabric 39\_ weft knit terry fabric (weft), 13\_plaid (warp)  
 Figure 137: 10\_jute, real (right) and virtual (left)  
 Figure 138: 36\_woven-overcoat, real (right) and virtual (left)  
 Figure 139: 05\_gabardine, real (right) and virtual (left)  
 Figure 140: 39\_ weft knit terry, real (right) and virtual (left)  
 Figure 141: Step bending 36\_overcoat fabric weft (left) and warp (right)  
 Figure 142: Cyclic load – unload test sample 11\_flannel  
 Figure 143: Comparison cyclic tensile test at two speeds, 1mm/s and 10mm/s for sample 24\_satin  
 Figure 144: creep test sample 24\_satin, 11-flannel and 38\_weft knit  
 Figure 145: Comparison creep test and cyclic measurement for fabric 11\_flannel  
 Figure 146: Elastic tensile potential EP calculated for the first fabric selection  
 Figure 147: Comparison EP and EMT, warp  
 Figure 148: Shear elastic potential GP calculated for the first fabric selection  
 Figure 149: Friction profile 01\_denim warp (left), weft (right)  
 Figure 150: Friction profile fabric 03\_cord warp (left) weft (right)  
 Figure 151: Friction profile fabric 15\_velvet warp (left) weft (right)  
 Figure 152: Friction profile fabric 05\_gabrdine warp (left), 14\_tweed warp (right)  
 Figure 153: MIU in weft and warp direction for the first fabric selection  
 Figure 154: Scheme of friction evaluation [Tribo]  
 Figure 155: Comparison of three obtained friction parameters  
 Figure 156: Pipeline of validation experiment  
 Figure 157: Scanning process of the real mannequin (left), virtual mannequin (right)  
 Figure 158: 2D pattern and sewing of the real dress  
 Figure 159: Digitalization process (left), digitized 2D pattern (center), virtual dress (right)  
 Figure 160: Real comfort performance  
 Figure 161: Virtual comfort performance  
 Figure 162: Comfort fitting  
 Figure 163: Fabric 38\_single-jersey: real and virtual drape (left), fabric 36\_overcoat fabric: real and virtual drape (right)  
 Figure 164: Fabric 41\_warp-knit: real and virtual drape  
 Figure 165: Comparison virtual simulation (left), scanned real fabric as point-cloud (center), scanned real fabric as polygons (right)  
 Figure 166: Set up of the real experiment  
 Figure 167: Diagram illustrating the real and the virtual force – deformation relationship  
 Figure 168: Virtually recreated experiment  
 Figure 169: Vicon Motion Tracking

Figure 170: Virtual skirt 38\_weft-knit jersey  
 Figure 171: Virtual skirt 38\_weft-knit jersey  
 Figure 172: Virtual skirt 04\_linen  
 Figure 173: Virtual skirt 39\_weft-knit terry fabric  
 Figure 174: Virtual skirt 11\_flannel  
 Figure 175: Real and virtual dress 24\_satin  
 Figure 176: Fabric 38\_weft-knit on a moving sphere, left real fabric, right virtual simulation  
 Figure 177: Fabric 36\_overcoat fabric on a moving sphere, left real fabric, right virtual simulation  
 Figure 178: Fabric 11\_flannel around two cylinders that move apart  
 Figure 179: Jacket for the Leapfrog project [Leapfrog 08]

## **Annex K: List of Tables**

Table 1: KES-f calculated characteristic fabric hand values  
 Table 2: FAST calculated characteristic fabric hand values [FAST 95]  
 Table 3: Different applications of fabric objective measurement technology  
 Table 4: Fabric properties and their relation to performance and appearance in wear and handle  
 Table 5: Data ranges  
 Table 6: Data ranges regarding various types of materials and structures  
 Table 7: FAST data extensibility warp, weft and shear, \* exceeded the test machine limit - 21%  
 Table 8: FAST data bending  
 Table 9: FAST data weight, thickness and friction  
 Table 10: Overview of input parameters of different simulation applications  
 Table 11: Overview of input parameters in the applied simulation system  
 Table 12: + = important, o = medium, - not important  
 Table 13: + = important, o = medium, - not important  
 Table 13a: + = important, o = medium, - not important  
 Table 14: + = important, o = medium, - not important  
 Table 15: Required aesthetical (visual) accuracy for different parts of a garment  
 Table 16: Required functional (felt) accuracy for different parts of a garment  
 Table 17: Fabric deformations at their SW  
 Table 18: Correlation of KES-f and ITT  
 Table 19: Maximum body distance-changes for men  
 Table 20: Maximum body distance-changes for women  
 Table 21: Measurement results for the determination of the point of rupture  
 Table 22: Shear deformations of the FAST measurement  
 Table 23: Various bending values of 5 fabric samples

Table 24: typical viscosity values [Handbook]

Table 25: Various types of friction in various the simulation applications

Table 26: Suitability of standard measurement methods

Table 27: Suitability of various measuring methods

Table 28: Tensile measurement specification

Table 29: Shear measurement specification

Table 30: Bending measurement specification

Table 31: Friction measurement specification

Table 32: Mannequin's body measurements

Table 33: Summary of error margins, \*calculated with a waist girth of 60cm

Table 34: Key factors for real and virtual garment prototyping